ROLE OF CYTOKININ AND ETHYLENE DURING SENESCENCE IN BROCCOLI (*BRASSICA OLERACEA* VAR. *ITALICA*).

A thesis presented in partial fulfilment of the requirements for the degree of

Doctor of Philosophy

at

Massey University

NIGEL ESTEVEN GAPPER

2003

Massey University
COLLEGE OF SCIENCES

Institute of Molecular BioSciences
Private Bag 11 222,
Palmerston North,
New Zealand
Telephone: 64 6 356 9099
Facsimile: 64 6 350 5688
Email: IMBS@massey.ac.nz

TO WHOM IT MAY CONCERN

This is to state that the research carried out for my PhD thesis entitled "Role of cytokinin and ethylene during senescence in broccoli (*Brassica oleracea* var *italica*)" in the Institute of Molecular BioSciences at Massey University, Palmerston North, New Zealand is all my own work. This is also to certify that thesis material has not been used for any other degree.

Candidate

Nigel Gapper

Date: 14 April 2003

Massey University
COLLEGE OF SCIENCES

Institute of Molecular BioSciences
Private Bag 11 222,
Palmerston North,
New Zealand
Telephone: 64 6 356 9099
Facsimile: 64 6 350 5688
Email: IMBS@massey.ac.nz

TO WHOM IT MAY CONCERN

This is to state that the research carried out for the PhD thesis entitled "Role of cytokinin and ethylene during senescence in broccoli (*Brassica oleracea* var *italica*)" was done by Nigel Gapper in the Institute of Molecular BioSciences at Massey University, Palmerston North, New Zealand. This thesis material has not been used for any other degree.

Chief Supervisor

Paula Jameson
Professor of Plant Biology

Date: 14 April 2003

Massey University
COLLEGE OF SCIENCES

Institute of Molecular BioSciences
Private Bag 11 222,
Palmerston North,
New Zealand
Telephone: 64 6 356 9099
Facsimile: 64 6 350 5688
Email: IMBS@massey.ac.nz

CERTIFICATE OF REGULATORY COMPLIANCE

This is to certify that the research carried out in the Doctoral Thesis entitled "Role of cytokinin and ethylene during senescence in broccoli (*Brassica oleracea* var *italica*)" in the Institute of Molecular BioSciences at Massey University, New Zealand:

(a) is the original work of the candidate, except as indicated by appropriate attribution in the text and/or in the acknowledgements;

(b) that the text, excluding appendices/annexes, does not exceed 100,000 words;

(c) all the ethical requirements applicable to this study have been complied with as required by Massey University, other organizations and/or committees which had a particular association with this study, and relevant legislation.

GMO 01/CFP00 update of HURST 3
GMO 00/CFP00 update of HURST
GMO 99/CFP00 HURST
GMO 00/CFR002 CHRISTEY

Please insert Ethical Authorisation code(s) here (if applicable): ERMA APPROVAL NUMBERS THROUGH CROP + FOOD RESEARCH

Candidate's Name: Nigel Gapper

Signature: Nigel Gapper

Date: 14 April 2003

Supervisor's Name: Professor Paula Jameson

Signature: P E Jameson

Date: 14 April 2003

Dedication

This thesis is dedicated

to my parents

Brian and Linda

Abstract

Broccoli (*Brassica oleracea* var. *italica*) deteriorates rapidly following harvest. The two plant hormones ethylene and cytokinin are known to act antagonistically on harvest-induced senescence in broccoli: ethylene acts by accelerating the process, whereas additional cytokinin delays it. The overall aim of this thesis was to gain a better understanding of how these two hormones control postharvest senescence. The effects of exogenous cytokinin (6-benzyl aminopurine, 6-BAP), 1-aminocyclopropane-1-carboxylic acid (ACC) and sucrose on senescence-associated gene expression were measured in both wild-type plants and transgenic plants harbouring an antisense tomato ACC oxidase gene (*pTOM13*). Exogenous cytokinin caused both a reduction (*BoACO*) and an increase (*BoACS*) in ethylene biosynthetic gene expression as well as reduced expression of genes encoding sucrose transporters and carbohydrate metabolising enzymes, indicating a significant role for cytokinin in the delay of senescence.

Transgenic broccoli was produced using *Agrobacterium tumefaciens*-mediated transformation. Ethylene biosynthesis was targeted *via* an antisense *BoACO2* gene fused to the harvest-induced asparagine synthetase (AS) promoter from asparagus. In addition, broccoli was transformed with constructs harbouring the *Agrobacterium tumefaciens* isopentenyl transferase (*ipt*) gene using the senescence-associated SAG_{12} and floral-associated MYB_{305} gene promoters to enhance the levels of cytokinin either during senescence or in floral tissue, respectively.

The presence of the antisense AS-ACO construct was associated with an increased rate of transformation when compared to control constructs. Physiological analyses of mature plants showed that the antisense AS-ACO gene construct caused delayed senescence in both detached leaves and detached heads. Gene expression analyses of harvested floret tissue from AS-ACO lines showed decreases in transcript levels of senescence marker genes compared to wild-type and transgenic control lines, as well as a reduction in

expression of sucrose transporter and carbohydrate metabolising genes, confirming the key role of ethylene in the promotion of senescence.

In addition, genes involved with cytokinin biosynthesis and metabolism were isolated by PCR using primers based on *Arabidopsis* clones. The four broccoli *ipt* sequences aligned closely to four of the *Arabidopsis* sequences and were subsequently named *BoIPT4*, *BoIPT5*, *BoIPT6* and *BoIPT7*. A cytokinin oxidase clone (*BoCKX*) was also isolated from broccoli. The four *BoIPT* genes were expressed in a number of different tissues, suggesting that the different genes may be involved in different biological processes in the plant. *BoIPT4* was expressed early and *BoCKX* expressed late in florets during senescence.

A model depicting the regulation of senescence in broccoli through the expression of cytokinin biosynthesis and metabolism genes, and their interaction with ethylene and carbohydrate metabolism is presented and discussed.

Acknowledgements

There are many people that have been involved with my PhD project, both directly and indirectly, I wish to thank you all for your help and support over the past four years of my life. First and foremost I would like to express my many thanks to my supervisors, Professor Paula Jameson, Dr Ross Lill, Dr Marian McKenzie and Dr Mary Christey. Paula, thank you for believing in my ability over the past seven years. You took me on when others might have thought twice, these hands that are large, are very capable after all. You nurtured, moulded and made me the scientist I am today, I cannot thank you enough. Ross, my gratitude for giving me the opportunity to work within the infrastructure at Crop & Food Research. You have taught me to think outside of the square, I have very much enjoyed discussions we have had. Marian, your scientific input into the project has been very prominent from the outset. Thank you for your role as a mentor on a day-to-day basis, your door was always open and I appreciated this very much. Mary, thank you for sharing your tissue culture expertise. Without your skills, the project would never have taken shape the way it has.

I must pay a very special acknowledgement to Dr Simon Coupe. Your scientific input throughout the duration of my PhD was nothing less than outstanding. You taught me many of the skills that I have used throughout my PhD for which I am very grateful. You call me the 'PCR God', well in turn I must call you the 'Molecular Biology God'. Thank you Simon, working with you was always a pleasure, and I wish you all the best with your career.

My gratitude for the help I received from Drs Michael McManus and Richard Scott for the ACC oxidase biochemistry. I must also thank the people who have provided me with technical assistance. Robert Braun, Gill Reader and Astrid Erasmuson from the Lincoln C&FR. Ian King, Steve Arathoon, Andrew Mullan, Beverley Hoffmann, Jan Manson and Ranjith Pathirana from Palmerston North C&FR. Robert Lamberts for photography and

Anthony Corbett for photography and excellent poster preparation. For advice on statistical analyses, I must pay a special thank you to Dr John Koolard.

Drs Erin O'Donohue, Jocelyn Eason, Chris Winefield, Donald Hunter, Kevin Davies, Karen Neilsen, Huaibi Zhang, Julian Heyes, Kathy Schwinn, Simon Deroles, Mr Brent Page, Mr Murray Boase and Mr Ed Morgan thank you for useful discussions we have had either in the lab, at the card table or while walking the corridors. Theresa Lill, Tatyana Pinkney, Lyn Watson, Sheryl Somerfield, Dacey Ryan, Yongjin Shang, Michael Bennett, David Horgan, John Javellana, Glen Shingleton, Jason Johnston, Gayle Marshall, Toni Waugh, Lisa Harvey, Lei Wang and Vern Collette, thank you all for making the Lab a very happy place to work in. Thank you also to Dr John Clemens and members of Paula and John's Research group at Massey, for friendship and scientific discussion.

I would like to make a special thank you to Malcolm McKinnon, Managing Director of Audio Progress Ltd, Craig Black and Hayden Sinclair from Creative Sounds, Jordan Reyne, Rob McDermott, Anna McKenzie (Fran), Regan Hawea and the many bands and artists I have worked with over the past four years. Also, the C&FR indoor cricket team, "The Chosen Ones", and the C&FR "Hackers and Hunters Elite Golf Group". Thank you all for your friendship and the chance to do something other than science. You have all given me opportunities I have relished that have stopped me going insane. Big ups to you all!!!!!!

No acknowledgement would be complete without thanking the funding bodies. Thank you to the Foundation for Research Science and Technology for supplying the funding for this project through C&FR. In addition, The Royal Society of New Zealand, The New Zealand Society for Horticultural Science, and The Institute of Molecular BioSciences, Massey University, provided funds for international conference travel.

Finally I would like to thank my family, my mum and dad, Linda and Brian, my nana Winefred, and my brother Leyton. Your support and encouragement during my PhD has been invaluable.

Table of Contents

List of Figures

List of Tables

Abbreviations

A_{260}	absorbance at 260 nm
A	adenine
ABA	abscisic acid
ACC	1-aminocyclopropane-1-carboxylic acid
ACO	1-aminocyclopropane-1-carboxylic acid oxidase
ACS	1-aminocyclopropane-1-carboxylic acid synthase
ADP	adenosine diphosphate
AHK	*Arabidopsis* histidine kinase
AHP	*Arabidopsis* histidine phosphotransfer
AMP	adenosine monophosphate
ARR	*Arabidopsis* response regulator
AS	Asparagine synthetase
AS-ACO	AS-promoter, antisense BoACO2 gene construct
AtCKX	*Arabidopsis thaliana* cytokinin oxidase
AtIPT	*Arabidopsis thaliana* isopentenyl transferase
ATP	adenosine triphosphate
6-BAP	6-benzylamino purine
BCIP	5-bromo-4-chloro-3-indoyl phosphate
Bo18S	*Brassica oleracea* 18S ribosomal subunit
BoACO	*Brassica oleracea* 1-aminocyclopropane-1-carboxylic acid oxidase
BoACS	*Brassica oleracea* 1-aminocyclopropane-1-carboxylic acid synthase
BoCAB	*Brassica oleracea* chlorophyll a/b binding protein
BoCKX	*Brassica oleracea* cytokinin oxidase
BoCP	*Brassica oleracea* cysteine protease
BoHK	*Brassica oleracea* hexokinase
BoIPT	*Brassica oleracea* isopentenyl transferase
BoINV	*Brassica oleracea* acid invertase
BoMLP	*Brassica oleracea* metallothionein-like protein
BoPI	*Brassica oleracea* protease inhibitor

BoSUC	*Brassica oleracea* sucrose transporter
bp	base-pairs
BSA	bovine serum albumin
°C	degrees Celsius
C	cytosine
CA	controlled atmosphere
CaMV 35S	cauliflower mosaic virus 35S promoter
cDNA	cDNA clone
CKI	cytokinin insensitive
cm	centimetre
CPPU	*N*-2-2chloro-4 pyridyl-*N'*-phenylurea
CRE	cytokinin receptor
Da	Daltons
dATP	2'-deoxyadenosine 5'-triphosphate
dCTP	2'-deoxycytidine 5'-triphosphate
dGTP	2'-deoxyguanosine 5'-triphosphate
DMAPP	dimethylallylpyrophophate
DMP	dimethyl formamide
DMSO	dimethyl sulphoxide
DNA	deoxyribonucleic acid
DNase	deoxyribonuclease
dNTP	deoxynucleotide triphosphate
DPU	diphenyl urea
DTT	dithiothreitol
dTTP	2'-deoxythymidine 5'-triphosphate
EDTA	ethylenediaminetetracetic acid
ETR	ethylene receptor
EREBP	ethylene response element biding protein
ERF	ethylene response factor
FPLC	fast performance liquid chromatography

g	gram
G	guanine
GC	gas chromatography
GCR	G-protein coupled receptor
GFP	green fluorescent protein
GMO	genetically modified organism
GTP	guanosine triphosphate
GUS	ß-glucuronidase
h	hour
Hyg	hygromycin
hpt	hygomycin phosphotransferase gene
IAA	indole acetic acid
iP	isopentenyladenine
iPA	isopentenyladenosine
iPDP	isopentenyladenosine-5-diphosphate
iPMP	isopentenyladenosine-5-monophosphate
ipt	isopentenyl transferase gene
IPT	isopentenyl transferase protein
IPTG	isopropyl-β-*D*-thiogalactopyranoside
IPTP	isopentenyladenosine-5-triphosphate
k	kilo
Kan	kanamycin
kb	kilo base-pairs
kDa	kilo Daltons
KV	kilo volts
L	litre
LB	Luria-Bertani (media or broth)
LSC	leaf senescence clone
LSD	least significant difference
M	molar, moles per litre

MAPK	mitogen activating protein kinase
min	minute
µg	micro gram
mg	milligram
µL	microlitre
mL	millilitre
µM	micro molar, micro moles per litre
mM	milli-molar, milli moles per litre
MOPS	3-[*N*-morpholino] propanesulphonic acid
mRNA	messenger ribonucleic acid
MYB_{305}	floral specific MYB_{305} promoter
NaHAc	sodium acetate
NBT	*p*-nitroblue tetrazolium chloride
ng	nanogram
nM	nano-molar, nano moles per litre
NOS	nopaline synthase
nptII	neomycin phosphotransferase gene
OCS	octopine synthetase
OD_{600}	optical density at 600 nm
OD_{660}	optical density at 660 nm
ORF	open reading frame
PCR	polymerase chain reaction
PIPES	piperazine-*N,N'-bis*-2-ethanesulphonic acid
PFU	plaque forming unit
pg	picogram
pmol	pico-molar, pico moles per litre
pTOM13	tomato 1-aminocyclopropane-1-carboxylic acid oxidase
rATP	ribooxyyadenosine triphosphate
rCTP	ribooxyycytidine triphosphate
rGTP	ribooxyyguanosine triphosphate

RH	relative humidity
Ri	root-inducing (plasmid)
RNA	ribonucleic acid
RNase	ribonuclease
rpm	revolutions per minute
RT	room temperature
RT-PCR	reverse transcriptase polymerase chain reaction
rUTP	ribooxyyuradine triphosphate
SAG	senescence-associated gene
SAG_{12}	senescence-associated gene promoter
SAM	*S*-adenosyl-*L*-methionine
SAP	shrimp alkaline phosphatase
SDG	senescence-down-regulated
SDS	sodium dodecyl suphate
SSC	saline sodium citrate buffer
T	thymine
TBS	tris-buffered saline solution
T-DNA	transfer DNA
TE	tris-EDTA buffer
TEMED	*N*,*N*,*N*',*N*'-tetramethylethylenediamine
Ti	tumour-inducing (plasmid)
Tris	tris(hydroxymethyl)aminomethane
Tween 20	polyoxyethylenesorbitan monolaurate
t-RNA	transfer-RNA
U	uracil
UV	ultra violet light
V	volts
vir	virulence gene
v/v	volume per volume
v/v/v	volume per volume per volume

w/v	weight per volume
Z	zeatin
ZR	zeatin riboside

Chapter 1

Introduction

1.1 OVERVIEW

Broccoli (*Brassica oleracea* var. *italica*) is an important vegetable crop in New Zealand. Sales totalled $19M in 1996, ranking it the sixth most popular vegetable purchased by the New Zealand public (Statistics NZ, 1996). Exports of broccoli and cauliflower increased by 79% over the eight years prior to 1996, from 20.5 to 99 tons (Statistics NZ 1988-1996). Further, recent research has shown broccoli contains compounds that may prevent cancer. This has enhanced the popularity of the crop throughout the western world, potentially providing novel niche export markets in the northern hemisphere. Broccoli is a product of relatively low value, hence export to overseas markets is by sea. However, broccoli is also highly perishable and export by sea freight often requires storage periods of between 25 and 40 days. Such extended storage periods can only be achieved if great care is taken during postharvest handling. Excellent initial quality, rapid pre-cooling and optimum storage conditions are crucial (Ryall and Lipton, 1979). Consequently, there is considerable interest in finding new methods of reducing the rate of deterioration of broccoli heads following harvest.

Harvested broccoli comprises a mass of green floral buds (florets), and thick fleshy flower branchlets or stalks attached to the central plant axis, collectively termed the head (Figure 1.1). Harvesting causes a series of stresses to broccoli, including wounding and separation from water, nutrient and hormone supply. As an immature tissue, harvested broccoli is unable to maintain metabolic homeostasis and deterioration can occur rapidly (Tian et al., 1997).

Symptoms of deterioration include chlorophyll loss from sepals (de-greening or yellowing of the head), opening of florets, offensive odour, and fungal decay (Irving and Joyce, 1995). The most obvious change during postharvest senescence of broccoli

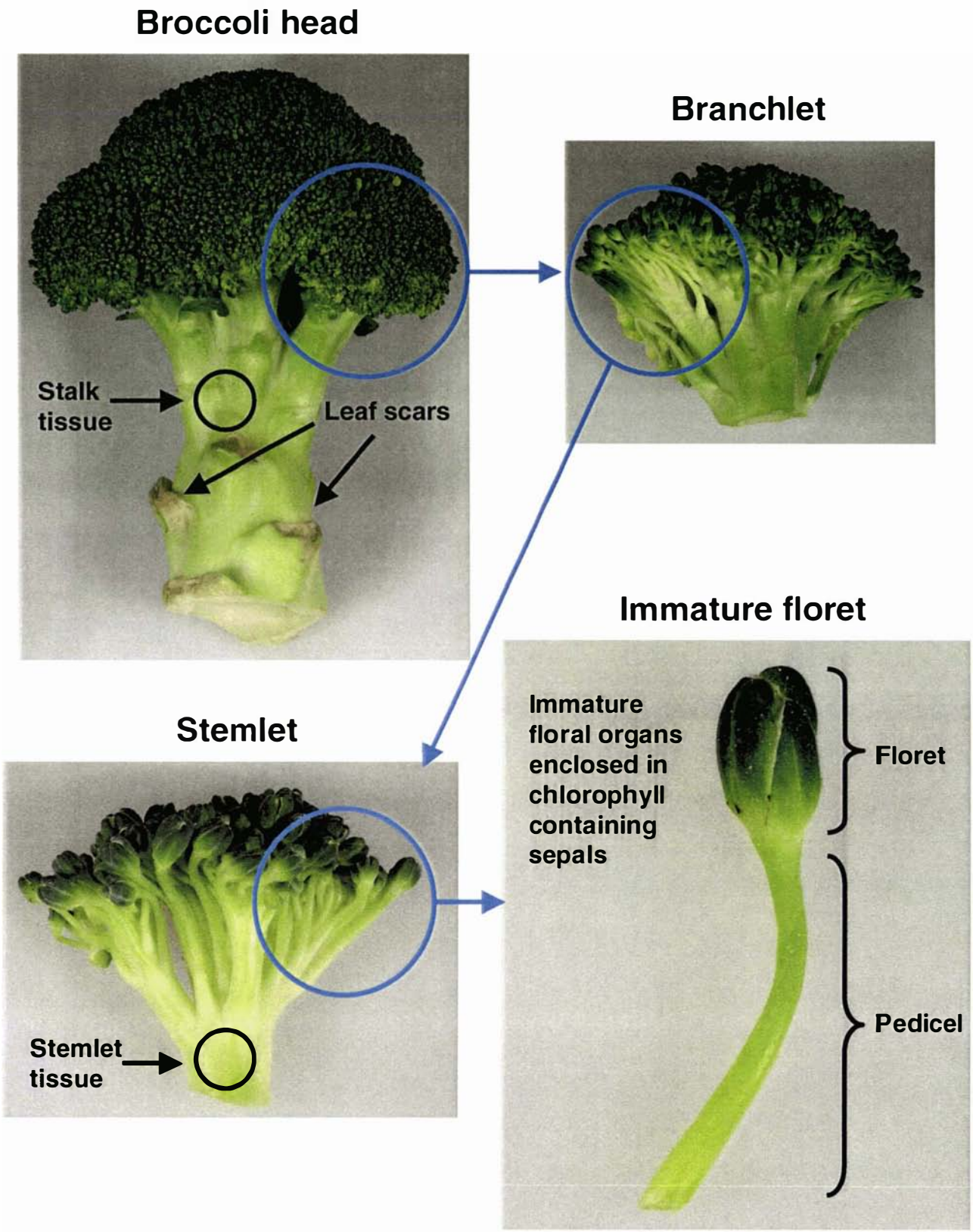

Figure 1.1 Pictures of broccoli tissues. Photographs show the different tissue types found within the harvested broccoli head.

is the yellowing of sepals. Exogenous ethylene accelerates loss of chlorophyll from sepals (Tian et al., 1994), and exogenous cytokinin or ethylene antagonists have been shown to decrease the rate of chlorophyll loss from sepals (Dedolph et al., 1962; Dostal et al., 1965; Gilbart and Dedolph, 1965; Wang, 1977; Shewfelt et al., 1983; Rushing, 1990; Clarke et al., 1994) and prevent offensive odour development, thus extending the storage life of broccoli after harvest.

In order to delay postharvest senescence, Henzi et al., (1999a) expressed an antisense ACC oxidase gene from tomato in broccoli. Although these transgenic plants showed reduced ethylene production in mature flowers, the authors reported that postharvest senescence was not arrested or effectively delayed. Since exogenous cytokinin has been shown to delay postharvest senescence in broccoli, even in the presence of added ACC (Clarke et al., 1994), the aim of this study was to determine the effects of altered ethylene and cytokinin biosynthesis during the harvest-induced senescence of broccoli.

1.2 BROCCOLI

Broccoli is harvested when the flowering heads are immature and growing rapidly (Pogson et al., 1995a). The head of broccoli is comprised of numerous immature florets arranged in whorls upon a fleshy stem (Figure 1.1). Each broccoli floret is made up of male and female reproductive organs surrounded by immature petals, and enclosed in chlorophyll-containing sepals. At harvest the florets are still closed and have not yet been pollinated.

The first visual sign of broccoli senescence is chlorophyll loss or sepal yellowing (Wang, 1977). Sepal yellowing commences between 24 h and 48 h after harvest and is essentially completed by 96 h at 20°C (Tian et al., 1994). Other symptoms of postharvest deterioration include opening of florets, offensive odour and fungal decay (Irving and Joyce, 1995). Early physiological changes which take place within the first 24 h of harvest include loss of soluble sugars, starch, proteins, phospholipids, organic acids, reduced respiration and accumulation of ammonia (King and Morris, 1994; Clarke et al., 1994). Changes in gene expression take place, which correlate with the

biochemical changes observed, such as the accumulation of asparagine synthetase, acid invertase and cysteine protease transcripts (Downs and Somerfield, 1997; Coupe et al., 2003a; Coupe et al., 2003b). Further, Page et al. (2001) showed that the expression of a number of senescence-related genes were induced during postharvest senescence in broccoli, often before any signs of deterioration occurred.

Recommended storage conditions vary in the literature, but 0°C is a common temperature used as broccoli does not suffer chilling injury, and deterioration increases rapidly at higher temperatures (Wang and Hrushka, 1977). Storage life ranges from three to four weeks in air at 0°C (Makhlouf et al., 1989), versus two to three days in air at 20°C (Wang, 1977). A relative humidity (RH) of 95% has been recommended for broccoli storage. Lower RH resulted in dehydration whilst higher RH resulted in development of soft rots (Henzi, 1999). Hot water treatment of broccoli following harvest caused reduced chlorophyll loss (Tian et al., 1996), reduced ethylene production and delayed sucrose loss (Tian et al., 1997). However, Forney and Jordan (1998) reported that hot water dips could lead to induction of volatile compounds. Postharvest storage can also be extended using a controlled atmosphere of 1% O_2 and/or 10% CO_2 (Lipton and Harris, 1974), 0.5% O_2 and 10% CO_2 at 0°C, or 1% O_2 and 10% CO_2 at 10°C (Izumi et al., 1996). However, since these postharvest treatments are often not sufficient, delaying senescence through the use of recombinant DNA technology is being investigated.

1.3 SENESCENCE

Leaf senescence is known to be a pre-programmed sequence of highly regulated biochemical and physiological events comprising the final stages of development, from the mature fully expanded state until organ death. The changes, which take place during senescence, are tightly regulated by specific gene expression events, coordinated at the cellular and tissue level (Smart, 1994). Cells remain viable and show tight metabolic regulation until the end of senescence (Thomas and Stoddart, 1980; Stoddart and Thomas, 1982; Matile, 1992).

At maturity, when the tissue is at full assimilatory capacity, mesophyll tissue begins to lose its green colour and turns yellow or red. The colour change is due to both the degradation of chlorophylls compared with carotenoids, and the unmasking or synthesis of new compounds such as anthocyanins and phenolics (Matile, 1992). During senescence the photosynthetic apparatus is dismantled and nutrients are exported to young growing tissues and storage organs. Abscission marks the end of leaf senescence in many species and requires very precisely localised and timed senescence in the petiole (Smart 1994).

More recently, molecular approaches have been used to understand the regulation and progression of leaf senescence. It is clear that leaf senescence is regulated as a controlled developmental process and that changes in gene expression occur. Specific sets of genes, designated senescence-down-regulated genes (SDGs), are down-regulated during senescence and include genes that encode proteins involved with photosynthesis (Hinderhofer and Zentgraf, 2001). Approximately 100 genes whose transcript abundance is increased during leaf senescence have been isolated from a variety of plant species such as *Arabidopsis*, rapeseed, tomato, maize, rice tobacco, potato and bean (Smart et al. 1994; Buchanan-Wollaston, 1994; Buchanan-Wollaston, 1997; Buchanan-Wollaston and Ainsworth, 1997; Nam 1997; Weaver et al. 1997; Quirino et al., 2000).

Many of these genes are generally referred to as senescence associated genes (SAGs) or leaf senescence clones (LSCs). General terms are often used to describe the clones, as definite functionality has not always been assigned to the induced gene. However, the putative roles assigned to many of these uncharacterised genes are of the type that would be expected during this developmental phase. Many of the SAG or LSC genes encode degradative enzymes such as proteases and nucleases, as well as enzymes involved in chloroplast dismantling and chlorophyll breakdown (Chandlee, 2001). Selected SAGS and SDGs were used as senescence markers in this work. SAGs included *BoCP5*, a broccoli cysteine protease clone (homologue to *SAG2* from *Arabidopsis thaliana*) and *BoMLP*, a broccoli cDNA encoding a metallothionein-like protein. The SDG used was *BoCAB1*, a broccoli cDNA encoding a chlorophyll a/b

binding protein. GenBank accession numbers to these and other clones used in this thesis are listed in Table 2.3 in Methods and Materials.

Approaches used to isolate senescence-associated genes have included differential cDNA screening, differential display and cDNA subtraction methods. However, only a limited number of senescence-associated genes have been isolated in this way, most of which possess moderate basal levels of expression prior to leaf senescence (He et al., 2001).

He et al. (2001) developed *Arabidopsis* senescence enhancer trap lines (SELs) harbouring a GUS reporter gene linked to a minimal promoter. Of 1300 lines screened, 147 lines were identified that expressed the GUS reporter gene in senescent leaves only (and not non-senescing leaves). This method provided large scale screening of mutants based on expression data and needless cloning of unidentified, non-target genes was avoided. Further, analysis of the effects of six senescence-promoting factors (ethylene, jasmonic acid, abscisic acid, brassinosteroids, dehydration and darkness) enabled the establishment of a regulatory network model for leaf senescence in *Arabidopsis*.

Leaf senescence is controlled by a number of endogenous and external factors through a regulatory network. Environmental cues include drought stress, extreme temperature, nutrient deficiency, and pathogen infection. Internal factors include reproduction and plant growth regulators such as abscisic acid, ethylene, jasmonic acid and salicylic acid (Smart, 1994; Morris et al., 2000). There is an overlap of gene expression events between senescence and stress-, pathogen- and hormone-response (Park et al., 1998; Weaver et al., 1998; Quirino et al., 1999). Recently, Hinderhofer and Zentgraf (2001), using suppression subtractive hybridisation, isolated a SAG clone, WRKY53, which is part of a super family of transcription factors that are thought to participate in the control of a wide variety of biological processes including pathogen defense and trichome development (Eulgem et al., 2000). WRKY53 is expressed very early during leaf senescence in *Arabidopsis*, and may play a key regulatory role in senescence. However the molecular mechanisms underlying leaf senescence remain poorly understood (He et al., 2001).

At the level of the whole plant, a number of different types of senescence have been characterised. Monocarpic senescence occurs as a consequence of reproduction, sequential senescence results from the competition for resources between lower leaves and younger leaves present on the same stem of a plant, and autumnal senescence is a consequence of daylength and temperature (Smart, 1994). External factors can also cause senescence, such as pathogen attack, desiccation, temperature, minerals and wounding.

Crops such as broccoli and asparagus are harvested when the inflorescences are immature and still rapidly growing so, once removed from source of water, nutrient and hormone, these tissues senesce rapidly. Investigation of the range of external and internal factors that cause senescence suggests that after the process has been triggered, the consequences are not identical. It appears that certain symptoms can become disconnected from the rest (Smart, 1994). Becker and Apel (1993) showed that genes induced during senescence of detached organs were not necessarily induced during natural senescence, demonstrating that the two processes were not identical. Further, the same gene may be induced by different environmental stimuli. For example, the expression of LSC54, which encodes a metallothionein-like protein, was up-regulated in both *Brassica napus* and *Arabidopsis* during senescence. However, the LSC54 promotor::GUS construct was also up-regulated during fungal infection in transgenic *Arabidopsis.* As pathogen infection resulted in the induction of a hypersensitive response and localised cell death, the authors suggested that there were similarities between the inductive signalling pathways of cell death in the hypersensitive response and natural leaf senescence. However, Pontier et al. (1999) observed clear differences in the expression profiles of markers of the hypersensitive response and natural senescence. Furthermore, Oh et al. (1996) showed that the expression of the *Arabidopsis* SAGs, *sen1*, *sen2*, *sen3*, *sen4* and *sen5,* was up-regulated during dark-induced senescence by a range of hormone treatments (ethylene, ABA and methyl jasmonate). However, expression levels varied depending on the senescence-inducing treatment used.

Weaver et al. (1998) carried out a comprehensive study using detached and attached leaves of *Arabidopsis*. The expression profiles of the SAGs were monitored in response to senescence induced by age (natural senescence), dehydration, darkness, ABA and ethylene treatments. In most cases SAGs were up-regulated in a similar fashion in attached or detached leaves, although some variation was seen for dehydration and different hormone treatments in terms of individual SAG response. This variation of SAG response to each of the different senescence-inducing treatments suggests that different regulatory mechanisms act on the individual SAGs, although overlapping mechanisms also do exist.

In asparagus spears, which are essentially an immature inflorescence and which deteriorate rapidly following harvest, some of the same genes and proteins detected during the harvest-induced senescence in spears were also present during natural foliar senescence (King et al., 1995). Transcripts for three harvest-induced cDNA clones were found to accumulate during natural foliar senescence, suggesting that the regulatory mechanisms may be similar in both situations. Two of the transcripts showed homology with ß-galactosidase and asparagine synthetase. Both of these enzymes are known to be involved with the remobilisation of carbon and nitrogen respectively. King et al. (1995) considered that the deterioration in the spear was due to a programmed senescence process, which was harvest-induced.

Downs and Somerfield (1997) reported that an asparagine synthetase transcript also increased in quantity during postharvest senescence in broccoli. When harvest-induced senescence of broccoli was compared with natural foliar senescence, changes not only in gene expression, but also phenotypical and compositional changes such as chlorophyll loss (degreening), losses in membrane lipids and proteins were similar (Page et al., 2001). Further, Page et al. (2001) showed that many senescence-induced genes were up-regulated before any visual signs of deterioration were observed in the harvested heads. These observations suggest that deterioration of broccoli could be considered to also be due to a programmed senescence process induced by harvest.

1.3.1 Regulation of senescence

During the process of senescence, chlorophyll and photosynthetic proteins are degraded (Humbeck et al., 1996) and carbon and nitrogen is remobilised from senescing tissues such that the original sink tissues become source tissues. There are several factors that can be manipulated to either accelerate or delay and thus regulate this process.

1.3.1.1 Ethylene and senescence Ethylene is considered to play a prominent role in the regulation of senescence, acting like a catalyst during senescence. Ethylene has been observed to accelerate many of the physiological changes normally associated with senescence. For example, McGlasson et al. (1975) observed in tomato leaf discs, that ethylene production and respiration decreased and then increased as in the climacteric in flowers and fruit. In another study, Aharoni et al. (1979) revealed that the increase of both ethylene production and respiration coincided with rapid chlorophyll degradation in dark-induced senescence of bean, tobacco, and sugar beet leaf discs. Treatment with silver ions, which inhibit ethylene action by interfering with the binding sites of ethylene (Sisler et al., 1986), delayed chlorophyll loss (Arahoni et al., 1979). Other antagonists of ethylene also cause delayed senescence.

More direct evidence for the role of ethylene during leaf senescence has been obtained through work with transgenic and mutant plants. Picton et al., (1993) used an antisense gene to produce tomato plants in which ACC oxidase (the ethylene-forming enzyme) was inhibited. These plants showed a delay of leaf yellowing of around one week. Further, Bleeker et al. (1988) studied an ethylene-insensitive mutant of *Arabidopsis* and reported that rosette leaf senescence was delayed in the mutant compared with the wild-type plants. Furthermore, Grbić and Bleeker (1993) reported that the expression of photosynthesis-associated genes was higher in the mutant than the wild-type, and that the expression of senescence-associated genes was delayed in ethylene-insensitive mutants.

King and Morris (1994) studied the physiological changes occurring within the first few hours of harvest of broccoli. During early postharvest senescence and through the preharvest-postharvest continuum, carbon dioxide produced from heads of container

grown broccoli and from heads, branchlets and florets of field-grown broccoli decreased markedly during the first 12 h of postharvest storage before stabilising. The respiratory quotient shifted toward a more oxidative metabolism in parallel with the respiratory decline. Ethylene production during storage showed no relationship to yellowing. However, time until the onset of yellowing was related to the basal levels of ethylene production. In contrast, detailed physiological studies of individual broccoli florets held at 20°C in darkness after harvest showed that ethylene production increased markedly as sepals yellowed (King and Morris, 1994).

Tian et al. (1994) observed that respiration rate and ethylene production were similar from branchlets or entire heads, although the magnitude of ethylene and carbon dioxide production seemed to be diluted by the stem tissue. Tian et al. (1994) suggested that the reproductive structures (stamens and pistil) may have a role in determining the rate of sepal yellowing, as removing them from florets reduced the rate of sepal degreening. The pistil and stamens also had seven-fold higher levels of ACC oxidase activity and more than double the ethylene production of other floret tissues. Changes in ACC oxidase activity mirrored the levels of ACC in these tissues. Tian et al. (1994) confirmed the climacteric status of harvested broccoli by exposure of heads to 0.5% propylene. Propylene stimulated respiration and ethylene production and accelerated sepal degreening (measured as chlorophyll and Hue angle decline). Pogson et al. (1995a) observed high expression of ACC oxidase 2 (*BoACO2*) transcript only in pistil and stamen tissue following harvest. They proposed that ethylene produced, as a result of the rapid and large increase in *BoACO2* transcript within the reproductive structures after harvest, was one of the main signals influencing sepal yellowing in broccoli.

1.3.1.2 Cytokinins and senescence The cytokinins appear to be the major group of senescence-retarding hormones in plants. There is a great deal of indirect evidence, which suggests cytokinins play an important role in senescence (van Staden et al., 1988; Noodén et al., 1990). Indeed, for example, external application of cytokinin to detached cuttings, single leaf or localised area results in the retention of green colour (Richmond and Lang, 1957). The effect of exogenous application of cytokinin to attached leaves,

still connected to the root system is less pronounced but the delay or retardation of senescence may still be observed (Fletcher, 1969; Adedipe and Fletcher, 1971). Cytokinins delay senescence in many species and may cause regreening of yellow leaves in some species (Dyer and Osbourne, 1971; Venkatarayappa et al., 1984). Young tobacco leaves can synthesise their own cytokinins, while mature and senescing leaves appear to have lost this capability (Singh et al., 1992). This difference has been proposed as a factor in controlling sequential senescence in tobacco.

Many studies have reported that leaf senescence is usually correlated with a decrease in active cytokinin in the leaves (and frequently high levels of *O*-glucosides), and roots have been implicated as the major source of cytokinins for mature leaves (Noodén et al., 1990 and papers therein). Root-produced cytokinins are carried through the xylem into the leaves with the transpiration stream. It has been suggested that cytokinins act by preventing oxidising reactions, which produce free radicals (Grossman and Lesham 1978). Lipoxygenase-mediated lipid oxidation produces free radicals, which are hyperactive and can cause damage to biological materials within plants, which is an essential facet of senescence. Further, Grossman and Lesham (1978) showed that exogenous cytokinin application to pea plants lowered lipoxygenase activity considerably. They suggested that lipoxygenase repression, induced by cytokinin, is a contributing factor to the overall anti-senescence action of the hormone.

Clarke et al. (1994) showed that chlorophyll a was the major (80%) contributor to total chlorophyll content in green sepals of broccoli and that degradation of chlorophyll a during postharvest senescence was the major contributor to colour change in yellowing broccoli, and that exogenous application of cytokinin was sufficient to delay chlorophyll loss and delay ammonia accumulation. Treatment of harvested broccoli with silver ions (which desensitises tissue to ethylene action) also delayed senescence, but less so than the cytokinin treatment. Clarke et al. (1994) proposed that cytokinin may delay senescence by stimulating chlorophyll production at the site of application, inhibiting the degradative processes that occurred following harvest or, indirectly, by desensitising the tissue to ethylene. They suggested that it was unlikely that treatment of

cytokinin inhibited ethylene biosynthesis, since applied cytokinins had been observed to stimulate ethylene synthesis (Rushing, 1990).

Recently developed molecular biology techniques have enabled the possibility of genetically modifying cytokinin biosynthesis and metabolism to influence plant development. Genes controlling cytokinin biosynthesis have been isolated from *Agrobacterium tumefaciens* (e.g. McKenzie et al., 1994), the bacterium responsible for crown gall disease. The genes responsible for the regulation of cytokinin biosynthesis in plants remained, until recently, elusive. The bacterial cytokinin synthase gene (*ipt*) codes for the enzyme isopentenyl transferase and has been used to elevate cytokinin levels in a number of transformed plants including tobacco, *Arabidopsis*, *Petunia* and *Kalanchoë* (Medford et al., 1989; Smart et al., 1991; McKenzie et al., 1994). Increased cytokinin production in these plants caused a variety of growth responses including delayed senescence. Undesirable responses included inhibition of root growth and increased bushiness, a result of constitutive over-production of cytokinins.

To alleviate the problem of constitutive over-production of cytokinins, inducible, developmental, or tissue specific gene promoters have been fused to the *ipt* gene (Gan and Amasino, 1995; McKenzie et al., 1998). Chen et al. (2001) successfully transformed broccoli using the SAG_{12}-IPT construct as used by Gan and Amasino (1995). These authors observed a delay in both natural leaf senescence, and harvest-induced senescence of heads.

1.3.1.3 Sugars and senescence There are few reports linking sugars to the regulation of senescence. However, evidence is growing supporting the idea that simple sugars such as sucrose and hexose are involved with regulating the process. Simple sugars have been implicated as molecules involved in transduction of many signals within the plant (for review see Smeekens, 2000). Further, Wingler et al. (1998) showed that added sugar accelerated senescence even in the presence of senescence retardant cytokinin. However, this group measured the extent of senescence by the level of activity of an NADH-dependent hydroxypyruvate reductase enzyme involved with photosynthesis. As the product of photosynthesis is sucrose, it is possible that this enzyme was under

negative feedback regulation by sugars. Consequently, in the presence of excess sugar, the expression and activity of the enzyme was reduced, regardless of the senescence status of the leaf. In retrospect, a better marker of senescence could have been chosen by Wingler et al. (1998).

Coupe et al. (2003a) proposed that sugars are involved in regulating senescence by showing that some of the gene expression changes that take place during harvest-induced senescence in both broccoli and asparagus, could be modified by exogenous supply of sucrose. The expression of asparagine synthetase, an enzyme involved with nitrogen mobilisation in asparagus, was up-regulated during senescence and was negatively regulated by sucrose (Davies et al., 1996). Further, cysteine protease transcript levels that normally increase during senescence in broccoli, were reduced upon feeding with additional sucrose (Coupe et al., 2003b). Another treatment that delayed senescence, controlled atmosphere, in addition to reducing senescence-associated transcript levels, caused a reduction in the expression of genes encoding enzymes responsible for the transport of sucrose, (Coupe et al., unpublished), and the metabolism of sucrose, invertase (Coupe et al., 2003a) and hexokinase (Ryan et al., 2002). Further, over-expression of an *Arabidopsis* hexokinase in tomato induced senescence (Dai et al., 1999). Consequently, the interaction between cytokinin, ACC, sucrose and transcripts encoding enzymes involved in carbohydrate transport and metabolism were investigated.

1.4 ETHYLENE

1.4.1 Ethylene and plant development

Ethylene is a gaseous hormone that has been used to manipulate plant development for hundreds or even thousands of years. Fruits were ripened by the burning of incense by the Chinese (Yang and Dong, 1993). Further, Philippino and Puerto Rican mango and pineapple growers used bonfires around their crops to initiate and synchronise flowering (Salisbury and Ross, 1985). The first statement that fruits release a gaseous compound that stimulated ripening was in 1910 by H. H. Cousins reporting to the Jamaican Agricultural Department, who suggested oranges should not be shipped with bananas,

as the bananas were ripening prematurely due to the release of gaseous substances from the oranges. However, it is likely that any ethylene released was produced by fungi associated with the oranges, as healthy oranges produce virtually no ethylene. It was not until 1934 that R. Gane showed that ethylene was synthesised by plants and was responsible for faster ripening (Salisbury and Ross, 1985).

However, it was Neljubow (1901) who first established that ethylene (a compound present in illuminating gas) affected plant growth. He reported that treatment of etiolated pea seedlings with illuminating gas caused thickening of the stem, inhibition of root and hypocotyl elongation (more pronounced curvature of the apical hook) and horizontal growth. These three findings collectively make up what is now referred to as the triple response.

Ethylene is involved with a wide range of different growth and developmental processes in plants including seed germination, emergence of seedlings through the soil (probable physiological significance of the triple response), root production and growth, shoot elongation, flower initiation, fruit ripening, nodulation of legumes, response to pathogens, abscission and senescence (see Section 1.3.1.1).

1.4.2 Mode of action of ethylene

How does a single compound influence or regulate so many growth and developmental processes? Current evidence suggests that ethylene perception and signal transduction rather than metabolism are the mediators of ethylene action, as the products of ethylene metabolism do not elicit ethylene responses and ethylene effects can be mimicked by other hydrocarbons (McKeon et al., 1995). The receptor for ethylene and some of the ethylene transduction components have now been identified in *Arabidopsis* by Chang and Meyerowitz, 1995; Chang, 1995) and the generally accepted current model is shown in Figure 1.2.

The ethylene receptor was first found by screening mutant *Arabidopsis* seedlings for the lack of the triple response after treatment with ethylene (Bleecker, 1988). The mutant, *etr1*, was shown to lack a number of ethylene responses that were present in the wild-

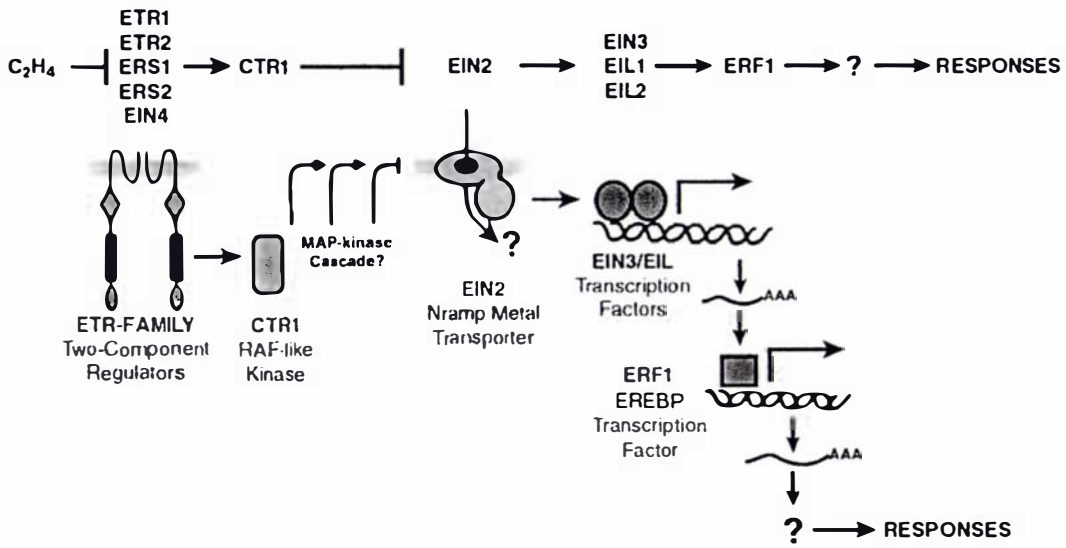

Figure 1.2 The genetic interactions and biochemical identities of components of the ethylene signal transduction pathway. The ordering of components into a hypothetical linear pathway is based on both genetic (epistasis) analysis, ectopic gene expression studies, and biochemical interactions. Progressing from left to right, ethylene is thought to regulate negatively a family of membrane-associated receptors that are related to the bacterial two-component superfamily of catalytic receptors. The histidine-kinase transmitter domains of members of the receptor family interact with the regulatory domain of the Raf-like kinase CTR1. This receptor/CTR1 complex negatively regulates a membrane protein (EIN2) related to a superfamily of metal transporters. The cytoplasmic C-terminal domain of EIN2 positively signals downstream to the EIN3 family of transcription factors located in the nucleus. A target of the EIN3 transcription factors is the promoter of the ERF1 gene, a member of a second family of transcription factors. ERF1 is rapidly induced in response to ethylene and is capable of activating a subset of ethylene responses when ectopically expressed. This figure was reproduced from Hende and Bleecker (2000) with permission.

type, and also had reduced ethylene binding capacity. The gene encoding ETR1 was subsequently cloned (Chang et al., 1993), and showed sequence homology to a superfamily of catalytic receptors in bacteria known as two-component regulators (Wurgler-Murphy and Saito, 1997).

Two-component regulators are typically composed of a sensor protein with an input domain that receives signals and a catalytic transmitter domain that autophosphorylates on an internal histidine residue. The second component is a response regulator protein, which is composed of a receiver domain that receives phosphate from the transmitter on an aspartate residue and an output domain that mediates responses depending on the phosphorylation state of the receiver. The transmitter domain of ETR1 has all the conserved residues essential for histidine kinase activity and is capable of autophosphorylating on the conserved histidine when expressed in yeast (Gamble et al., 1998).

The sensor component of these two-component regulators contains an input domain that interacts directly with a signalling ligand. The N-terminal hydrophobic domain of ETR1 showed no homology to any other functional domain in protein databases. The importance of this novel domain for ethylene signalling was suggested because all point mutations that caused insensitivity to ethylene *in planta* were located to this domain (Chang et al., 1993). Schaller and Bleecker (1995) demonstrated high affinity binding of ethylene to ETR1 when expressed in yeast. Further, Rodriguez et al. (1999) showed that the 128 residues of the hydrophobic domain of ETR1 were necessary and sufficient for ethylene binding activity. Both the ability to bind ethylene, and the homology to the bacterial two-component regulators suggests that the ETR1 protein is in fact an ethylene receptor.

Four other genes have been isolated from *Arabidopsis* that are related to ETR1 (Hua et al., 1995; Hua et al., 1998; Sakai et al., 1998). They are split into two groups based on structural similarities. The ETR1-like family includes *ETR1* and *ERS1* and is characterised by similar hydrophobic N-terminal domains and a conserved histidine kinase domain. The ETR2-like subfamily, which includes *ETR2*, *ERS2* and *EIN4*, has

an additional hydrophobic structure compared to the ETR1-like subfamily, and lacks some of the elements considered necessary for catalytic activity in the histidine kinase domain (Bleecker and Kende, 2000).

The next enzyme thought to be involved in ethylene signalling is CTR1. *CTR1* was cloned by Keiber et al. (1993) and sequence analysis showed that the gene encodes a protein related to mammalian Raf kinases that initiate mitogen-activated protein kinase (MAPK) cascades. The homology of CTR1 with MAPKKKs suggests that ethylene signalling may operate through a MAP-kinase cascade. Although genes homologous to MAPKKs and MAPKs exist in *Arabidopsis*, none are known to be associated with ethylene signalling. Further, biochemical and yeast two-hybrid experiments indicate that CTR1 interacts directly with the transmitter domains of ethylene receptors (Clarke et al., 1998). However, ethylene treatment caused enhanced MAPK-like activity and phosphorylated MAPK-like protein accumulation in *Arabidopsis* (Novikova et al., 2000).

Loss of function mutations in CTR1 and/or multiple receptor genes leads to constitutive activation of the ethylene-response pathway, suggesting that the receptors form a complex with CTR1, which negatively regulates responses in the absence of ethylene. Ethylene binding to receptors would then reduce the activity of the ETR/CTR1 complex and result in a derepression of the pathway (Bleecker and Kende, 2000). Ethylene signalling downstream of CTR1 is not very well understood. The protein encoded by EIN2 is related to the eukaryotic Nramp family of metal-ion transporters (Alonso et al., 1999) and is required for ethylene signalling, acting somewhere between CTR1 and the EIN3 family of transcriptional regulators (Chao et al., 1997). A loss of function mutation in EIN3 caused a reduced responsiveness to ethylene, and EIN3 was shown to encode a nuclear protein (Chao et al., 1997). Over-expression of EIN3 and related genes, EIL1 and EIL2, caused constitutive activation of response pathways (Figure 1.2).

Sensing of ethylene causes up-regulation of a number of transcripts that are responsible for eliciting the ethylene response, such as chitinases (Ishage et al., 1991), cellulase (Ferrarese et al., 1995) and cysteine protease (Jones et al., 1995). Promoter elements for

all these ethylene-induced genes contain a conserved 11 base pair sequence TAAGAGCCGGCC, known as the GCC box. These ethylene response elements (EREs) are crucial for ethylene signalling, as deletion of these elements causes loss of ethylene response (Shinshi et al., 1995), and addition of these elements to a minimal cauliflower mosaic virus (CaMV) 35S promoter conferred ethylene responsiveness (Ohme-Takagi and Shinshi, 1995). The ethylene response factor (ERF1) gene was identified by Solano et al. (1998) and was found to have a target promoter for the EIN3 family of proteins (Figure 1.2). ERF1 is a member of a group of plant-specific transcription factors referred to as ethylene-response-element-binding-proteins (EREBPs). EREBPs were originally identified as trans-acting DNA binding proteins that bound to specific elements in ethylene-inducible genes (Ohme-Takagi and Shinshi, 1995). *ERF1* expression was rapidly induced by treatment with ethylene in *Arabidopsis* (Solano et al., 1998) and heterodimers of EIN3 were shown to interact *in vitro* with a promoter element of ERF1. Further, when *ERF1* is constitutively expressed in an EIN3 mutant background, ethylene reponsiveness is restored. These results suggest that ERF1 is in the primary transduction chain downstream of the previously identified components and clearly indicate that a transcriptional cascade is operating in ethylene signalling (Bleeker and Kende, 2000).

Not only the ability to sense ethylene, but also changes in sensitivity to ethylene appear to be important. For example, a particular developmental state is required for response to ethylene for both ripening tomato fruits (Grierson and Kaber, 1986) as well as senescing leaves (Bleecker and Patterson, 1997).

The concentration of ethylene also plays an important role. Transgenic tomato fruit with lowered levels of ethylene production ripen more slowly (Klee, 1993) and in some cases fail to ripen altogether (Oeller et al., 1991). Furthermore, transgenic tomato plants unable to produce high levels of ethylene in response to flooding stress, when compared with wild-type plants, displayed reduced epinastic curvature of the petioles (English et al., 1995). These findings suggest that ethylene production is also an important aspect of how this hormone regulates a diverse array of responses in plants. This, together with the fact that the two dedicated ethylene biosynthetic enzymes, ACC synthase and ACC

oxidase, are encoded by multi gene families in plants that are differentially expressed, may provide another tier of regulation for this hormone.

1.4.3 Ethylene biosynthesis

Ethylene production is regulated in both a developmental manner and by external factors, both biotic and abiotic. Generally speaking, ethylene production is high in young fruit, vegetative and floral tissues during the periods of cell division, but declines during cell expansion before it increases once again during the later stages of tissue development, ripening and senescence (Abeles et al., 1992).

This pattern was reported recently in *Trifolium repens* (white clover) by Hunter et al. (1999). Ethylene was produced at significantly higher levels in the apex and immature leaves of the stolon, compared with more mature leaves. However, there was a rapid increase in ethylene biosynthesis during the final stages of leaf development, senescence.

Abiotic stresses include mechanical wounding, bending, rubbing, radiation, elevated temperatures, chilling, dehydration, and various chemical stimulants such as heavy metal ions, herbicides, defoliants and gases such as sulphur oxide and ozone (Abeles et al., 1992). Biotic stresses include infection of tissues by viruses, bacteria, fungi, insects and nematodes. All these stresses, both abiotic and biotic, can lead to elevated ethylene production, a phenomenon referred to as 'stress ethylene' (Abeles et al., 1973).

The biosynthetic pathway of ethylene has been well characterised in higher plants (Adams and Yang, 1979; Yang and Hoffman, 1984) (Figure 1.3), but little is known regarding ethylene synthesis in lower plants (Osbourne et al., 1996). In higher plants ethylene is predominately formed through the ACC-mediated pathway (Yang and Hoffman, 1984), and the two key enzymes of the pathway, ACC synthase and ACC oxidase have been identified (Yang and Hoffman, 1984; Kende, 1993). ACC synthase catalyses the conversion of *S*-adenosyl-L-methionine (SAM) to the cyclic amino acid 1-aminocyclopropane-1-carboxylic acid (ACC). A bi-product of the ACC synthase catalysed step is 5'-methylthioadenosine, which is utilised for the production of new

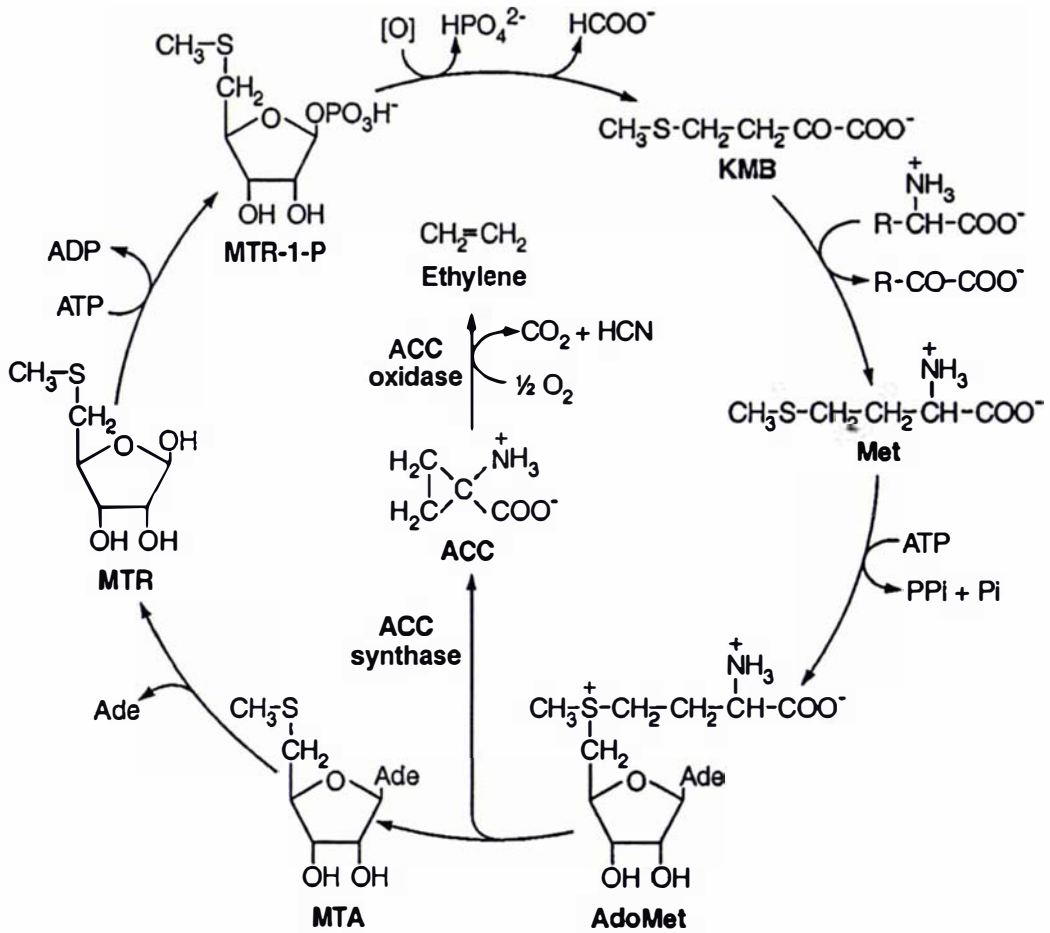

Figure 1.3 The ethylene biosynthetic pathway and the methionine cycle. ACC, 1-aminocyclopropane-1-carboxylic acid; Ade, adenine; AdoMet, *S*-adenosyl-L-methionine; KMB, 2-keto-4-methylthiobutyric acid; Met, L-methionine; MTA, 50-methylthioadenosine; MTR, 50-methylthioribose; MTR-1-P, 50-methylthioribose-1-phosphate. Modified from Miyazaki & Yang (1987). This figure was reproduced from Hende and Bleecker (2000) with permission.

ethylene via a modified methionine cycle. This salvage pathway preserves the methylthio group through every revolution at the expense of one ATP molecule (Figure 1.3). Thus high rates of ethylene biosynthesis can occur even when the free pool of methionine is low (Bleeker and Kende, 2000). ACC oxidase converts the ACC intermediate to ethylene by oxidation. In addition to this, the ACC intermediate can also be conjugated into a metabolically inert compound, *N*-malonyl-ACC, by ACC-*N*-malonyl transferase.

1.4.3.1 ACC synthase ACC synthase activity is stimulated by ethylene (Bufler, 1984), it the first committed step of the pathway and is generally regarded as the rate-limiting step of ethylene biosynthesis. cDNA clones encoding ACC synthase have now been isolated from tomato (van der Straten et al., 1990; Sato et al., 1991; Rottman et al., 1991; Yip et al., 1992), zucchini (Huang et al., 1991), apple (Dong et al., 1991), broccoli (Pogson et al., 1995b; Kato et al., 2002; Gonzalez and Botella, personal communication), white clover (Murray, 2002) and *Arabidopsis* (Liang et al., 1992; Van der Straeten et al., 1992; Liang et al., 1995). This enzyme is encoded by a divergent multigene family in all plant species analysed so far. The expression of ACC synthase genes has been best studied in tomato where there is a family of at least nine members (Van der Straeten et al., 1990; Rotmann et al., 1991; Olsen et al., 1991; Yip et al., 1992; Lincoln et al., 1992). The emerging picture is that ACC synthase genes are expressed differentially in response to several developmental, environmental and hormonal factors.

1.4.3.2 ACC oxidase The identification of the enzyme responsible for the conversion of ACC to ethylene proved difficult. Initial biochemical approaches used to isolate active enzyme failed due to the instability and low abundance of the enzyme. Molecular biology was utilised to isolate the first plant gene that encoded an ethylene-forming-enzyme. The ACC oxidase clone, *pTOM13*, was isolated from a ripe tomato fruit library (Slater et al., 1985). The cloning of *pTOM13* enabled closer biochemical analyses of the enzyme. The predicated amino acid sequence of pTOM13 was similar to the enzyme flavanone 3-hydroxylase. Complete recovery of enzyme activity was achieved *in vitro*

from melon fruit using factors (Fe^{2+} and ascorbate) that had been shown to be crucial to preserve activity of the hydroxylase (Ververidis and John, 1991).

Expression studies showed that levels of pTOM13 transcript correlated positively with ethylene evolution in wounded leaves and ripening fruit (Holdsworth et al., 1987). Tomato plants transformed with an antisense pTOM13 gene produced very low levels of ethylene and the ripening of the fruits was significantly delayed, further supporting the hypothesis that the pTOM13 protein was involved with ethylene biosynthesis (Hamilton et al., 1990). ACC oxidase genes have now been cloned from a variety of tissues from several plant species including orchid flowers (Nadeau et al., 1993), mung bean epicotyls (Kim and Yang, 1994), petunia floral tissues (Tang et al., 1994), broccoli floral tissues (Pogson et al., 1995a), melon leaf tissues (Lasserre et al., 1996), carnation floral tissues (ten Have and Woltering, 1997), sunflower seedling tissue (Liu et al., 1997), geranium floral tissue (Clark et al., 1997), and white clover leaf tissues (Hunter et al., 1999).

Pogson et al. (1995a) isolated two ACC oxidase clones from broccoli floret tissue, *BoACO1* and *BoACO2*, both having high sequence identity to pTOM13 (71% and 70% respectively). Pogson et al. (1995a) suggested that *BoACO1* contributed to basal levels of ethylene production. Since *BoACO2* increased rapidly within the reproductive structures in response to harvest and produced an ethylene signal, the authors suggested, that *BoACO2* regulated postharvest senescence. The isolation of this gene, therefore, provided access to a broccoli-specific ACC oxidase gene, which could be expressed in the antisense orientation, to reduce harvest-induced production of ethylene.

1.5 CYTOKININS

1.5.1 Cytokinins and plant development

Cytokinins are a class of plant hormones that play a central role in growth and development. Cytokinins were first discovered in the 1950s because of their ability to induce plant cell division (Miller et al., 1955). Soon after their discovery, Skoog and Miller (1957) hypothesized the cytokinin-auxin theory of plant morphogenesis:

cytokinin, together with auxin, plays an essential role in organogenesis, having a major influence on the development of roots and shoots and their growth. A number of reports have described cytokinins to have either a stimulatory or inhibiting role for different developmental processes such as root growth and branching, seed germination, de-etiolation, flower and fruit development, control of apical dominance, chloroplast development, leaf senescence and plant-pathogen interactions (for review see Mok, 1994). These processes are also influenced by other stimuli (for example light and other plant hormones), and the physiological and developmental outcomes reflect a highly integrated response to multiple stimuli (Haberer and Kieber, 2002).

The cytokinins are a group of plant hormones, which are involved with a number of plant growth and developmental processes (Mok, 1994). Some of these include *de novo* bud formation during tissue culture (Stabel et al., 1990; Zhang, 1998), germination and seed dormancy (Shultz and Small, 1991), release of apical dominance (Wickson and Thimann, 1958; Li and Bangerth, 1992), leaf expansion (Brock and Cleland, 1989), cell division (Miller et al., 1956; Lewis et al., 1996; Riou-Khamlichi et al., 1999) and delay of senescence (Clarke et al., 1994; Gan and Amasino, 1995). Reviews by Horgan (1984), Mok (1994) Mok and Mok (2001) and Schmülling (2001) cover these topics in more detail.

Conclusions about the biological function(s) of cytokinin have mainly been due to the exogenous application of compounds, and more recently endogenously enhanced levels by ectopic expression of bacterial cytokinin synthase genes. However, it is sometimes difficult to separate the effects of cytokinin from those of other plant hormones, as cytokinin can act either synergistically or antagonistically with auxin, and induce the production of ethylene, so the effect on whole plant morphology is not easily recognized as directly related to cytokinins. Further, isolation of cytokinin mutants has not been very successful, due to the fact that impairment of cytokinin biosynthesis or action is likely to be lethal. These constraints to some extent explain the slow progress in cytokinin research compared with other plant hormones. However, the recent identification of a cytokinin receptor, of the key biosynthesis gene, and of genes

involved with metabolism, now provide the molecular biology tools for in depth study into the role cytokinins play in growth and development in plants.

1.5.2 Structure

Naturally occurring cytokinins are N^6-substituted adenine derivatives, and modifications to this structure occur either on the purine ring itself (Figure 1.4), or on the side chain (isoprenoid or aromatic side-chains) (Figure 1.5). These changes from the basic adenine ring result in differing biological activity. For example, the *trans*-isomer of zeatin is highly active in bioassays but *cis*-zeatin is virtually inactive.

1.5.3 Biosynthesis

There are two groups of cytokinins extracted from plants: The 'free' cytokinins, extractable in aqueous alcoholic solutions, and the 'bound' cytokinins, extractable after alkaline hydrolysis and associated with the tRNA. The isoprenoid-type cytokinins are the most abundant, but several species also contain adenine derivatives with aromatic substituents. In addition, there is a group of synthetic diphenylurea-type (DPU) cytokinins that are structurally different to the adenine-type cytokinins, but which appear to bind to the cytokinin receptor (see later, Section 1.4.5).

Biosynthesis of the tRNA cytokinins occurs during post-transcriptional processing (Hall, 1973). Mevalonic acid pyrophosphate provides a five carbon branched chain which undergoes enzymatic modification leading to Δ^2-isopentenyl pyrophosphate. This is then condensed with the appropriate adenosine molecule in the tRNA (Chen and Hall, 1969) by Δ^2-iPP:tRNA-Δ^2-isopentenyltransferase (Bartz and Söll, 1972).

The 'free' cytokinins may derive from the hydrolysis of tRNA cytokinin to their nucleotide constituent. However, there is evidence to suggest additional sources of 'free' cytokinin. Structural differences exist between 'free' and 'bound' cytokinins and 'bound' cytokinin turnover appears not to be rapid enough to support the levels of 'free' cytokinin in the plant (Trewavas, 1970; Hall, 1973; Stuchbury et al., 1979). Further, the non-active *cis*-zeatin is the major cytokinin in tRNA, although this can be metabolised to the active *trans*-zeatin by *cis-trans*-isomerases (Bassil et al., 1993).

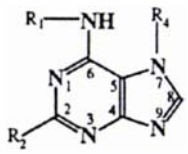

Adenine with substituent groups R_1, R_2, R_4

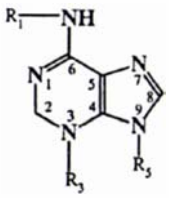

Adenine with substituent groups R_1, R_3, R_5

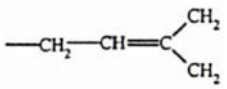

Unsaturated branched chain

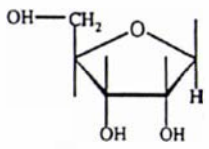

Ribosyl moiety

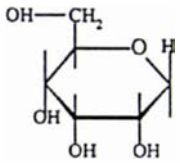

Glucosyl moiety

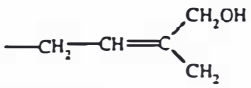

Unsaturated branched chain with hydroxyl group

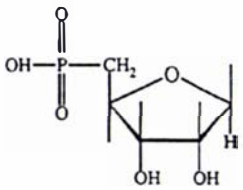

Nucleotide moiety

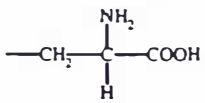

Alanine moiety

Form	Name		Substituents
Bases	isopentenyladenine	iP	R_1 unsaturated branched chain
	zeatin	Z	R_1 unsaturated branched chain + hydroxyl group
Ribosides	isopentenyladenosine	iPA	R_1 unsaturated branched chain R_5 ribosyl moiety
	zeatin riboside	ZR	R_1 unsaturated branched chain + hydroxyl group R_5 ribosyl moiety
Nucleotides	isopentenyl adenosine-5'-monophosphate	iPNT	R_1 unsaturated branched chain R_5 nucleotide moiety
	zeatin riboside-5'-monophosphate	ZNT	R_1 unsaturated branched chain + hydroxyl group R_5 nucleotide moiety
N-glucose conjugate	e.g. zeatin-7-glucoside	e.g. Z7G	R_1 unsaturated branched chain + hydroxyl group $R_{3,4 \text{ or } 5}$ glucosyl moiety
N-alanine conjugate	e.g. lupinic acid	e.g. Z9A	R_1 unsaturated branched chain + hydroxyl group R_5 alanine moiety

Figure 1.4 Cytokinin structure – modifications to the purine ring. This figure was reproduced from McKenzie (1996) with permission.

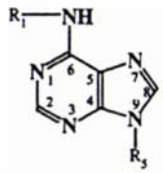

Adenine with substituent groups R_1 and R_5

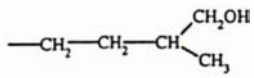

Saturated branched chain with hydroxyl group

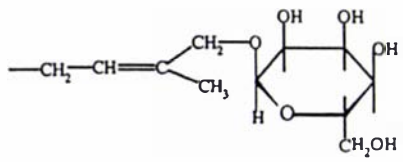

Unsaturated branched chain with glucosyl moiety

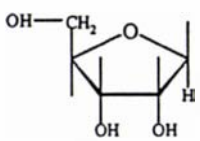

Ribosyl moiety

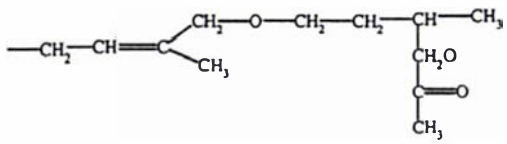

Unsturated branched chain with acetyl moiety

Form	Name		Substituents
Dihydroderivatives	dihydrozeatin	DZ	R_1 saturated branched chain + hydroxyl group
	dihydrozeatin riboside	DZR	R_1 saturated branched chain + hydroxyl group R_5 ribosyl moiety
O-glucosyl derivatives	e.g. zeatin-*O*-glucoside	e.g. ZOG	R_1 unsaturated branched chain + glucosyl moiety
O-acetyl derivatives	e.g. *O*-acetyl zeatin riboside	e.g. OAcZR	R_1 unsaturated branched chain + acetyl moiety R_5 ribosyl moiety

Figure 1.5 Cytokinin structure – modifications to the side chain. This figure was reproduced from McKenzie (1996) with permission.

Furthermore, the breakdown of tRNA occurs in all tissues, while cytokinin production has been proposed to be localised in root tips, shoot meristems and immature seeds and must be highly regulated (Mok and Mok, 2001).

Although the biosynthesis of tRNA-associated cytokinins is well understood, only recently has progress been made towards understanding the *de novo* biosynthesis of the 'free' cytokinins. Knowledge in this area has been restricted due to the very low levels of cytokinin found in plants, making biochemical studies very difficult. Also the lack of genetic mutants, which have been very useful in the study of many biosynthetic pathways including those of the other plant hormones gibberellin and abscisic acid, has limited progress in this area.

The generally accepted model of biosynthesis was based on the studies of microorganisms capable of *de novo* biosynthesis of cytokinins. The proposed pathway involved the addition of DMAPP to the N^6 position of adenosine-5-phosphate by an isopentenyl transferase to give the cytokinin nucleotide isopentenyl adenosine-5-monophosphate (iPNT), (Figure 1.6). Subsequent enzymatic modification of iPNT yielded the many other forms of cytokinin nucleotides, ribosides, free bases and glucosides.

The recent completion of the sequencing of the *Arabidopsis* genome enabled Takei et al. (2001) and Kakimoto (2001a) to independently identify a total of nine *ipt*-homologues, designated *AtIPT1* to *AtIPT9* by *in silico* analysis. Phylogenetic analyses suggested *AtIPT2* and *AtIPT9* encoded putative tRNA-*ipt*, while the other seven *AtIPTs* were more closely related to the bacterial *tmr* and *ipt* genes. Expression of these seven genes in *E. coli* resulted in the excretion of iP and zeatin, confirming that these *AtIPTs* encoded cytokinin biosynthetic enzymes (Takei et al., 2001). Further, Kakimoto (2001a) over-expressed *AtIPT4* constitutively *in planta* using the CaMV 35S promoter, and observed shoots regenerated independent of cytokinin in the culture media. Purified AtIPT4 utilised ADP and ATP preferentially over AMP as a substrate, unlike the bacterial IPT enzymes. The immediate products of the plant enzymes are probably

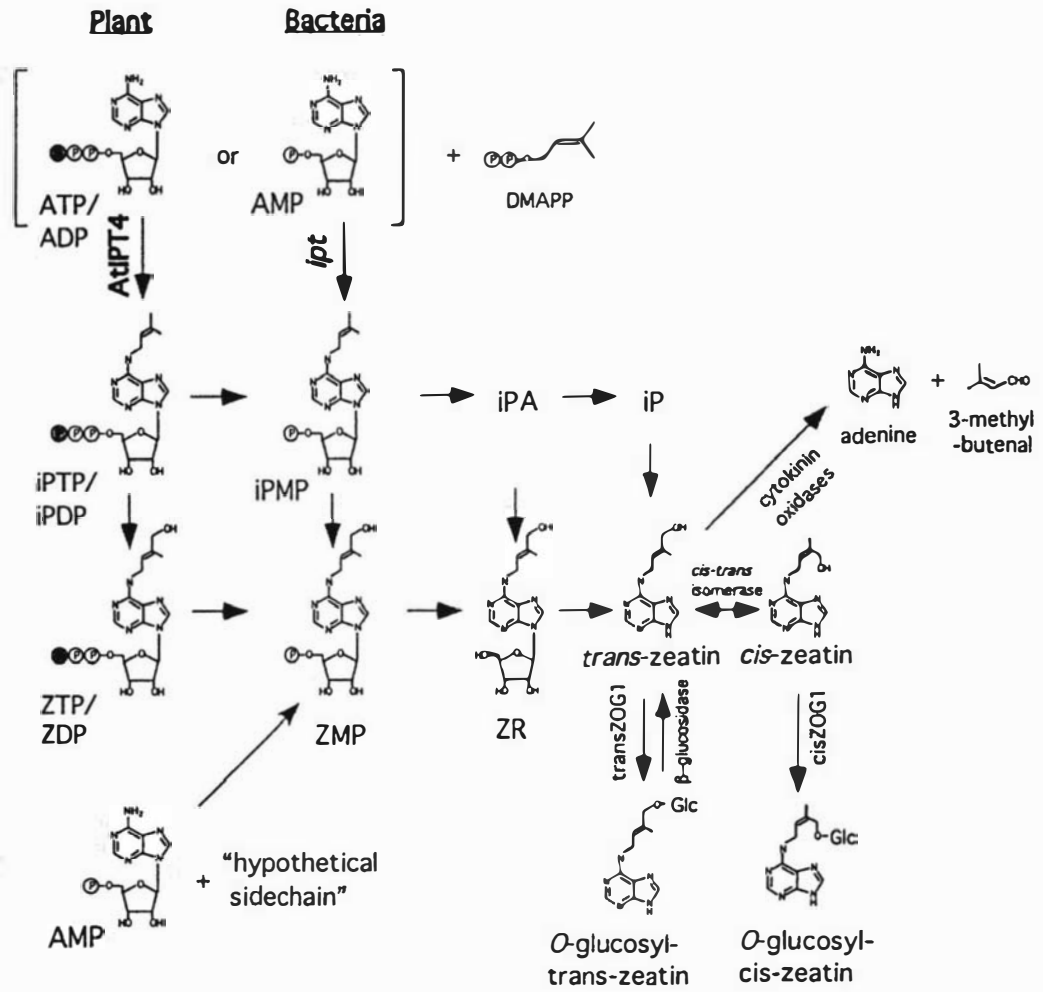

Figure 1.6 Proposed biosynthetic and metabolic pathway for cytokinins. Left, The proposed biosynthesis of zeatin tri-/diphosphate in *Arabidopsis*. Both ADP and ATP are likely substrates for the plant IPT enzyme, and these and their di- and triphosphate derivatives are indicted together (e.g. ATP/ADP). The biosynthesis of cytokinins in bacteria (e.g. *A. tumefaciens*) is compared next to it. Right, Several possible modifications and the degradation of zeatin. This figure was reproduced from Harberer and Kieber (2002) with permission.

isopentenyladenosine-5'-triphosphate (iPTP) and isopentenyladenosine-5'-diphosphate (iPDP), which are then converted to zeatin (Figure 1.6). Furthermore, Kakimoto (2001b) isolated the promoter sequences of several *AtIPTs* and fused them to GUS reporter gene. He observed that some of the genes displayed distinct, tissue specific patterns of expression. This result suggests that cytokinin production could be site specific and could add another tier of regulation to the mode of action of cytokinin.

More recently Zubko et al. (2002) using activation tagging, identified an *ipt* gene from *Petunia hybrida*. *P. hybrida* was transformed with T-DNA sequences containing elements, which enhance the expression of genes adjacent to the site of T-DNA integration. After screening 10,000 transformants, one showed a shooting phenotype. The mutant was designated shooting (*sho*). The cloned gene encoded an IPT protein with sequence homology to those isolated from *Arabidopsis*. Constitutive expression of *PtSHO in planta*, under the control of the CaMV 35S promoter enhanced the levels of N^6-isopentenyl adenosine derivatives, in contrast to the ectopic expression of bacterial *ipt* genes, which cause elevated levels of zeatin *in planta* (Smart et al., 1994; Martineau et al., 1994; McKenzie et al., 1998).

1.5.4 Metabolism

Addition of the side chain DMAPP to form iPNT is regarded as the rate-limiting step of cytokinin biosynthesis. However, the nucleotide appears to be rapidly hydroxylated to *trans*-zeatin derivatives. Feeding experiments, carried out using ^{14}C-labelled adenine, produced only radioactively labelled zeatin derivatives, no iP conjugates were detected (Stuchbury et al., 1979; Palni et al., 1983). Likewise, when ^{14}C-labelled iP was supplied, ZNT was the major constituent labelled, and very little radioactive iP or iPNT was detected (Palni and Horgan, 1983). Hydroxylation of iPNT is therefore regarded as a key event in cytokinin biosynthesis/metabolism. Conjugation, hydrolysis, reduction and oxidation follow hydroxylation. A diagram of cytokinin biosynthesis and metabolism is given in Figure 1.6.

1.5.4.1 Conjugation Conjugation occurs at the purine ring or the side chain resulting in ribosides and nucleotides, glucosides and amino acid conjugates. Ribosides and nucleotides are the most abundant conjugates found (McGaw, 1987). The ribosyl moiety only occurs on the 9-position of the purine ring, and may have one, two, or three phosphate groups attached forming nucleotides (Figure 1.4).

1.5.4.2 Hydrolysis Hydrolysis is the major form of metabolism of the ribosides and nucleotides. Two 5'-ribonucleotidase enzymes, which catalyse the hydrolysis of iPNT and iPA (Chen and Kristopeit, 1981a), and an adenine nucleotidase, which converts iPA to iP (Chen and Kristopeit, 1981b), have been characterised in wheat germ. *O*-glucosides have also been shown to be hydrolysed (McGaw et al., 1985).

1.5.4.3 Reduction Reduction of the cytokinin side chain leads to dihydro derivatives (Figure 1.5). The dihydro derivatives often have side chain conjugates, and are frequently detected as radioactive products during feeding experiments (Summons et al., 1979; Palmer et al., 1981).

1.5.4.4 Oxidation Oxidative cleavage of the cytokinin N^6-side chain appears to be the major fate of Z, iP, ZR and iPA (Jameson, 1994). Whittey and Hall, (1974) purified a cytokinin oxidase from *Zea mays* kernals, which was able to cleave iP and iPA yielding adenine and adenosine. Generally, dihydro derivatives, or derivatives bearing bulky substituents on side chains (*O*-glucosides) are resistant to attack by cytokinin oxidase (McGaw and Horgan, 1983), although some exceptions may exist (Laloue and Fox, 1989; Gerhäuser and Bopp, 1990). The genes of two very similar cytokinin oxidases have been isolated from *Zea mays* (Houba-Herin et al., 1999; Morris et al., 1999). Heterologous expression in moss protoplasts confirmed the predicted cytokinin oxidase activity. Further, *Arabidopsis* homologues have also been detected by *in silico* analyses and cloned (Bilyeu et al., 2001). The cloning of these cytokinin oxidase genes has provided for the first time the ability to reduce the levels of cytokinin in planta.

Werner et al. (2001) recently developed transgenic tobacco plants constitutively expressing *Arabidopsis* cytokinin oxidase genes. This allowed the determination of the

morphological consequences of reduced endogenous cytokinin. Transgenic plants exhibited increased rates of cytokinin oxidase activity, and reduced amounts of iP and zeatin-type cytokinins compared to wild-type plants. Phenotypically, the transgenic plants showed a dwarf growth pattern as a consequence of retarded shoot development. The growth of the root system was enhanced. Shoot apical meristems also had fewer cells in the transgenic lines compared to wild-type plants.

The oxidative nature of cytokinin oxidase genes has recently been questioned. Galuszka et al. (2001) purified a cytokinin oxidase enzyme to near homogeneity from wheat and barley grains. The wheat enzyme is a 60 kDa monomeric protein, its N-terminal amino acid sequence shows similarity to putative cytokinin oxidase proteins from *Arabidopsis*, but not to the enzyme previously isolated from maize. Oxygen was not required for enzyme activity and hydrogen peroxide was not produced during the catalytic reaction, so the enzyme behaved like a dehydrogenase rather than an oxidase. The question arises as to whether these authors have purified an enzyme, which is generally regarded as a cytokinin oxidase, or have they isolated another enzyme that is also involved in cytokinin degradation. The identity of this enzyme was shown by a short amino acid sequence, although the family of predicted protein sequences in the databases are quite divergent. However, the authors of this work suggest that the maize enzyme previously purified to near homogeneity by Morris et al., (1999) and Houba-Herin et al., (1999), may also behave as a dehydrogenase rather than an oxidase.

1.5.5 Mode of cytokinin action

While for ethylene most evidence suggests that signal transduction regulates ethylene action, it is likely that control of biosynthesis and of the metabolism of cytokinins may be as important as perception and signal transduction, for the regulation of the many plant processes cytokinin influences. This suggestion arises partly because a number of the naturally occurring cytokinin metabolites can themselves elicit cytokinin responses in bioassays. Bearing this in mind, the structure of the cytokinin is of crucial importance.

For many decades plant scientists have been searching for cytokinin binding proteins that could serve as cytokinin receptors (reviewed by Mok and Mok, 2001). Receptors require two properties: they must specifically bind the ligand and subsequently trigger biological responses specific to that ligand. Over the last few years considerable progress has been made, with the first cytokinin receptor and some of the downstream signalling genes being cloned and characterised (for reviews see Estelle, 2001; Schmulling, 2001; Schmulling, 2002; Deruère and Kieber, 2002, Harberer and Kieber, 2002). Recently, molecular approaches were used to isolate three genes, *CKI1* and *GCR1,* encoding proteins putatively implicated in cytokinin signal transduction (Kakimoto, 1996; Plakidouu-Dymock et al., 1998), and CRE1, which is considered to be a cytokinin receptor (Inoue et al., 2001).

Kaikmoto (1996) isolated the *CKI1* gene by T-DNA tagging. *Arabidopsis* callus was transformed with a T-DNA containing enhancer elements. After integration, this construct deregulates the expression of genes adjacent to the site of integration creating a dominant mutation. Mutant calli were characterised by rapid cellular proliferation, were green and produced shoots even in the absence of cytokinin in the medium. The resulting cloned *CKI1* gene showed sequence homology to *ETR1*, the ethylene receptor, suggesting *CKI1* could be a cytokinin receptor. While the *CKI1* gene probably encodes products that are involved in cytokinin signalling, where it fits into the pathway is unknown. To confirm its function as a receptor, the ability of the CKI1 protein to bind cytokinins remains to be demonstrated.

A different type of putative cytokinin receptor belonging to the G-protein coupled receptors (GCR) was identified by Plakidou-Dymock et al. (1998). The *GCR1* gene was isolated from *Arabidopsis* by PCR using primers homologous to seven trans membrane-spanning (7TM) receptors, which are often coupled to G proteins. Antisense expression of this gene conferred insensitivity to cytokinins. Root growth of the transformed plants became resistant to exogenous cytokinin. However, Kanyuka et al. (2001) have recently retracted their earlier findings and suggest that it is unlikely GCR1 is involved at all with cytokinin signalling.

Very recently, Inoue et al. (2001) isolated a mutant they called cytokinin response 1-1 (CRE1-1). The *cre1-1* mutant exhibited reduced responses to cytokinin. The cloned gene had a sequence similar to a histidine kinase two-component regulator and was, surprisingly, quite divergent from *CKI1* with only 25% amino acid identity in the amino terminal half of the proteins, the regions containing the histidine kinase and regulatory domains. Further, the extracellular domains of the two proteins are completely different suggesting against a common ligand.

Heterologous complementation was used to show CRE1 was a cytokinin receptor (Inoue et al., 2001). The well-characterised two-component regulator from the yeast *Saccharomyces cerevisiae* relies on the sensor histidine kinase SLN1, the transmitter YPD1 and the response regulator SSK1. The phosphorelay cascade phosphorylates SSK1, which keeps it from activating a MAPK cascade leading to cell division. In mutant strains of yeast that do not contain SLN1, growth in the absence of galactose is lethal due to the activation of SSK1 (galactose regulates the expression of a gene product which inhibits SSK1). The *CRE1* gene was expressed in this mutant strain of yeast, and cell division took place both in the presence and absence of galactose, when CRE1 was activated by cytokinin. Thus SLN1 was complemented by CRE1 when activated by cytokinin, providing evidence that CRE1 is a cytokinin receptor. This experiment also demonstrated that YPD1 was also required for the cytokinin-dependent rescue indicating that CRE1 acts through a phosphotransfer mechanism. The cytokinin molecules that have been shown to have high activity in bioassays such as *trans*-zeatin and 6-benzylamino purine could rescue mutant cells in the absence of galactose, while *cis*-zeatin was ineffective. Thidiazuron, a diphenylurea-type cytokinin, also activated CRE1. The DPU-type cytokinins inhibit cytokinin oxidase *in vitro*, and this was postulated as their mode of action *in vivo* (Jones and Schreiber, 1997). However, the activity of thidiazuron in the yeast assay suggests this compound may in fact stimulate the receptor *in vivo*. This is an extraordinary observation given the structural differences of thidiazuron and zeatin-type cytokinins. Yamada et al. (2001) confirmed by expression of CRE1 in yeast that cytokinin (both naturally occurring and synthetic) does bind directly to CRE1 with high affinity. The above result then explains the potency of

DPU-like analogues such as CPPU, which elicit cytokinin responses on exogenous application.

Suzuki et al. (2001) also used similar approaches to directly test the cytokinin sensing capabilities of three *Arabidopsis* histidine kinases AHK2, AHK3 and AHK4 (AHK4 is now known to be CRE1). The genes for these histidine kinases were expressed in a mutant strain of another yeast (*Schizosaccharomyces pombe*) and also in mutant strains of *E. coli*, both organisms lacking all of their histidine kinases. Only AHK4/CRE1 was able to complement mutations in these organisms in response to cytokinin. However, both AHK2 and AHK3 are homologous to CRE1 throughout their entire sequence, including the putative ligand-binding domain and also share the presence of two response regulator domains in their C-terminus. Further, Hwang and Sheen (2001) demonstrated that both AHK2 and AHK3 may regulate the promoter of a primary response gene in a cytokinin-dependent manner. These results suggest then that AHK2 and AHK3 are indeed cytokinin receptors in *Arabidopsis* (Harberer and Keiber, 2002).

The steps downstream of CRE1, and other cytokinin responsive histidine kinases, are complex and still need further dissection. Hwang and Sheen (2001) have proposed the model shown in Figure 1.7 based on their own and a number of other group's experiments. Because histidine kinase activity and phosphoryl transfer are required for CKI1 and CRE1 action, these histidine kinases probably act on histidine phosphotransfer proteins. *Arabidopsis* histidine phosphotransfer (AHPs) proteins have been shown to interact with CKI1 *in vitro*, and both AHP1 and AHP2 have been shown to be translocated into the nucleus in a cytokinin-dependent manner. It is proposed that these AHP proteins act like a bridge, transmitting a signal from the site of perception, probably at the plasma membrane, to the effectors within the nucleus, which consist of a third class of components in phosphorelays, the response regulators (Hwang and Sheen, 2001).

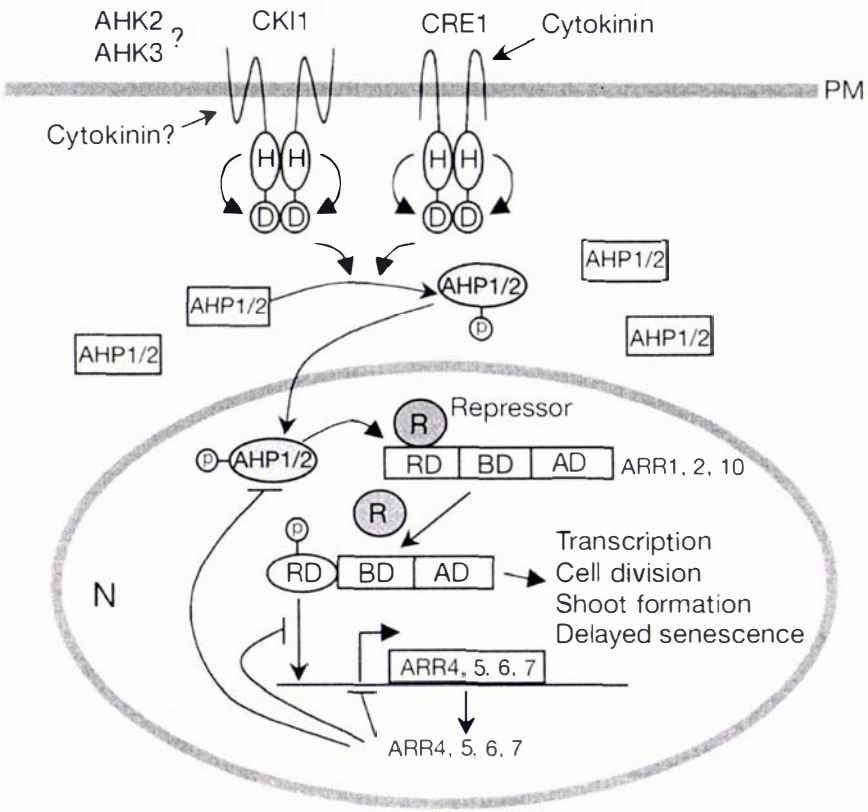

Figure 1.7 Model of the cytokinin signal transduction pathway in *Arabidopsis*. Cytokinin signal is perceived externally or internally by multiple histidine protein kinases at the plasma membrane. On perception of the cytokinin signal, histidine protein kinases initiate a signalling cascade through phosphorelay that results in the nuclear translocation of AHP proteins from the cytosol. Activated AHP proteins interact with sequestered ARR proteins or ARR complexes, and release the activation type of ARR proteins from putative repressors in the nucleus. The liberated ARR proteins bind to multiple *cis* elements in the promoters of target genes. The transcription activation is essential for cell proliferation, shoot formation, and delayed senescence. Activation of the repressor-type of *ARR* genes as cytokinin primary response genes provides a negative feedback mechanism. RD, response domain; BD DNA-binding domain; AD, transcription activation domain; PM, plasma membrane; N, nucleus; R, putative repressor; H, histidine; D, aspartate. This figure was reproduced from Hwang and Sheen et al. (2001) with permission.

Arabidopsis response regulators (ARRs) form two families, type-A and type-B ARRs. Type-A ARRs include ARR4, ARR5, ARR6 and ARR7 and are composed solely of a receiver domain; type-B ARRs includes ARR1, ARR2 and ARR10, which, in addition to the receiver domain, also contain an output domain. The C-terminal output domain activates transcription and binds to DNA in a sequence-specific manner. The type-B ARRs are also nuclear-localised proteins. Transcript levels of the type-A ARRs increase in response to cytokinin but not the type-B ARRs. Hwang and Sheen (2001) proposed that repressors were present to control cytokinin response because ectopic expression of type-B ARRs conferred a constitutive cytokinin response. Further, when type-A ARRs were over-expressed, they repressed their own expression in protoplasts, providing a possible negative feedback regulation of cytokinin signalling. Type-B ARRs also exerted an element of regulation on the transcription of type-A ARRs.

One should bear in mind that other components might be and probably are involved with the downstream signalling of cytokinin. In the example of ethylene signalling, histidine phosphotransfer proteins are not involved, rather the Raf kinase-like protein, CTR1 interacts directly with receptors (see Section 1.3.2). Further, ethylene receptors inactivate CTR1 in the presence of ethylene, causing derepression of the signalling pathway. However, cytokinin binding to receptors causes activation of the downstream signals. This indicates that, although the two systems share the utilisation of histidine kinase two-component regulators as their receptors, the way in which they are utilised in hormone signalling is completely different. The near future should see significant refinement of this cytokinin model as the tools are now in place to analyse the interactions amongst the elements involved.

1.5.6 Cytokinin activity

Although the metabolism of the cytokinins is very complex, it is possible to tentatively assign biological function to various forms. Bioassay is the standard method of studying the biological activity of cytokinins and whilst exogenous application of cytokinin cannot be expected to accurately mimic the action of endogenously produced cytokinin, such methods have provided valuable information regarding the possible function of the

many cytokinin forms. Briefly, the ribosides and free bases, are regarded as metabolically active, whereas the 9-glucosides are generally regarded as non-active forms of cytokinins and the *O*-glucosides as storage forms able to be turned over to release active cytokinin. The dihydro-derivatives are stabilised forms unable to be oxidised (Jameson, 1994).

1.6 ETHYLENE and CYTOKININ INTERACTIONS

Ethylene and cytokinins are known to regulate a number of different plant growth and developmental processes. The way in which these two plant hormones interact is now becoming better understood. It is becoming apparent that cytokinin and ethylene can act both synergistically and antagonistically.

Cytokinin has been shown to induce ethylene biosynthesis in a number of plant species (Cary et al., 1995), although the mechanism for this induction is not well understood. In mung bean hypocotyls, exogenous 6-BAP caused an increase in ACC synthase activity (Yoshii et al., 1980). To understand how cytokinins regulate ethylene biosynthesis, Vogel et al. (1998) isolated *Arabidopsis* mutants that did not respond to cytokinin treatment by increased ethylene biosynthesis (lack of the triple response). One of these mutants was found to be mutated in a member of the ACC synthase gene family, *ACS5*. *ACS5* was responsible for elevated ethylene levels in response to cytokinin and appeared to be regulated by a post-transcriptional mechanism, as cytokinin-induced perturbation of the carboxy terminus of *ACS5* resulted in ethylene over-production.

Hamant et al. (2002) studied the interactions of KNAT2 with ethylene and cytokinin. KNAT2 belongs to the family of KNOX proteins involved with regulating the architecture of the shoot apical meristem. When the genes encoding these proteins are ectopically expressed *in planta,* phenotypes indicative of cytokinin over-expression resulted (Ori et al., 1999; Frugis et al., 2001). Cytokinin levels were increased, indicating a clear link between KNOX genes and cytokinin signalling. It has been suggested that cytokinins could act downstream of KNOX, due to the *de novo* synthesis of cytokinin, following ectopic expression of *KNOX* genes. However, Hamant et al.

(2002) observed up-regulation of *KNAT2* transcript in response to exogenous cytokinin, suggesting a positive feedback mechanism may exist for at least the *KNAT2* member of the *KNOX* family.

KNAT2 was down-regulated in response to the ethylene precursor, ACC, reducing the number of cells in the shoot apical meristem markedly. Conversely, some of the ethylene insensitive mutant phenotypes were suppressed when *KNAT2* was ectopically expressed in the *ctr* background. Further, localisation of *KNAT2* gene expression increased in area in the ethylene resistant *etr1-1* mutant, or in response to exogenous cytokinin. The authors of this work concluded that cytokinins and ethylene act antagonistically in the meristem via KNAT2 to regulate meristem activity. Further, they suggested that cytokinin signalling could be divided into an ethylene-dependent pathway, that would control the response of cytokinins in the root and in the dark, and a KNAT-dependent pathway. The latter pathway would control the response of cytokinins that are induced in the light and are antagonistic to ethylene, such as cotyledon epinasty, leaf lobing, delayed senescence and enhanced capacity to regenerate. At this stage it is uncertain whether KNAT2 interacts with the cytokinin pathway directly via its antagonistic effect on ethylene.

Although Hamant et al. (2002) have provided a model (Figure 1.8), further work is needed to understand the consequences of the interactions between cytokinins, KNAT2 and ethylene in the shoot apical meristems. The regulation of other growth and developmental processes may also involve interaction between these two hormones.

Hall et al. (2001) proposed that cytokinin has a role in regulating the early stages of ethylene signal transduction. Activation of MAPK cascades by GTP-binding proteins can be inhibited by exogenous application of cytokinin (Novikova et al., 1999). The inactivation of MAPK cascade resulted in the desensitisation of senescing *Arabidopsis* leaves to ethylene, resulting in delayed senescence. During this thesis, gene expression experiments were carried out to elucidate whether cytokinin-ethylene interactions existed at the level of ethylene biosynthesis during postharvest senescence in broccoli (see Chapter 3 for details).

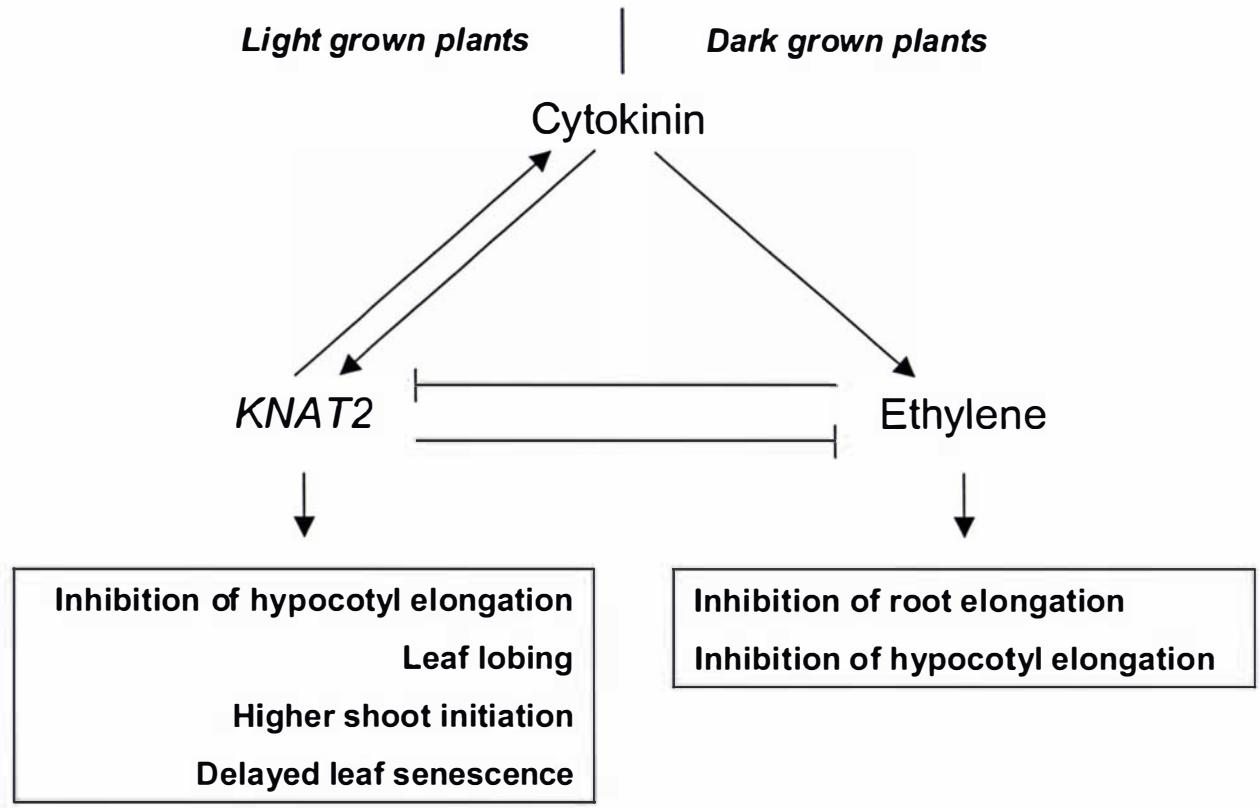

Figure 1.8 Putative position of KNAT2 in the cytokinin and ethylene network. The order of the elements in the pathway is based on the data from Cary et al.(1995) and Smalle and Van der Straeten (1997). In the dark, the cytokinin responses shown are some of those examined in wild-type plants in the presence of either 6-BAP or ACC. In the light, the cytokinin responses shown are some of those examined either in cytokinin over-producers or in KNAT2 transgenic lines. This figure was reproduced from Hamant et al. (2002) with permission.

1.7 TRANSFORMATION

Many strategies have been devised for gene transfer into plants, but few are successful for a wide range of species. Direct gene transfer, in which naked DNA is introduced into the plant either by electroporation, microinjection or DNA bombardment have been successfully used for monocotyledonous plant transformation. Often problems of gene silencing, due to incorporation of multiple copies of genes into plant genomes, have arisen from these techniques. *Agrobacterium*-mediated gene transfer has been successful for many dicotyledonous plants. This method exploits the natural gene transfer capacity of this soil borne bacterium, and is the main method for transformation of *Brassica oleracea* (Puddephat et al., 1996).

1.7.1 *Agrobacterium*-mediated transformation

Agrobacterium is a soil borne bacterium, which infects wound sites in a wide range of plant species. This infection causes crown gall tumours or hairy roots. Abnormal growth responses result from a natural gene transfer event. This unique inter-kingdom genetic transfer involves the transfer of a specific region of DNA (T-DNA) of the tumour-inducing (Ti) or the root-inducing (Ri) plasmid, integration, and expression in the plant genome. The T-DNA encodes enzymes responsible for the biosynthesis of phytohormones and proteins affecting the sensitivity of plant cells to these hormones. Thus expression of these genes results in tumour or hairy root development. Also encoded on the T-DNA are opines, modified amino acids, which the bacterium uses as a carbon and nitrogen source (Grant et al., 1991). The enzymes involved with the catabolism of opines are encoded elsewhere on these plasmids and are not transferred to the plant (Grant et al., 1991).

T-DNA regions are bordered by conserved 25 base pair sequences known as the left and right borders. Any sequences found between these borders are transferred and integrated into the plant nuclear DNA. *Vir* genes are found on the Ti and Ri plasmids, and encode genes, which are responsible for the excision, transfer and integration of the T-DNA from the bacterium into the nuclear DNA of plant cells. Products of the *vir* genes facilitate the transfer of any DNA located between the left and right borders, whether or

not they are present within the same plasmid. This enables the use of binary vectors in conjunction with disarmed Ti plasmids or armed Ri plasmids (van Wordragen and Dons, 1992).

1.7.2 *Agrobacterium*-mediated transformation of broccoli

Promising transformation results have been obtained using *Agrobacterium rhizogenes* for broccoli, but the impact of *rol* gene expression on phenotype is a limiting factor. Abnormalities have been reported to varying degrees after *A. rhizogenes* transformation of broccoli (Bertomie and Jouanin, 1992; Christey and Sinclair, 1992; Christey et al., 1997; Christey, 1997; Henzi et al., 1999a and 1999b; Henzi, 1999).

Henzi et al., (1999b) published an improved procedure for *A. rhizogenes*-mediated transformation of broccoli with an antisense ACC oxidase gene (pTOM13, from tomato). This procedure used compounds that enhanced the virulence of *A. rhizogenes*, and a *Brassica campestris* feeder cell layer. Intact cotyledons or leaf explants of three broccoli cultivars (Green Beauty, Shogun and Green Belt) were co-cultivated with *A. rhizogenes* strain A4T harbouring the binary vector pLN35 containing genes encoding an antisense ACC oxidase gene (35S-ACO-5'7') and neomycin phosphotransferase II (NOS-NPTII-NOS). Two cultivars were successfully transformed, Shogun and Green Beauty, with a transformation efficiency of 35% and 17% respectively. Integration of the T-DNA into the plant genome was confirmed using the polymerase chain reaction (PCR) and Southern analyses.

Although there was an initial increase in ethylene production compared with non-transformed control plants, transformed antisense ACC oxidase plants produced less ethylene in fully open mature flowers 50 h after harvest then did the wild-type flowers (Henzi et al., 1999a). Also, flowers showed a decrease in respiratory activity when compared with control plants. ACC oxidase enzyme activity was initially higher in transgenic plants, consistent with the higher initial ethylene production. ACC oxidase activity did not increase 50 h after harvest when ethylene production rapidly increased. However, a biological based assay was employed and not an *in vitro* assay as is regularly used to determine ACO activity, now that stable enzyme extraction conditions

have been developed. Henzi et al., (1999a) interpreted these results as suggesting that two underlying ethylene production pathways may operate, only one of which (the second increase) was down-regulated by the introduction of the antisense ACC oxidase gene. Ethylene production from mature heads of the ACC oxidase antisense plants was lower than normal wild-type plants after harvest (Henzi, 1999), however senescence was not effectively delayed.

Transgenic plants generated by *A. rhizogenes* transformation often exhibit an altered phenotype due to the expression of the rol genes (*rol A*, *B*, *C* and *D*) present on the T-DNA of the Ri plasmid. This altered phenotype is characterised by several morphological changes (see *rol* gene expression below) including wrinkled leaves, shortened internodes, reduced apical dominance, reduced fertility, altered flowering and plageotropic roots (Tepfer, 1989). The antisense ACC oxidase broccoli plants showed, to varying degrees, an altered and undesirable phenotype associated with the *Rol* genes transferred from the Ri plasmid when compared to untransformed control plants (Henzi, 1999). Consequently, the results presented by Henzi et al., (1999a and b) are confounded by the presence of the *rol* loci, which traditionally cause cytokinin-like effects, (such as the abnormal phenotypes observed to some degree in Henzi's (1999) plants), such as reduced apical dominance and shortened internodes.

Similar abnormalities in phenotype have not been reported for *A. tumefaciens*-mediated transformation, due to the disarming of the Ti plasmid of phytohormone and opine biosynthesis genes. However, *A. tumefaciens*-mediated transformation of broccoli generally results in low transformation efficiency. In fact transformation efficiency is frequently so low that it cannot be measured effectively.

Transformation efficiency could be increased by manipulating either or both the explant and bacterium virulence. This can be achieved either by increasing the number of competent plant cells by pre-culturing explants on regeneration medium prior to co-cultivation, improved induction of *vir* genes through use of cell feeder layers or by the addition of phenolic compounds such as acetosyringone or use of opines (Henzi, 1999).

Metz et al., (1995) reported an *A. tumefaciens*-mediated transformation system for broccoli, based on that of Toriyama et al., (1991), with an overall transformation efficiency of 6.5%. They concluded that important factors for high efficiency regeneration and high transformation rate included the use of a cell feeder layer, perforated petri dish sealants that allow ethylene diffusion, precultured seedling explants, and appropriate co-cultivation period. Moloney et al., (1989) reported an *A. tumefaciens*-mediated transformation procedure for *Brassica napus*. This system was developed for broccoli and was trialled using a number of different broccoli cultivars and *A. tumefaciens* strains (Mary Christey, personal communication). Chapter 4 of this thesis has been published in part and describes this transformation procedure (Gapper et al., 2002; reprint attached in the rear of thesis).

1.7.3 Promoters

Because constitutive over-expression of genes involved with the regulation of plant hormones often leads to unwanted pleiotropic effects on plant morphology, it is ideal to target such genetic manipulation in a temporal- or spatial-specific manner to avoid undesirable effects on normal plant growth and development. The importance of this consideration to gain beneficial horticultural performance from such biotechnological approaches was recently reviewed in a dedicated session at a recent IPGSA meeting (Klee and Clark, 2001). The promoters used in this study were chosen because they were likely to be expressed either following harvest or localised within floral tissue.

1.7.3.1 Asparagine Synthetase (AS) The expression of asparagine synthetase (AS) is significantly up-regulated in *Asparagus* following harvest. Up-regulation occurs rapidly, within a few hours of harvest. Davies and King (1993) proposed that the rapid accumulation of the AS transcript was induced by carbohydrate stress. Recently, the promoter region of AS was fused to β-glucuronidase (GUS), and transformed into broccoli and *Arabidopsis* (Kenel et al., 1999; Winichayakul et al., unpublished). Postharvest induction of the AS-promoter showed an increase in GUS expression in the leaves of both *Arabidopsis* and broccoli. Further, Kenel (2000) showed that the AS-promoter was controlled by influxes of both carbon and nitrogen. In this project a

chimeric gene containing the AS promoter from asparagus and an antisense ACC oxidase from broccoli was constructed and transformed into broccoli.

1.7.3.2 SAG_{12} Gan and Amasino (1995) developed a chimeric gene responsible for the auto-regulated production of cytokinin. They isolated a group of genes classified as senescence associated genes (SAG) from *Arabidopsis*, and removed the promoter sequences. One of these promoters, SAG_{12}, was linked to the isopentenyl transferase gene from *A. tumefaciens*, to form the chimeric auto-regulatory gene responsible for the inhibition of leaf senescence when introduced to plant genomes. The SAG_{12}-promoter has been used successfully to drive the expression of *ipt* in plant species including tobacco and rice (Gan and Amasino, 1995; Fu et al., 1998), altering the pool of cytokinin specifically during senescence, and thus inhibiting senescence. The SAG_{12}-IPT construct was introduced into broccoli during this project. Chen et al. (2002) recently showed that expression of SAG_{12}-IPT in broccoli was sufficient to delay senescence in both leaves and heads.

1.7.3.3 MYB_{305} Genes involved in the synthesis of flavonoid pigments represent a convenient model for the study of transcriptional activation in plants. One of these gene products, the MYB_{305} protein from *Antirrhinum majus* (snapdragon), is expressed specifically in the floral tissue of this species and is involved with the transcriptional activation of some flavonoid genes (Sablowski et al., 1994). By removing the native MYB_{305} promoter, Sablowski et al. (1995) showed the ectopic activation of a target promoter (phenylalanine ammonia-lyase (PAL2)) by over-expression of MYB_{305} protein in leaf cells of tobacco. Recently, Kenel (2000) reported the MYB_{305} promoter was sufficient to drive the expression of β-glucuronidase (GUS) in broccoli. GUS activity was present in low levels in the sepals of flowers, and in axillary meristems. In this work, the *ipt* gene from *A. tumefaciens* was introduced into to broccoli under the control of the MYB_{305} floral-associated gene promoter.

1.8 AIMS and OBJECTIVES

This project is a component of the Foundation for Research Science and Technology-funded programme, Biochemistry and Genetics of Vegetable Quality, being conducted at the New Zealand Institute for Crop & Food Research, Lincoln and Palmerston North sites. The overall objective of the programme is to determine the biochemical and genetic factors affecting quality attributes of vegetable crops so that improved cultivars can be developed. This project is part of a study of how shelf-life of highly perishable vegetables can be controlled.

Broccoli serves as a useful model for the study of crop deterioration. Broccoli is grown year round (dependant on cultivar choice), so obtaining tissue is generally not a problem. It is closely related to the fully sequenced model plant *Arabidopsis*, so that genes that have been isolated from *Arabidopsis* should be able to be isolated from broccoli with relative ease based on the homology of the two genomes. Further, broccoli is transformable by *Agrobacterium*-mediated transformation, so genes can be up- or down-regulated and *in vivo* function assigned. Broccoli is also sensitive to both the plant hormones ethylene and cytokinin, which have antagonistic effects on harvest-induced senescence. Consequently, the aims of this project were:

- To determine the effects of exogenous cytokinin, sucrose and ACC on senescence-associated and ethylene biosynthetic gene expression in broccoli following harvest, in both wild-type and transgenic plants expressing an antisense tomato ACC oxidase gene (Henzi, 1999). The aim of this work was to understand how these compounds regulate postharvest senescence in broccoli.

- To produce transgenic broccoli plants by *A. tumefaciens*-mediated transformation with an antisense ACC oxidase construct induced by harvest, as well as to introduce constructs that will induce cytokinin biosynthesis in a temporal- and spatial- specific manner, with the aim of delaying harvest-induced senescence.

- To produce a double transformant, one chimeric gene responsible for over-production of cytokinin and the other responsible for inhibition of ethylene biosynthesis, by crossing suitable transgenic parental lines or cloning and introducing a binary vector containing the two sets of genes. The aim here was to alter both ethylene and cytokinin biosynthesis following harvest to observe if altering both phytohormones would produce further extension of shelf-life compared to plants altered for only one factor.

- To determine the effects of reduced ethylene on postharvest senescence in broccoli, by monitoring the expression of genes associated with senescence in transgenic plants and comparing their profiles to those in wild-type plants.

- To isolate and characterise genes encoding enzymes involved with the biosynthesis and metabolism of cytokinins, in order to better understand the way in which the levels of these compounds are regulated in broccoli during harvest-induced senescence.

Chapter 2

Methods and Materials

Methods and materials that are common to the experimental Chapters are described in this Chapter.

2.1 CHLOROPHYLL REFLECTANCE AND DETERMINATION

Colour of florets was measured non-destructively by reflectance as described by King and Morris (1994), using a chromameter (model II; Minolta, Osaka, Japan) with an 8 mm measuring head and D-65 (6504K) illuminant. Reflectance was measured as Hue angle (180° = green, 90° = yellow), on equally spaced sites around the circumference of each branchlet, head or leaf.

Chlorophyll determinations were made according to Moran and Porath (1980) and Clarke et al. (1994). Up to 100 mg of freshly harvested broccoli floret or leaf tissue was immersed in 1 mL of cold (4°C) *N,N*-dimethyl formamide (DMF). The mixture was then incubated at 4°C in darkness for 48 h, and the $A_{664.5}$ and A_{647} of the extractant was determined following dilution. Chlorophyll concentrations were then calculated as described by Inskeep and Bloom (1985) using the following equations:

Chlorophyll a = $12.7\ A_{664.5} - 2.97\ A_{647}$ (mg mL^{-1})

Chlorophyll b = $20.7\ A_{647} - 4.26\ A_{664.5}$ (mg mL^{-1})

Total chlorophyll = $17.9\ A_{647} - 8.08\ A_{664.5}$ (mg mL^{-1})

2.2 DNA MANIPULATION

All DNA was stored at –20°C or 4°C until required.

2.2.1 Plasmid preparations

Reagents:

- Solution 1 – 50 mM glucose, 10 mM EDTA, 25 mM Tris-HCl pH 8.0
- Solution 2 – 0.2 M NaOH, 1% SDS (w/v)
- Solution 3 – 3 M potassium acetate, 11.5% (v/v) glacial acetic acid

Plasmid DNA was prepared using one of three different methods throughout the work presented here as outlined below. All three protocols relied on the alkaline lysis of bacterial cells to yield plasmid DNA (Sambrook et al., 1989). For mini-preparations of plasmid DNA, 3-5 mL of liquid LB culture containing the appropriate antibiotic for selection was grown for 16 h at 37°C. *E. coli* cells (1.5 mL) were pelleted at 14000 rpm for 5 min in a bench top centrifuge. The supernatant was aspirated away and the cells resuspended in 100 µL of Solution 1. The cells were then lysed by the addition of 100 µL of Solution 2, and the tube inverted 5-6 times gently. The lysed cells were then neutralised by the addition of 150 µL of Solution 3, and the tube inverted 5-6 times gently. Phenol:chloroform:isoamyl alcohol (25:24:1, v/v/v, 500 µL) was added and the tube shaken vigorously, followed by centrifugation at 14000 rpm in a bench top microcentrifuge for 10 min. The resulting supernatant was removed to a new tube and the nucleic acid precipitated by the addition of an equal volume of isopropanol, or 1/10 volume 3 M sodium acetate + 2.5 volumes ethanol. The nucleic acid was pelleted by centrifugation at 14000 rpm for 5 min in a bench top microcentrifuge. The resulting pellet was washed in 70% (v/v) ethanol, air dried and resuspended in 50-100 µL 1x TE containing 20 µg mL^{-1} DNase free RNaseA. The method was up-sized (two or three times) for binary and other low copy number plasmid vectors.

QIAGEN™ and CONCERT™ mini, midi and maxi Rapid Plasmid Purification Systems were routinely used for plasmid isolation as per the manufacturer's instructions. Generally commercially purchased systems were used when very clean (for sequencing reactions) or very large quantities (for insert preparation) of plasmid DNA was needed, or when binary vectors or low copy number plasmid DNA was extracted. In addition, the QIAGEN™ mini preparation system was used to isolate plasmid DNA from *Agrobacterium tumefaciens* cells to check for successful transformation. The resulting

plasmid DNA was transformed into *Escherichia coli*, then extracted by alkaline lysis and checked by restriction digest and PCR analyses.

2.2.2 Restriction digests

Restriction digests were carried out using enzymes and 10 x reaction buffer purchased from Roche (SuRE cut enzymes and Buffers). Plasmid and genomic DNA (0.1-10 μg) was digested in reactions varying between 10-200 μL in volume, at 25 or 37°C for between 1 and 16 h. Larger volumes and longer reaction times were used for complete digestion of genomic plant DNA. Digestion of small amounts of plasmid was routinely carried out in smaller volumes with short incubation times.

2.2.3 Agarose gel electrophoresis

DNA fragments were separated on 1 x TBE or 1 x TAE 0.7-2% (w/v) agarose gels containing ethidium bromide (0.5 μg mL^{-1}). The gels were run at 30-100V for between 1 and 20 h, depending on fragment size. Invitrogen (LIFE TECHNOLOGIES) DNA markers and standards were used to estimate fragment size. DNA was visualised by exposure to UV illumination in the presence of ethidium bromide in the gel.

2.2.4 Insert preparations

DNA fragments used as inserts for ligations or radio labelled for hybridisation experiments were cut from 1 x TBE or 1 x TAE agarose gels under UV illumination. The fragments isolated from gels were purified using High Pure PCR Product Purification Kits (Roche) or the QIAGEN mini elute system.

2.2.5 DNA bluntening reactions

Bacteriophage T4 DNA polymerase (Roche) or the Klenow fragment of *E. coli* DNA polymerase I (Roche) were used to blunten appropriately digested DNA inserts or vectors as described to Sambrook et al. (1989). The recessed 3' termini were end-filled by the DNA polymerase activity of the Klenow fragment of *E. coli* DNA polymerase I. Both Bacteriophage T4 DNA polymerase and the Klenow fragment of *E. coli* DNA polymerase I have 3'-5' exonuclease activity that was used to remove protruding 3' termini.

2.2.6 Ligation reactions

Ligation reactions were carried out using 1 unit T4 DNA ligase (Roche or Promega) per 100 ng vector DNA, and the appropriate volume of 10 x or 2 x ligation buffer supplied by the manufacturer. The standard T4 DNA ligase reaction using 10 x buffer was incubated at 4°C for 16 h. Similar reactions using 2 x rapid ligation buffer were complete after 5 min incubation at ambient room temperature. Molar ratios of 1:1. 1:3 and 3:1 of vector:insert DNA were routinely used. Some blunt ligations required higher insert concentrations to drive ligation reactions so molar ratios of 1:5 and 1:10 of vector:insert DNA were chosen. Molar ratios were calculated using the following equation:

$$\frac{\text{Amount of vector (ng)} \times \text{size of insert (kb)}}{\text{Size of vector (kb)}} \times \text{molar ratio of } \frac{\text{insert}}{\text{vector}} = \text{amount of insert (ng)}$$

2.2.7 Addition of linkers

Not I (New England Biolabs) and *Not* I-*Eco* RI (Pharmacia Biotech) linkers were ligated to blunt-ended DNA fragments as described by Sambrook et al. (1989). Up to 0.5 μg of blunt-ended DNA, 2 μg of phosphorylated *Not* I or *Eco* RI-*Not* I linker, 10 μL of 2 x rapid ligation buffer and 10 units of T4 DNA ligase (Roche) were mixed in a final volume of 20 μL and incubated at ambient room temperature for 5 min. Following ligation, the resulting fragment was digested with the appropriate restriction enzyme as described in Section 2.2.2, and cloned into the appropriate restriction site of the selected vector.

2.2.8 Dephosphorylation of linearised plasmid DNA

Linearised plasmid DNA was dephosphorylated using Shrimp Alkaline Phosphatase (SAP) to remove 5' phosphates (Roche) as per the manufacturer's instructions. Up to 1 pmol 5'-terminal phosphorylated DNA fragments either 5' protruding or 5' recessive ends were incubated with 1 unit of SAP at 37°C for 10 min. Up to 0.2 pmol 5'-terminal phosphorylated DNA fragments blunt-ended were incubated with 1 unit of SAP at 37°C for 60 min. Following dephosphorylation reactions, SAP was deactivated by incubation at 65°C for 15 min, the dephosphorylated fragments were then used without further

purification for ligation reactions. Dephosphorylation of plasmid vectors prior to ligation reactions ensures self-ligation of the vector occurs at very low frequency.

2.2.9 Bacterial culture

Media used:

- LB - 10 g L^{-1} bacto-tryptone, 5 g L^{-1} yeast extract, 10 g L^{-1} NaCl, for solid media 1.5% (w/v) bactoagar was added
- YEB - 1g L^{-1} yeast extract, 5g L^{-1} beef extract (Bovril), 0.5 g L^{-1} bacto-peptone, 0.5 g L^{-1} sucrose, 0.5 g L^{-1} $MgSO_4.7H_2O$, pH 7.0, for solid media 1.5% (w/v) bactoagar was added

E. coli strains were grown on/in LB or liquid medium at 37°C under appropriate antibiotic selection. *A. tumefaciens* was grown on/in either LB or YEB or liquid medium at 28°C under appropriate antibiotic selection. Bacterial cultures grown in liquid medium were aerated by constant orbital shaking at 240-300 rpm.

2.2.10 Bacterial transformation

Media used and reagents:

- LB - 10 g L^{-1} bacto-tryptone, 5 g L^{-1} yeast extract, 10 g L^{-1} NaCl
- YEB - 1g L^{-1} yeast extract, 5 g L^{-1} beef extract (Bovril), 0.5 g L^{-1} bacto-peptone, 0.5 g L^{-1} sucrose, 0.5 g L^{-1} $MgSO_4.7H_2O$, pH 7.0
- SEM buffer - 10 mM piperazine-*NN'-bis*-2-ethanesulphonic acid (PIPES), 55 mM $MnCl_2$, 15 mM $CaCl_2$, 250 mM KCl, pH 6.7

2.2.10.1 Competent cells Competent *E. coli* cells for heat shock transformation were prepared as described by Sambrook et al. (1989) or purchased (DH5α, Invitrogen LIFE TECHNOLOGIES). An overnight culture (100 mL) was grown in liquid LB medium at room temperature (ca. 22°C), or to an OD_{600} 0.4-0.8 (0.6 optimal). Cells were chilled on ice for 20 min, followed by harvesting by centrifugation at 3000 x g at 4°C for 10 min. The cells were then resuspended in 20 mL ice-cold filter sterilised SEM buffer. The resuspended cells were incubated on ice for 5 min, followed by centrifugation at 3000 x g for 10 min. The cells were resuspended in 6 mL ice cold filter sterilised SEM buffer and 460 µL DMSO was added. The cells were divided into 200 µL aliquots, snap frozen in liquid nitrogen and stored at –70°C until required.

Competent *A. tumefaciens* cells for electroporation were prepared as described by Sambrook et al. (1989), or purchased (LBA4404, Invitrogen, LIFE TECHNOLOGIES). A culture (250 mL) was grown in YEB media at 28°C until an OD_{600} of between 0.5-0.7 was reached. The cells were harvested by centrifugation at 3000 x g at 4°C for 10 min. The cells were resuspended in 250 mL of cold 10% glycerol. The cells were again pelleted as above and resuspended in 200 mL ice cold 10% glycerol. The process was repeated as above with reduction in volume continuously from 150 mL, 100 mL, 50 mL to finally 500 µL 10% glycerol. Cells were divided into 40 µL aliquots and stored at –70°C until required.

2.2.10.2 Transformation *E. coli* strains DH5α (Invitrogen, LIFE TECHNOLOGIES) or XL-1 blue (Stratagene) were transformed by heat shock at 42°C (Sambrook et al. 1989). Competent cells (50-100 µL) stored at –70°C were thawed on ice, plasmid DNA or ligation reaction mix were then added, and left to incubate on ice for 30 min. Subsequently, the cells were heat shocked at 42°C for 1 min, and returned to ice for 2 min. Cells were then left to recover with the addition of 900-950 µL L-Broth at 37°C for at least 1 h followed by plating on appropriate selective media. For transformation of *E. coli* cells using ligation reactions, often blue/white colour screening was used to determine which cells contained the inserted DNA fragment, by addition of X-gal and IPTG to the surface of selective media (Sambrook et al. 1989). The pUC based vectors pBLUESCRIPT® (Stratagene), pGEM®-5Zf, pGEM®-7Zf, pGEM®-T Easy (Promega), and binary vectors pART27 (Gleave 1992) and pBJ49 used in this work all have the gene encoding the *lacZ* α-peptide, allowing recombinants to be selected by blue/white colour screening.

A. tumefaciens strains LBA4404, GV3101, and AGL1 were transformed by electroporation. Competent cells stored at –70°C were thawed on ice. Plasmid DNA (1 µL) was combined with 20 µL of competent cells and placed in an electroporation cell (Gene Pulser® Cuvette, BioRad) and the cells electroporated with a 12 KV cm^{-1} charge (Cell Porator BRL LIFE TECHNOLOGIES). Immediately following electroporation the cells were recovered by the addition of 1 mL of TB (terrific broth) and shaken at 28°C for 2-4 hours. The cells were then plated on solid agar media with appropriate antibiotic selection and incubated at 28°C for three days.

2.3 BINARY VECTORS

Cloning strategies for the different binary vectors used in this thesis are outlined in detail in the Chapters they relate to most closely. A summary of the binary vectors used is shown in Table 2.1.

2.4 GENOMIC DNA EXTRACTION

Reagents:

- Extraction buffer - 200 mM Tris HCl (pH 7.5), 200 mM NaCl, 25mM EDTA, 0.5% (w/v) SDS

Genomic DNA was extracted by one of two methods. For PCR, a mini preparation method described by Edwards et al. (1991) was used to extract genomic DNA. Leaf discs were homogenised in 400 μL of cold extraction buffer and the extractant centrifuged. DNA was then precipitated from the supernatant (300 μL) with 300 μL cold (-20°C) isopropanol. The DNA was pelleted by centrifugation, air dried and resuspended in 100 μL H_2O.

For Southern analysis, genomic DNA was extracted using the Nucleon Phytopure Kit, as per the manufacturer's instructions (Amersham). Ground leaf tissue (0.5 g) was mixed and incubated at 37°C for 30 min with 2.3 mL Solution I, 23 μL β-mercaptoethanol, and 4.6 μL RNase A (10 mg mL^{-1}). Subsequently, 0.75 mL of Solution II was added, mixed, and incubated at 75°C for 10 min with occasional mixing by gentle inversion of the tubes. After incubation, the sample was placed on ice for 20 min, followed by the addition of 1 mL cold (-20°C) chloroform and 100 μL of Phytopure resin. The solution was again mixed and centrifuged at 1300 x g for 10 min. The DNA from the upper aqueous phase was cleaned with phenol:chloroform:isoamyl alcohol (25:24:1, v/v/v) and then precipitated by addition of an equal volume of cold (-20°C) isopropanol. The DNA pellet was subsequently washed in 70% (v/v) ethanol, air-dried and resuspended in 1x TE buffer.

Table 2.1 Binary vectors. TERM, terminator; 35S, Cauliflower mosaic virus 35S promoter; NOS3', nopaline synthase terminator; OCS3', octopine synthetase terminator; IPT, isopentenyl transferase; BoACO2 broccoli ACC oxidase 2; SAG_{12}, senescence associated gene promoter. AS, asparagine synthetase promoter; BoIPT, broccoli isopentenyl transferase; AtIPT *Arabidopsis* isopentenyl transferase.

Vector name	Description	Plant selectable marker
pBJ49	Binary vector based on pART27	Hygromycin b
pPN1	MYB_{305}-IPT-TERM cloned into the *Not* I site of pBJ49	Hygromycin b
pPN11	SAG_{12}-IPT-NOS3' cloned into the *Not* I site of pBJ49	Hygromycin b
pART27	Base Binary vector (Gleave, 1992)	Kanamycin
pPN10	AS-antisenseBoACO2-OCS3' cloned into the blunt-ended *Not* I site of pART27	Kanamycin
pPN92	35S-GUS	Kanamycin
pPN109	SAG_{12}-IPT-NOS3' cloned into the *Not* I site of pART27	Kanamycin
pPN110	MYB_{305}-IPT-TERM cloned into the *Not* I site of pART27	Kanamycin
pPN111	MYB_{305}-IPT-TERM::AS-antisenseBoACO2-OCS3' cloned into the *Not* I site of pART27	Kanamycin
pPN112	AS-antisenseBoACO2-OCS3' cloned into the *Not* I site of pART27	Kanamycin
pPN113	SAG_{12}-IPT-NOS3':: AS-BoACO2-OCS3' cloned into the *Not* I site of pART27	Kanamycin
pPN114	35S-antisenseBoIPT5-OCS3' cloned into the *Not* I site of pART27	Kanamycin
pPN115	35S-BoIPT4-OCS3' cloned into the *Not* I site of pART27	Kanamycin
pPN117	35S-BoIPT6-OCS3' cloned into the *Not* I site of pART27	Kanamycin
pPN118	35S-BoIPT7-OCS3' cloned into the *Not* I site of pART27	Kanamycin
pPN119	35S-AtIPT4-OCS3' cloned into the *Not* I site of pART27	Kanamycin
pPN120	*A. tumefaciens* native IPT gene, promoter and coding region, cloned into the blunt-ended *Not* I site of pART27	Kanamycin

2.5 RNA EXTRACTION

Reagents:

- Extraction Buffer - 100 mM Tris-HCl pH 9.0, 200 mM NaCl, 15 mM EDTA, 0.5% (v/v) sarkosyl, 0.8% (v/v) β-mercaptoethanol (added fresh)
- 1 x TE - 10 mM tris HCl, 1 mM EDTA, pH 8.0

Total RNA was extracted using one of two methods. The first method used TRIzol™ (Invitrogen, LIFE TECHNOLOGIES) following the manufacturers instructions. Plant material was ground in a precooled mortar and pestle in liquid nitrogen. Ground broccoli tissue (0.5 g) was homogenised in 5 mL TRIzol reagent and incubated at room temperature for 5 min. Chloroform (1 mL) was then added, mixed and incubated at room temperature for 3 min, before centrifugation for 15 min, to separate phases. RNA was then precipitated from the aqueous phase by the addition of 2.5 mL isopropanol. The pelleted RNA was then washed with 75% (v/v) ethanol, air dried and resuspended in RNase free water.

The second method was adapted from that described by Houdebine and Puissant (1995). Plant material was ground in a precooled mortar and pestle in liquid nitrogen. Ground broccoli tissue (1 g) was homogenised in 4 mL extraction buffer with β-mercaptoethanol, followed by the addition of 4 mL of phenol. Solutions were mixed by vortex, 0.8 mL of 24:1 (v/v) chloroform:isoamyl alcohol added, mixed by vortex once more, then 3 M sodium acetate added (280 µL). Samples were mixed by vortex, and placed on ice for 15 min, followed by centrifugation at 10,000 x g for 10 min. The upper aqueous phase was transferred to a fresh tube and an equal volume of phenol:chloroform:isoamyl alcohol (25:24:1, v/v/v) added. Samples were again mixed by vortex and centrifuged at 10,000 x g for 10 min. The upper aqueous phase was transferred to a fresh tube and an equal volume of chloroform was added. The tubes were mixed by vortex and centrifuged at 10,000 x g for 10 min. The resulting upper aqueous phase was precipitated with an equal volume of isopropanol. Nucleic acid was pelleted by centrifugation at 10,000 x g for 10 min, immediately after addition of isopropanol. The pellet was washed with 70% (v/v) ethanol and the pellet dried and resuspended in 1 mL RNase free water. Lithium chloride (8 M 0.5 mL) was added to

selectively precipitate RNA from genomic DNA. The precipitating RNA was left to incubate at 4°C for 2-3 h or overnight. The mixture was then centrifuged in a bench top microcentrifuge. The resulting RNA pellet was washed in 70% (v/v) ethanol, air dried and resuspended in RNase free H_2O. Genomic DNA from the supernatant was precipitated by the addition of 1/10 volume 3 M sodium acetate + 2.5 volumes of absolute ethanol. DNA was pelleted by centrifugation, the pellet washed in 70% (v/v) ethanol, air-dried and resuspended in 20 µg RNase A in 1 x TE.

Total RNA was quantified (A_{260}) using a spectrophotometer. The RNA was used for northern analyses as well as semi-quantitative RT-PCR analyses and RT-PCR gene isolation.

2.6 POLYMERASE CHAIN REACTION - PCR

PCR was carried out in either a Perkin Elmar Cetus, a Hybaid Touchdown or a Techne PHC-3 thermal cycler. The standard 50 µL PCR reaction contained 5 µL 10x PCR buffer, 1 µL dNTPs (10mM), 2 µL each primer (10 µM), and 1 unit of Taq polymerase (5u μL^{-1}) (Roche, QIAGEN) or Platinum Pfx (5u μL^{-1}) (Invitrogen, Life technologies). The remaining volume was made up of H_2O, Mg^+ (final concentration 1.5 µM) and template DNA (1-10 ng plasmid DNA, 10-100 ng genomic DNA). PCR conditions varied depending on primers used, expected product size and polymerase used for the reaction. Sequences of all primers used are provided in Table 2.2.

2.7 REVERSE TRANSCRIPTASE POLYMERASE CHAIN REACTION – RT-PCR

RT-PCR was carried out in a Techne PHC-3 thermal cycler. Two methods of RT-PCR were used. Firstly, a one step method (QIAGEN™ One step RT-PCR Kit) was used as described by the manufacturer for gene isolation. DNase treated total RNA (1 µg) was combined with 5 µL 5x One Step RT-PCR buffer, 2 µL dNTPs (10 mM), 1 µL each primer (forward and reverse) (25 µM), 1 µL RNase Inhibitor (10 u μL^{-1}), 2 µL of One Step RT-PCR enzyme mix, and RNase free H_2O to give a final volume of 25 µL. The

Table 2.2 Names and sequences of oligo nucleotides used

Primer name	Sequence
NPTII A	5'-ATGACTGGGCACAACAGACCATCGGCTGCT-3'
NPTII B	5'-CGGGTAGCCAACGCTATGTCCTGATAGCGG-3'
IPT3	5'-GTCCAATGCTGTCCTCAAC-3'
IPT4	5'-ATACATTCCGAACGGATGAC-3'
HPT 175 Fow	5'-GCCGTCAACCAAGCTCTGATAGA-3'
HPT 314 Fow	5'-CAGAAGAAGATGTTGGCGACCTC-3'
HPT 899 Rev	5'-ATGTAGGAGGGCGTGGATATGTC-3'
HPT 764 Rev	5'-AGAGCCTGACCTATTGCATCTCC-3'
ROL B Fow	5'-AAAGTATGCTACCATTCCCCA-3'
ROL B Rev	5'-CCCATAAGCCACGACATCATA-3'
IPT Pro 520 Fow	5'-CTTTCAAGGAGACAGCCATG-3'
IPT Cod 12O6 Rev	5'-CATATCGATATCCATCGATC-3'
IPT Cod 717 Fow	5'-CGGTCCAACTTGCACAGGAAAGAC-3'
BoACO2 311 Fow	5'-CGACATCCCGGATATGTCAGATGA-3'
BoACO2 893 Rev	5'-GGCTCCTTGGGCTGAAACTTGACT-3'
AtCKOX 693 Fow	5'-TTAGGAGGTTTGGGTCAATTCGG-3'
AtCKOX 1187 Rev	5'-TATGGGAAGTTCCTCATCCATGGC-3'
AtIPT 190 Fow	5'-TTGTCATCATGGGTGCCACCGG-3'
AtIPT 362 Fow	5'-TTCCTCACCATCTTCTCGGCG -3'
Oligo dT	5'-TTTTTTTTTTTTTTTTT-3'
AtCKOX 1222 Rev	5'-AGAGKTTAGCCAHGGATGHGG-3'
AtCKOX 706 Rev	5'-ATHCCRAAYTGHCCCAAACCTCC-3'
AtCKOX 165 Fow	5'-TGACTTCGGHAACATHHCGCCG-3'
BoACS1 48 Fow	5'-ATGGGTTTTAGAACACCCGG-3'
BoACS1 448 Rev	5'-AATGTTCGATACACGCGC-3'
BoACS2 213 Fow	5'-TGATCGGATCGTCCTCACCG-3'
BoACS2 960 Rev	5'-ATCCAACAGAACAACCCTGC-3'
BoACS3 138 Fow	5'-CCTTAAAGAGTTCAGACAGC-3'
BoACS3 749 Rev	5'-CGCATGACACAACCGAGTCG-3'
BoACS1 Fow	5'-TGGTTAAGTTCACCAATGAC-3'
BoACS2 Fow	5'-TCCTCGACTTCTGCGTACGC-3'
BoACS3 Fow	5'-TAGTCCGATTCGTCACGAAA-3'
BoACS1 Rev	5'-GGTGGTTAACTCTGCGTG-3'
BoACS2 Rev	5'-TTCCACAATTGTCTCGTA-3'
BoACS3 Rev	5'-TAGGGTAAAAACACCATGCC-3'
pTOM13 Fow	5'-AGATGAGAGAGCCAACACC-3'

pTOM13 Rev	5'-AAATCTTGGCTCTTTGGC-3'
AtIPT 844 Rev	5'-CTTTSAYNBCHHACCGCC-3'
AtIPT 769 Rev	5'-CSKATMGYCTTCCDWATCCC-3'
AtIPT 506 Rev	5'-AYGWAHGAGTTGGATCCTCC-3'
AtIPT1 Fow	5'-ATGACAGAACTCAACTTCCAC-3'
AtIPT1 Rev	5'-CTAATTTTGCACCAAATGCCG-3'
AtPT3 Fow	5'-ATGATCATGAAGATATCTATG-3'
AtIPT3 Rev	5'-ACGTGGTTACAACTGATCAC-3'
AtIPT4 Fow	5'-ATGAAGTGTAATGACAAAATG-3'
AtIPT4 Rev	5'-TTGCGGTGATATTAGTCC-3'
AtIPT5 Fow	5'-ATGAAGCCATGCATGACGG-3'
AtIPT5 Rev	5'-CCTGTTTTACCTCACCGGG-3'
AtIPT6 Fow	5'-ATGACCTTGTTATCACCACC-3'
AtIPT6 Rev	5'-CTAAACTTCCAACAAACTTC-3'
AtIPT7 Fow	5'-ATGAAGTTCTCAATCTCATC-3'
AtIPT7 Rev	5'-CTTTTCATATCATATTGTGGG-3'
AtIPT8 Fow	5'-ATGCAAAATCTTACGTCCACA-3'
AtIPT8 Rev	5'-TGCAGCTCACACTTTGTCTTT-3'
Vir GMT 24	5'-GCGGTAGCCGACAG-3'
Vir GMT 25	5'-GCGTCAAAGAAATA-3'
BoACS2&3 1076 Fow	5'-CGGARYYTGGMTGGTTTAGG-3'
BoACS2&3 1003 Fow	5'-GAGMTCGAGCTTTGGSAT-3'
18S Fow (39.3)	5'-ACCTTACCAGGTCCAGAC-3'
18S Rev (39.3)	5'-AGTCAACGCGAGCTGATG-3'
As PRO-318 Fow	5'-ACGTGTT GACTGTTGAAGTGC-3'
T3	5'-AATTAACCCTCACTAAAGGG-3'
T7	5'-GTAATACGACTCACTATAGGGC-3'
SP6	5'-ATTTAGGTGACACTATAGAATACT -3'
AtACTIN Fow	5'-TTCAGCCACTTGTCTGTGAC-3'
AtACTIN Rev	5'-CGACATCACATTTCATGATGG-3'
BoCKOX1 Fow	5'-TTCACACAGGAAACAGCTATGA-3'
BoCKOX1 Rev	5'-CCGTGGCTCTTCACTAAATCAG-3'
BoIPT5 Fow	5'-CCAAGGAAACATGGTGGACG-3'
BoIPT5 Rev	5'-TCCGGTAGGAGAATATTGGCG-3'
BoIPT6 Fow	5'-ACTACCAAATTCGGGTCACCAC-3'
BoIPT6 Rev	5'-CATATGGTCGACCTGCAGGC-3'
BoIPT7 Fow	5'-CAACTCTTTCCTCCATCCTCAC-3'
BoIPT7 Rev	5'-CCTACTTCCACTTCCTCCGTCC-3'

reactions were placed in a thermal cycler (Techne PHC-3) under the following conditions: 50°C for 30 min, 95°C for 15 min, followed by 35 cycles of 95°C for 30 sec, 50°C for 30 sec, 72°C for 1 min, followed by final extension at 72°C for 10 min and 4°C soak.

The second method used was carried out in two steps, and was used for Semi-Quantitative RT-PCR and 'virtual northern' gene expression analyses. The RT reaction was carried out using Superscript enzyme™ II (Invitrogen, LIFE TECHNOLOGIES) as described by the manufacturer. DNase treated total RNA (up to 5 μg) was mixed with 1 μL oligo dT primer (100 μM), 1 μL RNase inhibitor (10 u μL^{-1}), 1 μL of dNTPs (10 mM) and RNase free H_2O to give a final volume of 13 μL. The reaction mix was incubated at 65°C for 5 min, and placed on ice immediately. Next, 4 μL 5x Superscript buffer and 2 μL of dithiothreitol (DTT) was added to the mix and then incubated at 42°C for 2 min. Superscript enzyme (1 μL) was added and mixed by pipetting gently up and down. The reaction mix was incubated at 42°C for 50 min followed by 70°C for 15 min. The resulting cDNA was quantified by fluorometric (Hoefer TKO100 Fluorometer) or spectrophotometric (Shimadzu UV-106A Spectrophotometer) analyses and used as template for PCR reactions as outlined in Section 2.6.

2.8 SOUTHERN AND NORTHERN ANALYSES

Reagents:

- Hybridisation buffer – 0.25 M sodium phosphate, pH 7.2, 7% (w/v) SDS, 1% (w/v) BSA, and 1 mM EDTA, pH 8.0
- 10 x SSC – 1.5 M NaCl, 150 mM trisodium citrate
- 10 x MOPS – 0.2 M 3-[N-morpholino] propanesulphonic acid (MOPS), 50 mM NaHAc, 10 mM EDTA, pH 7.0

For genomic Southern analysis, DNA (10 μg) was first digested with 80 units of *Eco*RV in a total volume of 200 μL for 16 h at 37°C. The digested DNA was then cleaned in an equal volume of phenol:chloroform:isoamyl alcohol (25:24:1, v/v/v). Subsequently, the digested DNA was precipitated by the addition of 1/10 volume 3 M NaHAc and 2.5

volumes ethanol. The precipitated DNA was centrifuged, and the pelleted DNA washed in 70% (v/v) ethanol, air dried and resuspended in 10 µL of water. The digested genomic DNA was run on a 1x TBE 0.7% (w/v) Agarose gel at 30 V for 20 h. The DNA was transferred onto a nylon membrane (Hybond N+, Amersham) using the downward alkaline (0.4 M NaOH) capillary method (Chomczynski, 1992). After transfer of DNA, the membrane was washed in 2 x SSC. The 1.7 kb *Eco* RV fragment from pLN35 was labelled with [β-^{32}P] dCTP using the ^{T7}Quickprime®DNA labelling Kit (Amersham) according to the manufacturer's instructions. The labelled DNA was separated from nucleotides by purification through microcolumns (ProbeQuant G-50, Amersham). The denatured labelled probe was added to membranes bathed in hybridisation solution (Church and Gilbert, 1984) and hybridised at 65°C for 16 h. Membranes were washed for 20 min in 3 x SSC, 1% SDS (w/v), 20 min in 2 x SSC, 1% SDS (w/v), 20 min in 1 x SSC, 1% SDS (w/v), 20 min in 0.5 x SSC, 1% SDS (w/v) and 20 min in 0.1x SSC, 1% SDS (w/v), at 65°C. After washing, films were exposed to membranes at –80°C.

For northern analysis, 10 to 40 µg of total RNA was denatured in 2.2 M formaldehyde, 50% formamide (v/v), 1x MOPS, 100 µg mL^{-1} ethidium bromide, by heating at 65°C for 15 min and then cooling on ice. The denatured RNA was then separated for 4 h at 80 V in 1.2% (w/v) agarose gels (0.7 M formaldehyde, 1 x MOPS). After electrophoresis, the RNA was transferred in 10 x SSC to nylon membranes (Hybond N+, Amersham) by downward capillary transfer (Chomczynski, 1992). After blotting, membranes were washed in 2 x SSC and the RNA was cross-linked to the membrane with a UV cross-linker (Hoefer UVC 500 UV Cross Linker). Probes of interest were prepared as described above. Hybridisation and membrane washing was carried out as described above.

2.9 VIRTUAL NORTHERN ANALYSES

RT-PCR products of RNA isolated from broccoli tissues were separated in a 1 x TBE, 1% agarose (w/v) gel, and blotted onto nylon membrane (Hybond N+, Amersham) as

described for Southern analyses. Membranes were then hybridised and washed as described for Southern analyses.

2.10 DNA SEQUENCING

Plasmid DNA was sequenced by primer sequencing. The chemistry used was the Big Dye Terminator Cycle Sequencing Ready Kit (Applied Biosystems). DNA to be sequenced was denatured and the single stranded molecules labelled with fluorescence labelled dideoxynucleotides using AmpliTaq® DNA polymerase. The labelled DNA fragments were analysed automatically in an ABI PRISM® 64 lane DNA Sequencer (Applied Biosystems). Samples under went electrophoresis in the system's vertical gel, followed by laser detection and computer analysis. The final data was provided as electrophogram printouts and the sequence as electronic ABI trace files.

2.11 DNA MANIPULATION SOFTWARE

All DNA sequence manipulation was carried out using the DNAstar software package.

2.12 cDNA CLONES

A list of cDNA clones used for experimental all work in this thesis is shown in Table 2.3, with a reference and GenBank™ accession number where available.

2.13 STATISTICAL ANALYSES

All statistical analysis was carried out using Genstat Fifth Edition software package (Lawes Agricultural Trust, Rothamsted Experimental Station, VSN International Ltd, UK). This software package was used to generate least significant differences (LSD's) by analysing raw data by analysis of variance (ANOVA). The LSD's generated by ANOVA were averages of a number of time points following harvest in many cases. Exact confidence intervals (CI's) were also calculated using this software.

Table 2.3 cDNA clones.

Clone name	Description of clone	Accession number	Reference
BoINV1	Broccoli acid invertase 1	AF274298	Coupe et al. (2003)
BoSUC1	Broccoli sucrose transporter 1	AY065840	Coupe et al. (unpublished)
BoSUC2	Broccoli sucrose transporter 2	AY065839	Coupe et al. (unpublished)
BoCP5	Broccoli cysteine protease 5	AF454960	Dr Simon Coupe[1]
BoHK1	Broccoli hexokinase 1	AF454961	Dr Simon Coupe[1]
BoPI	Broccoli protease inhibitor 1	AY065838	Dr Simon Coupe[1]
BoACO1	Broccoli ACC oxidase 1	X81628	Pogson et al. (1995a)
BoACO2	Broccoli ACC oxidase 2	X81629	Pogson et al. (1995a)
BoACS1	Broccoli ACC synthase 1	X82273	Pogson et al. (1995b)
BoACS2	Broccoli ACC synthase 2	AF338651	Gonzalez and Botella (unpublished)
BoACS3	Broccoli ACC synthase 3	AF338652	Gonzalez and Botella (unpublished)
BoMLP1	Broccoli metallothionein-like protein 1	AF458412	Dr Simon Coupe[1]
BoCAB1	Broccoli chlorophyll a/b binding protein 1	AF458406	Dr Simon Coupe[1]
Bo18S	Broccoli 18S ribosomal RNA gene	AF513990	Dr Simon Coupe[1]
pTOM13	Tomato ACC oxidase	A35021	Smith et al. (1986)
AtIPT7	*Arabidopsis* isopentenyl transferase 7	BAB59046	Kakimoto (2001) and Takei et al. (2001)[2]
BoCKX	Broccoli cytokinin oxidase	YTBE[3]	Isolated during this thesis
BoACTIN	Broccoli actin	YTBE[3]	Isolated during this thesis
BoIPT4	Broccoli isopentenyl transferase 4	YTBE[3]	Isolated during this thesis
BoIPT5	Broccoli isopentenyl transferase 5	YTBE[3]	Isolated during this thesis
BoIPT6	Broccoli isopentenyl transferase 6	YTBE[3]	Isolated during this thesis
BoIPT7	Broccoli isopentenyl transferase 7	YTBE[3]	Isolated during this thesis

[1]Personal communication.

[2]This *AtIPT7* sequence was amplified from *Arabidopsis* genomic DNA in this thesis.

[3]YTBE – Yet to be entered to the GenBank™ database.

Note: Figure 3.20 provides a schematic representation of where many of the products of these genes are located in relation to metabolism.

Chapter 3

Senescence-associated gene expression following harvest in broccoli.

3.1 INTRODUCTION

Cytokinin and ethylene have antagonistic effects during the harvest-induced senescence of broccoli. Exogenous cytokinin causes a delay in postharvest senescence (Clarke et al., 1994) whereas exogenously supplied ethylene accelerates the process (Tian et al., 1994). However, although exogenous cytokinin treatment was sufficient for preventing chlorophyll loss and reducing ammonia accumulation, this treatment was not sufficient to maintain 'at harvest' sucrose, glucose and fructose levels (Irving and Joyce, 1995; Downs et al., 1997). Sugars have in fact been implicated in regulating senescence, as they are needed to provide a carbon source to maintain high respiration rates in harvested immature tissues (Irving and Joyce, 1995). Simple sugars have also been implicated as signal transduction molecules (Smeekens, 2000).

It was the aim of this part of the project to trace the expression profiles of genes associated with senescence, ethylene biosynthesis, carbohydrate transport and carbohydrate metabolism following harvest in broccoli florets, in an attempt to unravel some of the very complex interactions involving cytokinins, ethylene and carbohydrates that regulate harvest-induced senescence of broccoli. In order to do this, gene expression profiles were traced in both wild-type and transgenic broccoli harbouring an antisense tomato ACC oxidase construct (Henzi et al. 1999b), following postharvest feeding with either water, sucrose, ACC and/or 6-BAP.

3.2 METHODS AND MATERIALS

3.2.1 Plant material and treatments

3.2.1.1 Experiment one: Broccoli (*Brassica oleracea* var. *italica* cv. Marathon) was harvested from a commercially grown crop located at Aokatere near Palmerston North, New Zealand. The heads were placed on ice and returned to the laboratory within 1.5 h of harvest. Branchlets were selected randomly and subjected to postharvest treatment in air, or vase fed in the water-based treatments. The water-based treatments included water, sucrose (2% w/v), ACC (1 mM), 6-BAP (2.21×10^{-4} M), and 6-BAP (2.21×10^{-4} M) + ACC (1 mM). Branchlets were treated through cut ends continuously during postharvest storage at 20°C in the dark. Floret tissue (including pedicel and some stemlet tissue) was shaved from the branchlets at critical times following harvest for later analyses. Rate of sepal yellowing following harvest was monitored by measuring colour by hue angle (refer to Section 2.1 for details). A total of three branchlets were individually measured for hue angle then pooled as one sample for molecular analyses.

3.2.1.2 Experiment two: Transgenic broccoli (*Brassica oleracea* var. *italica* cv. Green Beauty), harvested from a containment glasshouse located at Crop & Food Research Lincoln, New Zealand, was grown from seeds collected from primary transformant (T_0) plants. These plants had been produced by Henzi et al. (1999b) and harboured either a functional antisense or non-functional sense ACC oxidase gene from tomato, the pTOM13 gene construct. These plants had been transformed by *A. rhizogenes* strain A4T, harbouring the binary vector pLN35 (functional) or pLN34 (non-functional) (Figure 3.1). Plants genotypically and phenotypically similar to wild-type plants were selected from the T_1 segregants. PCR and Southern analyses were used to determine whether the T-DNA was present or not. T_1^- plants represent plants that did not have T-DNA present, where T_1^+ represents plants that have T-DNA present in their genome. Branchlets or whole heads were selected randomly and subjected to postharvest treatment in air or vase fed with the water-based treatments (water, ACC (1 mM), and 6-BAP (2.21×10^{-4} M)) and stored at 20°C in the dark. Floret tissue (including pedicel and some stemlet tissue) was shaved from the branchlets at critical times following

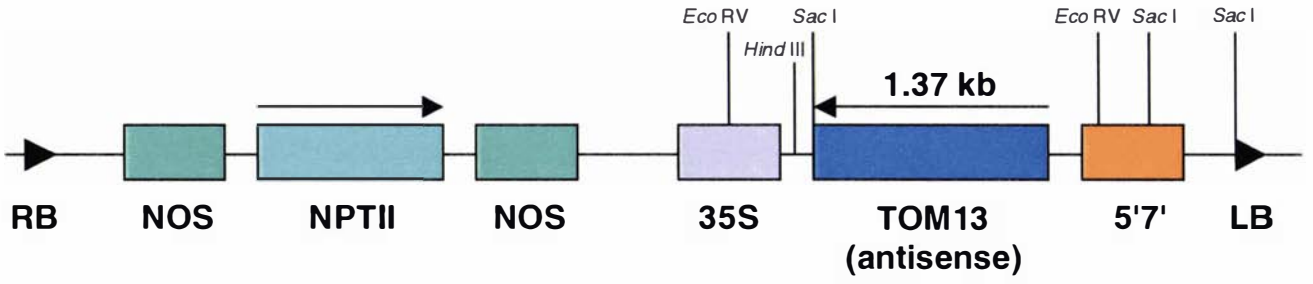

Figure 3.1 Schematic representation of the 5.2 kb T-DNA region (not to scale) of antisense *TOM13* construct pLN35 (redrawn from Henzi et al., 1999b). LB, left T-DNA border; RB right T-DNA border; NOS, promoter and terminator from the nopaline synthase gene from *A. tumefaciens*; *NPTII*, neomycin phosphotransferase II gene for kanamycin resistance; 35S promoter from the cauliflower mosaic virus; TOM13, tomato ACC oxidase cDNA in antisense orientation; 5'7', transcriptional terminator region. Arrows indicate 5' to 3' direction (sense →; antisense ←). pLN34 differs in that the orientation of the TOM13 fragment is reverse (sense orientation →) and also contains a cloning artifact at the 5' end making it non-functional.

harvest for later analyses. However, chlorophyll was extracted directly from floret tissue following harvest and treatment. Only one branchlet was used for each time point during this analysis.

3.2.2 Chlorophyll reflectance and determination

Details of these methods are outlined in Section 2.1.

3.2.3 RNA extraction and northern analyses

All RNA extraction in this chapter was carried out using TRIzol™ (Invitrogen) as per the manufacturer's instructions. Details of the method followed are outlined in Section 2.5). Northerns were carried out as described in Section 2.8. Descriptions of cDNAs used as probes are shown in Table 2.3.

3.2.4 Polymerase chain reaction (PCR)

Details of these methods are outlined in Section 2.6. Routinely, 30-40 cycles of PCR were carried out using specific primers to the *nptII*, *rolb* and *rolc* genes, and using an annealing temperature of 55°C for 30 s and an extension time of 30 s also.

3.2.5 Genomic DNA extraction and Southern analyses

Details of these methods are outlined in Sections 2.4 and 2.8 respectively.

3.3 RESULTS

3.3.1 Experiment one – wild-type plants

3.3.1.1 Sepal yellowing Branchlets of broccoli cv Marathon treated following harvest in air, water, sucrose, 6-BAP, ACC, and 6-BAP + ACC at 20°C in the dark for five days are shown in Figure 3.2. Sepal yellowing, measured as hue angle during postharvest storage is shown in Figure 3.3. Initial hue angle readings at harvest were around 130 and declined to around 110 in the four days (96 h) following for air-treated branchlets. All branchlets that underwent the water-based treatments maintained a high hue angle until three days (72 h) following harvest. At this point during storage, sepals from

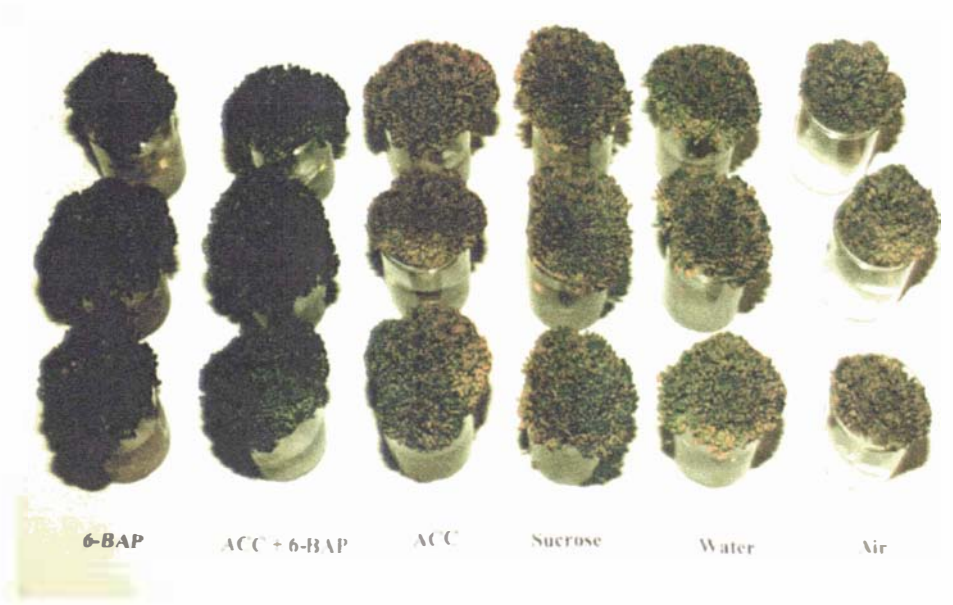

Figure 3.2 The influence of postharvest treatment of broccoli in 6-BAP (2.21 x 10^{-4} M), ACC (1 mM) + 6-BAP, ACC (1 mM), (2.21 x 10^{-4} M), sucrose (2% w/v), water and air after storage at 20°C, five days following harvest.

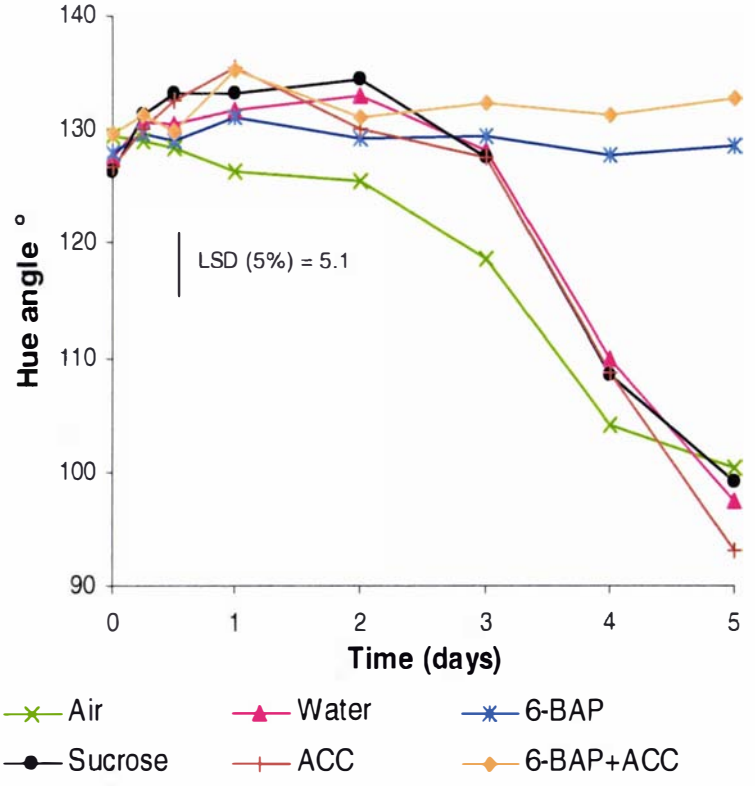

Figure 3.3 Changes in hue angle of broccoli branchlets treated in air, water, 6-BAP (2.21 x 10^{-4} M), sucrose (2% w/v), ACC (1 mM), 6-BAP (2.21 x 10^{-4} M) + ACC (1 mM), and held at 20°C in the dark following harvest.

branchlets treated with water, sucrose and ACC started to yellow, and by five days after harvest, these sepals were a similar colour to sepals from air-treated branchlets. Sepals from branchlets treated with 6-BAP either with or without added ACC remained green (hue angle ~ 130) throughout the five day postharvest period.

3.3.1.2 Northern analyses In general *BoACO1* transcript levels were detected at low levels at harvest (Figure 3.4). In florets from branchlets held in air transcript levels increased to reach a peak at 48 h and were maintained at this level until at least 120 h. All water-based treatments caused a reduction of *BoACO1* transcript accumulation when compared to air-treated florets. Water alone caused a greater reduction than both sucrose and ACC treatments. Exogenous 6-benzylaminopurine (6-BAP), even in the presence of added ACC, caused a further reduction of *BoACO1* transcript accumulation in florets after harvest compared to all other water-based treatments.

BoACO2 transcript was not detectable at harvest. *BoACO2* transcript levels increased from 24 h to peak at 48 h following harvest, and was maintained at this level until at least 72 h in florets from air-treated branchlets. All water-based treatments of branchlets caused a reduction of *BoACO2* transcript in florets following harvest. Water alone caused a further reduction of *BoACO2* transcript compared to sucrose and ACC treatments. Exogenous 6-BAP, even in the presence of ACC, caused a further reduction of *BoACO2* transcript accumulation after harvest compared to the water alone treatment.

BoACS1 transcript levels were detectable at harvest and increased slowly following harvest in air-treated broccoli material (Figure 3.5). Transcript levels increased in florets when branchlets were treated with water 48 and 72 h following harvest compared to air-treated branchlets. Sucrose and ACC appeared to reduce the levels of *BoACS1* transcript following harvest in comparison to water-treated florets. Exogenously fed 6-BAP caused the greatest level of *BoACS1* transcript but not in the presence of ACC. Both *BoACS2* and *BoACS3* transcript levels increased in florets following harvest in air-treated branchlets. The increase was reduced for all other wet treatments, although *BoACS2* transcript levels also increased slightly in response to exogenous 6-BAP.

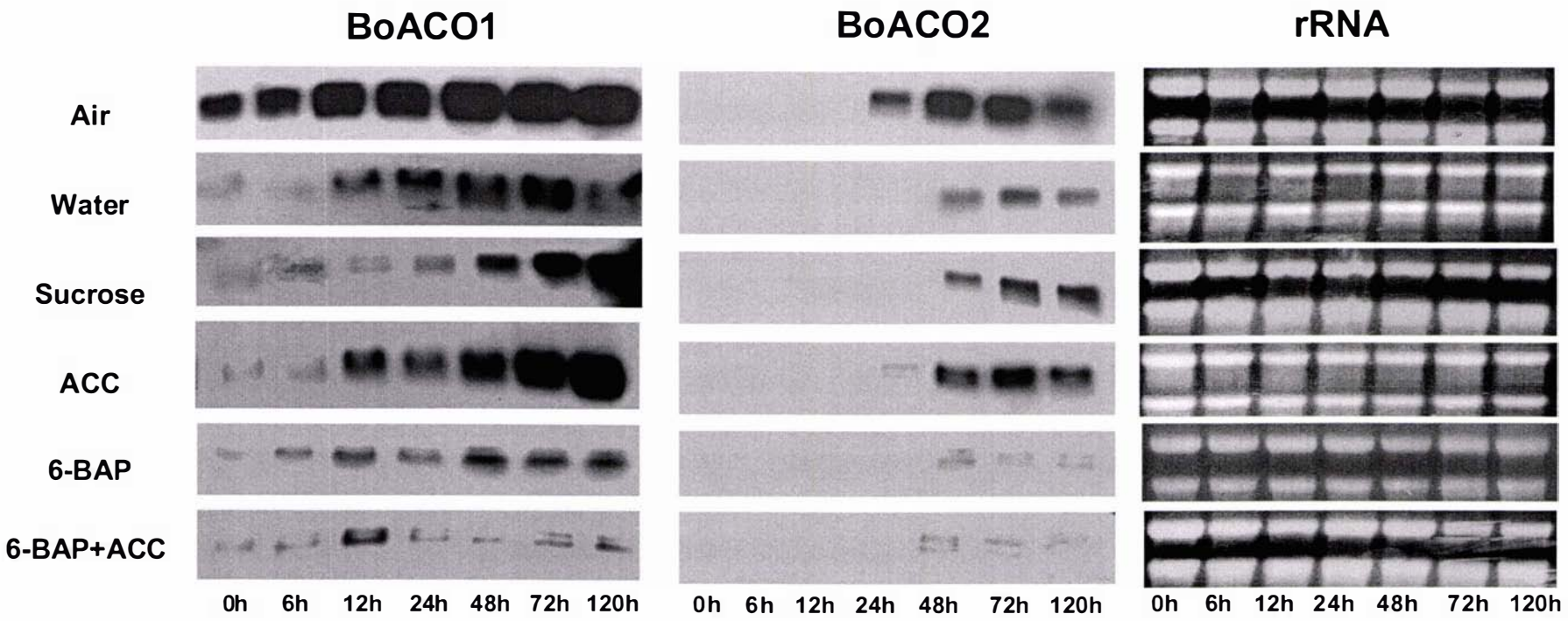

Figure 3.4 Autoradiographs showing the northern hybridisation of a 1.3 kb ^{32}P labelled *BoACO1* cDNA fragment and a 1.3 kb ^{32}P labelled *BoACO2* cDNA fragment, with total RNA from broccoli treated following harvest. Ten micrograms total RNA extracted from broccoli florets treated following harvest in air, water, sucrose (2% w/v), ACC (1 mM), 6-BAP (2.21×10^{-4} M) and 6-BAP (2.21×10^{-4} M) + ACC (1 mM), was denatured and separated in a 1.2% (w/v) agarose gel in 2.2 M formaldehyde, and then transferred to nylon membranes. For details of hybridisation and washing conditions, see Methods and Materials, Section 2.8. Membranes were not probed together in all situations so specific activity of probes may be different for each northern shown. However, experiments were repeated a number of times with similar results.

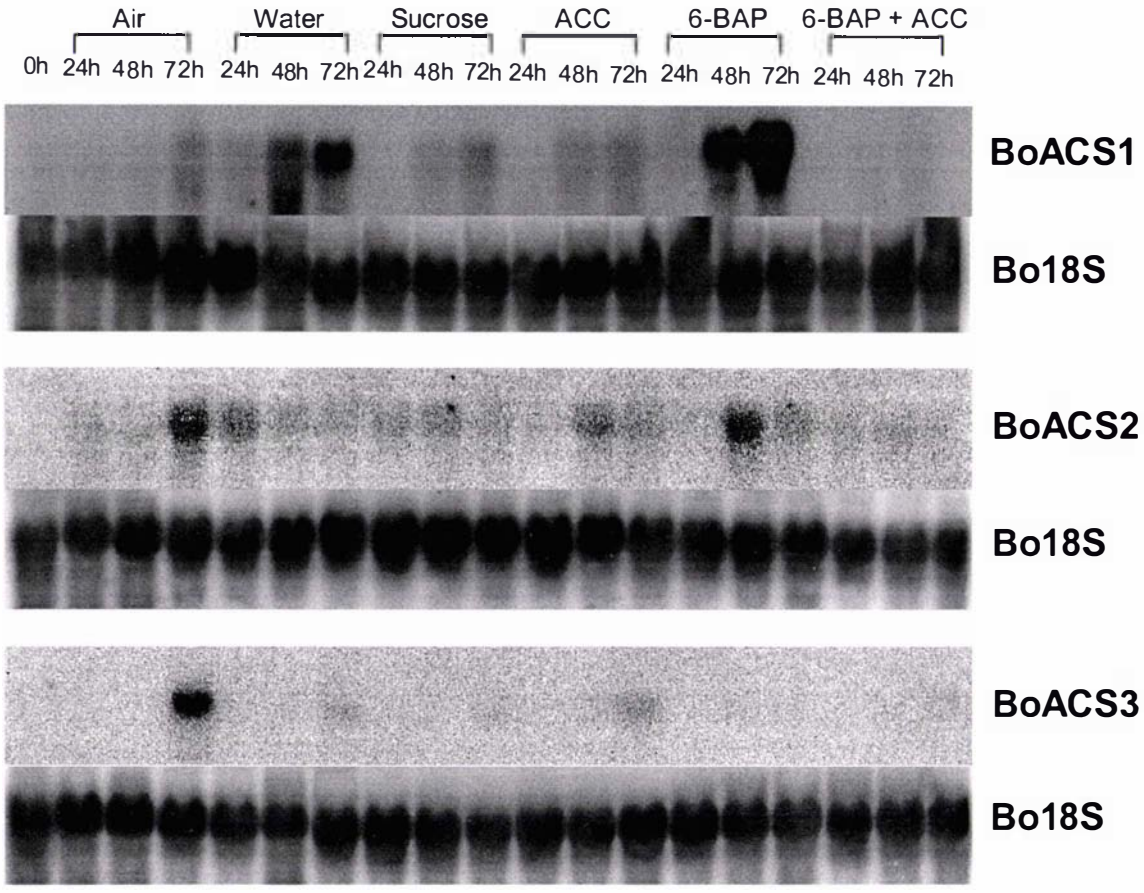

Figure 3.5 Autoradiographs showing the northern hybridisation of a 1.7 kb ^{32}P labelled *BoACS1* cDNA fragment, a 1.1 kb ^{32}P labelled *BoACS2* partial cDNA fragment, a 1.1 kb ^{32}P labelled *BoACS3* partial cDNA fragment and a 400 bp ^{32}P labelled *Bo18S* fragment, with total RNA from broccoli treated following harvest. Total RNA (20 μg) extracted from broccoli florets treated following harvest in air, water, sucrose (2% w/v), ACC (1 mM), 6-BAP (2.21×10^{-4} M) and 6-BAP (2.21×10^{-4} M) + ACC (1 mM), was denatured and separated in a 1.2% (w/v) agarose gel in 2.2 M formaldehyde, and then transferred to nylon membranes. For details of hybridisation and washing conditions, see Methods and Materials, Section 2.8. These northern experiments were repeated with similar results.

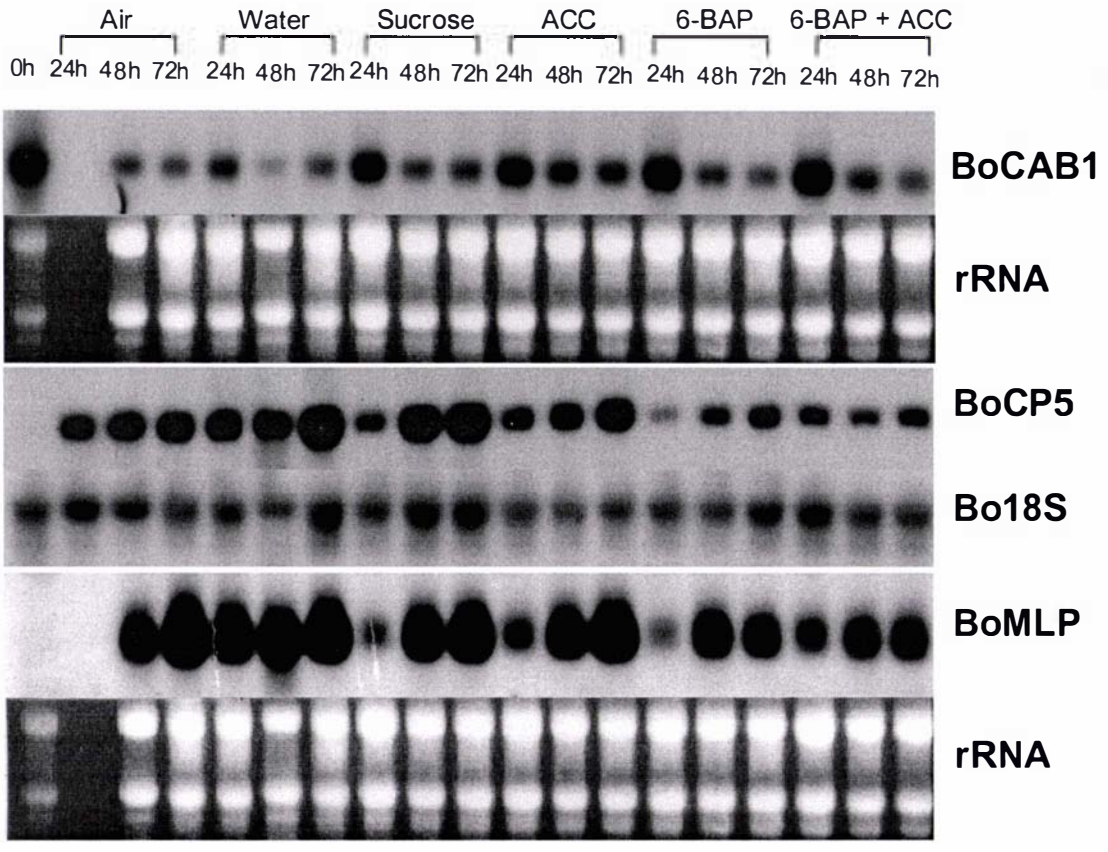

Figure 3.6 Autoradiographs showing the northern hybridisation of a 1.1 kb ^{32}P labelled *BoCAB1* cDNA fragment, a 1.3 kb ^{32}P labelled *BoCP5* cDNA fragment, a 500 bp ^{32}P labelled *BoMLP* cDNA fragment and a 400 bp ^{32}P labelled *Bo18S* fragment, with total RNA from broccoli treated following harvest. Total RNA (10 μg) extracted from broccoli florets treated following harvest in air, water, sucrose (2% w/v), ACC (1 mM), 6-BAP (2.21×10^{-4} M) and 6-BAP (2.21×10^{-4} M) + ACC (1 mM), was denatured and separated in a 1.2% (w/v) agarose gel in 2.2 M formaldehyde, and then transferred to nylon membranes. For details of hybridisation and washing conditions, see Methods and Materials, Section 2.8. Northern experiments conducted using the *BoCP5* probe were repeated with similar results.

Chlorophyll a/b binding protein (*BoCAB1*) transcript levels in florets were high at harvest and declined following harvest for air-treated branchlets (Figure 3.6). No RNA was detected by ethidium bromide staining in the 24 h air-treated lane. Treatment of branchlets with 6-BAP caused *BoCAB1* transcript levels to be maintained to slightly higher levels in florets 24 h following harvest compared to all other wet treatments, even in the presence of added ACC.

Cysteine protease (*BoCP5*) transcript levels in florets were low at harvest and increased within 24 h following harvest. This level was maintained at least until 72 h following harvest for air-treated branchlets (Figure 3.6). All water-based treated material had a similar transcript accumulation profile for *BoCP5* in florets except when branchlets were treated with exogenous 6-BAP. Even in the presence of ACC *BoCP5* levels were lower compared to all other treatments.

Metallothionein-like protein (*BoMLP*) transcript levels were low in florets at harvest and increased between 24 and 48 h following harvest in air. For all water-based treatments *BoMLP* transcript levels increased within 24 h following harvest (Figure 3.6). No RNA was detected by ethidium bromide staining in the 24 h air-treated lane. All hormone treatments caused a decrease in *BoMLP* transcript levels in florets 24 h following harvest compared to water alone. Exogenous treatment of branchlets with 6-BAP caused a further reduction of *BoMLP* transcript levels in florets at 48 and 72 h following harvest compared to all other treatments, even in the presence of added ACC.

The influence of exogenous feeding on the expression of sucrose transporter (*BoSUC*) genes in shaved broccoli florets following harvest is shown in Figure 3.7. *BoSUC1* transcript levels in florets increased in the 24 h following harvest. This level was maintained until at least 72 h following harvest for air-treated branchlets. Water and sucrose feeding caused transcript levels in florets to increase relative to air-treated branchlets. Exogenous treatment with ACC and 6-BAP (both separately and in combination) caused a reduction in *BoSUC1* transcript levels in florets 24, 48 and 72 h following harvest compared to the other water-based fed material. *BoSUC2* levels were low at harvest and increased in florets within 24 h and rose to high levels 72 h following

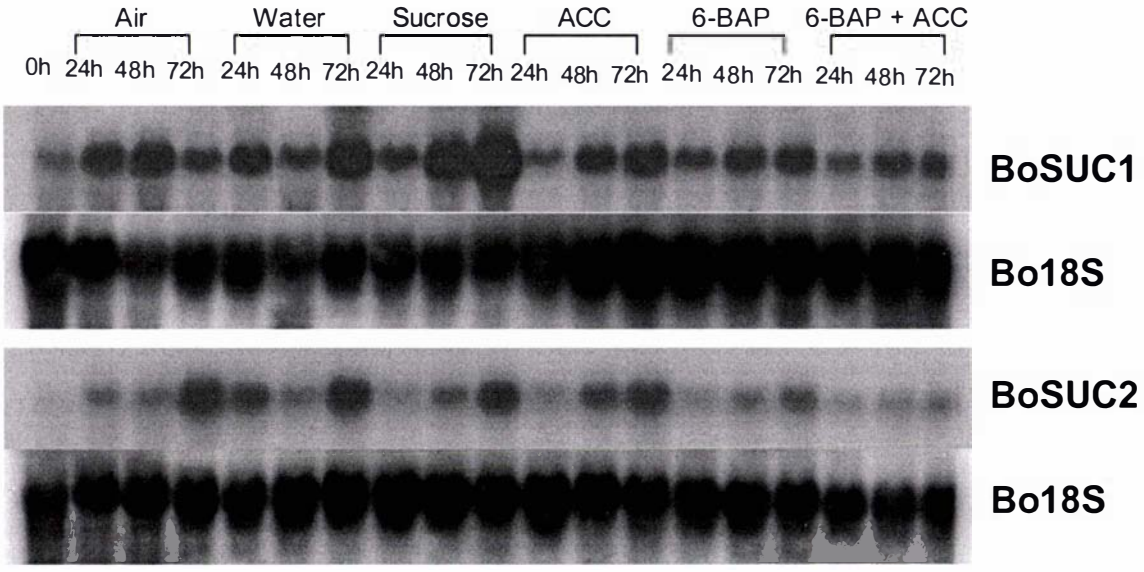

Figure 3.7 Autoradiographs showing the northern hybridisation of a 1.8 kb ^{32}P labelled *BoSUC1* cDNA fragment and a 1.7 kb ^{32}P labelled *BoSUC2* cDNA fragment and a 400 bp ^{32}P labelled *Bo18S* fragment, with total RNA from broccoli treated following harvest. Total RNA (20 μg) extracted from broccoli florets treated following harvest in air, water, sucrose (2% w/v), ACC (1 mM), 6-BAP (2.21×10^{-4} M) and 6-BAP (2.21×10^{-4} M) + ACC (1 mM), was denatured and separated in a 1.2% (w/v) agarose gel in 2.2 M formaldehyde, and then transferred to nylon membranes. For details of hybridisation and washing conditions, see Methods and Materials, Section 2.8. These northern experiments were repeated with similar results.

harvest in air-treated branchlets. All water-based treated branchlets had a similar expression profile for *BoSUC2* except for those exogenously treated with 6-BAP. Even in the presence of ACC, *BoSUC2* transcript levels were lower in florets treated with 6-BAP than all other treatments.

Acid invertase (*BoINV1*) transcript levels in florets were low at harvest and increased 48 to 72 h following harvest in air-treated branchlets (Figure 3.8). This expression profile was maintained for water-treated material. Treatment with sucrose caused an increase in *BoINV1* transcript levels at 48 hours following harvest compared to all other treatments. Treatment with 6-BAP and ACC (both separately and in combination) caused *BoINV1* transcript levels in florets to remain at basal levels following harvest. Hexokinase (*BoHK1*) transcript levels in florets increased 72 h following harvest in air-treated branchlets (Figure 3.8). This profile was maintained for all other treatments except for exogenous treatment with 6-BAP, where *BoHK1* transcript levels decreased slightly even in the presence of added ACC. Sucrose also caused a slight reduction in *BoHK1* transcript levels.

3.3.2 Experiment two – antisense pTOM13 plants

3.3.2.1 Selection of T_1^+ and T_1^- plants PCR and Southern analyses were used in tandem to determine the genotypes of broccoli plants grown from seed collected from *A. rhizogenes* derived primary transformant plants (T_0) harbouring an antisense *ACO* gene from tomato (*pTOM13*).

PCR was used as an initial screen to select plants that were transgenic (T_1^+) and plants that did not have inserted T-DNA present in their genome (T_1^-). PCR for *nptII*, *rolb* and *rolc* (for primer sequences, see Table 2.2 in Methods and Materials) was carried out and results tabulated (Table 3.1). An example of the PCR products run in an agarose gel is shown in Figure 3.9.

Figure 3.10 shows the hybridisation of a 1.7 kb pTOM13 DNA fragment from pLN35 following *Eco* RV digestion (see Figure 3.1) to *Eco* RV digested genomic DNA extracted from individual broccoli plants. In most cases, the *pTOM13* fragment

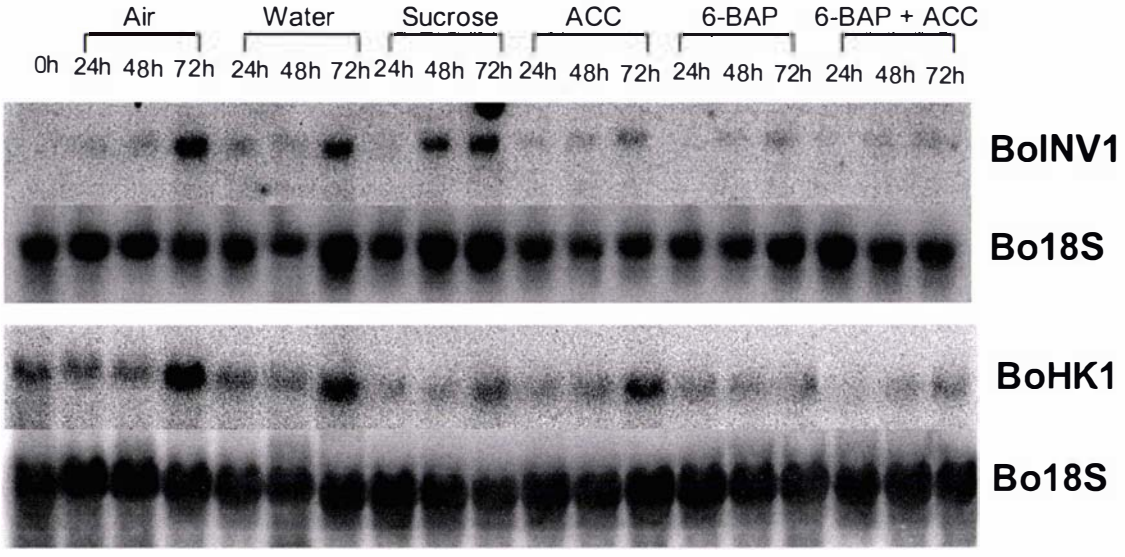

Figure 3.8 Autoradiographs showing the northern hybridisation of A. a 800 bp ^{32}P labelled *BolNV1* cDNA fragment and B. a 1.6 kb ^{32}P labelled *BoHK1* cDNA fragment, with total RNA from broccoli treated following harvest. Total RNA (10 μg) extracted from broccoli florets treated following harvest in air, water, sucrose (2% w/v), ACC (1 mM), 6-BAP (2.21×10^{-4} M) and 6-BAP (2.21×10^{-4} M) + ACC (1 mM), was denatured and separated in a 1.2% (w/v) agarose gel in 2.2 M formaldehyde, and then transferred to nylon membranes. For details of hybridisation and washing conditions, see Methods and Materials, Section 2.8. These northern experiments were repeated with similar results.

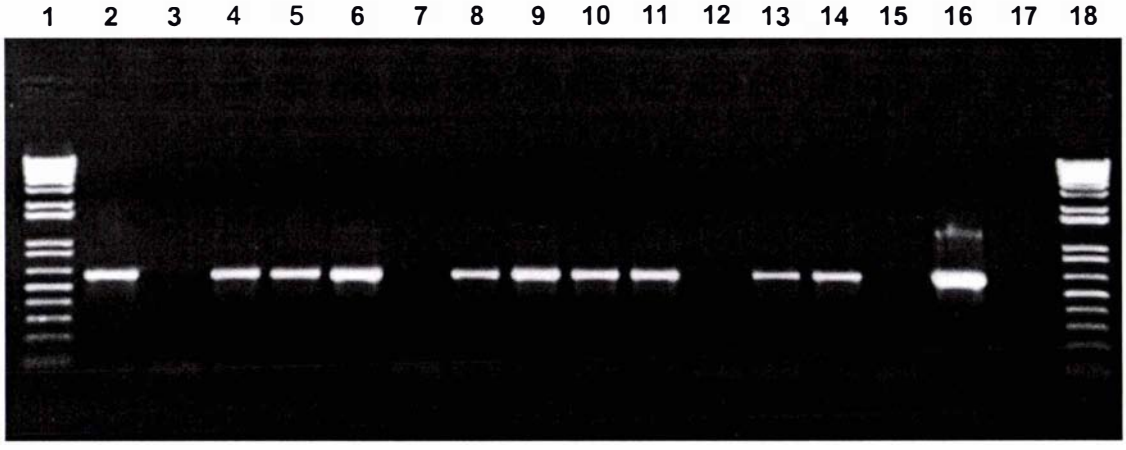

Figure 3.9 PCR amplification for *nptII* using genomic DNA from broccoli transformed with ACC oxidase construct pLN34 or pLN35 by *A. rhizogenes*. Lanes 1 and 18: 1 kb ladder markers; lanes 2 to 13: transgenic T_1^+ and T_1^- broccoli plants; lane 14: positive control (known transgenic cauliflower plant containing *nptII* confirmed by southern analysis); lane 15: wild-type plant; lane 16: positive control (pART27 vector containing *nptII*); lane 17: negative no DNA control (water).

Figure 3.10 Autoradiograph showing the Southern hybridisation of the 1.7 kb ^{32}P labelled TOM13 fragment of pLN35 with *Eco* RV digested genomic DNA from antisense TOM13 transgenic (T_1^+) and T_1^- broccoli plants. Lanes are labelled with individual plant number. The letter denotes the plant line: A = non-functional control Line 2 D (contains the T-DNA from pLN34), B = non-functional control Line 2 F (contains the T-DNA from pLN34), C = Line 6, D = Line 7 , E = Line 9 and G = Line 10. Numbers represent the GMO glasshouse number. Genomic DNA (10 µg) was separated on a 1% (w/v) agarose gel and blotted onto nylon membrane. All membranes were probed together with the 1.7 kb ^{32}P labelled TOM13 fragment from pLN35. For details of hybridisation and washing conditions, see Materials and Methods, Section 2.8.

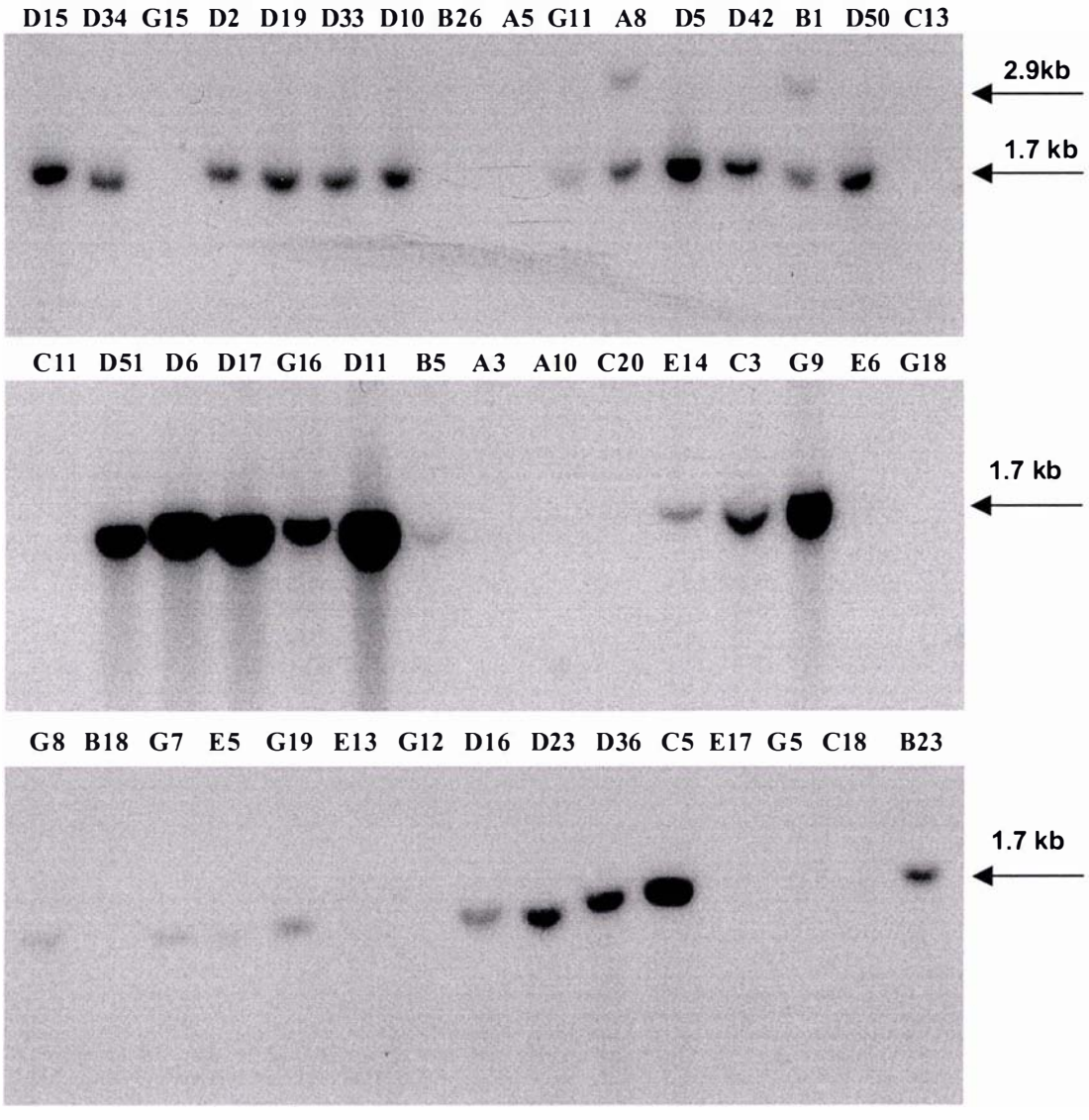
D15 D34 G15 D2 D19 D33 D10 B26 A5 G11 A8 D5 D42 B1 D50 C13
2.9kb
1.7 kb
C11 D51 D6 D17 G16 D11 B5 A3 A10 C20 E14 C3 G9 E6 G18
1.7 kb
G8 B18 G7 E5 G19 E13 G12 D16 D23 D36 C5 E17 G5 C18 B23
1.7 kb

hybridised to a single band of the 1.7 kb size indicating digestion of the genomic DNA was complete. A second band also appeared in two lanes (A8 and B1), at approximately 2.9 kb. This extra band could be the result of incomplete digestion of DNA, although these plants both originated from one individual transgenic line so it is possible that T-DNA rearrangement could be the cause of the extra band in this case. Figure 3.11 shows the hybridisation of the 1 kb *rolc* fragment to *Eco* RV digested genomic DNA extracted from individual broccoli plants. In most cases multiple bands are present for each positive lane. Results from the Southern analyses are shown in Table 3.1. In most cases the two separate Southern experiments conducted gave similar results.

3.3.2.2 Sepal yellowing Chlorophyll was extracted and measured as described in Section 2.1. The changes in chlorophyll content of whole florets of air-treated branchlets of Line 7, Line 9, Line 10 and segregating wild-type 'like' (T_1^-) plants are shown in Figure 3.12. Two of the transgenic lines, 9 and 10 had lower 'at harvest' whole floret chlorophyll content than T_1^- and T_1^+ Line 7 florets. Sepal yellowing in the three transgenic lines was less rapid when compared to sepal yellowing in T_1^- florets. Chlorophyll content appeared to increase between 48 and 72 h in Line 10 florets. This, although a statistically significant result seems unlikely, and could be due to development dis-similarities between the sample analysed in this case.

From this point onwards, due to the shortage of plant material, and growing space in containment glasshouse, only one transgenic line was analysed. Figure 3.13 shows the influence of hormone feeding on sepal yellowing for transgenic line 7 and T_1^- florets. Chlorophyll content was maintained to 'at harvest' levels for line 7 material treated in air. By contrast chlorophyll content of T_1^- material declined steadily over the 72 h following harvest in air-treated florets. 6-BAP treatment caused the slowest rate of sepal yellowing in both transgenic line 7 and T_1^- florets of all the wet treatments.

3.3.2.3 Northern analyses The influence of exogenous feeding on the expression of *ACO* genes in detached florets from T_1^- and transgenic antisense pTOM13 line 7 broccoli following harvest is shown in Figures 3.14 and 3.15. At harvest both *BoACO1* and *BoACO2* transcript levels in florets were low and increased rapidly to peak at 48-72 h

Figure 3.11 Autoradiograph showing the Southern hybridisation of the 1.0 kb ^{32}P labelled *rolc* fragment with *Eco* RV digested genomic DNA from antisense TOM13 transgenic (T_1^+) and T_1^- broccoli plants. Lanes are labeled with individual plant number. The letter denotes the plant line: A = non-functional control Line 2 D (contains the T-DNA from pLN34), B = non-functional control Line 2 F (contains the T-DNA from pLN34), C = Line 6, D = Line 7 , E = Line 9 and G = Line 10. Numbers represent the GMO glasshouse number. Genomic DNA (10 µg) was separated on a 1% (w/v) agarose gel and blotted onto nylon membrane. All membranes were probed together with the 1.0 kb ^{32}P labeled *rolc* fragment. For details of hybridisation and washing conditions, see Materials and Methods, Section 2.8.

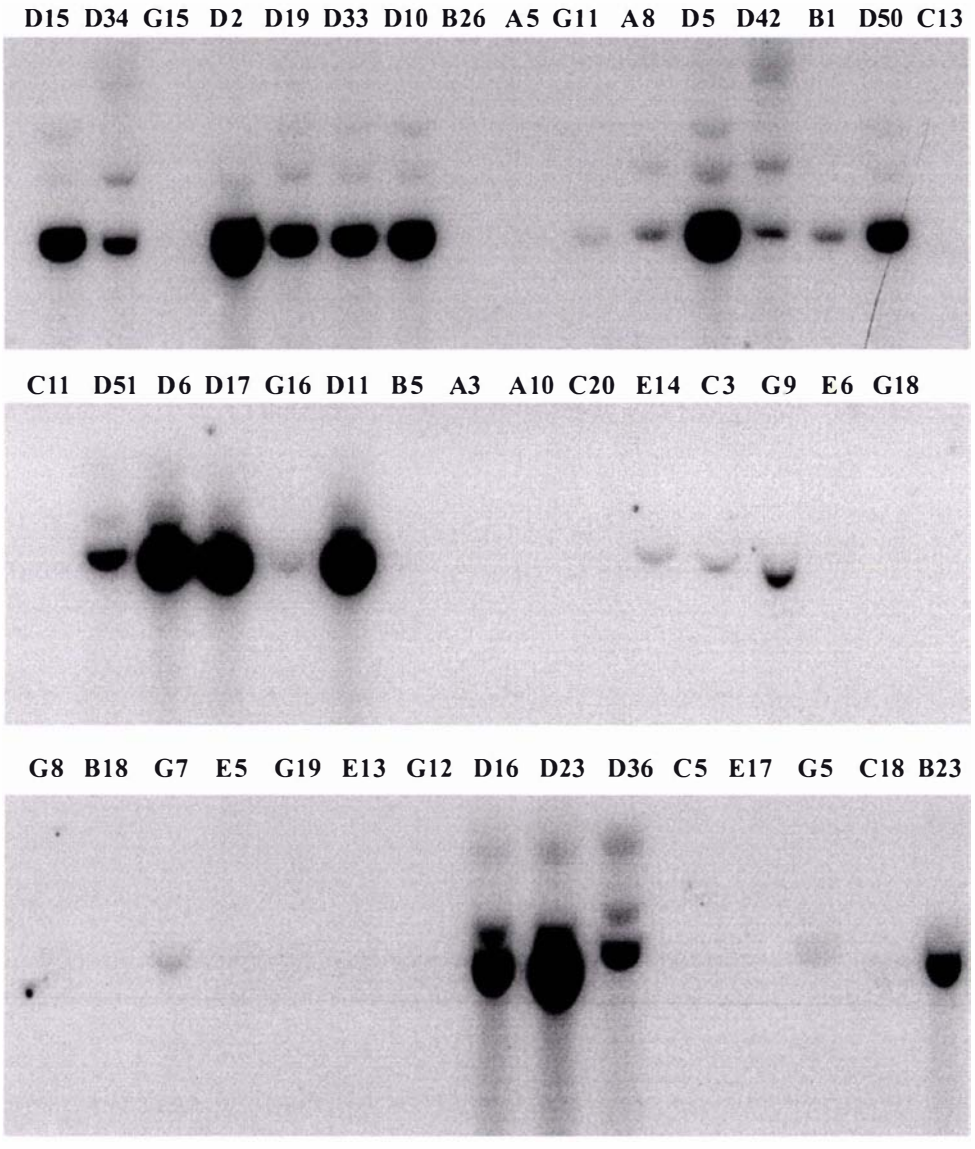
D15 D34 G15 D2 D19 D33 D10 B26 A5 G11 A8 D5 D42 B1 D50 C13
C11 D51 D6 D17 G16 D11 B5 A3 A10 C20 E14 C3 G9 E6 G18
G8 B18 G7 E5 G19 E13 G12 D16 D23 D36 C5 E17 G5 C18 B23

Table 3.1 PCR amplification, observational and Southern results from plants that were involved in postharvest experiments. The letter denotes the plant Line: A = non-functional control Line 2-D (parent contained the T-DNA from pLN34), B = non-functional control line 2-F (parent contained the T-DNA from pLN34), C = Line 6, D = Line 7, E = Line 9 and G = Line 10. Numbers represent the GMO glasshouse plant number.

Lines	PCR			Visual	Southern	
T_1^- (similar to wild-type)	***nptII***	***rolb***	***rolc***	**Visual**	***TOM13***	***rolc***
A3	- ve[a]	- ve	- ve	- ve	- ve	- ve
A5	- ve	- ve	- ve	- ve	- ve	- ve
G5	- ve	+ ve[b]	- ve	- ve	- ve	?[c]
G15	- ve	- ve	- ve	- ve	- ve	- ve
C13	- ve	- ve	- ve	- ve	- ve	- ve
C18	- ve	+ ve	- ve	- ve	- ve	- ve
C20	- ve	?	- ve	- ve	- ve	- ve
C11	- ve	- ve	- ve	- ve	- ve	- ve
B26	+ ve	?	- ve	- ve	- ve	- ve
B5	- ve	+ ve	+ ve	- ve	- ve	- ve
T_1^+ (TOM13 Line 7)	***nptII***	***rol b***	***rolc***	**Visual**	***TOM13***	***rol c***
D17	+ ve	+ ve	+ ve	- ve	+ ve	+ ve
D51	+ ve	+ ve	+ ve	- ve	+ ve	+ ve
D15	+ ve	+ ve	+ ve	- ve	+ ve	+ ve
D34	+ ve	+ ve	+ ve	- ve	+ ve	+ ve
D11	+ ve	+ ve	+ ve	+ ve	+ ve	+ ve
D6	+ ve	+ ve	+ ve	+ ve	+ ve	+ ve
D10	+ ve	+ ve	+ ve	+ ve	+ ve	+ ve
D2	+ ve	+ ve	+ ve	- ve	+ ve	+ ve
D42	+ ve	+ ve	+ ve	+ ve	+ ve	+ ve
D19	+ ve	+ ve	+ ve	+ ve	+ ve	+ ve
D50	+ ve	+ ve	+ ve	- ve	+ ve	+ ve
T_1^+ (TOM13 Line 10)	***nptII***	***rol b***	***rolc***	**Visual**	***TOM13***	***rol c***
G16	+ ve	+ ve	+ ve	+ ve	+ ve	+ ve
G7	- ve	+ ve	+ ve	+ ve	+ ve	+ ve
G9	+ ve	+ ve	+ ve	+ ve	+ ve	+ ve
G11	+ ve	+ ve	+ ve	+ ve	+ ve	+ ve
T_1^+ (TOM13 Line 9)	***nptII***	***rol b***	***rolc***	**Visual**	***TOM13***	***rol c***
E6	- ve	- ve	+ ve	+ ve	- ve	- ve

[a]-ve = absence of a PCR product, Southern hybridisation or visual symptom
[b]+ve = presence of a PCR product, Southern hybridisation or visual symptom
[c]? = unsure or unclear result

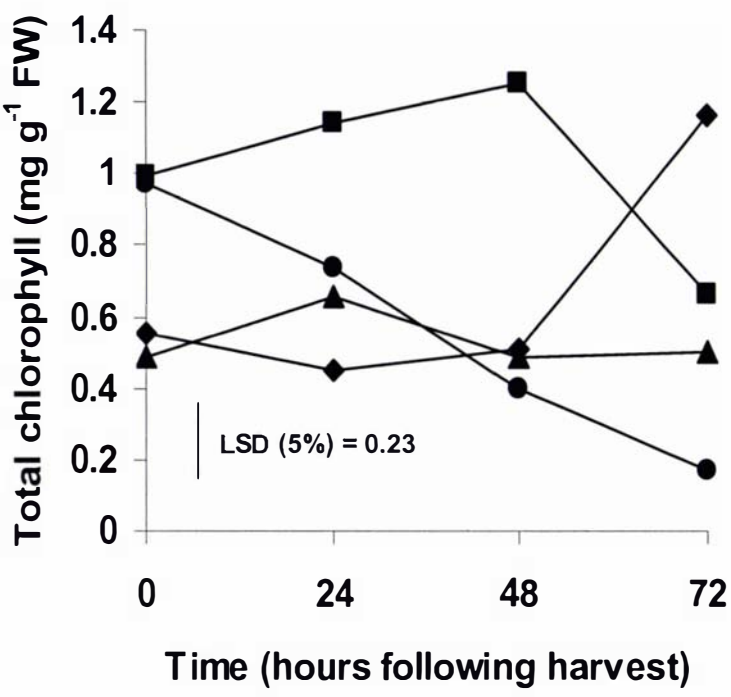

Figure 3.12 Changes in total chlorophyll in florets of antisense *TOM13* transgenic (T_1^+; Lines 7, 9 and 10) and T_1^- broccoli stored in air at 20°C in the dark following harvest. ● = T_1^-, ■ = Line 7, ▲ = Line 9, ◆ = Line 10.

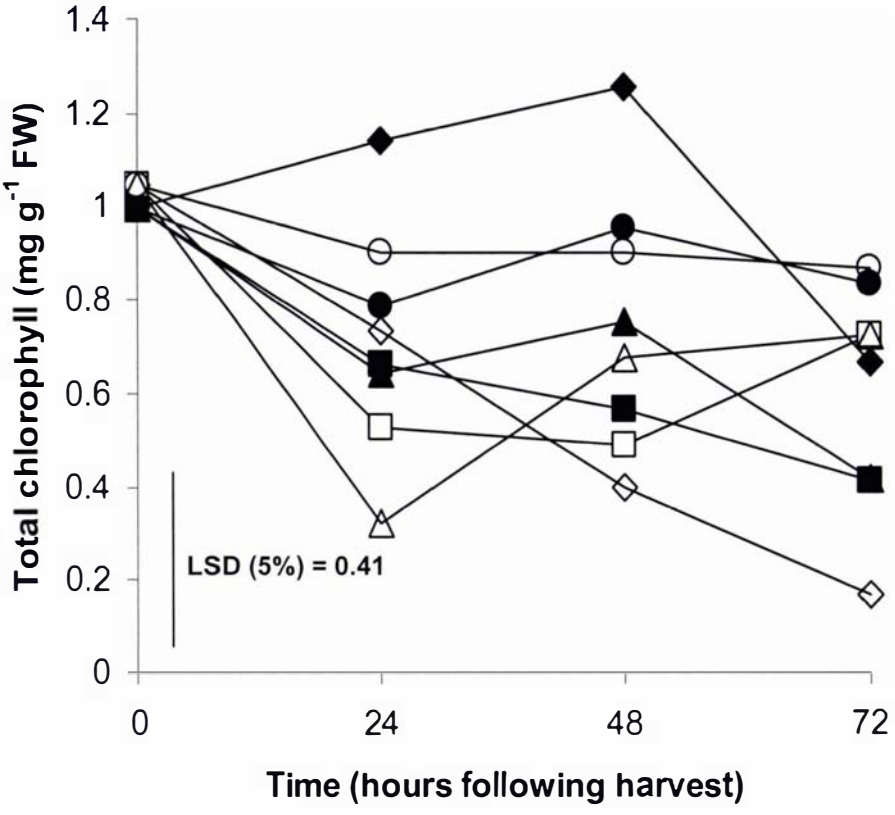

Figure 3.13 Changes in total chlorophyll of florets from T_1^- and antisense TOM13 transgenic line 7 (T_1^+) broccoli, during postharvest treatment in air, water, ACC and 6-BAP at 20°C in the dark. ◇ = air, □ = water, △ = ACC (1 mM) and ○ = 6-BAP (2.21×10^{-4} M). Filled symbols represent transgenic Line 7 (T_1^+) and open symbols represent T_1^-.

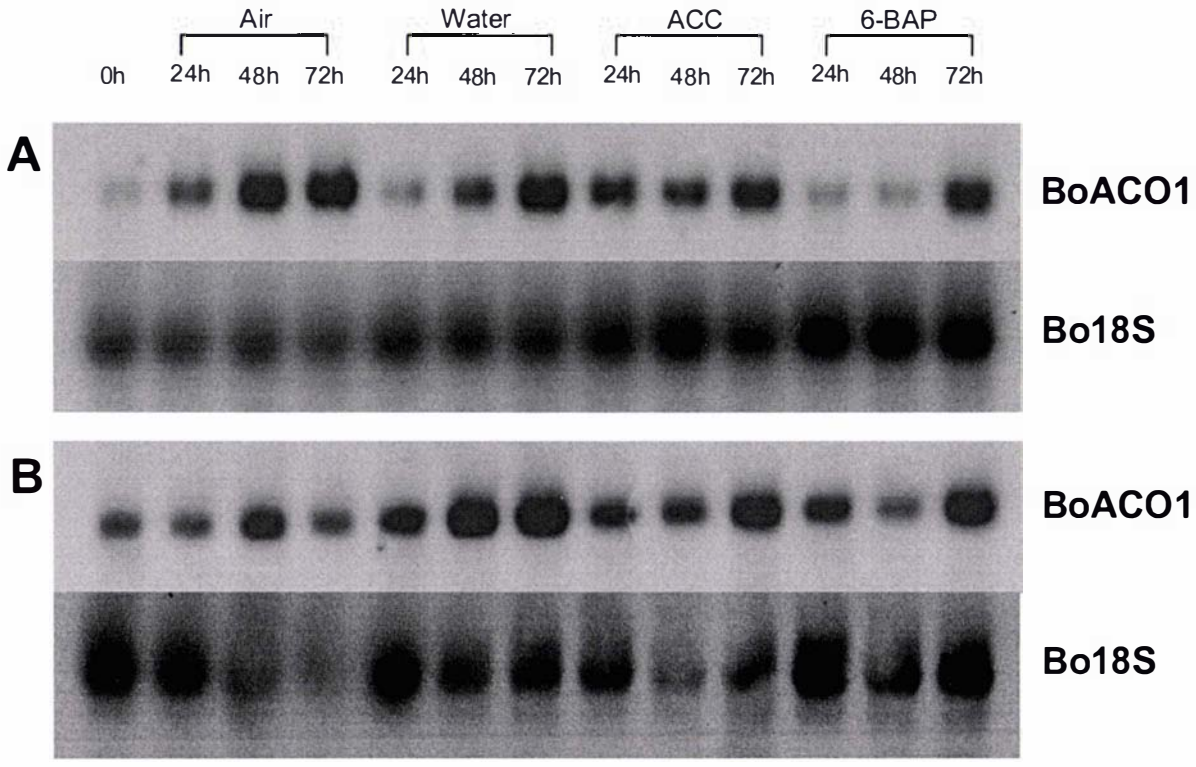

Figure 3.14 Autoradiographs showing the northern hybridisation of a 1.3 kb ^{32}P labelled *BoACO1* cDNA fragment and a 400 bp ^{32}P labelled *Bo18S* fragment, with total RNA from A. T_1- and B. antisense TOM13 Line 7 transgenic broccoli florets treated following harvest. Total RNA (10 µg) extracted from broccoli florets treated following harvest in air, water, ACC (1 mM) and 6-BAP (2.21×10^{-4} M), was denatured and separated in a 1.2% (w/v) agarose gel in 2.2 M formaldehyde, and then transferred to nylon membranes. All membranes were probed together with either a ^{32}P labelled *BoACO1*or *Bo18S* fragment. For details of hybridisation and washing conditions, see Methods and Materials, Section 2.8. These northern experiments were repeated with similar results.

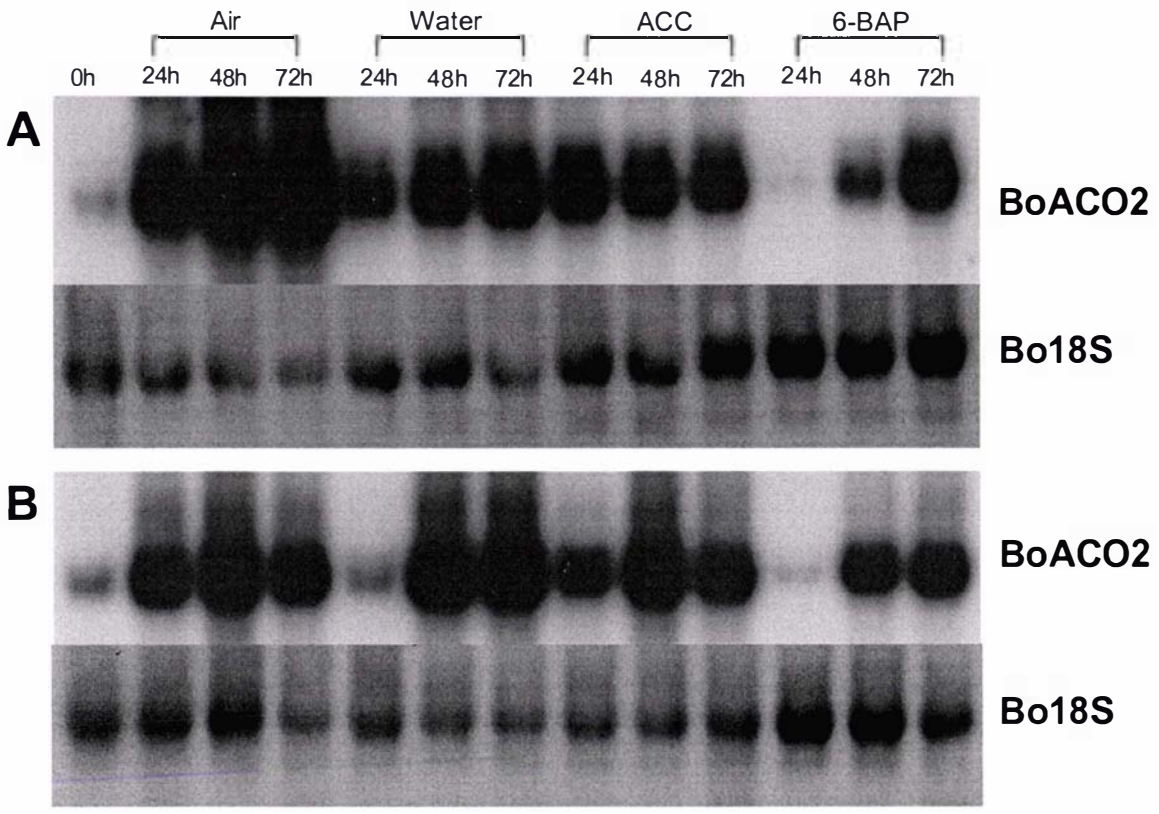

Figure 3.15 Autoradiographs showing the northern hybridisation of a 1.3 kb ^{32}P labelled *BoACO2* cDNA fragment and a 400 bp ^{32}P labelled *Bo18S* fragment, with total RNA from A. T_1- and B. antisense TOM13 Line 7 transgenic broccoli florets treated following harvest. Total RNA (10 µg) extracted from broccoli florets treated following harvest in air, water, ACC (1 mM) and 6-BAP (2.21×10^{-4} M), was denatured and separated in a 1.2% (w/v) agarose gel in 2.2 M formaldehyde, and then transferred to nylon membranes. All membranes were probed together with either a ^{32}P labelled *BoACO2* or *Bo18S* fragment. For details of hybridisation and washing conditions, see Methods and Materials, Section 2.8. These northern experiments were repeated with similar results.

after harvest, for both T_1^- and antisense *pTOM13* line 7 material treated in air. The overall transcript levels in florets appear to be similar for both T_1^- and transgenic antisense pTOM13 line 7 branchlets. All water-based treatments caused a small reduction in transcript accumulation in florets following harvest. The greatest decrease in transcript accumulation in florets following harvest was observed for branchlets treated with 6-BAP, particularly 24 h following harvest. The expression profile of *pTOM13* in antisense pTOM13 Line 7 florets following harvest was checked by northern analyses and no transcript was detected for *pTOM13* in any RNA sample (data not shown).

Figure 3.16 shows an unexpected result, regarding the up-regulation of *BoACS1* in response to 6-BAP treatment. *BoACS1* appeared to be present in two distinct bands. Analysis was difficult due to the general low expression of this gene compared to others following harvest. At harvest *BoACS1* transcript levels were easily detectable in florets and declined in the hours following harvest. These basal levels were maintained in florets through to 72 h following harvest for both T_1^- and antisense pTOM13 material, for all treatments with the exception of ACC. Less transcript appeared to be present at harvest in florets from antisense pTOM13 Line 7 plants compared to T_1^- florets. ACC caused an increase in *BoACS1* transcript levels in transgenic florets 72 h following harvest. *BoACS2* and *BoACS3* transcripts were not analysed in these tissues. However, other northern experiments carried out using RNA isolated from these tissues shows that 6-BAP also up-regulated the expression of *BoACS1* in T_1^- florets following harvest (data not shown).

The influence of exogenous feeding on the expression of senescence marker genes in detached florets from T_1^- and transgenic antisense pTOM13 line 7 broccoli following harvest is shown in Figures 3.17, 3.18 and 3.19. At harvest Chlorophyll a/b binding protein (*BoCAB1*) transcript levels were high in florets and declined rapidly following harvest for both T_1^- and antisense pTOM13 line 7 air-treated material (Figure 3.17). *BoCAB1* levels in florets were higher for all water-based treated branchlets 24 h following harvest than in the air-treated branchlets. Exogenous treatment of branchlets

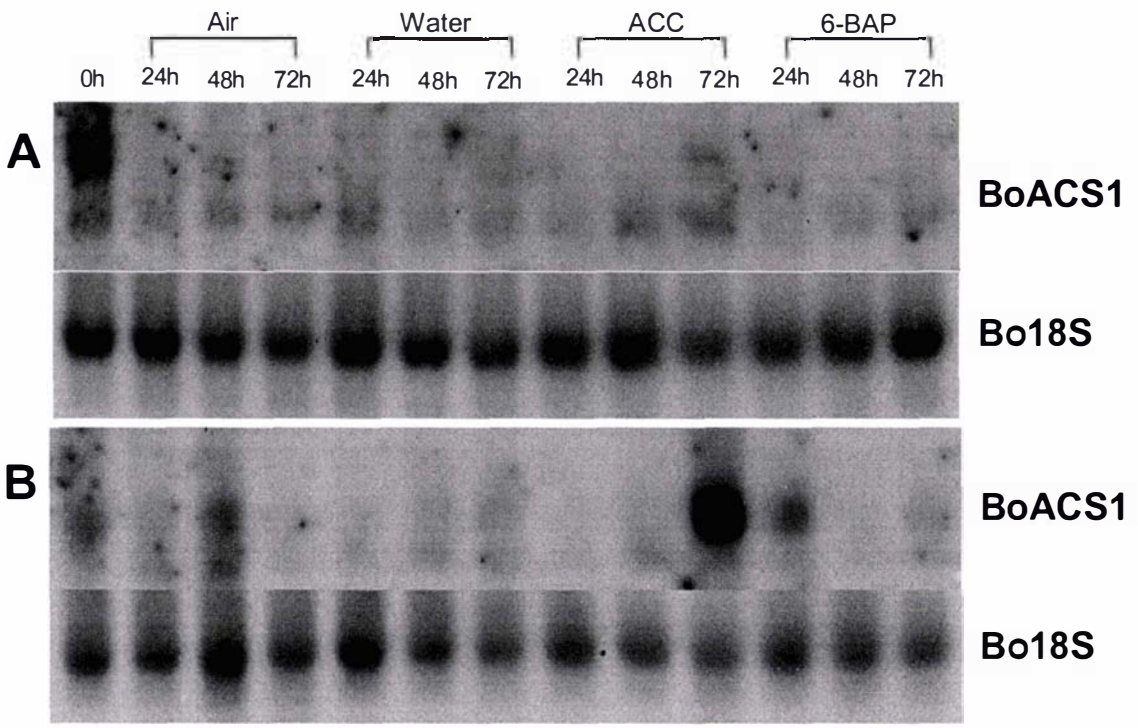

Figure 3.16 Autoradiographs showing the northern hybridisation of a 1.7 kb ^{32}P labelled *BoACS1* cDNA fragment and a 400 bp ^{32}P labelled *Bo18S* fragment, with total RNA from A. T_1 and B. antisense TOM13 transgenic broccoli florets treated following harvest. Total RNA (10 μg) extracted from broccoli florets treated following harvest in air, water, ACC (1 mM) and 6-BAP (2.21×10^{-4} M), was denatured and separated in a 1.2% (w/v) agarose gel in 2.2 M formaldehyde, and then transferred to nylon membranes. All membranes were probed together with either a ^{32}P labelled *BoACS1* or *Bo18S* fragment. For details of hybridisation and washing conditions, see Methods and Materials, Section 2.8. These northern experiments were repeated with similar results.

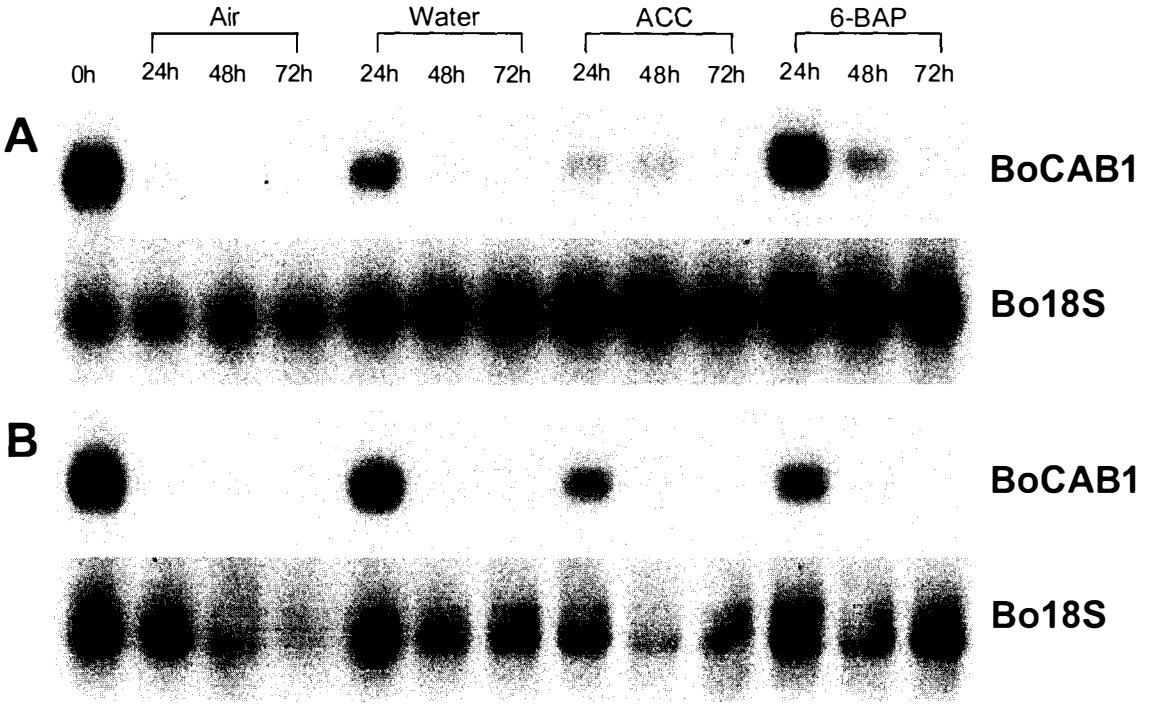

Figure 3.17 Autoradiographs showing the northern hybridisation of a 1.1 kb ^{32}P labelled *BoCAB1* cDNA fragment and a 400 bp ^{32}P labelled *Bo18S* fragment, with total RNA from A. T_1^- and B. antisense TOM13 transgenic broccoli florets treated following harvest. Total RNA (10 μg) extracted from broccoli florets treated following harvest in air, water, ACC (1 mM) and 6-BAP (2.21×10^{-4} M), was denatured and separated in a 1.2% (w/v) agarose gel in 2.2 M formaldehyde, and then transferred to nylon membranes. All membranes were probed together with either a ^{32}P labelled *BoCAB1* or *Bo18S* fragment. For details of hybridisation and washing conditions, see Methods and Materials, Section 2.8. These northern experiments were repeated with similar results.

with 6-BAP caused *BoCAB1* transcript levels to increase in florets 24-48 h following harvest compared to all other wet treatments (particularly in T_1^- florets).

Cysteine protease (*BoCP5*) transcript levels were low in florets at harvest and increased within 24 h following harvest, this level was maintained until at least 72 h following harvest for air-treated T_1^- and antisense pTOM13 line 7 branchlets although there was a reduction in transcript levels 72 h following harvest for antisense pTOM13 florets (Figure 3.18). All water-based fed branchlets had a similar transcript accumulation profile in florets except when treated with 6-BAP. *BoCP5* levels decreased compared to all other treatments in the presence of 6-BAP. The overall levels of *BoCP5* transcript in T_1^- and antisense pTOM13 line 7 florets appeared to be similar.

Metallothionein-like protein (*BoMLP*) transcript levels were low in florets at harvest and increased rapidly following harvest in air-, water- and ACC- treated T_1^- and antisense pTOM13 line 7 branchlets (Figure 3.19). 6-BAP treatment caused a delay in *BoMLP* transcript accumulation by 24 h in T_1^- florets and a reduction of *BoMLP* transcript levels in antisense pTOM13 line 7 florets 48 h following harvest.

3.4 DISCUSSION

Branchlets of broccoli (cultivar Marathon) were treated following harvest in air (dry control), or a variety of water-based treatments (water (control), sucrose, ACC, 6-BAP and 6-BAP + ACC) at 20°C in the dark for five days. Sepal yellowing was measured to monitor the rate of postharvest senescence using a chromameter (model II; Minolta, Osaka, Japan) as described by King and Morris (1994). For air-treated branchlets, the initial hue angle readings at harvest were around 130 and declined to around 110 in the 96 h following harvest (Figure 3.3), results which are comparable to those of King and Morris (1994).

Exogenous application of 6-BAP caused a delay in sepal yellowing even in the presence of applied ACC (Figures 3.2 and 3.3). This observation is consistent with the findings of Clarke et al. (1994). Applied 6-BAP also caused a reduction in the accumulation of

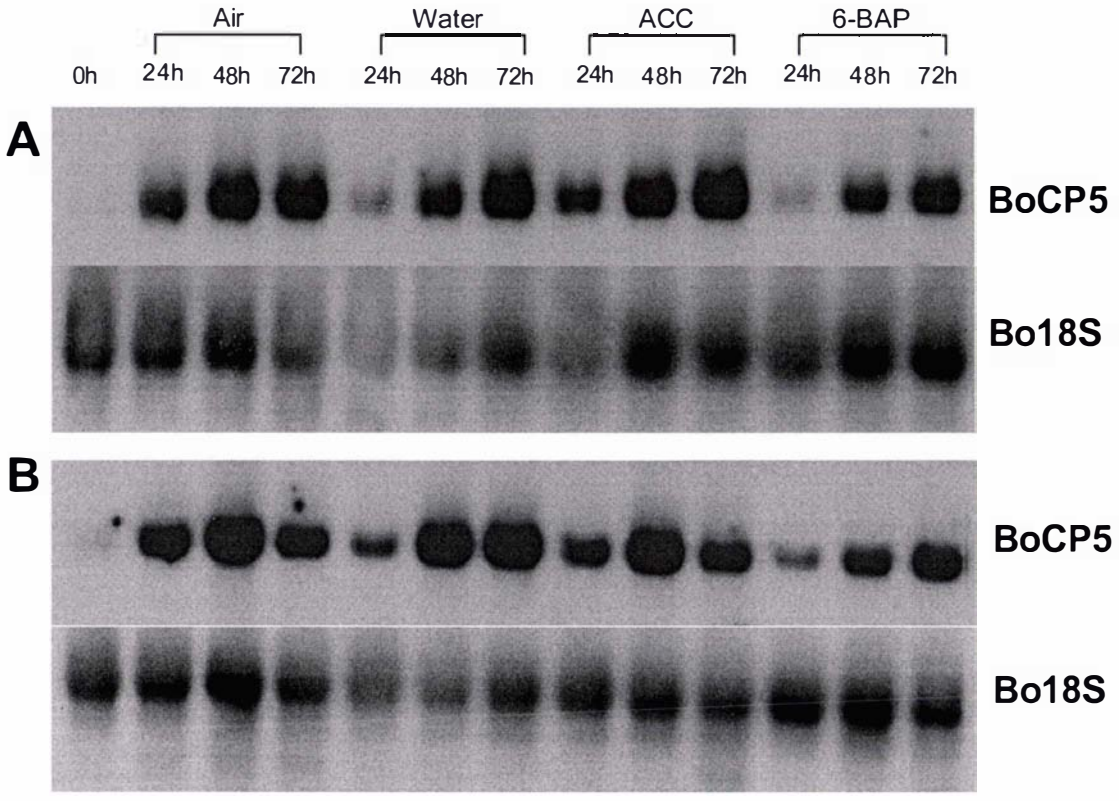

Figure 3.18 Autoradiographs showing the northern hybridisation of a 1.3 kb ^{32}P labelled *BoCP5* cDNA fragment and a 400 bp ^{32}P labelled *Bo18S* fragment, with total RNA from A. T_1^- and B. antisense TOM13 transgenic broccoli florets treated following harvest. Total RNA (10 μg) extracted from broccoli florets treated following harvest in air, water, ACC (1 mM) and 6-BAP (2.21×10^{-4} M), was denatured and separated in a 1.2% (w/v) agarose gel in 2.2 M formaldehyde, and then transferred to nylon membranes. All membranes were probed together with either a ^{32}P labelled *BoSAG2-4* or *Bo18S* fragment. For details of hybridisation and washing conditions, see Methods and Materials, Section 2.8. These northern experiments were repeated with similar results.

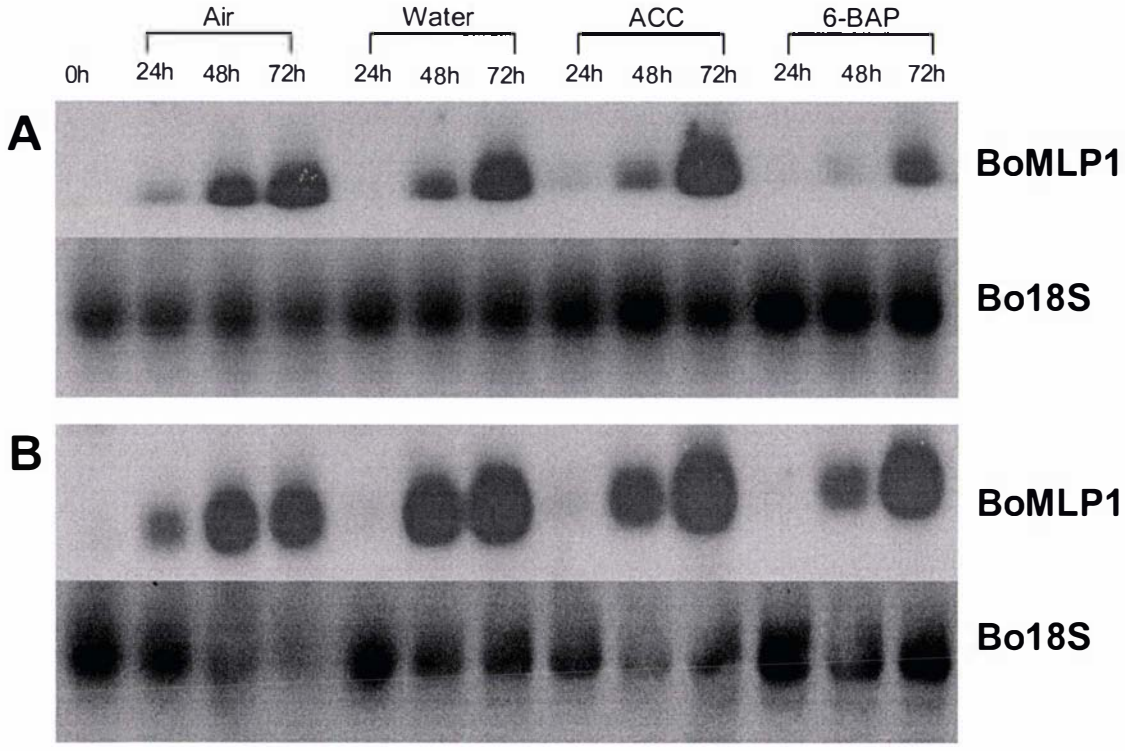

Figure 3.19 Autoradiographs showing the northern hybridisation of a 500 bp ^{32}P labelled *BoMLP1* cDNA fragment and a 400 bp ^{32}P labelled *Bo18S* fragment, with total RNA from A. T_1- and B. antisense TOM13 transgenic broccoli florets treated following harvest. Total RNA (10 μg) extracted from broccoli florets treated following harvest in air, water, ACC (1 mM) and 6-BAP (2.21×10^{-4} M), was denatured and separated in a 1.2% (w/v) agarose gel in 2.2 M formaldehyde, and then transferred to nylon membranes. All membranes were probed together with either a ^{32}P labelled *BoMLP1* or *Bo18S* fragment. For details of hybridisation and washing conditions, see Methods and Materials, Section 2.8. These experiemnts were repeated with similar results.

transcripts normally up-regulated during senescence (*BoCP5,* a cysteine protease; *BoMLP,* a metallothionein-like protein), and maintained transcript levels for chlorophyll a and b binding protein (*BoCAB1*) which is normally reduced rapidly following harvest (Figure 3.6). These observations suggest that exogenous application of 6-BAP is sufficient for delaying senescence in broccoli florets following harvest.

A schematic summary of a proposed model of how ethylene, cytokinin, and sugars may regulate different gene expression events during senescence in broccoli, based on observations from this research and citings in the literature, is shown in Figure 3.20. Genes encoding the enzymes responsible for the final stage of ethylene biosynthesis, namely *BoACO1* and *BoACO2* were down-regulated following exogenous treatment with cytokinin (Figure 3.4). These results suggest that cytokinins inhibit broccoli senescence by inhibiting ethylene biosynthesis. However, application of exogenous cytokinin also caused an increase in the level of both *BoACS1* and *BoACS2* (Figure 3.5) transcripts compared to all other wet treatments. The ACC synthase genes catalyse what is regarded as the first dedicated and rate limiting step of ethylene biosynthesis. 6-BAP may then both negatively and positively regulates ethylene biosynthesis.

Ethylene biosynthesis has been reported to be regulated by both positive and negative feedback by ethylene itself. During fruit ripening, the abundance of ACC synthase transcripts increased as ethylene production increased in both tomato and banana (Nakatsuka et al., 1998; Liu et al., 1999). Further, ethylene both positively and negatively regulated ethylene biosynthesis in mung bean hypocotyls. Exogenous ethylene increased ACC synthase transcript abundance whereas ACC oxidase transcript abundance was reduced (Kim et al., 2001). This feedback regulation by ethylene was reversed by the addition of the ethylene biosynthesis inhibitor aminooxyacetic acid (AOA) and the application of 6-BAP also abolished ethylene responsiveness with respect to the expression of ACC oxidase and synthase genes (Kim et al., 2001). Pogson et al. (1995a) showed that the gene expression of broccoli ACC oxidase (*BoACO2*) was positively regulated by ethylene during senescence in broccoli florets. It is possible that broccoli ACC synthase (*BoACS*) gene expression is under negative feedback control by ethylene during senescence in broccoli, and that 6-BAP treatment nullifies the potential

suppression by ethylene on *BoACS1* and *BoACS2* gene expression (Figure 3.5). Treatment with ACC, the precursor for ethylene, and with sucrose caused a reduction in *BoACS1* transcript abundance when compared to water treatment alone (Figure 3.5), and the effect of applied ACC was sufficient to over-ride the effects of exogenous 6-BAP. Furthermore, ACC treatment also caused an increase in *BoACO* (in particular *BoACO1*) transcript levels following harvest compared to water fed control tissue (Figure 3.4). It appears then that ACC might act as a negative regulator of ethylene biosynthesis at *BoACS* and a positive regulator at *BoACO* in broccoli florets during senescence.

It is clear from the work presented here that exogenous application of cytokinin alters the expression of genes involved in ethylene biosynthesis. However, Clarke et al. (1994) suggested that cytokinins exerted their inhibitory effect on senescence in broccoli by desensitising the tissue to ethylene. Further, Kim et al. (2001) showed that exogenous application of 6-BAP also had an inhibitory effect on ethylene action, apart from the ability to inhibit ethylene biosynthesis. Furthermore, Hall et al. (2001) suggested that cytokinins were involved in the early regulation of ethylene signal transduction. In pea epicotyls, treatment with ethylene led to the activation of monomeric GTP-binding proteins responsible for the activation of mitogen-activated protein kinase (MAPK) cascades (Novikova et al., 1997) and the receptor-directed inhibitor 1-methylcyclopropene (MCP) antagonised the activation of these GTP-binding proteins. In leaves of *Arabidopsis*, a similar effect was shown by the application of cytokinin: GTP-binding protein activation was antagonised, and leaf senescence was delayed (Novikova et al., 1999). One might then hypothesise that cytokinins regulate ethylene action at both the level of biosynthesis and at the level of perception during senescence in broccoli. However, it is possible that 6-BAP may cause the effect on ethylene biosynthesis by inhibiting the feedback regulation of ethylene rather than directly on the biosynthetic genes (Figure 3.20). This then, would support the hypothesis that cytokinin nullifies the feedback regulation of ethylene by desensitisation of the receptors to the hormone (if ethylene is not perceived, ACS is up-regulated and ACO is down regulated).

Figure 3.20 A schematic representation of the proposed regulation of ethylene biosynthesis, carbohydrate transport and carbohydrate metabolism by ethylene, ACC, sucrose and 6-BAP in broccoli florets. Ethylene induces the expression of *BoACO2* (Pogson et al., 1995) and suppresses the expression of broccoli ACC synthase genes (Kim et al., 2001). 6-BAP and to some extent ACC blocks the signalling pathway of ethylene, nullifying the induction of *BoACO2* gene expression by ethylene. 6-BAP also nullifies the suppression of *BoACS1* and *BoACS2* gene expression by ethylene, but this activation is reversed by ACC. 6-BAP also nullifies the trigger responsible for the induction of *BoSUC1*, *BoSUC2*, *BoINV1* and *BoHK1* gene expression following harvest. Arrow lines with + or – symbols represent the proposed signalling pathway. + and – indicate the inductive and suppressive effects on the expression of genes respectively.

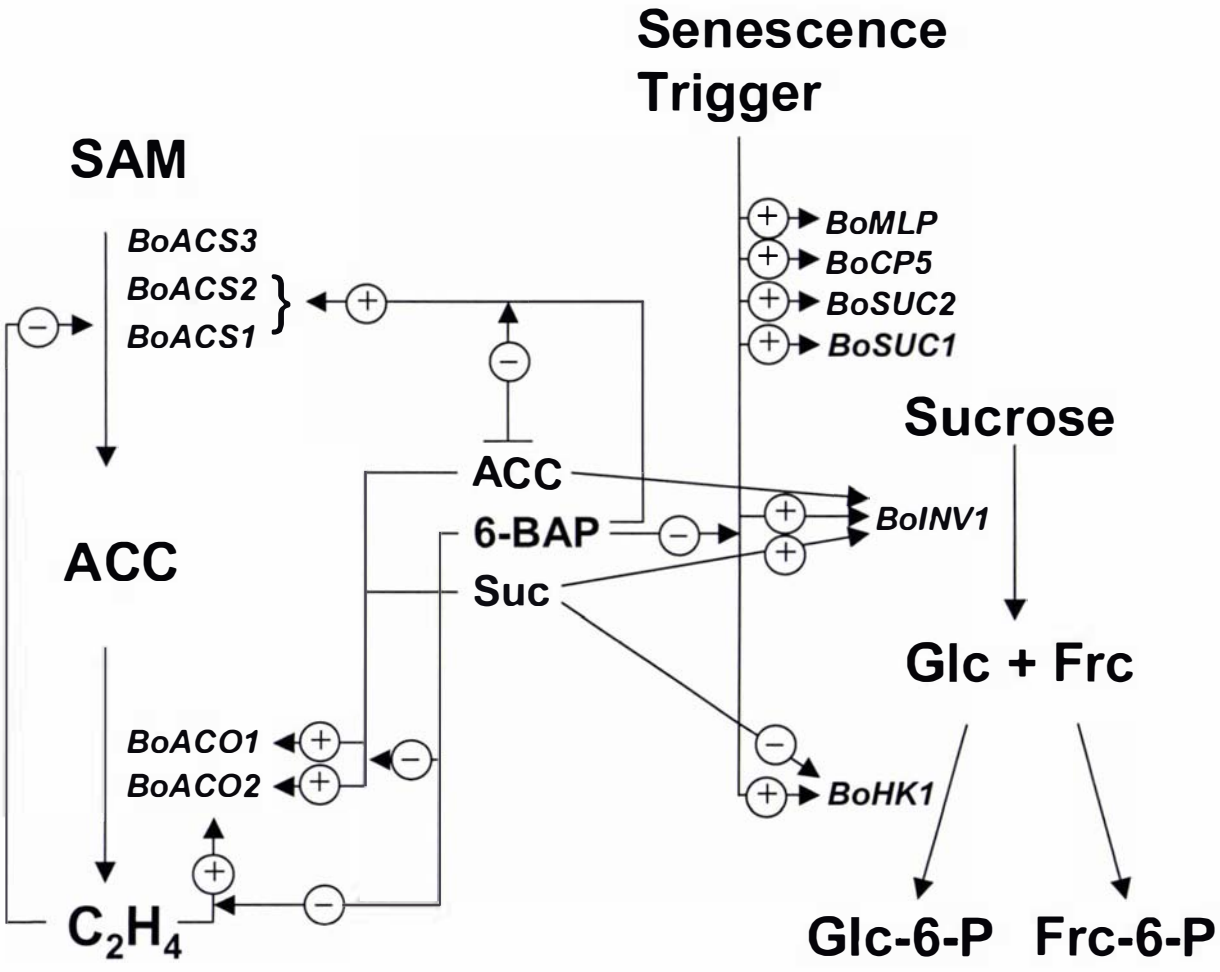
Senescence
Trigger
SAM
BoACS3
BoACS2
BoACS1
BoMLP
BoCP5
BoSUC2
BoSUC1
Sucrose
ACC
6-BAP
Suc
BoINV1
ACC
Glc + Frc
BoACO1
BoACO2
BoHK1
C2H4
Glc-6-P
Frc-6-P

Broccoli is an immature tissue, which has a very high respiratory rate. Once harvested this immature tissue, instead of being a sink for carbon, becomes a source because, to maintain the high levels of respiration, carbohydrates must be utilised. Harvest then triggers the up-regulation of genes encoding enzymes involved with the active energy-dependent loading of sucrose into the phloem by sucrose transporters, as well as genes encoding enzymes involved in sucrose metabolism (Coupe et al., 2003a). Invertase (*BoINV1*) enzymes are responsible for the irreversible cleavage of sucrose into fructose and glucose. Hexokinase (*BoHK1*) enzymes are responsible for catalysing the initial step of glycolysis, the phosphorylation of glucose. Exogenous cytokinin caused reduced expression of genes involved in carbohydrate transport (*BoSUC1* and *BoSUC2*) and metabolism (*BoINV1*and *BoHK1*) (Figures 3.7 and 3.8 respectively). These results suggest that because cytokinin application reduces senescence in broccoli, somehow it desensitises the trigger to up-regulate the expression of transcripts involved with carbohydrate metabolism and transport. However, Irving and Joyce (1995) showed that although exogenous cytokinin was sufficient to prevent chlorophyll loss in broccoli, it did not prevent the depletion of carbohydrates in florets following harvest. However, transport of exogenously fed cytokinin may not be rapid enough to the sites in florets where the main changes in gene expression involved in carbohydrate regulation of senescence to take place. Irving and Joyce (1995) also concluded that sucrose supply could be a discrete senescence factor with an effect independent of its role as a respiratory substrate.

Evidence is accumulating pointing towards simple carbohydrates being molecules involved with signal transduction (for review see Smeekens, 2000). It could be that in broccoli following harvest, exogenous cytokinin regulates not only ethylene biosynthesis and/or perception, but that signal transduction by simple sugars sucrose and hexose might also be regulated by cytokinin. The effects of the ectopic expression of a cytokinin synthase gene in the immature floral organs on the retention of simple sugars in these tissues would be interesting and could provide an answer to this question.

Seeds collected from primary transformants (T_0) harbouring an antisense ACC oxidase gene from tomato (pTOM13) (Green Beauty) (Henzi et al., 1999b), were sown and the resulting secondary transformant (T_1) plants analysed. Visual assessment and PCR was used as an initial screen to decide which plants had segregated from parent plants with transgenes present (T_1^+), or without transgenes present (T_1^-: genetically and phenotypically similar to wild-type). Southern analyses validated the initial visual observations and PCR analyses. Heads were harvested from mature plants and subjected to postharvest treatment in air, water, 6-BAP and ACC at 20°C in the dark. The shortage of plant material meant a scaled down experiment with up to only four treatments and three days postharvest storage. Three transgenic lines (Lines 7, 9 and 10), and T_1^- plants were chosen for treatment assessment in air, whilst line 7 and T_1^- material was treated with hormone following harvest. Line 7 has a normal phenotype, while Lines 9 and 10 carry a moderate to severe *rol* gene induced phenotype (Henzi, 1999).

Both transgenic Lines 9 and 10 had lower 'at harvest' whole floret chlorophyll content when compared to transgenic line 7 and T_1^- florets (Figure 3.12). This reduction in the initial chlorophyll content was also observed for leaf chlorophyll content (data not shown). However, the 'at harvest' chlorophyll content remained high in the 72 h following harvest for all three antisense pTOM13 lines analysed compared to T_1^- material. These results suggest that the antisense ACC oxidase gene present in these transgenic lines may be reducing ethylene production, inhibiting senescence and thus slowing down chlorophyll loss after harvest.

The influence of hormone treatment on sepal yellowing in both T_1^- and antisense pTOM13 (line 7) material is shown in Figure 3.13. It is evident that there was a lot of variation throughout this experiment as the 5% least significant difference (LSD) was very high (0.41). However, from these results it is safe to conclude that 'at harvest' chlorophyll content was maintained for antisense pTOM13 Line 7 material treated with air and 6-BAP, and also T_1^- material treated with 6-BAP. Possible reasons for the variation observed for these two experiments could be due to variation in developmental stage of the material harvested. It was observed above that initial chlorophyll content was different for different lines. Also, as the major losses in chlorophyll occur from 72

h following harvest (Clarke et al., 1994; King and Morris, 1994; Downs et al., 1997), care should be taken when making conclusions from these results. Further, it was noted during the growing season that the colour of the different plants varied markedly. It is possible then that the inconsistent chlorophyll results stem from some samples having more or less chlorophyll present at harvest with than other plants. A general trend observed in the glasshouse was that T_1^+ plants appeared to contain less chlorophyll than T_1^- plants.

If more tissue had been available at the time of harvest for these experiments, more data would have been collected by extending the time line following harvest and also increasing the number of replications. However, the decision to harvest over the first 72 h was made in order to collect tissue, which is sensitive to major changes in gene expression following harvest. It was hoped that characterisation of the expression of genes normally associated with early senescence processes in these tissues would give more valuable information regarding the senescence status of these plants following harvest.

Northern analyses were carried out on both antisense pTOM13 and T_1^-, wild-type 'like', material treated following harvest in air, water, ACC or 6-BAP. Total RNA was probed with the senescence-associated genes *BoCAB1*, *BoCP5* and *BoMLP* (Figures 3.17, 3.18 and 3.19 respectively). No significant changes in expression profiles were observed for any of the genes analysed with respect to differences in plant type (i.e. antisense pTOM13 Line 7 or T_1^-). These results suggest that changes in gene expression that are normally associated with a delay of senescence were absent in the antisense pTOM13 Line 7 plant samples. Postharvest treatment with 6-BAP caused an increase in the levels of *BoCAB1* transcript 24 h following harvest in wild-type treated florets, although very subtle changes were observed (Figure 3.6). Further, this postharvest treatment also caused a reduction of *BoCP5* and *BoMLP1* transcript levels 24 to 72 h following harvest (Figures 3.6). Similar results were expected if the antisense pTOM13 Line 7 tissues were reduced in senescence.

The PCR and Southern analyses clearly indicate that the pTOM13 lines were transformed (Figures 3.9 - 3.11). The question then arises, is the antisense pTOM13 expressed in these lines, and what effects can be seen on the *BoACO* transcript levels? If the antisense pTOM13 gene is expressed then we would expect one of two outcomes. 1) if antisense pTOM13 was expressed but unable to hybridise to *BoACO* transcript, detection of constitutively expressed *pTOM13* transcript and normal levels of *BoACO* transcript should be observed, or 2) if expressed antisense *pTOM13* was able to hybridise to *BoACO* transcript and induce the activation of double stranded RNA nucleases, no detection of *pTOM13* transcript and reduced levels of *BoACO* transcript should be observed. No *pTOM13* transcript was detected using northern analyses for postharvest treated material from Line 7. The expression profiles of *BoACO1* and *BoACO2* were similar for both antisense pTOM13 Line 7 and T_1^- material. It would appear that the pTOM13 gene was not expressed in the antisense pTOM13 Line 7 plants.

Henzi et al. (1999b) reported Line 7 contained six copies of the antisense pTOM13 gene. So many copies of a gene could lead to gene silencing and thus an inactive antisense gene. Henzi et al. (1999a) also reported a normal phenotype for the Line 7 plants. Consequently, it is possible that the *rol* genes were also silenced in these plants due to high copy number. It is interesting that in the T_1 plants, the *rolc* gene appears to be inherited in the same pattern as the antisense *pTOM13* gene (Figures 3.10 and 3.11). These data then provide an explanation for the fact that postharvest senescence was not effectively delayed and these plants displayed a normal phenotype.

Postharvest analysis of transgenic broccoli plants altered for cytokinin and ethylene status, away from the complicating influence of the *rol* genes will be interesting.

Chapter 4

Transformation of broccoli and *Arabidopsis* to alter ethylene and cytokinin biosynthesis

4.1 INTRODUCTION

In order to reduce ethylene evolution in broccoli, Henzi et al. (1999b) produced transgenic plants harbouring an antisense ACC oxidase gene from tomato (*pTOM13*). However, as discussed in Chapter 3, there are concerns regarding the reduced ethylene status of these plants. The antisense pTOM13 gene construct, while present in the genome of these plants, did not appear to be expressed in at least the one line which was analysed in detail. Further, the plants were produced by *Agrobacterium rhizogenes*-mediated transformation and some lines exhibited the aberrant phenotypes frequently associated with that form of transformation.

Similar abnormalities in phenotype have not been reported for *Agrobacterium tumefaciens*- mediated transformation. However, *A. tumefaciens*-mediated transformation of broccoli has generally resulted in very low transformation efficiency. Metz et al. (1995) published what is widely regarded as the most efficient procedure to transform broccoli using *A. tumefaciens*, with transformation rates sometimes exceeding 5%. Moloney et al. (1989) reported an *A. tumefaciens*-mediated transformation procedure for cotyledonary petioles of *Brassica napus*. They used a simpler method than Metz et al. (1995), which did not involve explant preculture prior to inoculation or the use of cell feeder layers. This procedure has been developed further for broccoli transformation (Judith Irwin, personal communication) and described here. A portion of this chapter has been published (Gapper et al., 2002).

The primary aims of the research reported in this chapter were to transform broccoli using *A. tumefaciens* and to produce lines with reduced ethylene and enhanced cytokinin status. To reduce ethylene biosynthesis in broccoli, a construct harbouring an

antisense ACO gene from broccoli (Pogson et al., 1995), driven by a harvest-induced asparagine synthetase (AS) promoter from asparagus (Moyle, 1997) was constructed. In addition, constructs designed to enhance cytokinin production were cloned using a cytokinin synthase gene from *A. tumefaciens* (*ipt*) driven by either the senescence associated gene promoter SAG_{12} (Gan and Amasino, 1995) from *Arabidopsis*, or the floral-associated gene promoter MYB_{305} from *Antirrhinum majus* (snapdragon). The longer term aim was to produce broccoli plants with both reduced ethylene biosynthesis as well as enhanced cytokinin biosynthesis by either crossing the single transgenic plants or by producing transgenic plants harbouring larger constructs to simultaneously alter both ethylene and cytokinin biosynthesis.

4.2 METHODS AND MATERIALS

4.2.1 Plant Material

4.2.1.1 Broccoli (*Brassica oleracea* var. *italica*) The broccoli cultivar, Triathalon, was used for all transformation experiments. Hypocotyl and cotyledonary petiole explants were used in all shoot regeneration and plant transformation experiments. *Agrobacterium tumefaciens* strains AGL1, GV3101 and LBA4404 harbouring the binary vectors pPN10, pPN109, pPN110, pPN111, pART27, pPN1, pPN11 and pBJ49 were used (for details see Table 2.1). The binary vectors contained either an antisense ACO gene from broccoli (*BoACO2*, Pogson et al., 1995a) driven by the harvest-induced asparagine synthetase (AS) promoter from asparagus (Moyle, 1997), the senescence auto-regulated SAG_{12}-IPT chimeric construct (Gan and Amasino, 1995), an IPT gene driven by the floral-associated MYB_{305} promoter from *Antirrhinum*, or a combination of these constructs (for details see Table 2.1). All the binary vectors were based on pART27 (Gleave, 1992), which contains the chimeric gene (*nos-nptII-nos*), which renders transformed plant cells resistant to kanamycin. pPN1 and pPN11 were made from the pART27 based vector pBJ49, which contains the chimeric gene (*nos-hpt-nos*), which renders transformed plant cells resistant to hygromycin.

4.2.1.2 *Arabidopsis*

Medium used:

- Germination medium - ½ x MS salts (Murashige and Skoog, 1962), L5 vitamins, 3% sucrose (v/v), 0.8 % Phytagar (w/v), pH 5.7.

The ecotype Columbia (Col-1) was used in all transformation experiments. Seeds were surface sterilised in absolute ethanol for 1 min followed by 20% (v/v) commercial bleach (active ingredient, 1 g L^{-1} sodium hypochlorite) for 20 min. The seeds were washed three times in sterilised water, plated on solid germination medium and placed at 4°C for 48 h prior to germination. Seedlings were grown with a 16 h photoperiod at 25°C for two weeks, ex-flasked and planted in soil, and then grown in a containment glasshouse under natural light with aerial watering. After a further 2-3 weeks growth, plants were ready for transformation using the floral dip method described by Clough and Bent (1998) using *Agrobacterium tumefaciens* strain AGL1 containing the binary vectors pART27, pPN10, pBJ49, pPN1 and pPN11 (for details see Table 2.1).

4.2.2 Binary vectors and cloning strategies

The T-DNA regions for all the cloned constructs from this section of work is shown schematically in Figure 4.1.

4.2.2.1 pPN10 - AS-BoACO2-OCS3' The strategy involving the cloning of this chimeric gene construct is shown in four steps in Figure 4.2.

I. The ACC oxidase 2 cDNA from broccoli (*BoACO2*) was cut from its pBLUESCRIPT vector by *Not* I digestion. These sites were then blunt-ended using T4 DNA polymerase. The blunt-ended BoACO2 fragment was then digested with *Xba* I and subsequently cloned into *Sma* I-*Xba* I digested pBLUESCRIPT. This vector was given the name pBoACO2.

II. The vector pASP3 (containing the asparagine synthetase (AS) promoter from asparagus) was digested with *Nco* I, and this site blunt-ended using T4 DNA polymerase. The AS insert was removed from pASP3 by digestion with *Eco* RI. The pBoACO2 vector was digested with *Pst* I, and this site was blunt-ended using T4 DNA polymerase. The linearised pBoACO2 vector

Figure 4.1 Schematic representation of the T-DNA regions (not to scale) of the binary vector constructs. LB, left T-DNA border; RB, right T-DNA border; NOS, promoter and terminator from the nopaline synthase gene from *A. tumefaciens*; *NPTII*, neomycin phosphotransferase II gene for kanamycin resistance; HPT, hygromycin phosphotransferase gene for hygromycin resistance; OCS3', 800 bp octopine synthase terminator from *A. tumefaciens*; BoACO2, 1.2 kb broccoli ACC oxidase 2 fragment in antisense orientaion; IPT, 700 bp isopentenyl transferase from *A. tumefaciens* in sense orientation ; IPT-TERM, 2 kb fragment containing isopentenyl transferase gene from *A. tumefaciens* in sense orientation and an unknown terminator sequence. AS promoter, 2 kb harvest-induced asparagine synthetase promoter from asparagus; SAG_{12} promoter, 2 kb senescence-associated gene promoter frrom *Arabidopsis*; MYB_{305} promoter, 3 kb floral-associated promoter from *A. majus*. Arrows indicate 5' to 3' direction (sense →; antisense ←). Useful restriction sites are also marked.

pPN10 (AS-ACO-OCS3' in pART27)

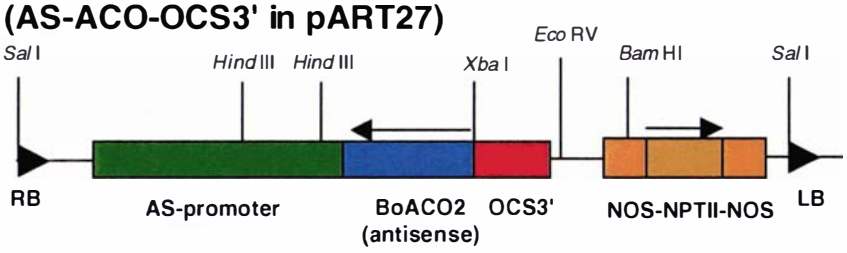

pPN109 (SAG_{12}-IPT-NOS3' in pART27)

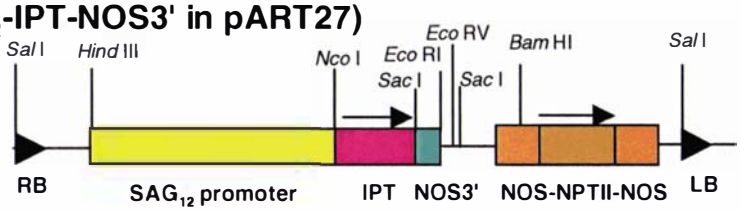

pPN11 (SAG_{12}-IPT-NOS3' in pBJ49)

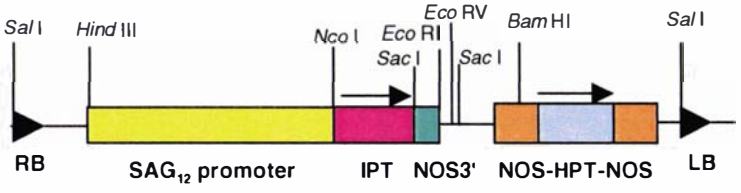

pPN110 (MYB_{305}-IPT-TERM in pART27)

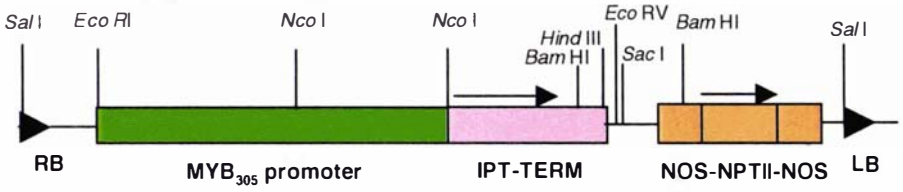

pPN1 (MYB_{305}-IPT-TERM in pBJ49)

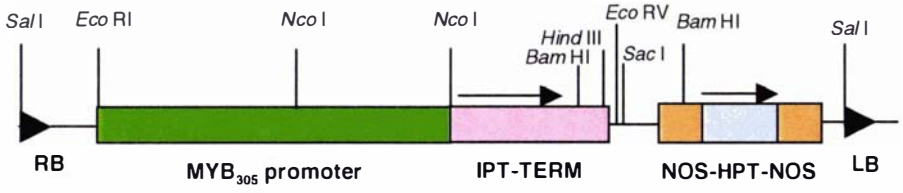

pPN111 (MYB_{305}-IPT-TERM::AS-ACO-OCS3' in pART27)

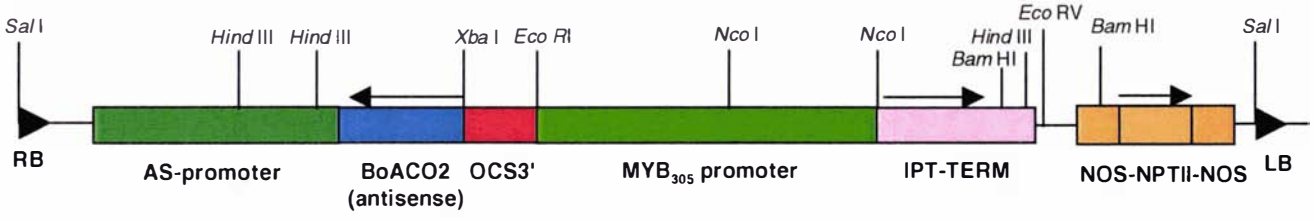

pPN112 (SAG_{12}-IPT-TERM::AS-ACO-OCS3' in pART27)

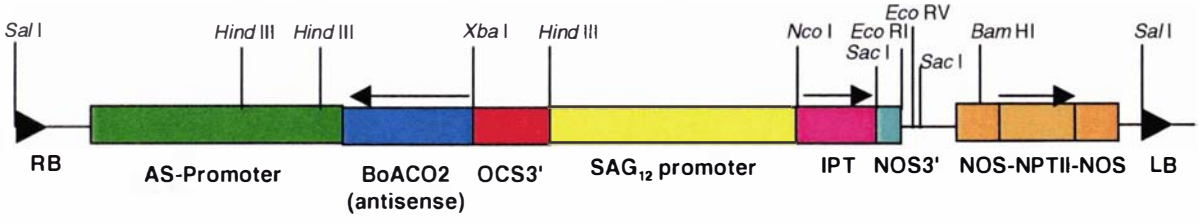

I

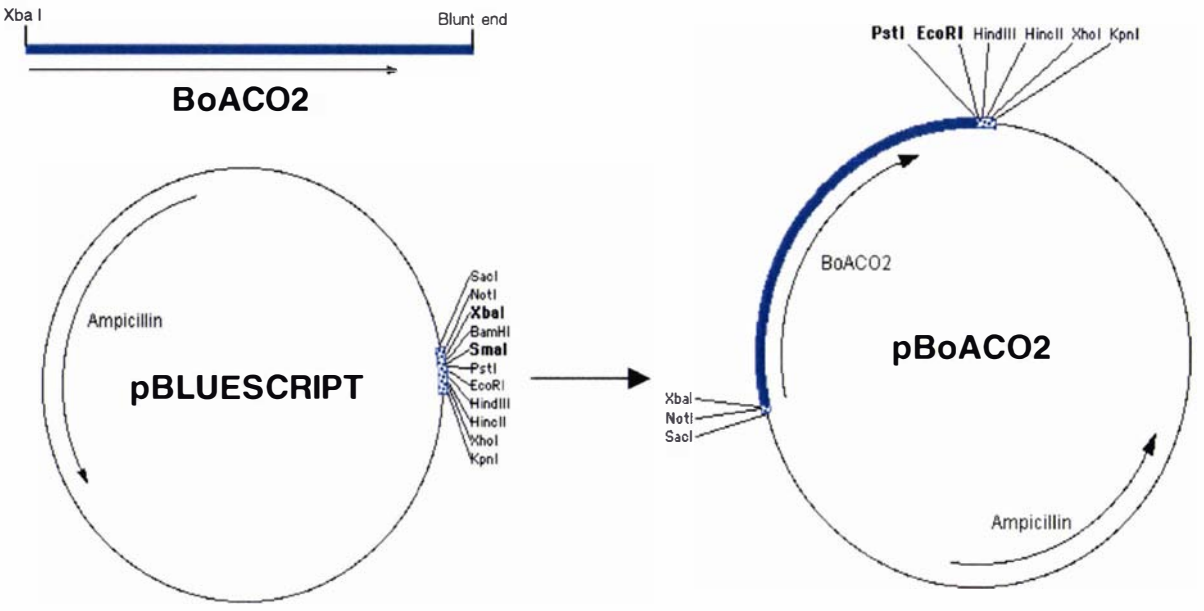

The BoACO2 fragment was digested with *Not* I then blunt ended and subsequently digested with *Xba* I. This fragment was then cloned into the *Xba* I and *Sma* I sites of pBLUESCRIPT to produce pBoACO2. Successful cloning was confirmed by restriction digest and PCR analyses (data not shown).

II

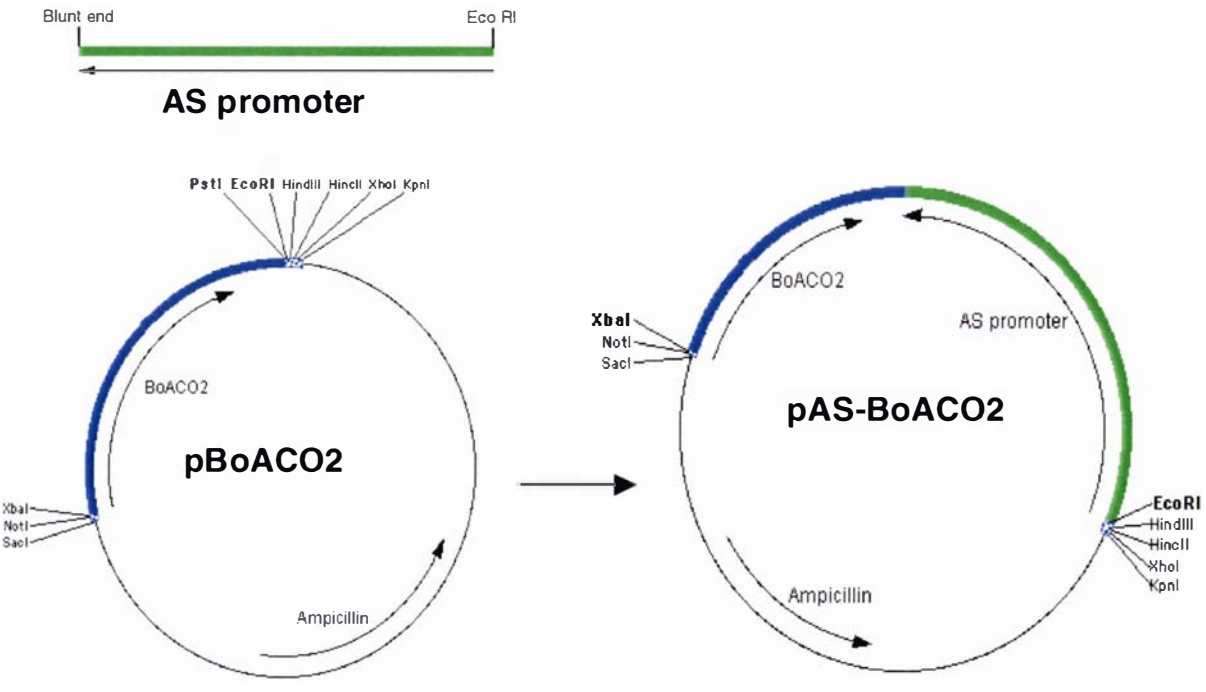

pBoACO2 was digested with *Pst* I and this site was subsequently blunt ended. The plasmid was then digested with *Eco* RI, and the *Eco* RI/blunt AS promoter fragment was cloned into these sites. pAS-BoACO2 was digested with *Xba* I and *Eco* RI to liberate the AS-BoACO2 fragment for subsequent cloning steps. Successful cloning was confirmed by sequencing (data not shown).

Figure 4.2 Cloning strategy of pPN10 binary vector.

III

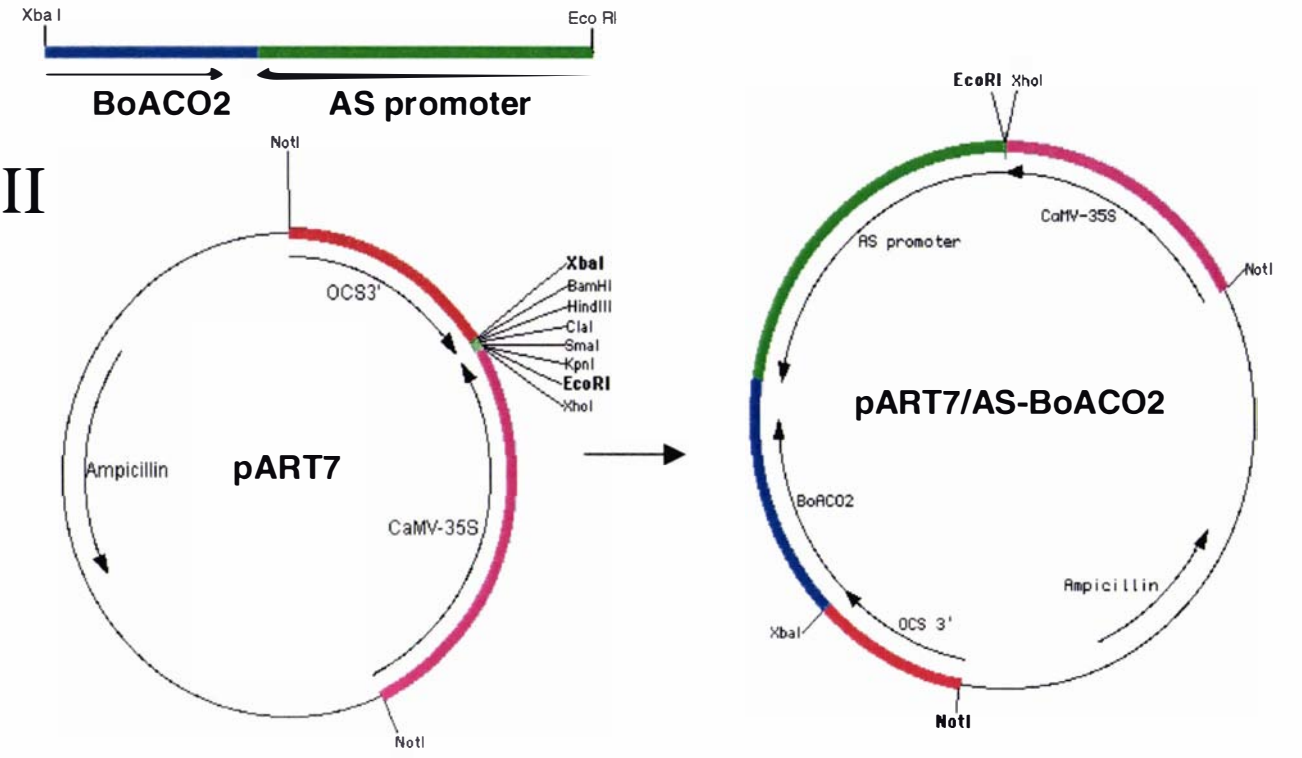

The *Eco* RI/*Xba* I AS-BoACO2 fragment digested from pAS-ACO2 was cloned into the *Xba* I and *Eco* RI sites of pART7 to generate a terminator (OCS3') to the antisense construct. pART7/AS-BoACO2 was digested with *Not* I and *Eco* RI to liberate the AS-BoACO2-OCS3' fragment, which was subsequently blunt ended. Successful cloning was confirmed by restriction digestion (data not shown).

IV

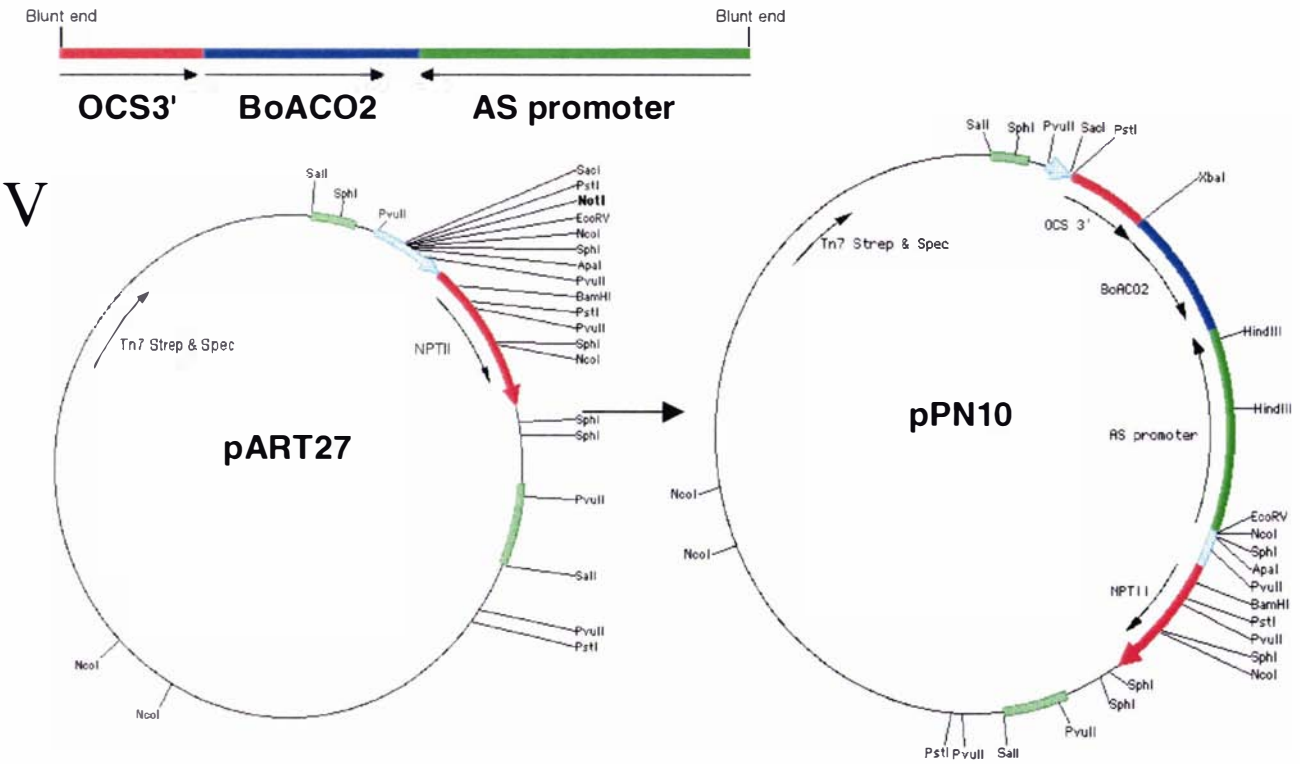

The blunt ended AS-BoACO2-OCS3' fragment was cloned into previously blunt ended *Not* I site of pART27 to produce the binary vector pPN10. Successful cloning was confirmed by PCR analysis (data not shown).

Figure 4.2 Cloning strategy of pPN10 binary vector (continued).

was then digested with *Eco* RI and the earlier prepared AS promoter was cloned into these blunt-ended sites. This vector was named pAS/BoACO2, and was sequenced in both directions using the T3 and T7 primer sites of the vector, to check orientation of the two inserted fragments.

III. The AS-BoACO2 insert was removed from pAS/BoACO2 by *Eco* RI-*Xba* I digestion, and cloned into the *Eco* RI-*Xba* I sites of pART7 (Gleave, 1992). This vector was named pART7/AS-BoACO2.

IV. *Eco* RI-*Not* I digestion of pART7/AS-BoACO2 yielded the 3.9 kb fragment containing the chimeric gene construct AS-BoACO2-OCS3'. This insert was then blunt-ended and cloned into the blunt-ended *Not* I site of pART27 (Gleave, 1992) to form the new binary vector pPN10.

4.2.2.2 pPN11 and pPN109 - SAG_{12}-IPT-NOS3' The pUC18 based vector pSG516 was donated by Dr Richard Amasino, and contained the chimeric gene SAG_{12}-IPT-NOS. The chimeric gene was removed from pSG516 by digesting with *Sph* I – *Sma* I. The released 3.2 kb fragment was then cloned into the *Sph* I and *Eco* RV sites of pGEM5zf vector to produce another *Not* I site at the terminator end of the chimeric gene. This vector was named pGEM5/SAG_{12}-IPT. *Not* I digestion of this vector yielded the 3.2 kb chimeric gene, which was cloned into the *Not* I sites of pBJ49 to produce the binary vector pPN11 and into pART27 to produce the binary vector pPN109.

4.4.2.3 pPN1 and pPN110 - MYB_{305}-IPT-TERM The pBLUESCRIPT based vector pGAK4 contained the chimeric gene MYB_{305}-IPT-TERM. *Not* I digestion of this vector yielded the 6kb fragment containing the chimeric gene. This *Not* I fragment was cloned into *Not* I digested pBJ49, to produce the binary vector pPN1 and into pART27 to produce the binary vector pPN110.

4.2.2.4 pPN111 – MYB_{305}-IPT-TERM::AS-BoACO2-OCS3' pART7/AS-BoACO2 was digested with *Eco* RI and this site was then blunt-ended using Bacteriophage T4 DNA polymerase, and *Not* I adapters (New England Biolabs) were ligated to this blunt site. This linearised vector was then digested with *Not* I to yield the 3.9 kb AS-BoACO2-OCS3' fragment, which was then cloned into the *Not* I site of pGEM5zf. This vector

was named pGEM/AS-BoACO2-OCS3', and was digested with *Not* I to yield the 3.9 kb AS-BoACO2-OCS3' fragment. pGAK4 was also digested with *Not* I to yield the 6kb MYB_{305}-IPT-TERM fragment. Both these *Not* I fragments were then cloned into the *Not* I site of pART27 in a three-way ligation to produce the binary vector pPN111.

4.2.2.5 pPN112 - SAG_{12}-IPT-NOS3'::AS-ACO2-OCS3' pART7/AS-BoACO2 was digested with *Eco* RI and this site was then blunt-ended using Bacteriophage T4 DNA polymerase. The SAG_{12}-IPT-NOS3' fragment of pSG516 was liberated by digestion with *Sma* I-*Sph* I. The *Sph* I site was blunt-ended using the Klenow fragment of *E. coli* DNA polymerase I. The blunt 3.2 kb SAG_{12}-IPT-NOS3' fragment was then cloned into the blunt-ended *Eco* RI site of pART7/AS-BoACO2. *Not* I digestion liberated a 7.1 kb SAG_{12}-IPT-NOS3'::AS-BoACO2-OCS3' fragment which was cloned into the *Not* I site of pART27 to produce the binary vector pPN112 (Gleave, 1992).

4.2.3 Transformation

4.2.3.1 Broccoli

Media used:

- Seed germination medium - 1 x MS salts, B5 vitamins, 3% sucrose (v/v), 0.8 % Phytagar (w/v), pH 5.7, poured into medium tubs (50 mm deep, 90 mm diameter).
- Co-cultivation medium - 1 x MS salts, B5 vitamins, 3% sucrose (v/v), 13.3 µM 6-benzyl amino purine (6-BAP) (3 mg L^{-1}), 0.8 % Phytagar (w/v), pH 5.7, poured into petri dishes (20 mm deep, 90 mm diameter).
- Selection medium - 1 x MS salts, B5 vitamins, 3% sucrose (v/v), 3 mg L^{-1} 6-benzyl-amino purine (6-BAP), 0.7 mM ticarcillin disodium (Timentin) (300 mg L^{-1}), 0.8 % Phytagar (w/v), pH 5.7, containing either 42.8 µM kanamycin (25 mg L^{-1}), or either 3.8 or 14.3 µM hygromycin B (2 or 7.5 mg L^{-1}), poured into plates (20 mm deep, 90 mm round).
- Rooting medium - 1 x MS salts, B5 vitamins, 3% sucrose (v/v), 0.35 mM ticarcillin disodium (Timentin) (150 mg L^{-1}), 0.8 % Phytagar (w/v), pH 5.7, containing either 85.6 µM kanamycin (50 mg L^{-1}), or 3.8 µM hygromycin B (2 mg L^{-1}), poured into medium tubs.
- Bacterial minimal culture medium - 7.6 mM $(NH_4)_2SO_4$, 1.7 mM sodium citrate, 78.7 mM K_2HPO_4, 0.33 M KH_2PO_4, 1 mM $MgSO_4$, 0.2% sucrose (w/v), pH 7.2.

A cotyledonary petiole and hypocotyl based system was modified from Moloney et al. (1989) and Judith Irwin (personal communication), and used as described by Gapper et al. (2002), and is shown by flow diagram in Figure 4.3. Seeds were surface sterilised in

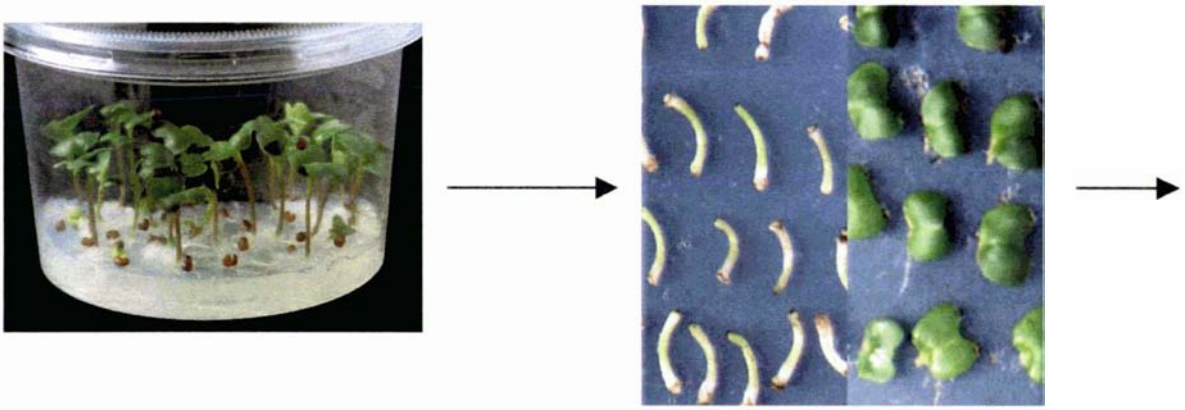

Hypocotyl and cotyledonary petiole explants excised from five day old seedlings and inoculated in *A. tumefaciens* culture (A_{660} 0.1), were co-cultivated for three days then transferred to selection media containing antibiotics.

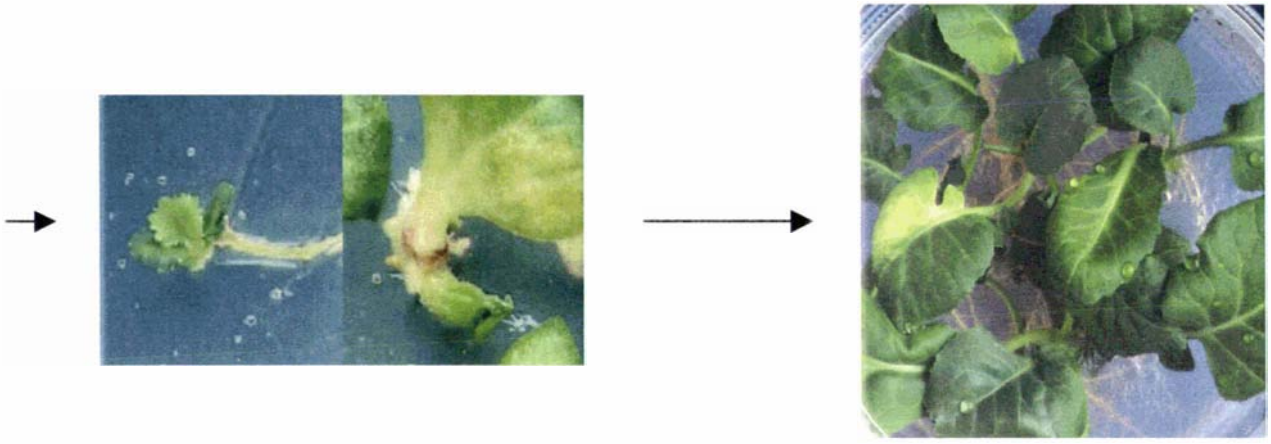

Putative transgenic shoots regenerated after between three and eight weeks from inoculated explants, and were transferred to hormone-free rooting media. Plant numbers were amplified clonally by adventious shoot regeneration. Once roots were established plantlets were exflasked and transferred to soil and grown to maturity in a containment glasshouse.

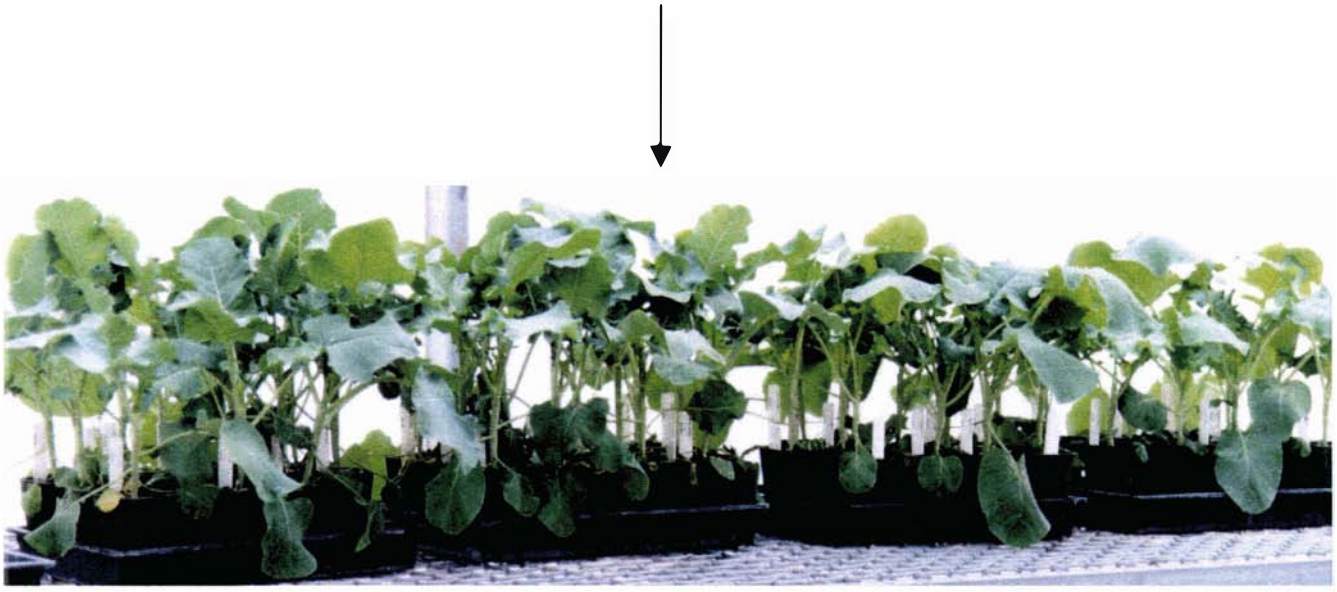

Figure 4.3 Flow diagram of the broccoli transformation procedure as described by Gapper et al. (2002).

absolute ethanol for one minute followed by 20% (v/v) commercial bleach (active ingredient, 1 g L^{-1} sodium hypochlorite) for 20 min followed by three washes in sterile water. After an initial overnight incubation at 4°C, sterilised seeds were germinated at 25°C with a 16 h photoperiod on solid germination media. Cotyledonary petiole and hypocotyl explants were then excised from 5 d old seedlings. Explants were inoculated with *A. tumefaciens* cultures, which had been grown in and subsequently diluted in minimal media to an OD_{600nm} of 0.1. The cut ends only of cotyledonary petioles were dipped briefly, while hypocotyls were fully immersed briefly, diluted in culture. The inoculated cut ends of the cotyledonary- petiole explants were planted at least 2 mm into co-cultivation media whereas hypocotyl explants were placed horizontally on top of the medium. The plates were sealed with micropore tape (3M). After 3 d of co-cultivation at 20 or 25°C (16 h photoperiod), the explants were transferred to selection media containing ticarcillin disodium (Timentin) and either kanamycin or hygromycin, with or without 29.4 μM silver nitrate (5 mg L^{-1}). Inoculated explants were transferred to fresh selection medium every two weeks. Kanamycin-resistant shoots were transferred to hormone-free rooting media containing kanamycin and Timentin, and hygromycin-resistant shoots were transferred to hormone-free media containing hygromycin and Timentin.

4.2.3.2 *Arabidopsis*

Media used:

- LB medium - 10 g L^{-1} bacto-tryptone, 5 g L^{-1} yeast extract, 10 g L^{-1} NaCl
- Inoculation medium - 5% sucrose (w/v), 0.05% silwet (v/v)

Plants with floral stalks 2-10 cm in length were chosen for transformation experiments. *Agrobacterium tumefaciens* strain AGL1 harbouring the binary vectors pART27, pBJ49, pPN1, pPN10 and pPN11 (for binary vector details see Table 2.1 in see Section 2.3) were grown in LB medium (500 ml) at 28°C under the appropriate antibiotic selection (for pART27 and pPN10 68.6 μM streptomycin sulphate (100 mg L^{-1}) and 85.6 μM kanamycin mono sulphate (50 mg L^{-1}); for pBJ49, pPN1 and pPN11 68.6 μM streptomycin sulphate and 95 μM hygromycin b (50 mg L^{-1})), until the culture reached an OD_{660} of around 1.0. The culture was then centrifuged at 3000g or 10 minutes at 4°C

to pellet the cells. The cells were then resuspended in inoculation media (1 L) to give a final OD_{660} of 0.5. *Arabidopsis* plants were then dipped in the *A. tumefaciens* culture for 1 min, making sure all floral tissue was inoculated. Plastic bags were then placed over the plants to avoid water loss and the covered plants placed in the dark for 24 h. The plastic bags were removed, and the plants were returned to the containment glasshouse under natural light with aerial watering. The plants were grown until siliques were mature, after which they were removed from watering, siliques dried and seeds collected. The resulting seeds were germinated as described above under the appropriate antibiotic selection (for pART27 and pPN10, 85.6 μM kanamycin (50 mg L^{-1}); for pBJ49, pPN1 and pPN11, 9.5 μM hygromycin (5 mg L^{-1})).

4.2.4 Molecular analyses

PCR, Southern, RT-PCR based 'virtual northern' and northern analyses were used individually or in combination to verify successful transformation of broccoli and *Arabidopsis*. For details of these techniques see Methods and Materials, Chapter 2.

4.2.5 Crosses

Transgenic (T_0) and wild-type (F_1) broccoli plants were self-fertilised, and crosses were also made to produce T_1 transgenic seed and F_2 wild-type seed. Pollen was collected on sterile toothpicks by gently brushing the anthers of open flowers. The pollen was transferred to the female reproductive structures of open flowers, again by gentle brushing. Pollinated flowers were marked by tagging and seeds collected once pods had matured. Seed produced from these crossing and 'selfing' experiments were not screened in the body of this work.

4.2.6 Experimental

The transformation experiments for broccoli outlined in this chapter are separated into three experiments. Experiment I was carried out at the Lincoln site of Crop & Food Research. All explants were co-cultivated and selected at 25°C, and under a 16 h photoperiod, with 20 explants per plate. Experiment II was carried out at the Palmerston North site of Crop & Food Research. All explants were co-cultivated and selected at 20°C with a 16 h photoperiod, and 10 cotyledonary petioles and 15 hypocotyls per plate.

Variables such as explant age and silver nitrate were also tested in this experiment. Experiment III was also carried out at the Palmerston North site, but conducted at 25°C.

4.3 RESULTS

4.3.1 Broccoli transformation

Shoot regeneration rates with no antibiotic selection were optimised at 3 mg L^{-1} 6-BAP for both hypocotyl and cotyledonary petiole explants for the cultivar Triathalon (Gapper et al., 2002). On this medium, approximately 75% of the cotyledonary petiole explants regenerated shoots while approximately 95% of the hypocotyl explants regenerated shoots.

Following *A. tumefaciens*-transformation of broccoli using strains and binary vectors described, green putative transgenic shoots regenerated between 3-12 weeks following co-cultivation on medium containing 3 mg L^{-1} 6-BAP and 300 mg L^{-1} ticarcillin disodium as well as the appropriate antibiotic selection. The green putative transgenic shoots were transferred to hormone-free media and selection was still maintained during root organogenesis (not all shoots regenerated roots, of which most were found to be non-transgenic escapes).

The level of kanamycin antibiotic selection (25 mg L^{-1}) for transformed broccoli shoots harbouring an *nptII* gene was previously optimised and has been reported (Metz et al., 1995, Henzi et al., 1999b). This level of kanamycin was sufficient to ensure only low levels of false positive shoots and a number of putative transgenic lines were produced using this level of selection (Table 4.1).

An initial level of 7.5 mg L^{-1} hygromycin was used to select for transgenic broccoli shoots harbouring an *hpt* gene. No putative transgenic plants were recovered from transformation experiments on this level of hygromycin, as all explants died rapidly under this selection pressure (Table 4.1; Experiment I, Lincoln). Subsequently, a shoot regeneration experiment using various levels of hygromycin (kill curve; 0-19 μM; 0-10 mg L^{-1}) revealed that 7.5 mg L^{-1} hygromycin was too high (Figure 4.4). However, a

Table 4.1 Results of broccoli transformation experiments. Transformation efficiency equals the number of independent transgenic lines obtained per 100 explants inoculated.

Construct	Selection (mg L^{-1})	Plasmid	Site	Co-cultivation temperature (^{o}C)	*A. tumefaciens* strain	Ag^{+} (+/-)	Explant type	Total explants	Total lines	Transformation efficiency (%) [4] (based on PCR)	Number of lines confirmed by Southern
AS-ACO	Kan 25	pPN10	Lincoln[1]	25	AGL1	-	hypocotyl	266	0	0 (0-1.4)	0
AS-ACO	Kan 25	pPN10	Lincoln[1]	25	GV3101	-	hypocotyl	272	3	1.1 (0.2-3.2)	3
AS-ACO	Kan 25	pPN10	Lincoln[1]	25	AGL1	-	petiole	526	9	1.7 (0.8-3.2)	9
AS-ACO	Kan 25	pPN10	Lincoln[1]	25	GV3101	-	petiole	541	14	2.6 (1.4-4.3)	14
pART27	Kan 25	pART27	Lincoln[1]	25	AGL1	-	hypocotyl	423	3	0.7 (0.1-2.1)	3
pART27	Kan 25	pART27	Lincoln[1]	25	GV3101	-	hypocotyl	201	4	2.0 (0.5-4.4)	4
pART27	Kan 25	pART27	Lincoln[1]	25	AGL1	-	petiole	845	0	0 (0-0.4)	0
pART27	Kan 25	pART27	Lincoln[1]	25	GV3101	-	petiole	402	1	0.2 (0-1.4)	1
MB-IPT	Hyg 7.5	pPN1	Lincoln[1]	25	AGL1	-	hypocotyl	250	0	EDE	N/A
MB-IPT	Hyg 7.5	pPN1	Lincoln[1]	25	GV3101	-	hypocotyl	272	0	EDE	N/A
MB-IPT	Hyg 7.5	pPN1	Lincoln[1]	25	AGL1	-	petiole	499	0	EDE	N/A
MB-IPT	Hyg 7.5	pPN1	Lincoln[1]	25	GV3101	-	petiole	545	0	EDE	N/A
SG-IPT	Hyg 7.5	pPN11	Lincoln[1]	25	AGL1	-	hypocotyl	271	0	EDE	N/A
SG-IPT	Hyg 7.5	pPN11	Lincoln[1]	25	GV3101	-	hypocotyl	312	0	EDE	N/A
SG-IPT	Hyg 7.5	pPN11	Lincoln[1]	25	AGL1	-	petiole	540	0	EDE	N/A
SG-IPT	Hyg 7.5	pPN11	Lincoln[1]	25	GV3101	-	petiole	623	0	EDE	N/A
pBJ49	Hyg 7.5	pBJ49	Lincoln[1]	25	AGL1	-	hypocotyl	243	0	EDE	N/A
pBJ49	Hyg 7.5	pBJ49	Lincoln[1]	25	GV3101	-	hypocotyl	201	0	EDE	N/A
pBJ49	Hyg 7.5	pBJ49	Lincoln[1]	25	AGL1	-	petiole	486	0	EDE	N/A
pBJ49	Hyg 7.5	pBJ49	Lincoln[1]	25	GV3101	-	petiole	402	0	EDE	N/A

MB-IPT	Hyg 2	pPN1	Lincoln[I]	25	AGL1	-	hypocotyl	100	4	4.0 (1.1-9.9)	0
MB-IPT	Hyg 2	pPN1	Lincoln[I]	25	AGL1	-	petiole	200	0	0 (0-1.8)	0
SG-IPT	Hyg 2	pPN11	Lincoln[I]	25	AGL1	-	hypocotyl	100	0	0 (0-3.6)	0
SG-IPT	Hyg 2	pPN11	Lincoln[I]	25	AGL1	-	petiole	200	0	0 (0-3.6)	0
MB-IPT	Hyg 2	pPN1	Palm Nth[II]	20	AGL1	-	hypocotyl	225	5	2.2 (0.7-5.1)	0
MB-IPT	Hyg 2	pPN1	Palm Nth[II]	20	AGL1	+	hypocotyl	225	3	1.3 (0.3-3.8)	0
MB-IPT	Hyg 2	pPN1	Palm Nth[II]	20	AGL1	-	petiole	450	0	0 (0-0.8)	0
MB-IPT	Hyg 2	pPN1	Palm Nth[II]	20	AGL1	+	petiole	450	3	0.7 (0.1-1.9)	0
SG-IPT	Hyg 2	pPN11	Palm Nth[II]	20	AGL1	-	hypocotyl	225	7	3.1 (1.3-6.3)	0
SG-IPT	Hyg 2	pPN11	Palm Nth[II]	20	AGL1	+	hypocotyl	225	4	1.8 (0.5-4.5)	0
SG-IPT	Hyg 2	pPN11	Palm Nth[II]	20	AGL1	-	petiole	450	1	0.2 (0-1.2)	0
SG-IPT	Hyg 2	pPN11	Palm Nth[II]	20	AGL1	+	petiole	450	1	0.2 (0-1.2)	0
pBJ49	Hyg 2	pBJ49	Palm Nth[II]	20	AGL1	-	hypocotyl	225	6	2.7 (1.0-5.7)	0
pBJ49	Hyg 2	pBJ49	Palm Nth[II]	20	AGL1	-	petiole	450	0	0 (0-0.8)	0
MB-IPT	Kan 25	pPN110	Palm Nth[III]	25	LBA4404	-	hypocotyl	1560	8	0.5 (0.2-1.0)	N/A
MB-IPT	Kan 25	pPN110	Palm Nth[III]	25	LBA4404	-	petiole	490	0	0 (0-0.8)	N/A
SG-IPT	Kan 25	pPN109	Palm Nth[III]	25	LBA4404	-	hypocotyl	1480	4	0.3 (0.1-0.7)	N/A
SG-IPT	Kan 25	pPN109	Palm Nth[III]	25	LBA4404	-	petiole	440	0	0 (0-0.8)	N/A
MB-IPT::AS-ACO	Kan 25	pPN111	Palm Nth[III]	25	LBA4404	-	hypocotyl	1500	3	0.2 (0-0.6)	N/A
MB-IPT::AS-ACO	Kan 25	pPN111	Palm Nth[III]	25	LBA4404	-	petiole	1500	0	0 (0-0.2)	N/A
							Totals	**19065**	**83**	**0.4**	

[I, II and III]Indiciate the experiment number

[4]Numbers in brackets represent exact 95% confidence intervals: if the confidence intervals of two populations don't overlap then they are highly significantly different from one another.

EDE = explants died early

N/A = not analysed

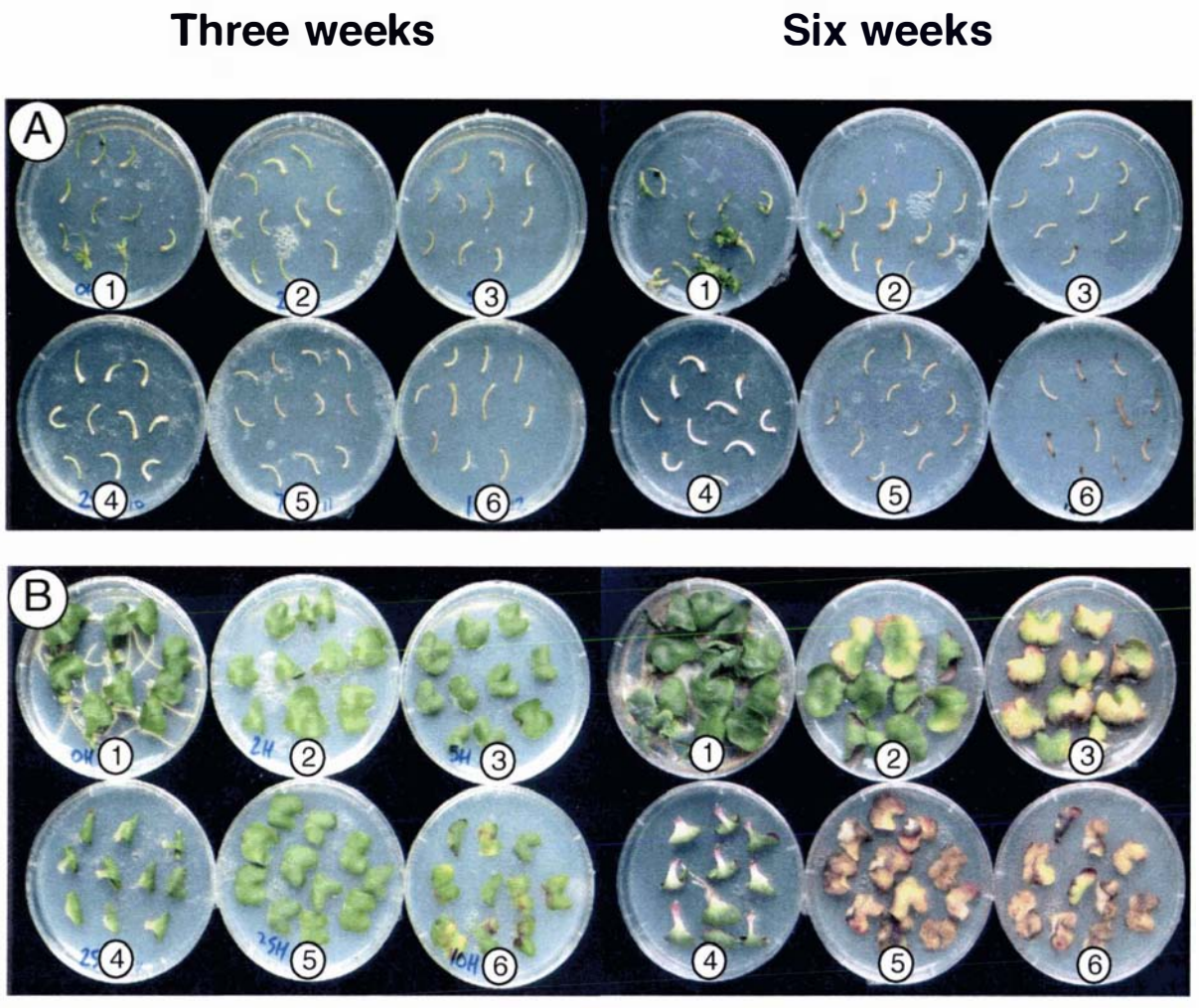

Figure 4.4 Influence of different levels of hygromycin (kill curve) on broccoli shoot regeneration from (A) hypocotyl and (B) cotyledonary petiole explants three and six weeks after excision from seedlings. 1 = no antibiotic control, 2 = 2 mg L^{-1} hygromycin, 3 = 5 mg L^{-1} hygromycin, 4 = 25 mg L^{-1} kanamycin, 5 = 7.5 mg L^{-1} hygromycin and 6 = 10 mg L^{-1} hygromycin.

number of putative transgenic lines were produced when selection pressure was lowered to 2 mg L^{-1} hygromycin in subsequent transformation experiments (Table 4.1; Experiment II, Palmerston North).

Transformation efficiency or rate was calculated based on the number of PCR positive lines obtained per 100 explants co-cultivated with *A. tumefaciens*. Across all experiments, the transformation rate was 0.4% but ranged from 0 to 4% (Tables 4.1). Transformation experiments conducted at the Lincoln site (Experiment I) were the most successful, with a rate of 1.0% for the AS-ACO (pPN10) and pART27 constructs (kanamycin selection) (Table 4.2). Transformation rate increased from 0.4% to 1.6% when pPN10 was used compared to the pART27 control plasmid. This increase was only observed for cotyledonary petiole explants (2.2% pPN10 petioles; 0.1% pART27 petioles). When hypocotyls were used, transformation rate decreased from 1.1% (pART27) to 0.6% (pPN10). Transformation rate was also higher for hypocotyls (1.9%) compared to cotyledonary petioles (0.1%) when pPN10 was excluded. The *A. tumefaciens* strain GV3101 (pART27 and pPN10, hypocotyls and cotyledonary petioles) had a transformation efficiency of 1.6% compared to AGL1, which was 0.6%. Transformation rate was relatively low for Experiment III (0-0.5%) and putative transgenic plants only regenerated from hypocotyl explants.

4.3.2 Molecular analysis of transgenic broccoli plants

PCR analyses were used as an initial molecular screen for putative transgenic shoots. If a positive PCR result occurred, the putative shoots were sub-cultured and grown further. Approximately 200 putative transgenic shoots were subjected to PCR analyses, and PCR products of the expected size were obtained for many of them (Figures 4.5 and 4.6). Based on these PCR results, 81 independent transgenic lines of broccoli were obtained using the cotyledonary petiole and hypocotyl transformation system: 26 AS-ACO lines, 23 MYB_{305}-IPT lines, 17 SAG_{12}-IPT lines, 3 AS-ACO::MYB_{305}-IPT lines, as well as 8 pART27 controls and 6 pBJ49 controls.

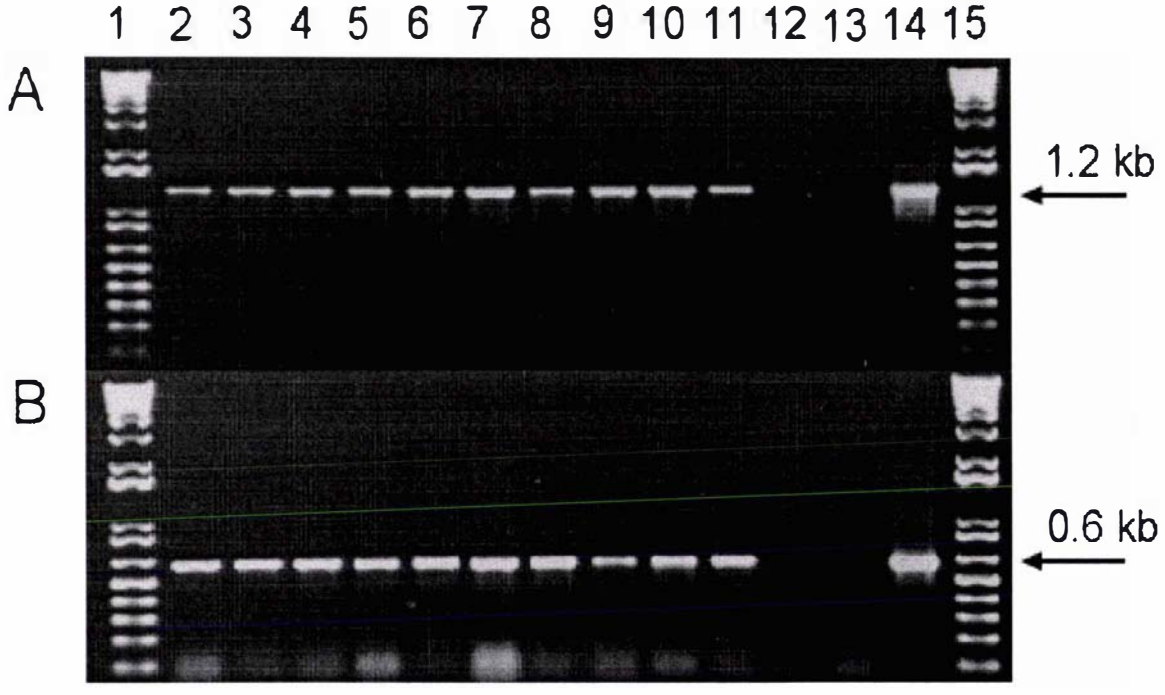

Figure 4.5 PCR amplification for (A), AS-ACO fragment and (B), *nptII* using genomic DNA from 10 individual broccoli lines transformed with the AS-ACO construct pPN10. Lane 1 and 15 1 kb plus ladder markers (Life Technologies), lanes 2 to 11 individual transgenic broccoli lines, lane 12 negative control (WT), lane 13 negative control (water) and lane 14 positive control (pPN10, plasmid DNA).

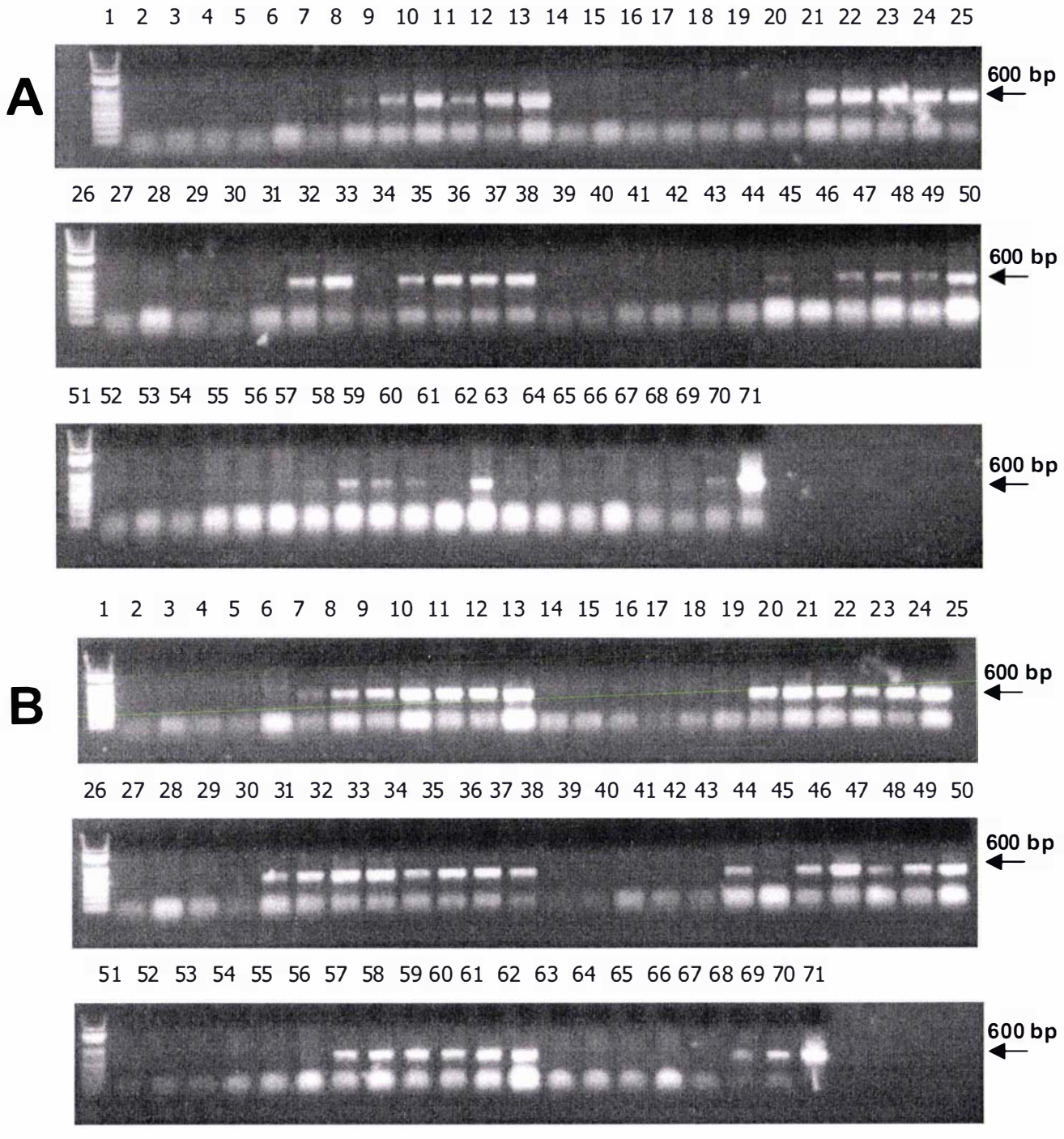

Figure 4.6 PCR amplification of (A), *ipt* gene and (B), *hpt* gene using genomic DNA from putative transgenic broccoli lines transformed with the SAG_{12}-IPT (pPN11), MYB_{305}-IPT (pPN1) or pBJ49 constructs. Lanes 1, 26 and 51 1 kb plus ladder markers (Life Technologies), lanes 2-25, 27-50 and 52-65 putative individual transgenic broccoli lines, lane 67 negative control (WT), lane 68 negative control (water) and lanes 69-71 positive controls (pBJ49, pPN1 and pPN11, plasmid DNA respectively).

Table 4.2 Combined effects on transformation rate. Effects of *A. tumefaciens* strain, construct and explant type on transformation efficiency of broccoli, for Experiment I (Lincoln), AS-ACO and pART27 constructs only.

Variable tested	Total explants	Total lines	Transformation efficiency (%)[1]
AS-ACO hypocotyl	538	3	0.6 (0.1-1.6)[2]
pART27 hypocotyl	624	7	1.1 (0.5-2.3)
AS-ACO petiole	1067	23	2.2 (1.4-3.2)
pART27 petiole	1247	1	0.1 (0-0.4)
AS-ACO total	1605	26	1.6 (1.1-2.4)
PART27 total	1871	8	0.4 (0.2-0.8)
GV3101 total	1416	22	1.6 (1.0-2.3)
AGL1 total	2060	12	0.6 (0.3-1.0)
hypocotyls total[3]	1074	20	1.9 (1.1-2.9)
petiole total[3]	2147	2	0.1 (0-0.3)

[1]Transformation efficiency equals the number of independent transgenic lines obtained per 100 explants inoculated.

[2]Numbers in brackets represent exact 95% confidence intervals: if the confidence intervals of two populations do not overlap then they are significantly different from one another.

[3]Numbers exclude AS-ACO construct

Southern analysis was used to confirm the transgenic nature of the PCR positive plants and to estimate the number of transgenes present. The size of the broccoli genome was estimated at 1.56 pg DNA $2C^{-1}$ nucleus by flow cytometry (Murray Hopping, personal communication). All calculations of plasmid DNA concentration for single copy equivalents were based on this genome size. For the AS-ACO lines (pPN10), a 550 bp *Hind* III fragment from the AS promoter was hybridised to broccoli genomic DNA from wild type and putative transgenic AS-ACO lines, as well as plasmid DNA at concentrations equivalent to 1, 3 and 5 copies of a single gene, digested with *Hind* III and *Xba* I (Figure 4.7). One single band (550 bp) was present for most of the lines indicating digestion had gone to completion. Multiple bands only occurred for lines

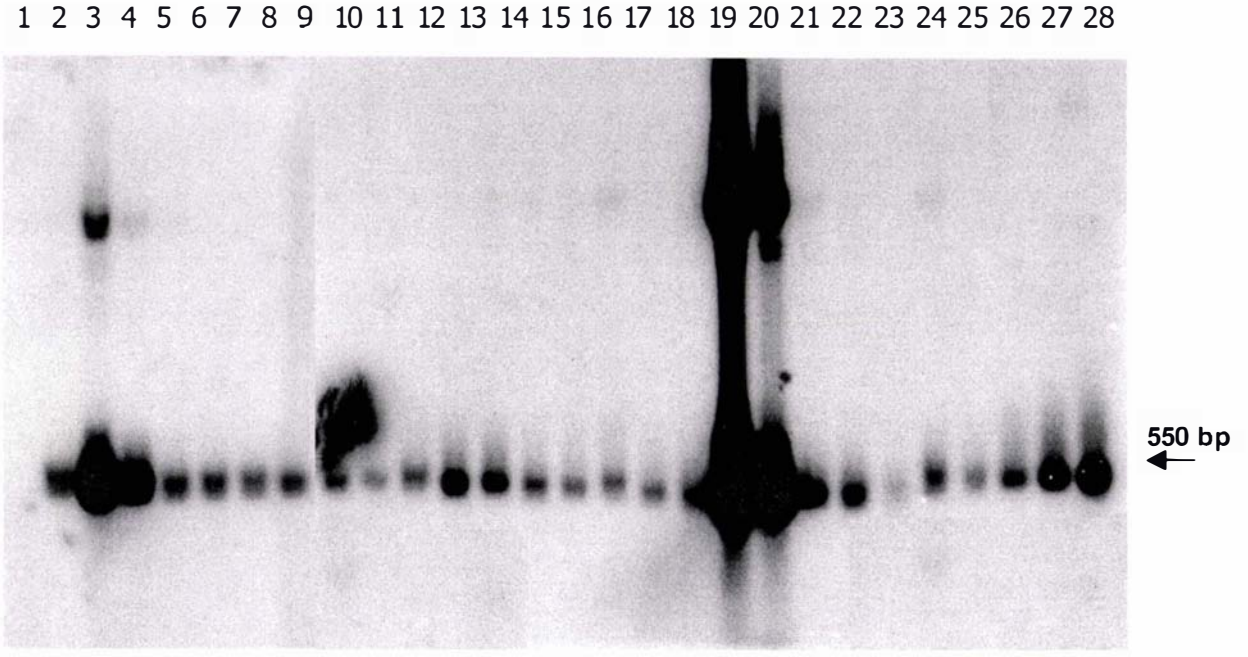

Figure 4.7 Autoradiograph showing the Southern hybridisation of the 550 bp ^{32}P labelled *Hind* III fragment of the AS promoter with *Hind* III-*Xba* I digested genomic DNA from 24 individual transgenic broccoli AS-ACO lines. Lane 1 WT, lanes 2-25 individual transgenic lines, lanes 26-28 1, 3 and 5 copies of plasmid DNA equivalents respectively. Genomic DNA (10 mg) was separated on a 1% (w/v) agarose gel and blotted onto nylon membrane. All membranes were probed together with the 550 bp ^{32}P labeled *Hind* III AS promoter fragment. For details of hybridisation and washing conditions, see Materials and Methods, Section 2.8.

containing many (>10) copies of the transgene, suggesting an alteration of the T-DNA. Differing intensities of the bands were compared by eye with the plasmid copy equivalent lanes, and copy number of inserted transgenes into the plant genome was estimated (Table 4.3). Further, a 600 bp *nptII* PCR product was also hybridised to the digested DNA, as well as to genomic DNA isolated from pART27 control plants digested with *Hind* III (Figure 4.8). Copy number of transgenes inserted into the broccoli genome was estimated by counting the number of bands present for each line (Table 4.3).

For the putative IPT lines from Experiments I and II (pPN1 and pPN11; hygromycin selection), 600 bp *hpt* and *ipt* PCR products were hybridised to broccoli genomic DNA from wild-type and putative transgenic IPT plants, as well as plasmid DNA at concentrations equivalent to 1, 3 and 5 copies of a single gene, digested with either *Eco* RV or *Eco* RI (Figure 4.9). No hybridisation occurred for any samples containing digested genomic DNA from these putative transgenic plants. Membranes were stripped and re-probed with a broccoli protease inhibitor (*BoPI*) cDNA provided by Dr Simon Coupe, which confirmed the presence of broccoli genomic DNA from all samples analysed (Figure 4.9). Undigested genomic DNA (40 μg) from wild-type, putative transgenic IPT plants, and pBJ49 control plants, was hybridised with 600 bp *ipt* and *hpt* fragments. No hybridisation occurred for either probe to the undigested genomic DNA (data not shown).

Northerns and RT-PCR based gene expression analyses were conducted in an effort to detect transgene-specific expression. The 600 bp *hpt* and *ipt* PCR fragments were used as probes against total RNA isolated from wild-type, putative IPT and pBJ49 transgenic plants, from a range of tissues. No hybridisation of these probes was observed (data not shown). Total RNA (DNase treated) was also used in more sensitive RT-PCR based 'virtual northern' analyses. Primers used were specific for *ipt* (IPT3 and IPT4) and also *18S* broccoli ribosomal binding protein (18S Fow and 18S Rev; Dr Simon Coupe, Personal Communication) gene amplification (for details of primer sequences see Table 2.2). No hybridisation of the *ipt* probe was observed for any of the samples analysed, although the *18S* probe did hybridise with all samples present (Figure 4.10).

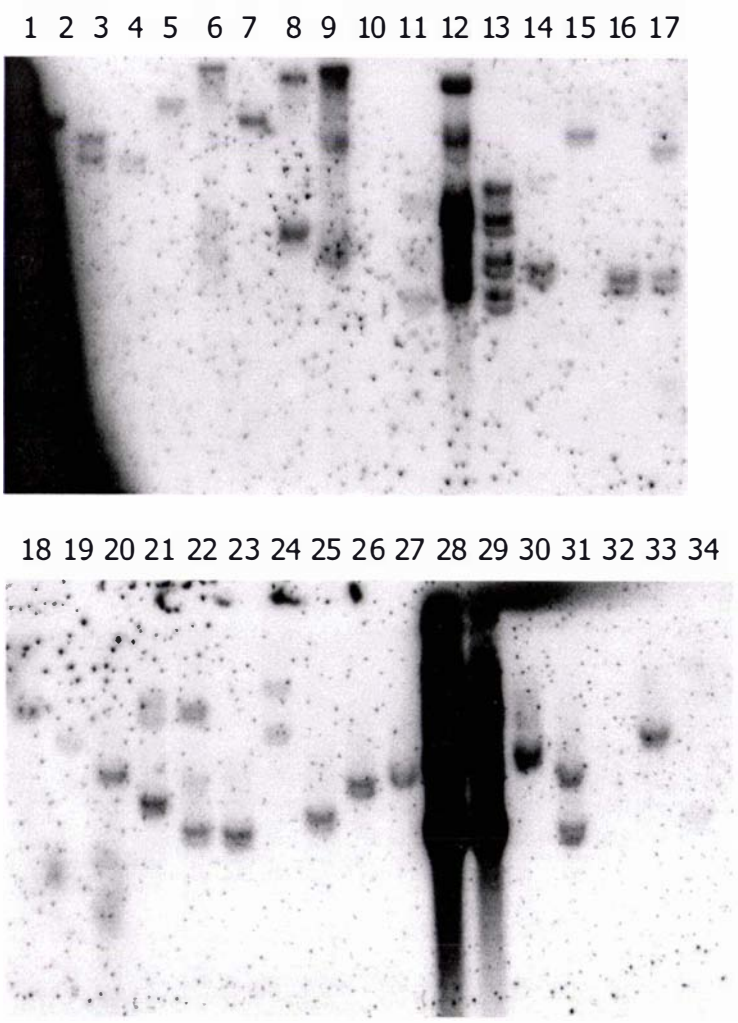

Figure 4.8 Autoradiographs showing the Southern hybridisation of the 600 bp ^{32}P labeled PCR amplified *nptII* fragment with *Hind* III-*Xba* I digested genomic DNA from 24 individual transgenic broccoli AS-ACO lines and 8 pART27 lines. Lane 1 pART27 plasmid control, lanes 2-9 individual transgenic pART27 lines, lane 10 WT, lanes 11-34 individual transgenic AS-ACO lines. Genomic DNA (10 µg) was separated on a 1% (w/v) agarose gel and blotted onto nylon membrane. All membranes were probed together with the 600 bp ^{32}P labeled *nptII* fragment. For details of hybridisation and washing conditions, see Materials and Methods, Section 2.8.

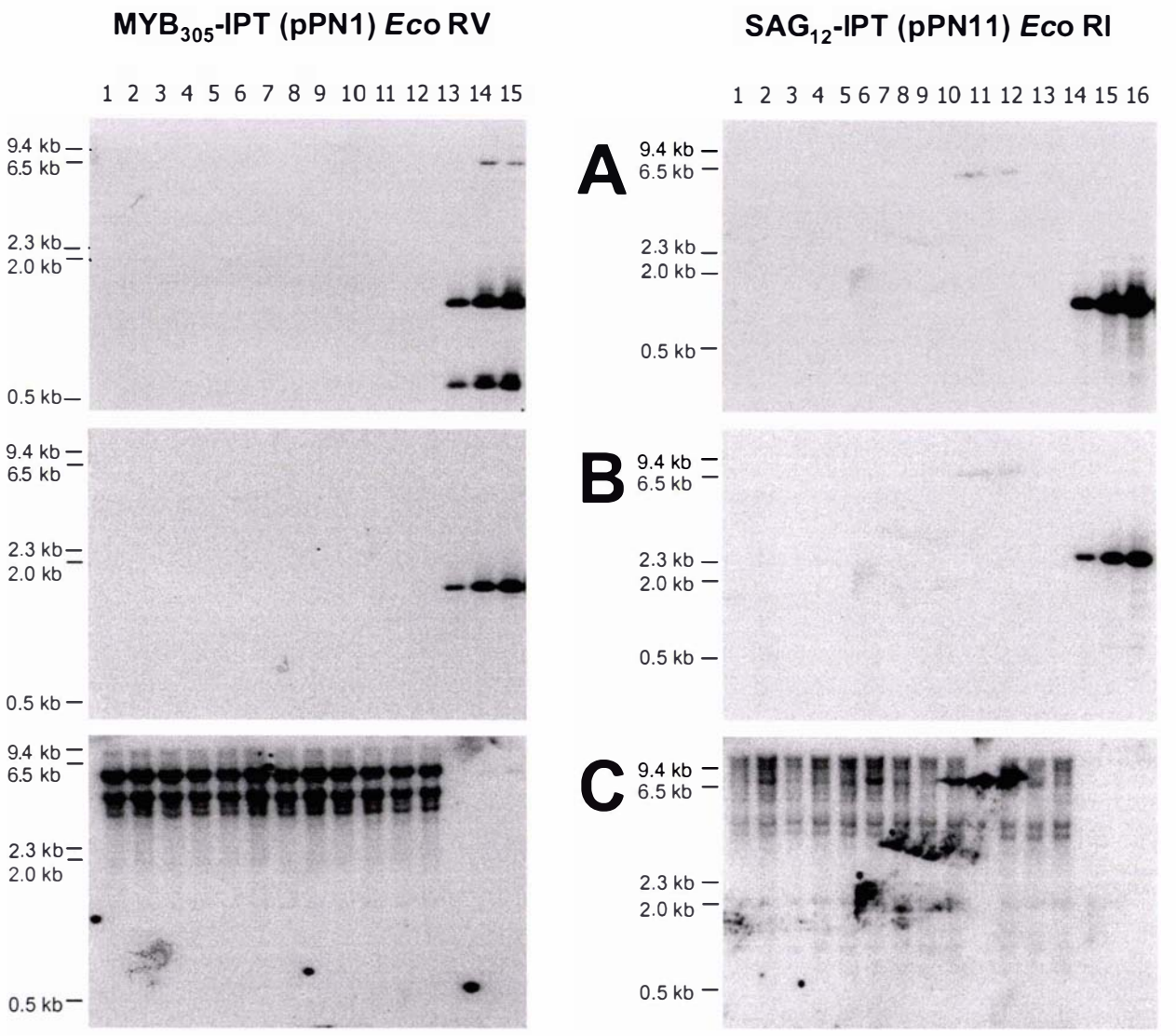

Figure 4.9 Autoradiographs showing the Southern hybridisation of (A) a 600 bp ^{32}P labelled PCR amplified *ipt* fragment, (B) a 600 bp ^{32}P labelled PCR amplified *hpt* and (C) an 800 bp ^{32}P labelled *BoPI* (broccoli protease inhibitor) PCR fragment with digested genomic DNA from putative individual transgenic broccoli MYB$_{305}$-IPT (pPN1) and SAG$_{12}$-IPT (pPN11) lines. For MYB$_{305}$-IPT (pPN1): Lanes 1-11 putative individual transgenic lines, lane 12 WT and lanes 13-15 1, 3 and 5 copies of plasmid (pPN1) DNA equivalents respectively. For SAG$_{12}$-IPT (pPN11): Lanes 1-12 putative individual transgenic lines, lane 13 WT and lanes 14-16 1, 3 and 5 copies of plasmid (pPN11) DNA equivalents respectively. Digested DNA (10 mg) was separated on a 1% (w/v) agarose gel and blotted onto nylon membrane. Membranes were stripped and reprobed. For details of hybridisation and washing conditions, see Materials and Methods, Section 2.8.

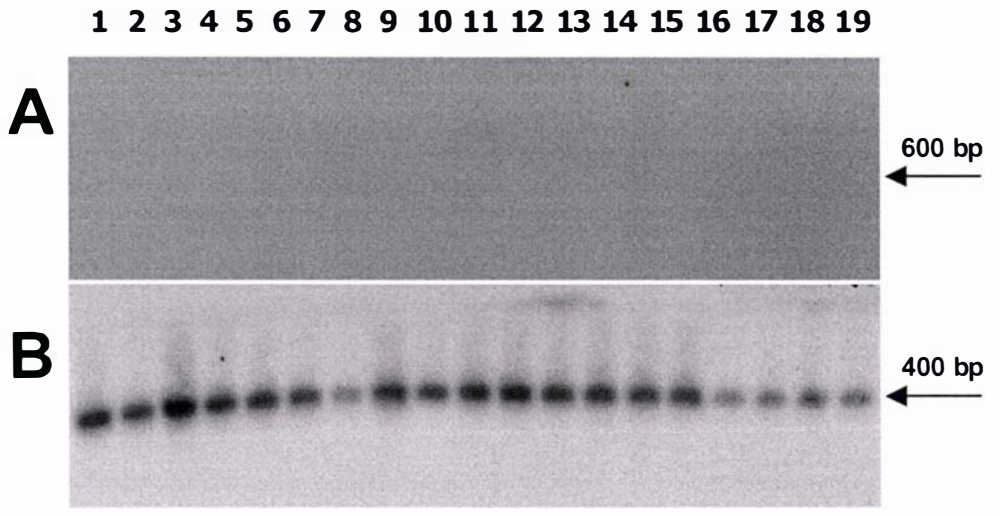

Figure 4.10 Autoradiographs showing the 'virtual northern' hybridisation of (A) a 600 bp ^{32}P labelled PCR amplified *ipt* fragment and (B) a 400 bp ^{32}P labeled PCR amplified *18S* fragment with RT-PCR products amplified from total RNA from selected tissues of putative transgenic lines. Lanes 1, 2 and 16 are WT samples, lanes 3-9 are putative SAG_{12}-IPT samples and lanes 10-15, 18 and 19 are putative MYB_{305}-IPT samples. For details of hybridisation and washing conditions, see Materials and Methods, Section 2.9.

Table 4.3 Copy number. Estimation of copy number by Southern analyses. The AS probe was a 550 bp *Hind* III fragment from the AS promoter, and was hybridised against *Hind* III-*Xba* I digested genomic DNA from transgenic broccoli harbouring the AS-ACO construct. The NPTII probe was a 600 bp PCR product amplified from the binary vector pART27 and was hybridised against genomic DNA digested with *Hind* III-*Xba* I from transgenic plants harbouring the *nptII* gene.

Line number	AS probe	NPTII probe
AS-ACO#1	2	1
AS-ACO#2	10	9
AS-ACO#3	5	4
AS-ACO#4	1	1
AS-ACO#5	1	1
AS-ACO#6	1	1
AS-ACO#7	1	2
AS-ACO#8	1	1
AS-ACO#9	1	1
AS-ACO#10	1	1
AS-ACO#11	2	2
AS-ACO#12	2	2
AS-ACO#13	1	1
AS-ACO#14	1	2
AS-ACO#15	1	1
AS-ACO#16	N/A	N/A
AS-ACO#17	1	1
AS-ACO#18	1	1
AS-ACO#19	N/A	N/A
AS-ACO#20	>10	>10
AS-ACO#21	>10	>10
AS-ACO#22	2	1
AS-ACO#23	1	2
AS-ACO#24	1	LU
AS-ACO#25	1	1
AS-ACO#26	1	LU
ART27#1	N/A	1 or more
ART27#2	N/A	2
ART27#3	N/A	1
ART27#4	N/A	1
ART27#5	N/A	1
ART27#6	N/A	1
ART27#7	N/A	2
ART27#8	N/A	3

N/A = not analysed

LU = lane under-loaded with genomic DNA so hard to visualise bands

Experiment III was conducted to produce transgenic broccoli IPT lines using the binary vectors pPN109 (SAG_{12}-IPT), pPN110 (MYB_{305}-IPT) and pPN111 (MYB_{305}-IPT::AS-ACO). Putative transgenic lines underwent PCR analyses as an initial screen (Figure 4.11). Subsequently tissue has been harvested to confirm PCR results by Southern analyses, which are currently being conducted by Crop & Food Research personnel. Initial postharvest trials were conducted with mature heads, although due to undesirable growing conditions for this cultivar during early summer, heads were unable to be assessed at similar developmental stages. Plants are currently being grown *in vitro* and will be subjected to glasshouse conditions when conditions become more suitable for broccoli, this again will be carried out by Crop & Food Research personnel.

4.3.3 *Arabidopsis*

Because there are often inherent problems with broccoli transformation procedures, early during this work it was decided, to introduce the cloned binary vectors into the model plant *Arabidopsis* as a contingency plan, as *Arabidopsis* is easily transformed and undergoes leaf senescence. *Arabidopsis* was transformed by the floral dip method described by Clough and Bent (1998) and a number of transgenic plants were produced harbouring pART27 and pPN10 constructs. No transgenic plants were recovered from experiments conducted using the pBJ49 based binary vectors pPN1 and pPN11 which utilise hygromycin resistance for selection. Putative transgenic plants were screened and grown under antibiotic selection (50 mg L^{-1} Kan). This together with PCR analysis provided indicative data of the transgenic nature of these plants (Figure 4.12). Thirteen independent transgenic lines containing the AS-ACO construct from pPN10 were grown in the containment glasshouse. Approximately half of these transgenic lines show an altered 'lettuce' phenotype, with a reduced rosette and crinkly leaves, and reduced floral bolting (Figure 4.13).

4.3.4 Phenotype

One of the main reasons for switching to *A. tumefaciens* from *A. rhizogenes* (even though transformation rates are generally lower for *A. tumefaciens*), was to produce transgenic plants with a normal looking phenotype, and so be able to assess easily the effects of either reduced ethylene or enhanced cytokinin on plant phenotype. While

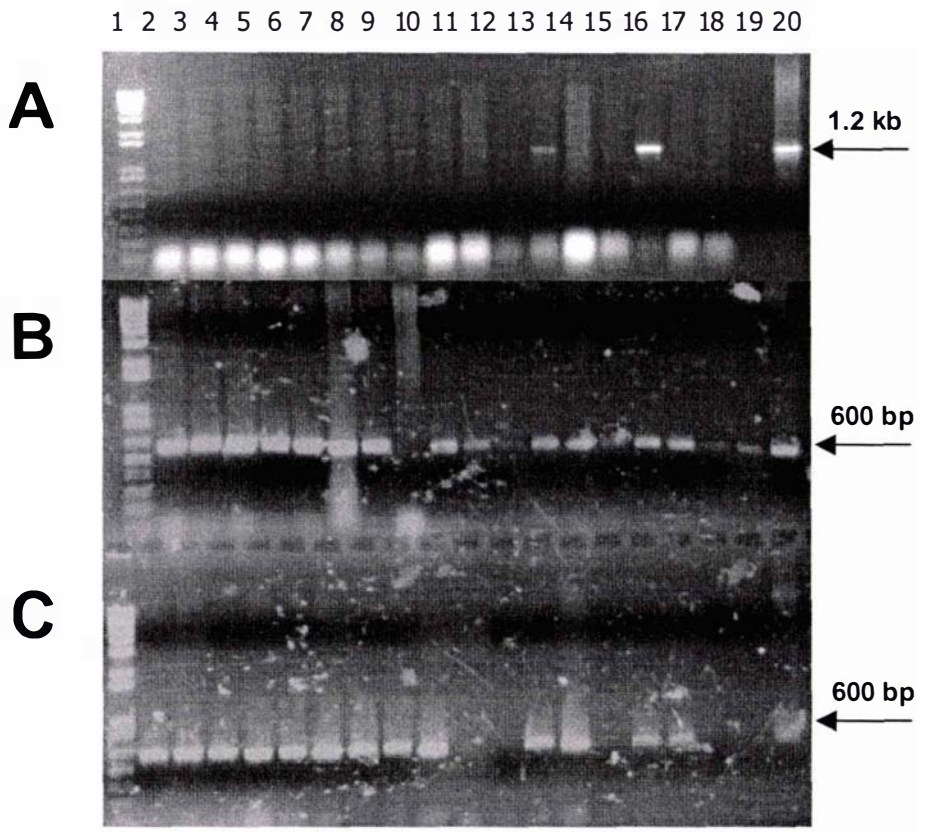

Figure 4.11 PCR amplification for (A), AS-ACO fragment and (B), *nptII* and (C) *ipt* using genomic DNA from individual broccoli lines transformed with the SAG_{12}-IPT (pPN109), MYB_{305}-IPT (pPN110) and MYB_{305}-IPT::AS-ACO (pPN111) constructs. Lane 1, 1 kb plus ladder markers (Life Technologies), lanes 2 to 17 individual transgenic broccoli lines, lane 18 negative control (WT), lane 19 negative control (water) and lane 20 positive control (pPN111, plasmid DNA).

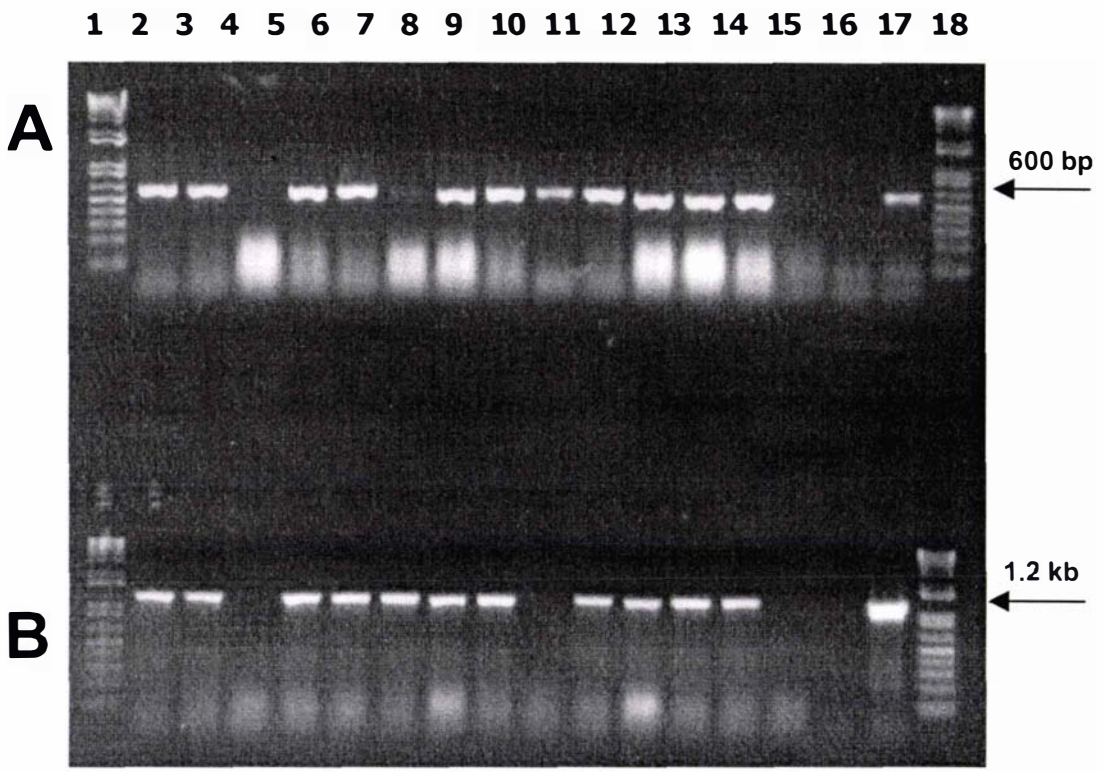

Figure 4.12 PCR amplification for (A), *nptII* and (B), AS-ACO fragment using genomic DNA from 13 individual *Arabidopsis* lines transformed with the AS-ACO construct pPN10. Lane 1 and 18 1 kb plus ladder markers (Life Technologies), lanes 2 to 14 individual transgenic *Arabidopsis* lines, lane 15 negative control (WT), lane 16 negative control (water) and lane 17 positive control (pPN10, plasmid DNA).

Figure 4.13 Photographs of 13 individual transgenic lines of *Arabidopsis* harbouring the AS-ACO construct growing in a containment glasshouse. (A) 2 weeks following exflasking and (B) 4 weeks following exflasking.

most of the individual transgenic lines looked phenotypically normal in culture, there were some abnormal phenotypes. Some of the AS-ACO lines had reduced leaf and root growth, altered leaf shape, elongated leaf petioles and shortened internodes in culture (Figure 4.14). A notable feature of AS-ACO Line 21 was an extended petiole phenotype (Figure 4.16). Some of the IPT lines had very reduced roots, reduced leaf size, reduced plant stature, increased bushiness and bleaching of leaves in culture (Figure 4.15) and in the glasshouse (Figure 4.16).

4.4 DISCUSSION

4.4.1 Optimisation of the protocol

Shoot regeneration experiments had been carried out previously by Dr Mary Christey with non-inoculated tissue on a range of 6-BAP concentrations (0-10 mg L^{-1}) to determine the optimal level of the hormone for subsequent transformation experiments for a number of commercially available F_1 hybrid cultivars (Dr Mary Christey, Personal Communication). Shoot regeneration rates had been optimised at 3 mg L^{-1} 6-BAP for both hypocotyl and cotyledonary petioles for Triathalon, as described by Gapper et al. (2002). Shoots regenerated at high rates for both explant types on this level of hormone: 75% of the cotyledonary petiole explants regenerated shoots while approximately 95% of hypocotyl explants regenerated shoots on 3 mg L^{-1} 6-BAP. Transient expression of a GUS reporter gene was higher both three and six weeks following co-cultivation for hypocotyl explants than for cotyledonary petiole explants (experiments conducted by Robert Braun, as described in Gapper et al., 2002). This result in combination with the shoot regeneration results, strongly suggests that hypocotyl explants were more useful for successful transformation than cotyledonary petioles. However, cotyledonary explants were still used for transformation experiments because they had been a successful explant choice for a number of other laboratories, using similar protocols (Mary Christey Personal communication; Metz et al., 1995; Cao et al., 1999; Chen et al., 2001).

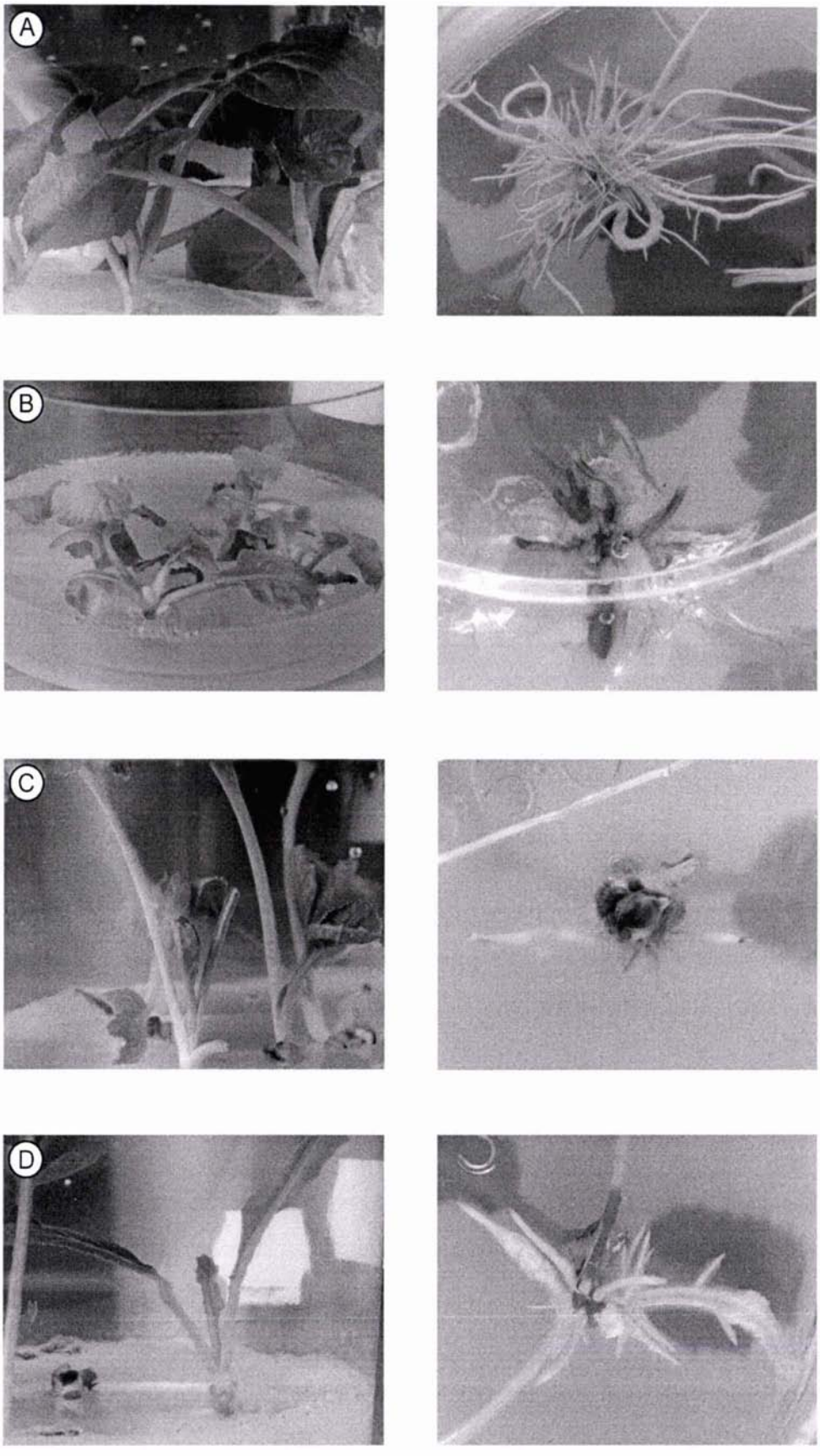

Figure 4.14 Transgenic and wild-type broccoli shoots and roots in culture. (A), wild type. (B-D), individual AS-ACO lines.

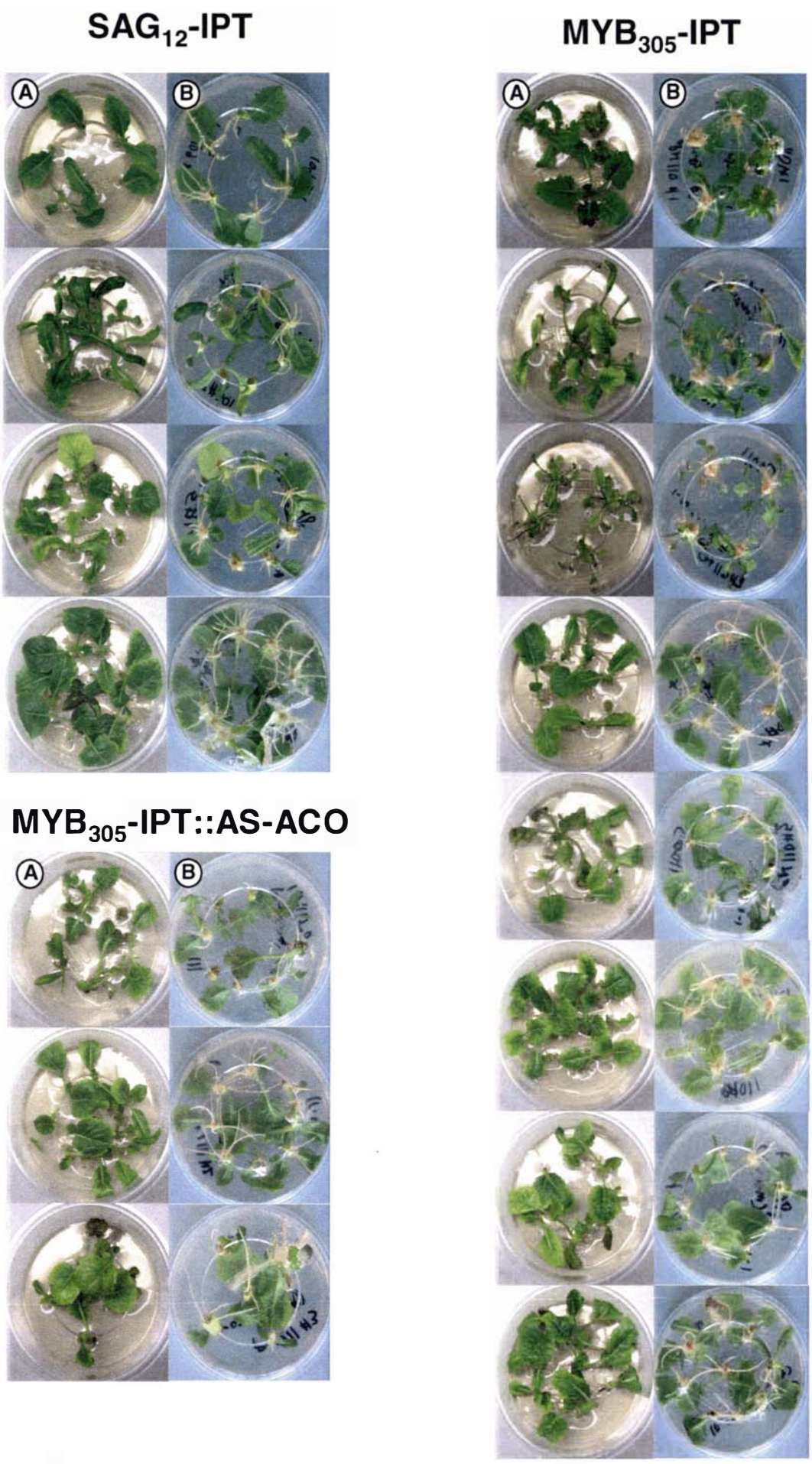

Figure 4.15 Photographs of putative transgenic broccoli plants harbouring SAG_{12}-IPT (pPN109), MYB_{305}-IPT (pPN110) and MYB_{305}-IPT::AS-ACO (pPN111) constructs growing in culture. Altered morphology is likely to be due to leaky expression of *ipt* genes, A = shoots, B = roots.

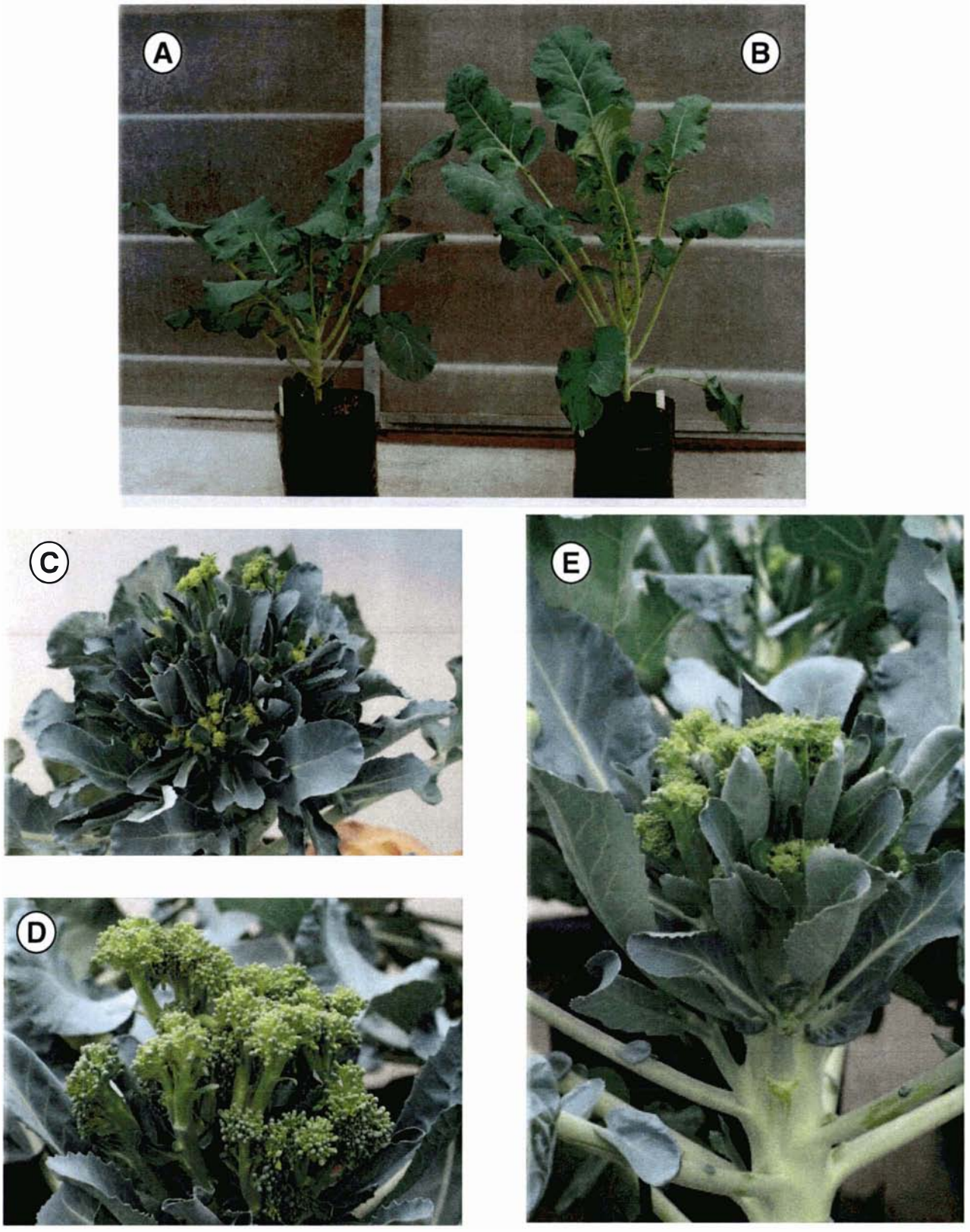

Figure 4.16 Putative transgenic plants harbouring IPT or AS-ACO constructs growing in containment glasshouse. (A) wild-type plant, and (B) an AS-ACO line (#21); (C), (D) and (E) putative IPT lines (selected on hygromycin), none of which were confirmed to be transgenic in nature by strigent molecular analyses.

Eighty independent PCR-positive putative transgenic lines were produced in this study. Southern analyses confirmed the transgenic nature all of the AS-ACO lines and pART27 control lines analysed (Figures 4.7 and 4.8). In many cases the stable integration of a single copy of a transgene into the broccoli genome occurred (Table 4.3). Unfortunately, Southern analyses did not confirm the PCR results for the putative IPT transgenic lines that were selected on hygromycin containing medium.

The original concentration of hygromycin used (7.5 mg L^{-1}) was shown to be toxic when 'kill curves' were subsequently set up (Figure 4.4). The original level of hygromycin was chosen because Cao et al. (1999) had successfully used 10 mg l^{-1} hygromycin for broccoli. This level was also used for successful selection and transformation of *Brassica rapa* varieties (Cho et al., 2001). Further, earlier 'kill curve' experiments had also conducted by Dr Mary Christey who concluded that any level up to 5 mg L^{-1} hygromycin would be suitable for selection purposes. An intermediate concentration was subsequently chosen for selection and 7.5 mg L^{-1} hygromycin was used. For subsequent transformation experiments, using the same binary vectors, the hygromycin concentration was lowered to 2 mg L^{-1} for selection. This level was low enough to let 'escape' or non-transformed shoots regenerate at a higher frequency than the kanamycin selection used (Figure 4.4). However, Southern analyses did not confirm the transgenic nature of the putative IPT lines from transformation experiments using this selection, suggesting selection conditions were insufficient.

Further molecular analyses were used in an attempt to confirm the initial positive PCR results for the putative IPT transgenic lines. PCR, using primers specific to *vir G* from the *A. tumefaciens* Ti plasmid, was carried out to ensure that *A. tumefaciens* contamination was not the cause of false positive results. No *A. tumefaciens*-specific PCR products were detected for any of the plant DNA samples analysed (data not shown). Northern and more sensitive RT-PCR based 'virtual northern' methods were also used, but no transgene-specific gene expression was observed for any RNA samples from any of the putative transgenic IPT lines (Figure 4.10).

These results do not explain the initial PCR results suggesting the transgenic nature of these plants. Register (1997) describes several inherent problems associated with this method, when it is used to screen for the presence or absence of transgenes in plant samples. A positive PCR result only indicates that sequences homologous to the primers exist in the sequence template, not the complete sequence being amplified. Further, a positive PCR result does not confirm whether the DNA used as a template is integrated into the plant genome. It does not preclude the possibility of contamination. More stringent analyses such as Southern or gene expression analyses (as was done here) or even biochemical analyses such as enzyme linked immuno sorbent assay (ELISA) are suggested for final confirmation of successful transformation.

Because no stringent results were obtained to confirm the transgenic nature of the IPT lines selected on hygromycin, it was decided to clone new binaries, using kanamycin as a selectable marker, as it was successful for the earlier transformation work using this antibiotic for selection. The new binary vectors were constructed using pART27 (Gleave, 1992) to produce pPN109 (SAG_{12}-IPT), pPN110, (MYB_{305}-IPT), pPN111 (MYB_{305}-IPT::AS-ACO) and pPN113 (SAG_{12}-IPT::AS-ACO). Subsequently, pPN109, pPN110 and pPN111 were used in broccoli transformation experiments and transgenic plants were generated. These plants are currently being grown at Crop & Food Research for further molecular and physiological analyses.

Successful transformation of *Arabidopsis* also proved difficult using hygromycin selection. No transgenic lines were produced, or at least selected using this antibiotic as a selectable marker. As mentioned above, transgenic *Brassica* crops have previously been produced using hygromycin as the selectable marker (Cao et al., 1999; Cao et al., 2001). However, these researchers used different binary vectors. This suggests that there may be a problem with the binary vector pBJ49, which was used in these cloning experiments. This vector has proved troublesome for the selection of transgenic plants for a number of other crops (Dr Huaibi Zhang, personal communication). Both *E. coli* and *A. tumefaciens* bacterial cultures harbouring pBJ49-based vectors grew under the selection pressure of hygromycin which indicated that the *hpt* gene present on the vector was functional, at least in the bacterial system. It is plausible to conclude then, that the

codons encoded by the *hpt* gene present on pBJ49 can be utilised by bacterial species, but this codon usage may not be favourable in plant systems.

For transformation experiments conducted with kanamycin for selection, transformation rate appeared to be greater for hypocotyl explants than for cotyledonary petiole explants (Tables 4.2, summary of the confirmed transformation experiments conducted in Experiment I), although this observation was not significant due to the influence of the AS-ACO construct on cotyledonary petiole transformation (See following Section, 4.4.2). However, for experiments conducted without this construct, transformation efficiency increased 19-fold for hypocotyls compared to cotyledonary petioles.

Different *A. tumefaciens* strains also had a significant effect on transformation efficiency. The strain GV3101 (pART27 and pPN10, hypocotyls and cotyledonary petioles) had a transformation efficiency of 1.6 % in contrast to strain AGL1 that was 0.6% (Table 4.2). AGL1 is regarded as one of the hypervirulent strains of *A. tumefaciens* (Lazo et al., 1991) and could have caused greater pathogenic effects compared to other strains such as GV3101, resulting in the death of plant tissue.

4.4.2 Effect of reduced ethylene biosynthesis on transformation rate

Transformation of *Arabidopsis* with the AS-ACO construct (AGL1/pPN10) using the floral dip method (Clough and Bent, 1998) confirmed the increased transformation rate seen for broccoli cotyledonary petioles in this work, as more transformants appeared to grow from seed collected from plants dipped in pPN10 cultures than pART27 cultures. Determining actual transformation rate for *Arabidopsis* is difficult due to the high numbers of seeds needed to screen, so the above result was simply observation based. However, the observed increase in transformation rate for the AS-ACO construct led to the hypothesis that antisense ACO expression lowered localised ethylene production which, in turn, caused an increase in transformation efficiency, due to either enhanced shoot regeneration or reduced susceptibility to the pathogenic effects of *A. tumefaciens* invasion. To simulate this, silver ions were added to selection media to block ethylene perception for experiments that did not involve the AS-ACO construct. Shoot regeneration has previously been increased by using similar treatments in a variety of

Brassica species (Chi et al., 1990; Palmer, 1992). Transformation efficiency has also been improved for a range of *B. napus* and *B. oleracea* varieties (De Block et al., 1989) and also for potato (Chang and Chan, 1991) with the addition of Ag^+ into culture media. However, the addition of 5 mg L^{-1} $AgNO_3$ into the media in experiments carried out here appeared to have no significant effect on the transformation efficiency for either explant type (Tables 4.1 and 4.2). In fact, Metz et al. (1995) reported that the addition of a $AgNO_3$ treatment (up to 10mg L^{-1}) inhibited shoot regeneration in both transformation and control experiments of broccoli.

However, Pua (2000) and Mo and Pua (2000) showed that blocking ethylene biosynthesis by using an antisense ACO construct in mustard led to increased transformation efficiency. Further, they found that the levels of free and conjugated polyamines were higher in their transgenic plants compared to controls. They also showed that exogenous polyamines promoted shoot regeneration. They suggested that the enhanced regeneration of the transgenic plants might be attributed to increased polyamine biosynthesis, due to the increased availability of the common biosynthetic precursor with ethylene, *S*-adenosyl methionine. Their data supports the hypothesis presented in this thesis, that transformation rate increases when ethylene biosynthesis is blocked by the AS-ACO construct, but not when ethylene perception alone is blocked by the addition of silver ions.

However, Metz et al. (1995) observed that inhibiting ethylene build up inside sealed plates by use of porous tape during the inoculation of explants by *A. tumefaciens,* was critical for high rates of transformation. It is possible then that ethylene may be influencing transformation rate at two different levels. Firstly, inhibition of ethylene biosynthesis causes increased biosynthesis of shoot regenerative enhancing compounds (the polyamines) and secondly, reduced ethylene causes plant cells to become less sensitive to the adverse effects of *A. tumefaciens* infection. Ethylene has been implicated in plant-pathogen interactions such as those described between tomato and *Xanthamonas campestris* (O'Donnell et al., 2001). Mutants, both ethylene-under-producing and ethylene-insensitive, had greatly reduced visible symptoms of infection, with the mutant plant cells demonstrating tolerance to pathogen infection. O'Donnell et

al. (2001) attributed this tolerance to the fact that the ethylene-regulated response to pathogen infection was switched off, as the infected mutant plant cells either produced no ethylene, or could not sense the ethylene produced. The transformed cells harbouring antisense ACC oxidase constructs may not be able to produce ethylene when under stress from *A. tumefaciens* invasion. They are thus able to tolerate the invasion and are able to regenerate more rapidly than transformed cells not harbouring such constructs.

4.4.3 Phenotype

The few abnormal phenotypes seen in some of the AS-ACO lines may be attributed to high copy number integration of T-DNAs into the plant genome, and subsequent gene disruption or gene silencing effects (Figure 4.15). However, some of the abnormalities could be due to the constitutive expression of the antisense ACO gene, thus reducing ethylene content or production during normal growth and development. Further, approximately half of the AS-ACO *Arabidopsis* transgenic lines also exhibited an altered phenotype (Figure 4.13), suggesting the AS promoter may be switched on during normal stages of development. Some of the cultured broccoli IPT lines (selected on kanamycin) also showed signs of promoter leakiness (Figure 4.15), with phenotype changes such as reduced or no roots and reduced plant stature which are typical of constitutive *ipt* expression (McKenzie et al., 1998). Also it is interesting to note that the putative broccoli transgenics selected on hygromycin also showed altered phenotypes, which could be attributed to enhanced cytokinin levels, such as floral bolting and shortened plant stature (Figure 4.16). However, these changes in plant morphology could have also been due to strenuous growing conditions in the containment glasshouse during summer. Other abnormalities could be due to the conditions during culture (i.e. somaclonal variation), as similar abnormalities were observed occasionally for adventitious shoots regenerated directly from wild-type and transgenic control plants.

Some of the abnormalities seen for transgenic lines produced during this thesis, are not unlike some of those associated with *A. rhizogenes* transformation. This reinforces the argument that any genetic manipulation that potentially causes marked changes in plant morphology must be conducted in a way to minimise the effect of the background

vector of transformation, hence the use of *A. tumefaciens* over *A. rhizogenes* throughout this work.

The plants described in this Chapter will be important in the elucidation of the interactions between ethylene and cytokinin during the postharvest senescence of broccoli. In the following Chapter, the work involving the characterisation of some of the transgenic lines is reported. The horticultural performance of the plants and the specificity of the gene promoters used is discussed.

Chapter 5

Characterisation of transgenic broccoli altered for ethylene and cytokinin biosynthesis.

5.1 INTRODUCTION

While the production of transgenic plants harbouring altered hormone status is not novel, the use of two of the gene promoters in this study is. Numerous reports in the literature advocate the use of specific promoters to drive the expression of cytokinin synthase genes in particular tissues, or at specific times, due to the often aberrant growth associated with constitutive expression of *ipt* genes *in planta*. However, most attempts to produce plants altered for either ethylene sensitivity or biosynthesis have utilised constitutive expression of target genes, usually using the cauliflower mosaic virus 35S promoter. Often such plants grow to reproductive maturity and show the expected phenotype of delayed ripening or senescence but have other undesirable phenotypes that reduce their horticultural performance. These pleiotropic effects are caused by constitutive expression of the target genes, sometimes resulting in phenotypes not unlike those observed during leaky expression of cytokinin synthase genes (Klee and Clark, 2001).

The production of transgenic broccoli which were transformed with an antisense *BoACO2* gene from broccoli (Pogson et al., 1995a), driven by a harvest-induced asparagine synthetase (AS) promoter from asparagus (Moyle, 1997) was described in Chapter 4. These plants were produced so that the influence of reduced ethylene biosynthesis during harvest-induced senescence in broccoli could be investigated. In addition, initial characterisation was performed of transgenic broccoli plants harbouring a cytokinin synthase gene (*ipt*) under control of either the senescence associated gene promoter SAG_{12} (Gan and Amasino, 1995), or the floral-associated gene promoter

MYB_{305}. The aim was to investigate the influence of additional endogenous cytokinin on postharvest shelf-life (SAG_{12}) and in the florets (MYB_{305}) of broccoli. In addition, initial characterisation of lines altered for both reduced ethylene and enhanced cytokinin production was conducted.

5.2 METHODS AND MATERIALS

5.2.1 Plant material

Transgenic broccoli heads (*Brassica oleracea* var. *italica* cv. Triathalon) were harvested from primary transformants (T_0 plants) from a containment glasshouse located at Crop & Food Research, Palmerston North. These plants harboured the antisense AS-ACO construct (pPN10), the SAG_{12}-IPT construct (pPN109), the MYB_{305}-IPT construct (pPN110), the AS-ACO::MYB_{305}-IPT double construct (pPN111) or the T-DNA from the control binary vector (pART27). The plants had been transformed by *Agrobacterium tumefaciens* strains LBA4404, GV3101 or AGL1 as described in Chapter 4. Wild-type plants (F_1) were grown alongside the primary transformants for comparison. Whole heads were subjected to postharvest storage at 20°C in the dark. Further, both AS-ACO line 7 and wild-type heads were subjected to 28 d of cool-storage at 1°C prior to shelf-life conditions (20°C in the dark for five days) to simulate export to the northern hemisphere. Whole heads were harvested and packaged in perforated plastic bags to reduce water loss (around 10 % of the water content was lost from heads over the 28 day period, as measured by weight (data not shown)).

Floret tissue (including pedicel and some stemlet tissue) was shaved from the whole heads and branchlets at critical times following harvest for later analyses. Chlorophyll reflectance (hue angle) was measured throughout postharvest senescence. Leaves of a similar developmental stage (third and fifth leaf from the apex) were also detached and stored at 20°C in the dark for up to ten days, and their rate of senescence monitored by measuring chlorophyll reflectance (hue angle) daily.

5.2.2 Chlorophyll reflectance

Details of these methods are outlined in Section 2.1. Chromameter readings were taken randomly through the middle portion of the head (usually six to eight readings) and random spots were chosen for leaves (three to eight readings). Measurements were made once a day at 0900 hours.

5.2.3 RNA extraction and northern analyses

All RNA extractions in this chapter were carried out either using TRIzol™ (Invitrogen) as per the manufacturer's instructions, or by the modified method of Houdebine and Puissant (1995) (details of the methods are outlined in Section 2.5). Northerns were carried out as described in Section 2.8.

5.2.4 RNA transcription

Reagents:

- [α^{32}P]rUTP (400-800Ci/mmol)
- Supplied in the Stratagene kit - 5x RNA transcription buffer, rATP (10 mM), rGTP (10 mM), rCTP (10 mM), DTT (0.75 M), T3 RNA polymerase, T7 RNA polymerase

Single stranded ribosomal RNA (rRNA) probes for *BoACO2* were made using an RNA transcription kit (Stratagene) according to the manufacturer's instructions. The pBLUESCRIPT vector pBoACO2 (5 μg) was linearised by digesting with either *Xho* I to give a T3 priming site for a sense transcript, or *Xba* I to give a T7 priming site for an antisense transcript. The digested plasmid was separated from non-digested plasmid in a 1 x TBE, 1% (w/v) agarose gel and purified from the gel (as described in Section 2.2.4). Approximately 300 ng of the resulting linearised template was used in the RNA transcription reaction incubated at 37°C for 30 min: 5 μL 5 x buffer, 1 μL rATP, 1 μL rGTP, 1 μL rCTP, 1 μL DTT, 5 μL [α^{32}P]rUTP, 10 units of T3 or T7 RNA polymerase and RNase free water to give a final volume of 25 μL. After the reaction, DNA template was removed by incubation at 37°C for 15 min with RNase free DNase (10 units). The single stranded probes were then ready for northern hybridisation (as described in Section 2.8).

5.2.5 ACC oxidase activity

5.2.5.1 Enzyme extraction

Reagents:

- Extraction buffer - 100 mM Tris-HCl, pH 7.5, 10% (v/v) glycerol, 2 mM DTT, and 30 mM sodium ascorbate

The activity of ACC oxidase was determined as described by Hunter et al. (1999) and Gong and McManus (2000). Floret tissue stored at –80°C and previously ground into a powder was extracted in 3-5 volumes of ice-cold extraction buffer. The slurry was filtered through Miracloth (Calbiochem) and centrifuged at 12000 x g for 10 min at 4°C. Solid ammonium sulphate was added to the supernatant to give a final saturation of 30% (164 g L^{-1} at 0°C) on ice for 30 min. The sample was centrifuged at 12000 x g for 10 min at 4°C, and solid ammonium sulphate was added to give a final saturation of 90% (402 g L^{-1} at 0°C). The salt was dissolved on ice for 60 min. The precipitated protein was collected by centrifugation at 12000 x g for 15 min at 4°C. The pellet was resuspended in extraction buffer, and the solution desalted using Sephadex G-25 (Amersham) column chromatography (see below).

5.2.5.2 G25 column chromatography

Reagents:

- Sephadex G25
- Extraction buffer - 100 mM Tris-HCl, pH 7.5, 10% (v/v) glycerol, 2 mM DTT, and 30 mM sodium ascorbate

Columns (G25) were prepared by placing one layer of GF-A glass micro fibre paper (Whatman) in the bottom of disposable 10 mL syringes (Becton Dickensen). The syringes were filled with a slurry of G25 (pre-equilibrated in extraction buffer) and left to settle out without drying the top of the columns. The column volume was approximately five volumes of G25 to one volume of enzyme extract. Samples were loaded onto the top of the column carefully, and eluted in one column volume of cold extraction buffer, straight into tubes on ice.

5.2.5.3 ACC oxidase assay

Reagents:

- Reaction buffer - 50 mM Tris-HCl, pH 7.5, 1 mM ACC, 10% (v/v) glycerol, 2 mM DTT, 30 mM ascorbate, 50 µM $FeSO_4$ and 30 mM $NaHCO_3$.

In vitro ACC oxidase activity was measured from 0.4 mL aliquots of the enzyme preparation warmed to 25°C, and then mixed with 1.6 mL of pre-equilibrated (25°C) reaction buffer in 9 mL capacity vacuum tubes (Vacutainer, Becton-Dickinson). Tubes were sealed and shaken at 25°C for 20 min. The resulting gas (1 mL aliquot of the headspace) was removed and the ethylene content measured with a gas chromatograph (GC-8A, Shimadzu, Kyoto, Japan).

5.2.5.4 Ethylene measurement Ethylene (1 mL samples) produced by the ACC oxidase assay was injected on to a Shimadzu GC-8A Gas Chromatograph (Shimadzu Corporation, Kyoto, Japan) fitted with a flame ionisation detector. The column used was a 2.5 m x 3 mm (I.D.) glass column (Shimadzu 8G2 6-2.0) and was prepacked with Porapak Q with a mesh size of 80/100 (Alltech Associates Inc., Deerfield, USA). Nitrogen was used as the carrier gas at a flow rate of 50 mL min^{-1}. The flame was generated by hydrogen and air at 50 kPa. The column was initially conditioned at 200°C for five hours, thereafter for 0.5 to 1 h before use. For sample measurement, the oven was set at 85°C, and the injector at 150°C. Ethylene sample peaks were identified by comparison with the retention time of an ethylene standard (0.101 ppm) (BOC Gases New Zealand Ltd.). Ethylene had a retention time of 1.5 min.

5.2.5.5 Calculation of ethylene concentration The concentration of ethylene in the 7 mL headspace of vacuum tubes was measured in ppm by comparison to the peak height obtained from a 1 mL injection of ethylene standard (0.101 ppm) (BOC Gases New Zealand Ltd.). The number of moles of ethylene present in the headspace of the vacuum tube could then be calculated using the following equation:

$$n=\frac{PV}{RT} \times ppm \times 10^{-6}$$

where:

n = total number of moles of ethylene in the headspace of the vessel
P = pressure (101325 Pa)
V = volume of headspace of vessel (m^3)
R = universal gas constant (8.314)
T = temperature (normal temperature and pressure (NTP) = 298 K)

5.3.6 Protein determination

Reagents:

- Coomassie Brilliant Blue G250 concentrate dye preparation (Bio-Rad)
- BSA (Bovine serum albumin, fraction V, standard grade, Sigma)

Protein concentration was measured by the method of Bradford (1976) using a commercially available dye (Bio-Rad). Generally, enzyme extracts were diluted 1:10 and aliquots (5-20 µL) were pipetted into the wells of a microtitre plate and made up to 160 µL with water. Bio-Rad reagent (40 µL) was then added and pipetted up and down to mix. After 5 min incubation at room temperature, the protein content was measured at 595 nm using an Anthos htII plate reader (Anthos Labtech Instruments, Salzburg, Austria) by comparison of a protein standard (0-5 µg standard curve of BSA).

5.2.7 Western analyses

Reagents:

- Transfer buffer – 25 mM Tris, 192 mM Glycine, 20 % (v/v) methanol, 10% (v/v) SDS
- 1 x TBS – 20mM Tris-HCl pH 7.6, 150 mM NaCl
- Blocking solution – 50 mM Tris-HCl pH 8.0, 150 mM NaCl, 0.3% (v/v) Tween 20, 1% (w/v) BSA
- Washing buffer – 1 x TBS, 0.05% (v/v) Tween 20
- Colour development buffer – 0.1 M Tris pH 9.5, 0.05 M $MgCl_2$, 0.1 M NaCl

Western blots were carried out using antibodies described by Hunter et al. (1999) and followed the method of Towbin et al. (1979) as described by McManus et al. (1994). The method used for SDS-PAGE was previously described by Laemmli (1970). Proteins were separated in an 8% (w/v) precast polyacrylamide mini gel (iGels, Gradipore, Australia) at 150 V for approximately 1 h. The gel was then blotted on to PVDF membrane (0.2 micron, Bio-Rad) at 4°C in transfer buffer overnight using Trans-Blot Electrophoretic Transfer Apparatus (Bio-Rad) at 12 V. The membrane was then exposed to blocking solution for 1 h at room temperature, followed by incubation with TRACO2 polyclonal antibody (Hunter et al., 1999) (whole sera was diluted 1:500 in blocking solution) for 2 h at room temperature with gentle shaking. The membrane was washed for 5 min, five times in washing buffer at room temperature with gentle shaking. The membrane was then incubated with secondary anti-rabbit antibody linked with

alkaline phosphatase diluted 1:10000 in blocking solution, for 1 h with gentle shaking at room temperature. The membrane was then washed for 5 min, five times in washing buffer, then 5 min, two times in 1 x TBS buffer. Colouration was developed by the addition of 10 mL of colour development buffer with the addition of 200 μL of NBT/BCIP solution (Roche). The colour reaction was stopped by washing the membrane with water twice.

5.3 RESULTS

5.3.1 Senescence of AS-ACO leaves

Leaves were detached from transgenic and wild-type broccoli plants at a similar stage of development, and stored at 20°C for up to ten days in the dark. Loss of greenness from leaves was measured by hue angle using a chromameter as previously described (see Section 2.1).

Initial hue angle readings were around 130 and declined rapidly following detachment, as the tissue became yellow (Figure 5.1). Leaves that were detached from position three from the apex yellowed more slowly than the leaves detached from position five from the apex. Leaves from a number of transgenic lines harbouring the AS-ACO construct maintained their greenness for longer than leaves detached from both wild-type and pART27 transgenic plants. However, eventually, all leaves from the older developmental stage (fifth leaf from the apex) from both transgenic and wild-type plants had yellowed. Not all the younger leaves (third leaf from the apex) yellowed completely by ten days following detachment. Figure 5.2 shows the reduced rate of detached leaf senescence of selected AS-ACO lines compared to wild-type leaves of a similar developmental stage.

Leaves from both wild-type and AS-ACO line 7 were also tagged early during development at a similar position to the apical meristem. Late during development these same leaves were measured for hue angle. Wild-type leaves had a hue angle value no higher than 90 (yellow) whereas transgenic AS-ACO Line 7 leaves had measured hue

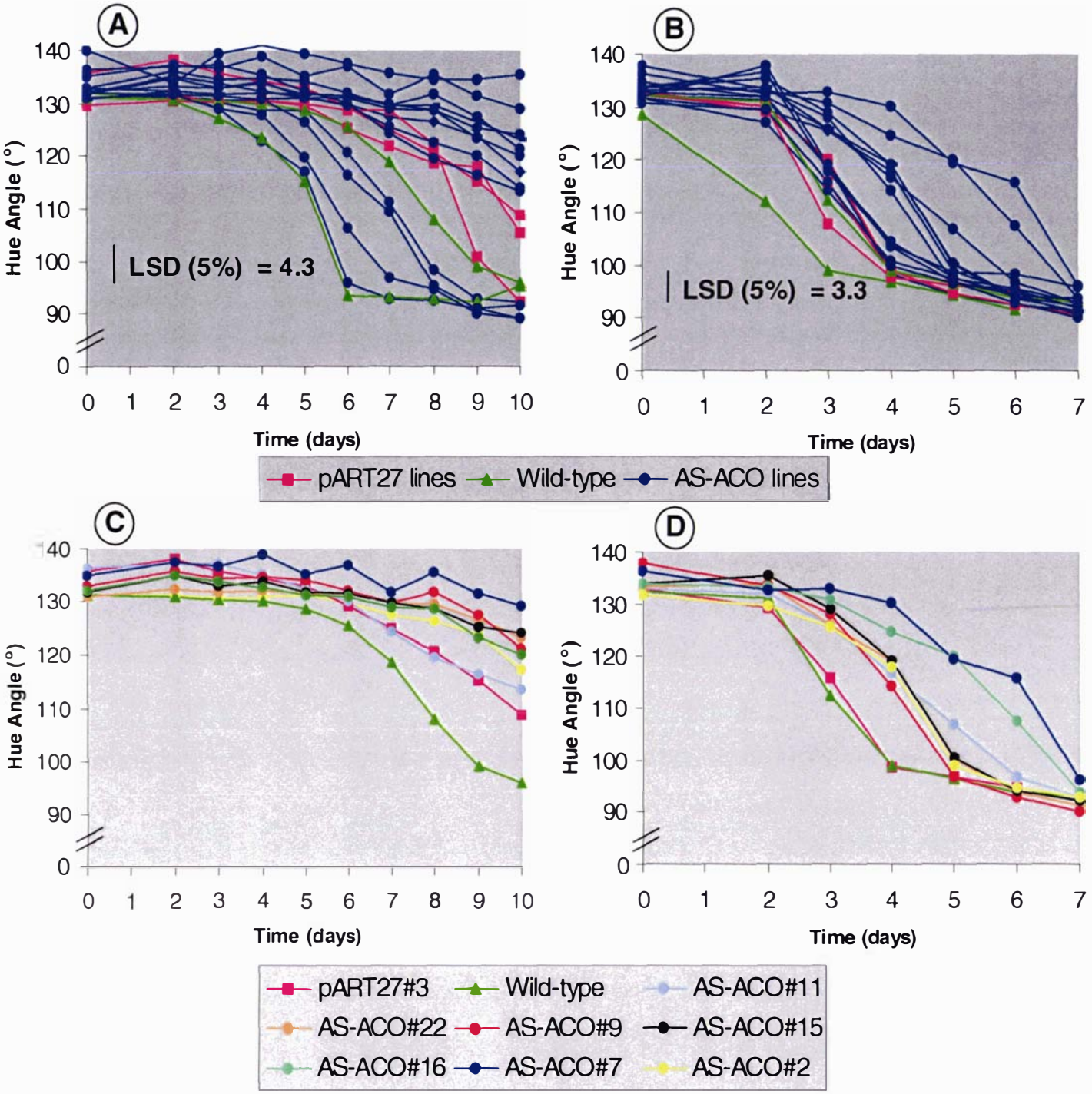

Figure 5.1 Hue angle of detached leaves of AS-ACO and control plants: A and C are measurements of the third leaf from the apex; B and D are measurements of the fifth leaf from the apex. Leaves were detached from transgenic and wild-type plants at a similar stage of development, and stored at 20°C for up to ten days in the dark. A and B represent all the data collected for the experiment, and C and D represent selected transgenic and control lines. Each data point represents the mean hue angle value for one individual leaf (n=3).

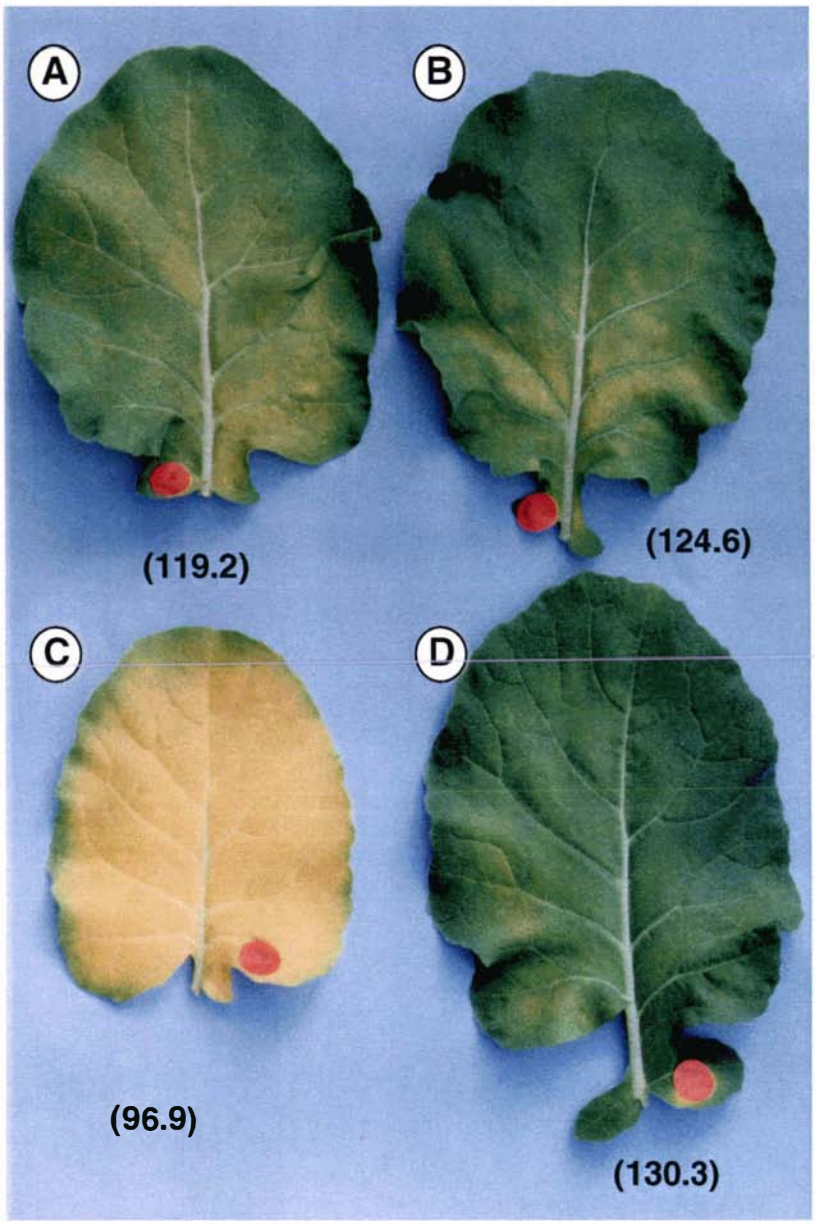

Figure 5.2 Detached leaf senecence of AS-ACO and wild-type plants.
Photographs show the fifth leaf from the apex detached from plants at a similar stage of development and stored at 20°C for four days in the dark. A. AS-ACO line 16, B. AS-ACO line 15, C. wild-type and D. AS-ACO line 7. Numbers in brackets represent the mean hue angle measurements (n=3) for individual leaves.

angle values of around 111 (still relatively green). The senescence of leaves still attached to the plant appeared to be delayed in AS-ACO line 7 plants when compared to wild-type plants (Figure 5.3).

5.3.2 Postharvest senescence of AS-ACO heads

Five transgenic lines were selected for postharvest trials, four containing the AS-ACO construct and a fifth containing the T-DNA from the control plasmid pART27, as well as wild-type heads for comparison. Note, however, that the wild-type heads were harvested and analysed at a different time to the transgenic plants. Figure 5.4 shows the rate of greenness loss in the five days following harvest of heads stored at 20°C in the dark. Those lines that contained the AS-ACO construct retained at harvest levels of chlorophyll after five days postharvest storage compared to the control pART27 line and the wild-type. By 48 h following harvest, for the control and wild-type, chlorophyll levels had started to decline and reached the low hue angle value of around 100 by day five. Figure 5.5 shows photographs of the heads (minus wild-type heads) analysed for hue angle, both four days (96 h) and five days (120 h) following harvest. The retention of greenness by the all four AS-ACO lines is very clearly shown in the photographs in comparison to the control transgenic line.

5.3.3 Characterisation of ACC oxidase in AS-ACO florets

5.3.3.1 Gene expression RNA transcription was used to produce both sense and antisense single stranded probes for northern analyses of *BoACO2* gene expression in the AS-ACO floret material following harvest. However, non-specific binding of both sense and antisense single stranded ribo-probes appeared to occur to ribosomal RNA. As a consequence, a single band of the size (~1.3 kb) corresponding to *BoACO2* was unable to be determined (Figure 5.6). Figure 5.7 shows the northern hybridisation of *BoACO1* with RNA isolated from florets of postharvest stored transgenic and wild-type heads. In all cases a similar profile of gene expression was seen for *BoACO1* in the five days following harvest for all the transgenic lines analysed, which appeared to be somewhat reduced compared to wild-type 48-72 h following harvest, but did appear to be similar to the transgenic control line (pART27).

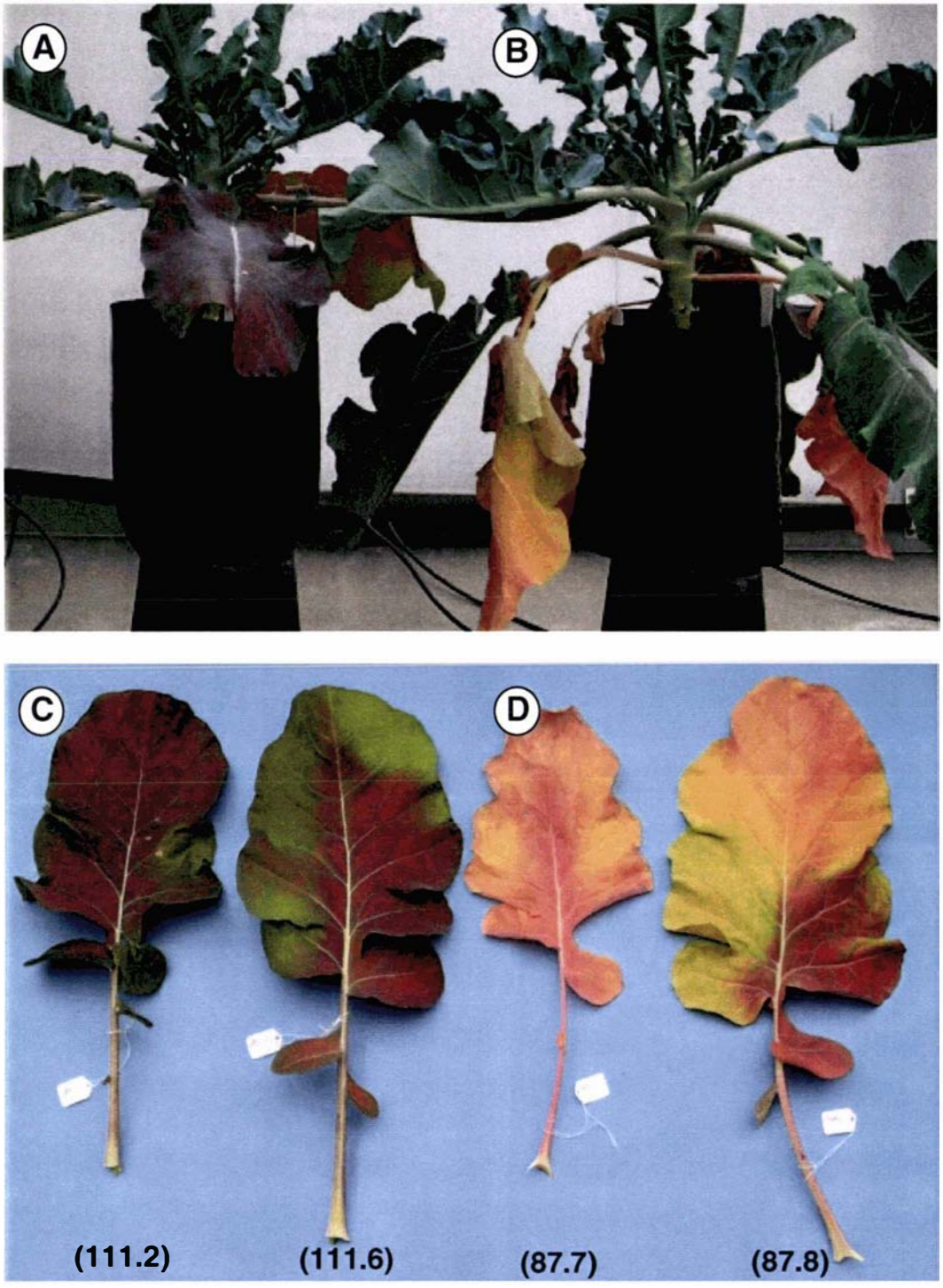

Figure 5.3 Natural leaf senecence of AS-ACO plants. Photographs show the natural leaf senescence of leaves: A and C, AS-ACO line 7; B and D wild-type plants and leaves. Leaves from AS-ACO line 7 and wild-type plants were tagged at an early and similar stage of development, then analysed after heads were removed. Numbers in brackets represent mean hue angle measurements (n=6) for the individual leaves.

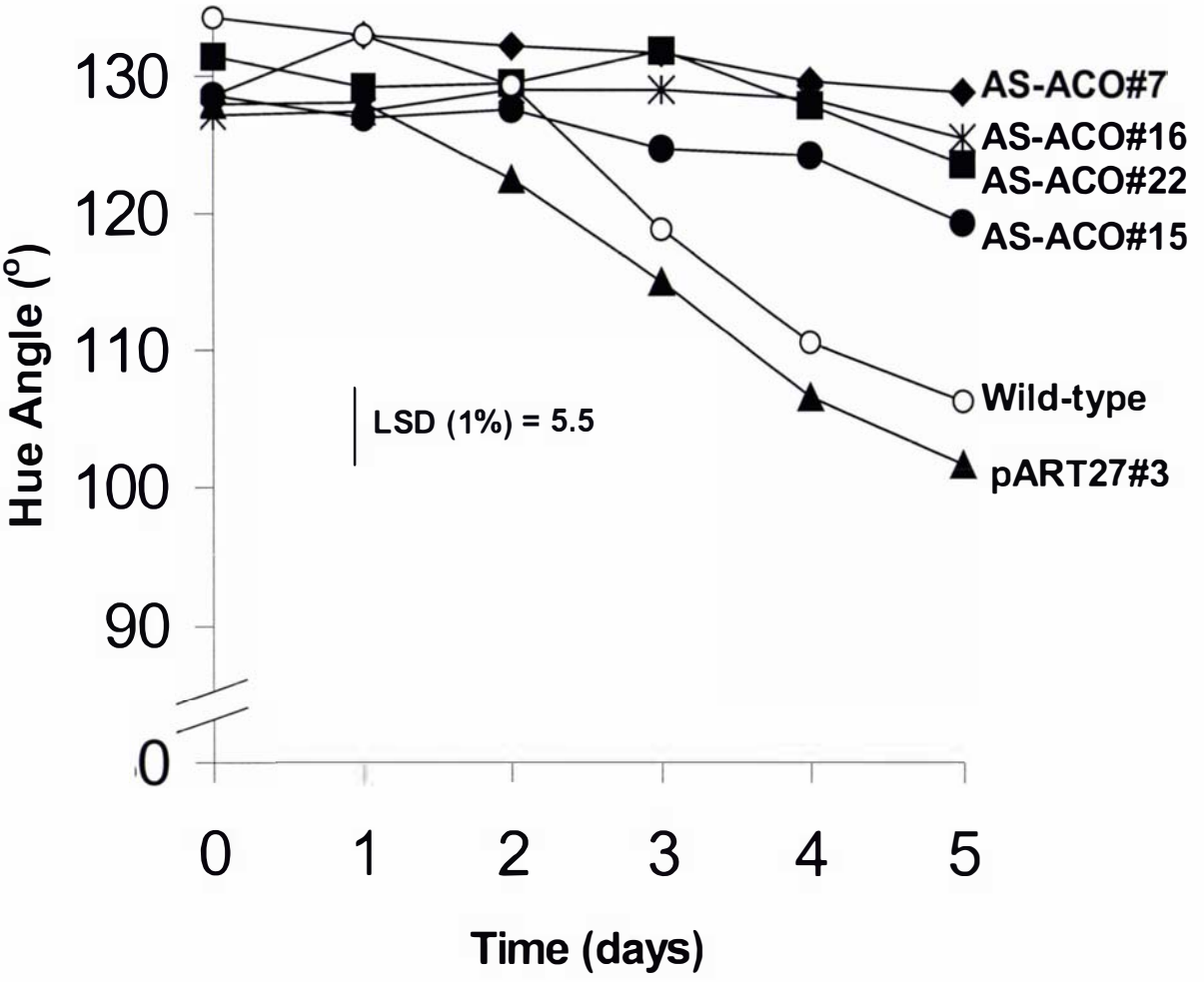

Figure 5.4 Hue angle of harvested heads from transgenic broccoli plants. Heads were harvested from transgenic AS-ACO and pART27 (control), and wild-type plants at a similar stage of development and stored at 20°C for up to five days in the dark. Each data point represents the mean hue angle value for one individual head (n=6).

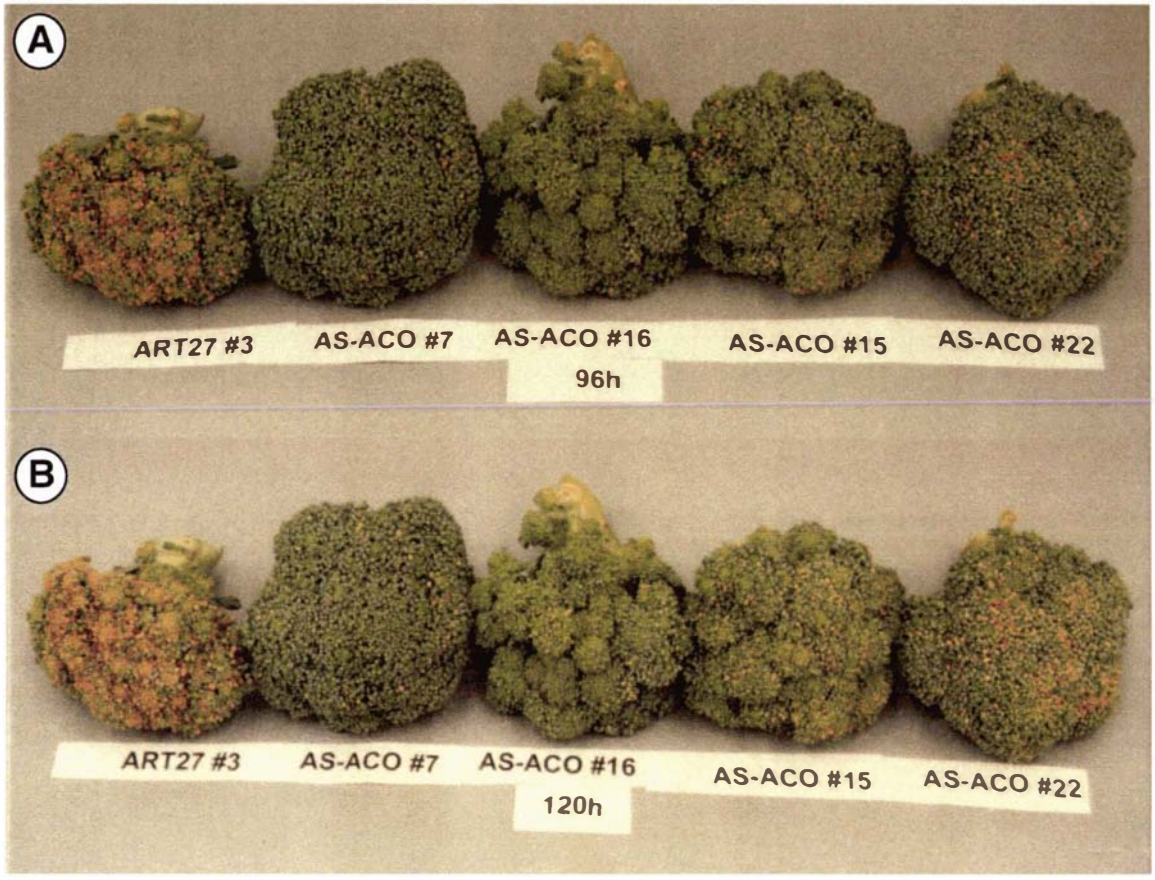

Figure 5.5 Senescence of heads from AS-ACO plants: A, after 96 h and B, after 120 h storage of transgenic broccoli heads harvested from AS-ACO and pART27 (control) plants at a similar stage of development and stored at 20°C in the dark.

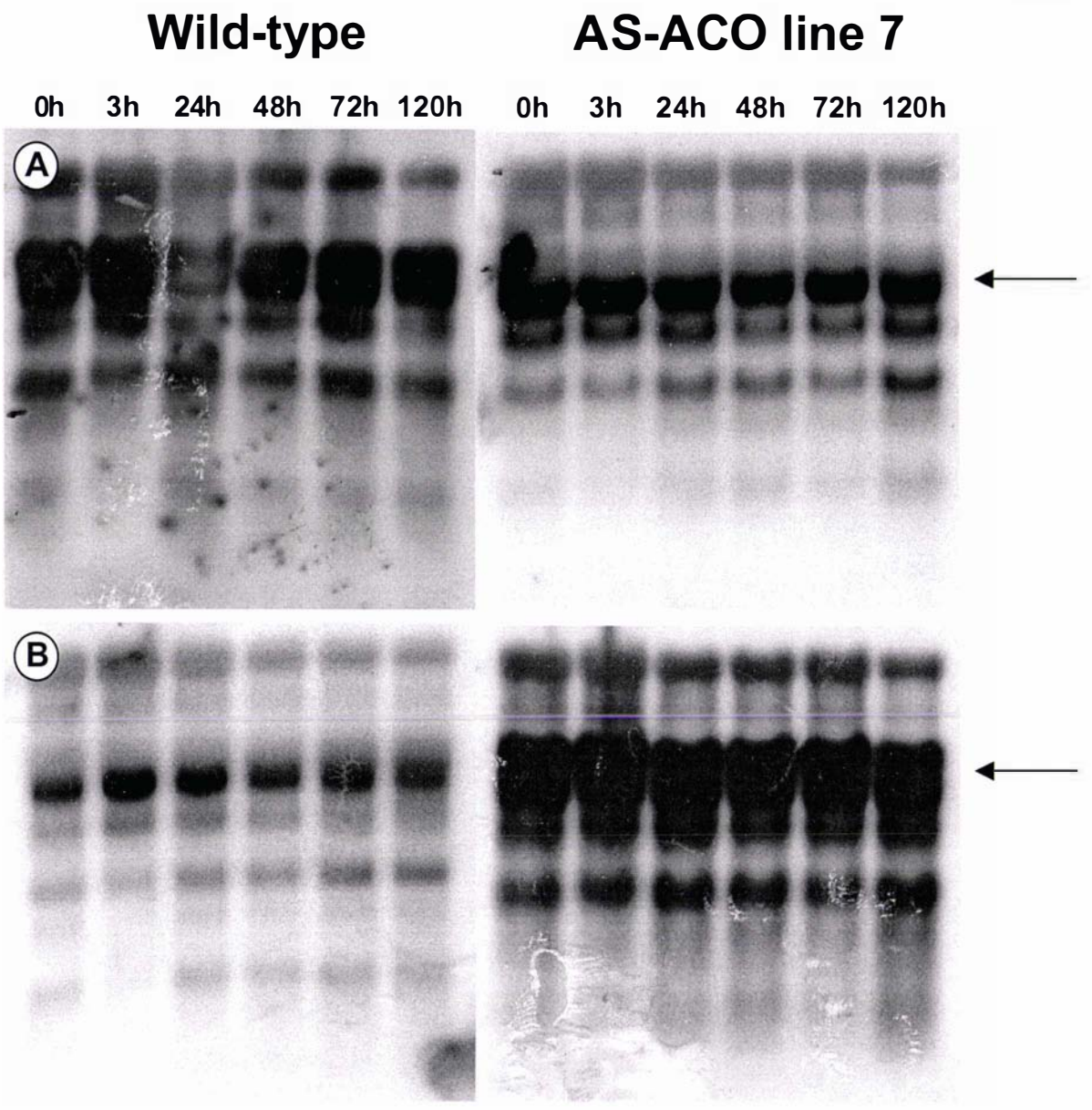

Figure 5.6 Autoradiographs showing the northern hybridisation of A, a 1.3 kb ^{32}P labeled single stranded sense *BoACO2* RNA fragment and B, a 1.3 kb ^{32}P labeled single stranded antisense *BoACO2* RNA fragment with total RNA from transgenic and wild-type broccoli following harvest. Total RNA (20 μg) extracted from broccoli florets treated following harvest in air, was denatured and separated in a 1.2% (w/v) agarose gel in 2.2 M formaldehyde, and then transferred to nylon membranes. For details of hybridisation and washing conditions, see Methods and Materials, Section 2.8. Arrows represent approximate expected position of 1.3 kb *BoACO2* hybridisation.

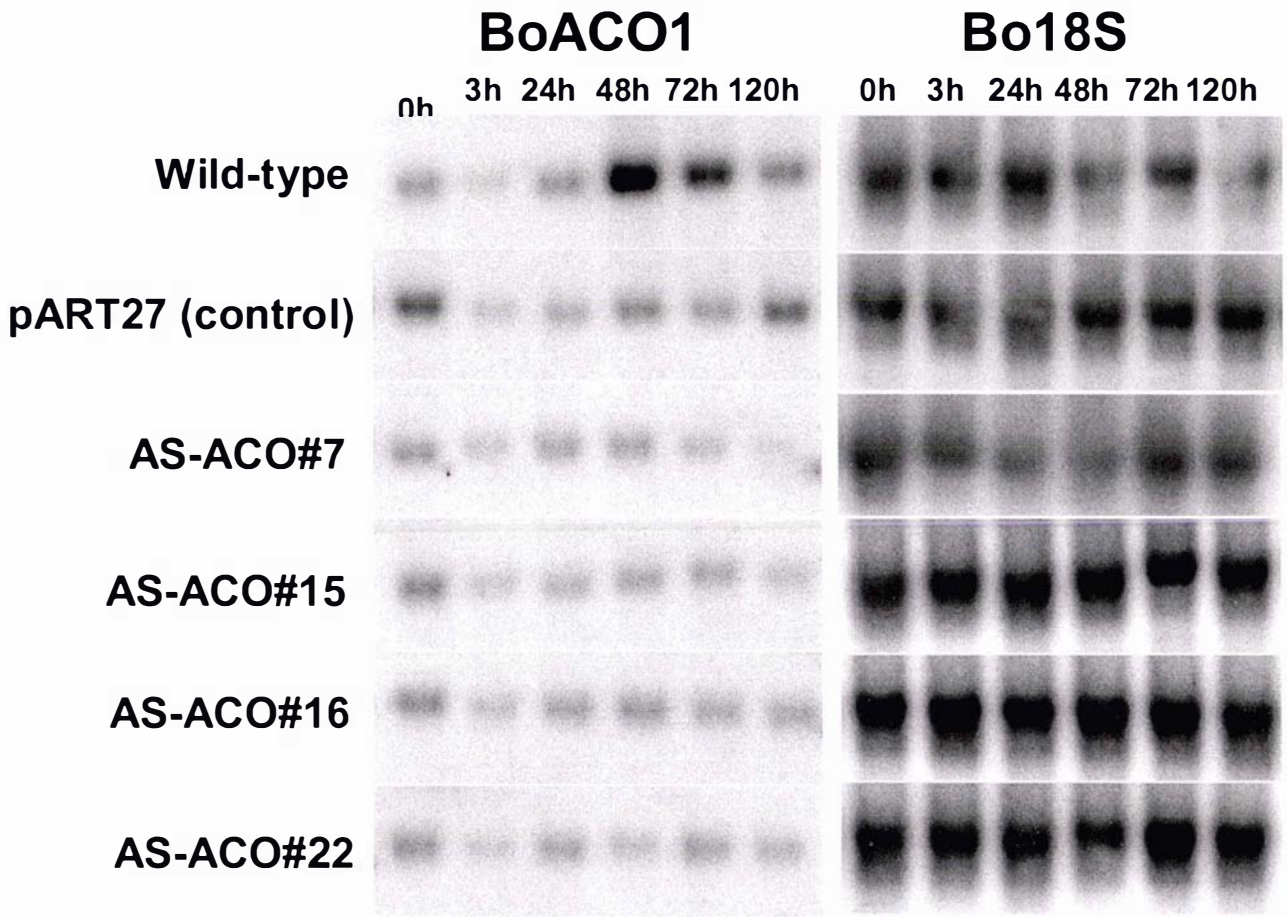

Figure 5.7 Autoradiographs showing the northern hybridisation of a 1.3 kp ^{32}P labeled *BoACO1* cDNA fragment and a 400 bp ^{32}P labelled *Bo18S* partial cDNA fragment with total RNA from transgenic and wild-type broccoli following harvest. Total RNA (20 μg) extracted from broccoli florets treated following harvest in air, was denatured and separated in a 1.2% (w/v) agarose gel in 2.2 M formaldehyde, and then transferred to nylon membranes. For details of hybridisation and washing conditions, see Section 2.8. These northern experiments were repeated with similar results.

5.3.3.2 *In vitro* ACC oxidase enzyme activity ACC oxidase activity was measured in enzyme preparations extracted from florets of postharvest stored heads of AS-ACO line 7 and wild-type plants. ACC oxidase activity increased from 24 h following harvest and continued to rise until at least 72 h following harvest in wild-type extracts (Figure 5.8). In AS-ACO line 7 extracts, ACC oxidase activity levels remained at basal levels throughout the 72 h period following harvest.

5.3.3.3 PAGE and western analyses Proteins from enzyme preparations were separated using PAGE and resulting gels were either stained with Coomassie blue stain or blotted on to PVDF membrane for western analyses. Figure 5.9 shows both PAGE and western analyses of extracts isolated from AS-ACO line 7 and wild-type florets following harvest. The main protein band visible in the PAGE gel was approximately 50 kDa in size. This band was proposed to be the Rubisco band (Michael McManus, personal communication). This band decreases in intensity in the wild-type 48 h and 72 h samples as compared to the equivalent AS-ACO samples. The TRACO2 polyclonal antibody recognised a 30-40 kDa band that increases in intensity in the 48 h and 72 h samples from wild-type extracts only. The protein levels for this band did not increase as in wild-type florets for the AS-ACO line 7 samples in the 72 h following harvest.

5.3.4 Gene expression during postharvest storage of AS-ACO florets

5.3.4.1 Senescence markers The expression profiles of the senescence marker genes encoding a metallothionein-like protein (*BoMLP*) and a cysteine protease (*BoCP5*) in transgenic and wild-type florets following harvest is shown in Figures 5.10 and 5.11 respectively. In the wild-type florets *BoMLP* transcript levels had increased by 24 h following harvest and rose to high levels by 48 h, and this level was maintained until at least 120 h following harvest. For all transgenic lines, the increase of *BoMLP* transcript levels appeared to be higher at 24 h following harvest than in the wild-type florets. However, these levels did not increase to the same levels observed for wild-type tissue, or pART27 controls, but were maintained at this level to at least 120 h following harvest for AS-ACO lines. However it should be noted that this transcript was present at harvest at higher levels in the pART27 control line compared to all other lines analysed.

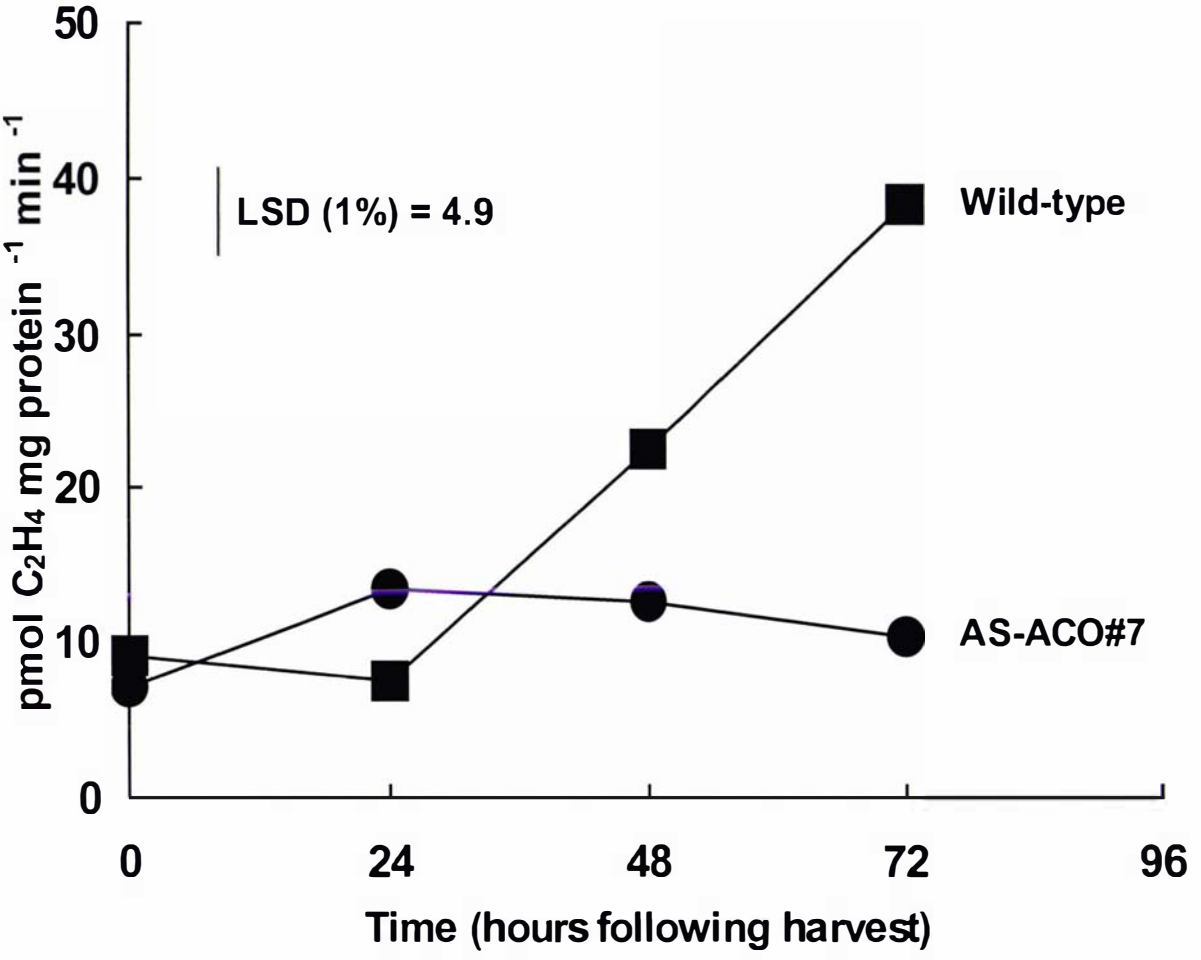

Figure 5.8 *In vitro* enzyme activity of ACC oxidase in crude enzyme extracts from wild-type and AS-ACO line 7 florets following harvest. Heads were harvested at a similar stage of development and stored at 20°C for up to five days in the dark. Each data point represents the mean ACC oxidase activity value of individual assays from one individual head (n=4).

Figure 5.9 Analyses of ACC oxidase in wild-type and AS-ACO Line 7 florets following harvest. A. Polyacrylamide gel electrophoresis (PAGE) analyses of enzyme extracts and B. western analyses of ACC oxidase in wild-type and AS-ACO line 7 florets following harvest. Heads were harvested at a similar stage of development and stored at 20°C in the dark (only up to three days (72 h) analysed here). Western analysis of ACO protein accumulation in extracts from broccoli florets from both AS-ACO line 7 and wild-type plants was detected using polyclonal antibodies raised against TRACO2 (Hunter et al., 1999). Antibody recognition was detected using an alkaline-phosphatase-linked secondary antibody.

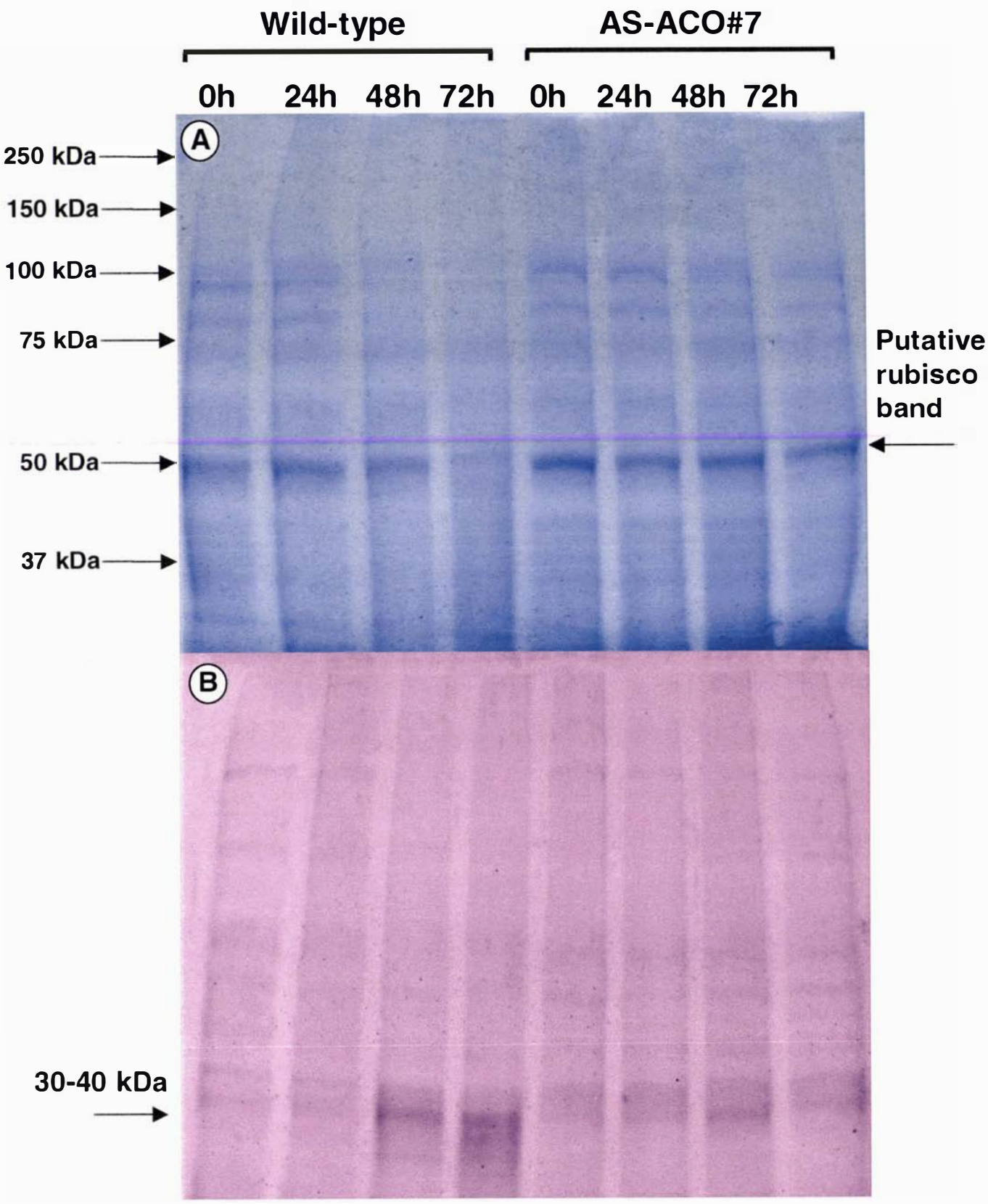
Wild-type
AS-ACO#7
0h
24h
48h
72h
0h
24h
48h
72h
A
250 kDa
150 kDa
100 kDa
75 kDa
50 kDa
37 kDa
Putative rubisco band
B
30-40 kDa

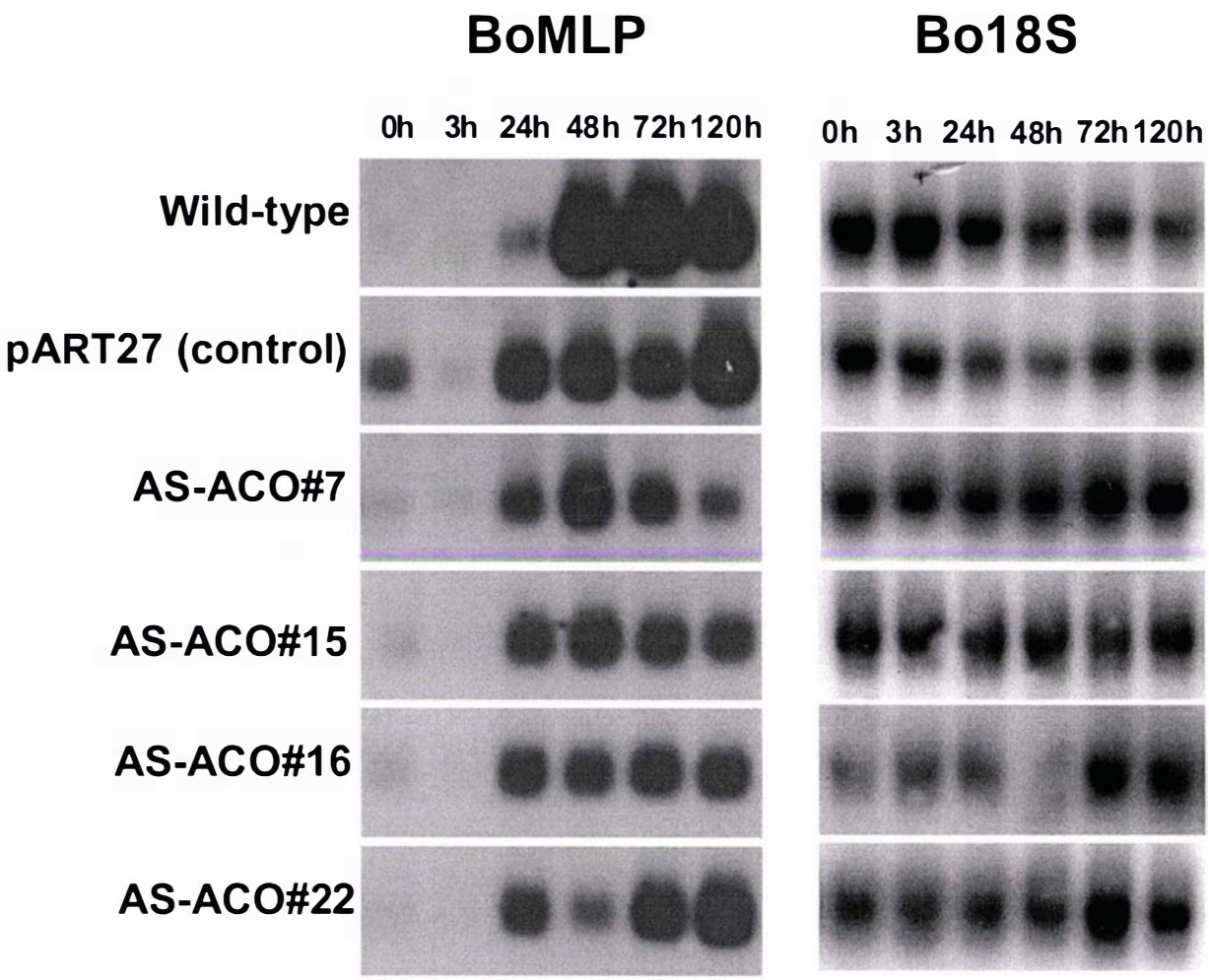

Figure 5.10 Autoradiographs showing the northern hybridisation of a 500 bp ^{32}P labelled metallothionein-like protein (*BoMLP*) cDNA fragment and a 400 bp ^{32}P labelled *Bo18S* partial cDNA fragment with total RNA from transgenic and wild-type broccoli following harvest. Total RNA (20 μg) extracted from broccoli florets treated following harvest in air, was denatured and separated in a 1.2% (w/v) agarose gel in 2.2 M formaldehyde, and then transferred to nylon membranes. For details of hybridisation and washing conditions, see Section 2.8. These northern experiments were repeated with similar results.

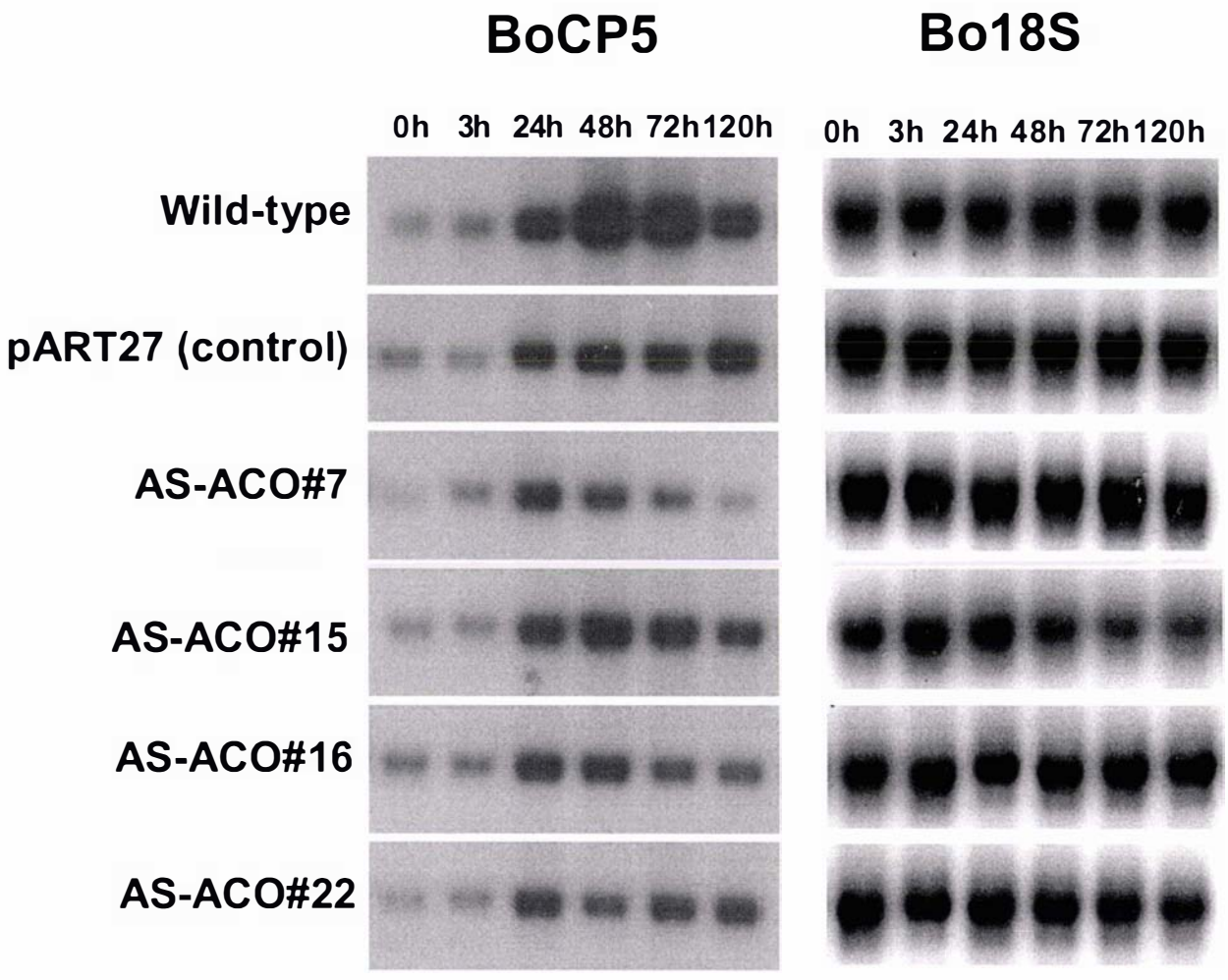

Figure 5.11 Autoradiographs showing the northern hybridisation of a 1.3 kb ^{32}P labelled cysteine protease (*BoCP5*) cDNA fragment and a 400 bp ^{32}P labelled *Bo18S* partial cDNA fragment with total RNA from transgenic and wild-type broccoli following harvest. Total RNA (20 μg) extracted from broccoli florets treated following harvest in air, was denatured and separated in a 1.2% (w/v) agarose gel in 2.2 M formaldehyde, and then transferred to nylon membranes. For details of hybridisation and washing conditions, see Section 2.8. These northern experiments were repeated with similar results.

BoCP5 transcript levels were present at low levels at harvest and increased at 24 h to reach the highest levels by 48-72 h following harvest in wild-type florets (Figure 5.11). By 120 h following harvest, *BoCP5* transcript levels started to decline in wild-type florets. This pattern was also observed for the pART27 control line, although the transcript levels did not increase to the same levels and no decline was observed 120 h following harvest. Generally for all AS-ACO lines analysed, *BoCP5* transcript levels appeared to be lower in comparison to both the wild-type and pART27 florets following harvest. In some cases (AS-ACO lines 7 and 16) *BoCP5* transcript levels appeared to decline in florets 72 h following harvest.

5.3.4.2 Carbohydrate metabolism *BoINV1* transcript level was low at harvest, increased at 72 h and continued to rise at 120 h in wild-type florets following harvest (Figure 5.12). This change in transcript profile was also observed for pART27, but appeared to be weaker in comparison to the wild-type profile. No increase in *BoINV1* transcript was observed for any of the transgenic lines harbouring the AS-ACO construct in the 120 h analysed following harvest.

BoHK1 transcript level was low at harvest, increased at 72 h and then declined at 120 h in wild-type florets following harvest (Figure 5.13). A slight increase was also observed for pART27 at 120 h following harvest, but the *BoHK1* transcript levels were lower in comparison to wild-type florets. No increase in the *BoHK1* transcript was observed for any of the transgenic lines harbouring the AS-ACO construct in the 120 h analysis period.

5.3.4.3 Sucrose transporters *BoSUC1* transcript levels increased markedly at 48 h and start to decline 72-120 h following harvest in wild-type florets (Figure 5.14). *BoSUC1* transcript was present at relatively high levels at harvest, declined immediately to basal levels by three hours, and then increased at 72-120 h in florets following harvest for pART27. Little change in *BoSUC1* transcript levels was observed for any of the AS-ACO transgenic lines analysed over the 120 h period following harvest in comparison to both wild-type and pART27 control florets.

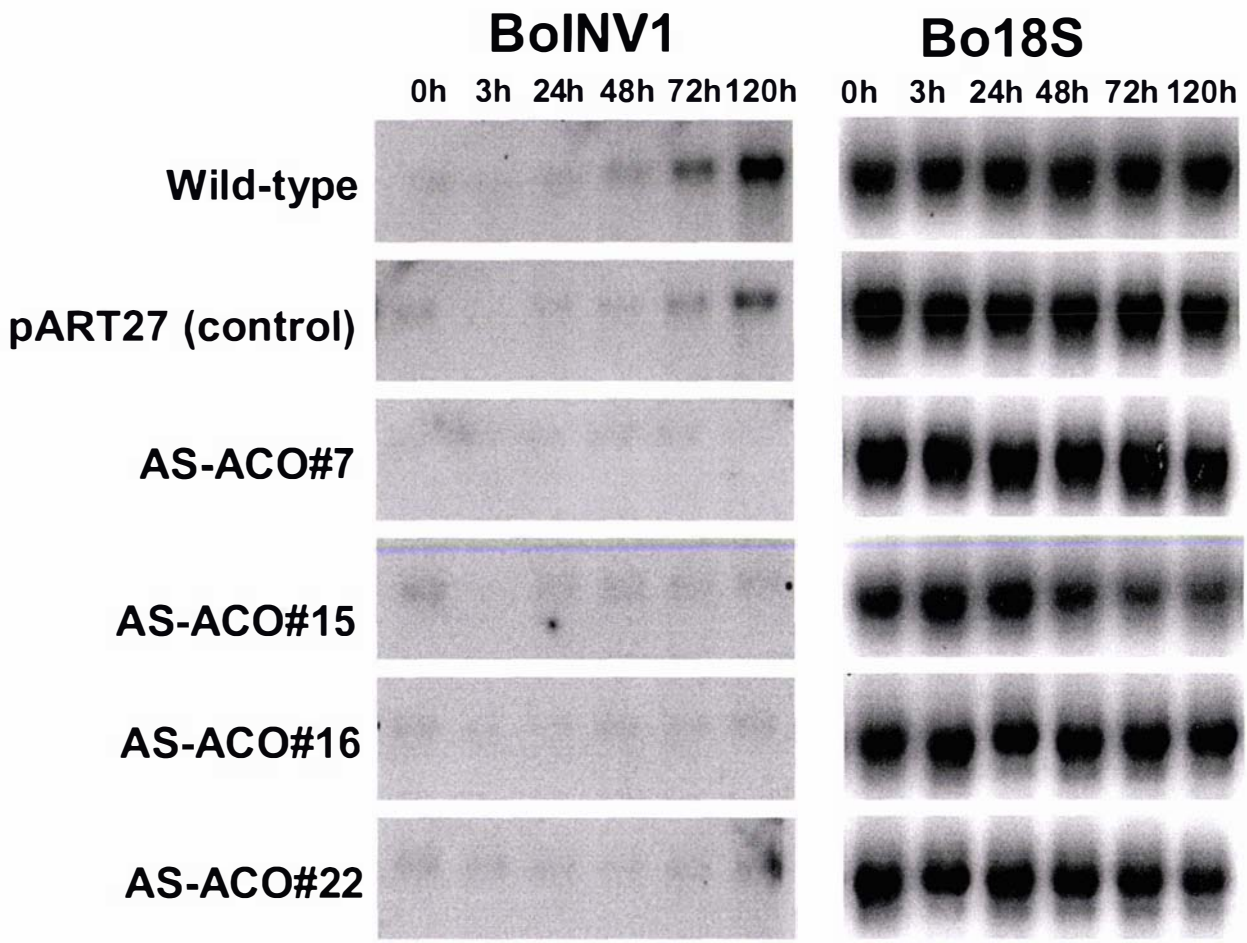

Figure 5.12 Autoradiographs showing the northern hybridisation of a 800 bp ^{32}P labelled acid invertase (*BoINV1*) cDNA fragment and a 400 bp ^{32}P labelled *Bo18S* partial cDNA fragment with total RNA from transgenic and wild-type broccoli following harvest. Total RNA (20 μg) extracted from broccoli florets treated following harvest in air, was denatured and separated in a 1.2% (w/v) agarose gel in 2.2 M formaldehyde, and then transferred to nylon membranes. For details of hybridisation and washing conditions, see Section 2.8.

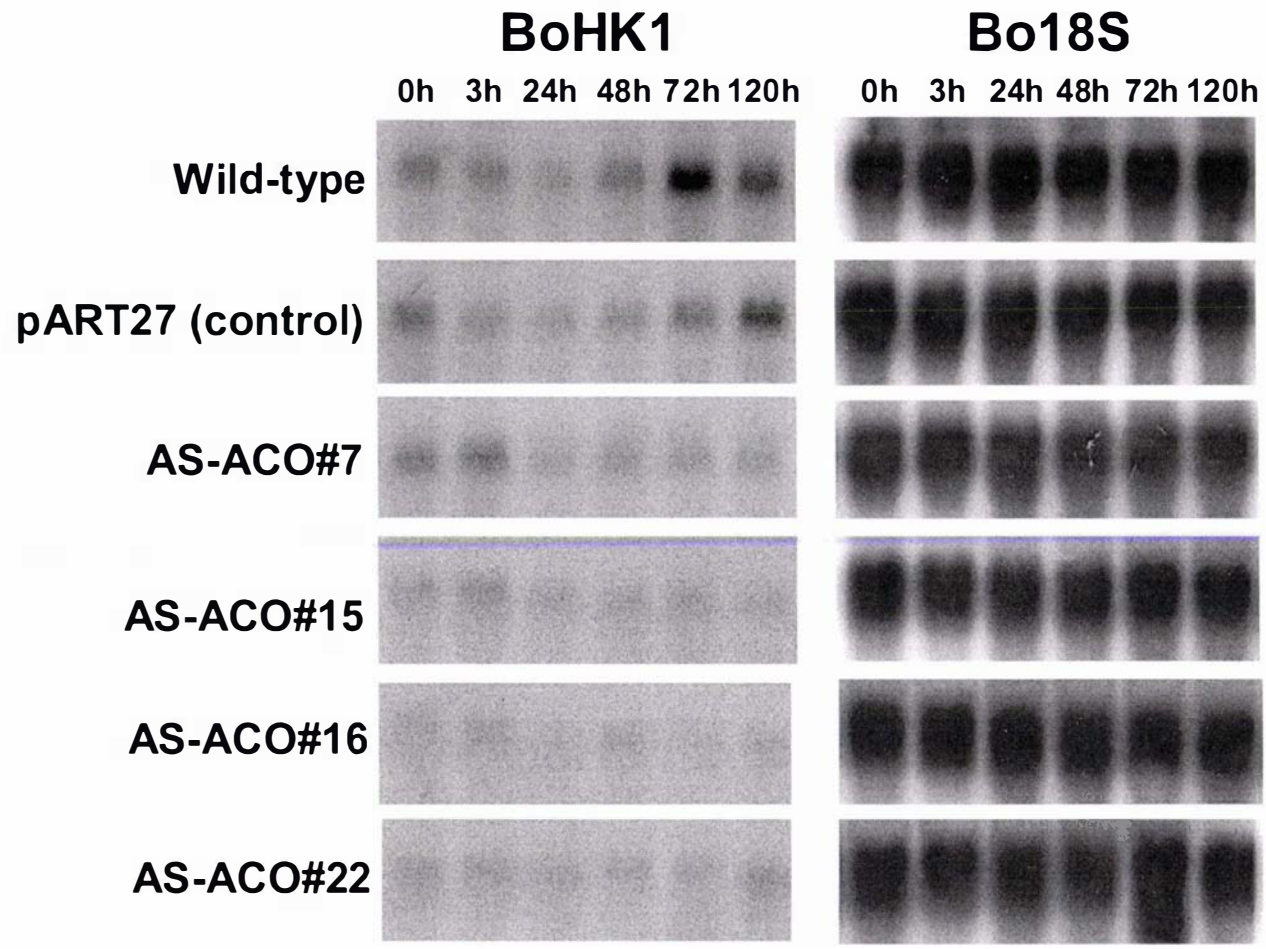

Figure 5.13 Autoradiographs showing the northern hybridisation of a 1.6 kb ^{32}P labelled hexokinase (*BoHK1*) cDNA fragment and a 400 bp ^{32}P labelled *Bo18S* partial cDNA fragment with total RNA from transgenic and wild-type broccoli following harvest. Total RNA (20 µg) extracted from broccoli florets treated following harvest in air, was denatured and separated in a 1.2% (w/v) agarose gel in 2.2 M formaldehyde, and then transferred to nylon membranes. For details of hybridisation and washing conditions, see Section 2.8.

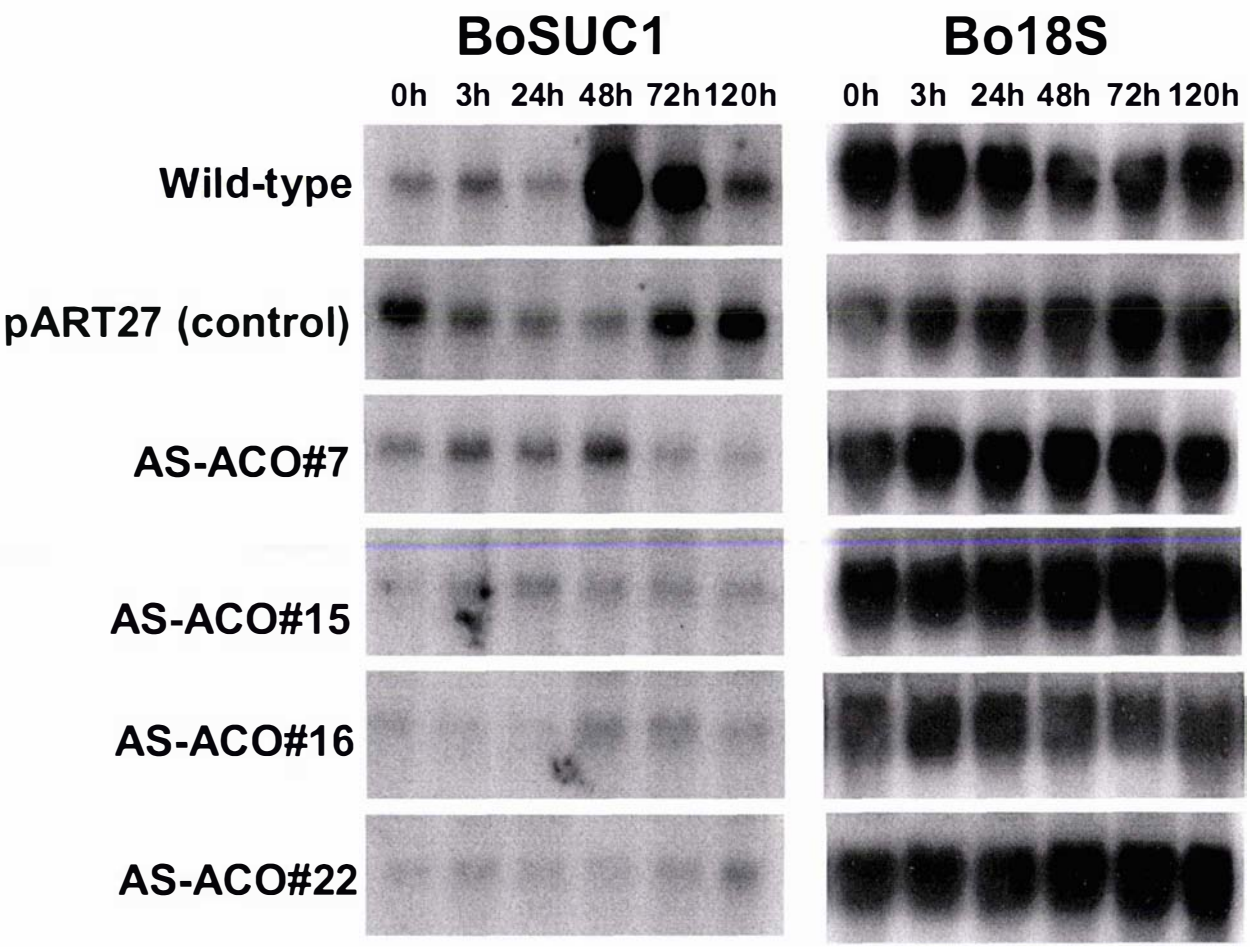

Figure 5.14 Autoradiographs showing the northern hybridisation of a 1.8 ^{32}P labelled sucrose transporter (*BoSUC1*) cDNA fragment and a 400 bp ^{32}P labelled *Bo18S* partial cDNA fragment with total RNA from transgenic and wild-type broccoli following harvest. Total RNA (20 μg) extracted from broccoli florets treated following harvest in air, was denatured and separated in a 1.2% (w/v) agarose gel in 2.2 M formaldehyde, and then transferred to nylon membranes. For details of hybridisation and washing conditions, see Section 2.8.

BoSUC2 transcript levels increased at 48 h, peaked at 72 h and declined by 120 h following harvest in wild-type florets (Figure 5.15). *BoSUC2* transcript had increased by 72 h and kept increasing at 120 h in florets following harvest for pART27. Little change in *BoSUC2* transcript levels was observed for any of the AS-ACO transgenic lines analysed over the 120 h period following harvest in comparison to both wild-type and pART27 control florets.

5.3.5 Influence of cool-storage on shelf-life of AS-ACO heads

The influence of cool-storage at 1°C for 28 days after harvest on the shelf-life of AS-ACO line 7 and wild-type heads is shown in Figure 5.16. Hue angle values declined after one day of shelf-life conditions for wild-type heads that were subjected to either 28 days cool-storage and or underwent shelf-life conditions without the cool-storage. A similar decline for both treatments occurred in the first three days of postharvest storage, when the decline for the cool-stored material accelerated compared to the non-cool-stored wild-type heads. The AS-ACO heads retained their at harvest greenness until after three days of shelf-life conditions. The AS-ACO heads that did not undergo cool-storage retained near at harvest hue angle levels, whereas the cool-stored AS-ACO heads had a similar hue angle value as non-cool-stored wild-type heads after five days of shelf-life conditions.

5.3.6 Influence of *ipt* constructs on plant morphology

Introduction of constructs for altered cytokinin, SAG_{12}-IPT (pPN109), MYB_{305}-IPT (pPN110) and AS-ACO::MYB_{305}-IPT (pPN111), caused altered plant morphology in broccoli plants both growing in culture (see Chapter 4 for details) and also when grown in the GMO containment house (Figure 5.17). At least one line for each of these constructs appeared to be bushier, with shortened plant stature. An altered floral bolting phenotype was also observed (Figure 5.17). However, some of the morphological changes (particularly floral bolting) maybe attributed to the hot growing conditions during early summer, which were not suitable for the cultivar used in this study.

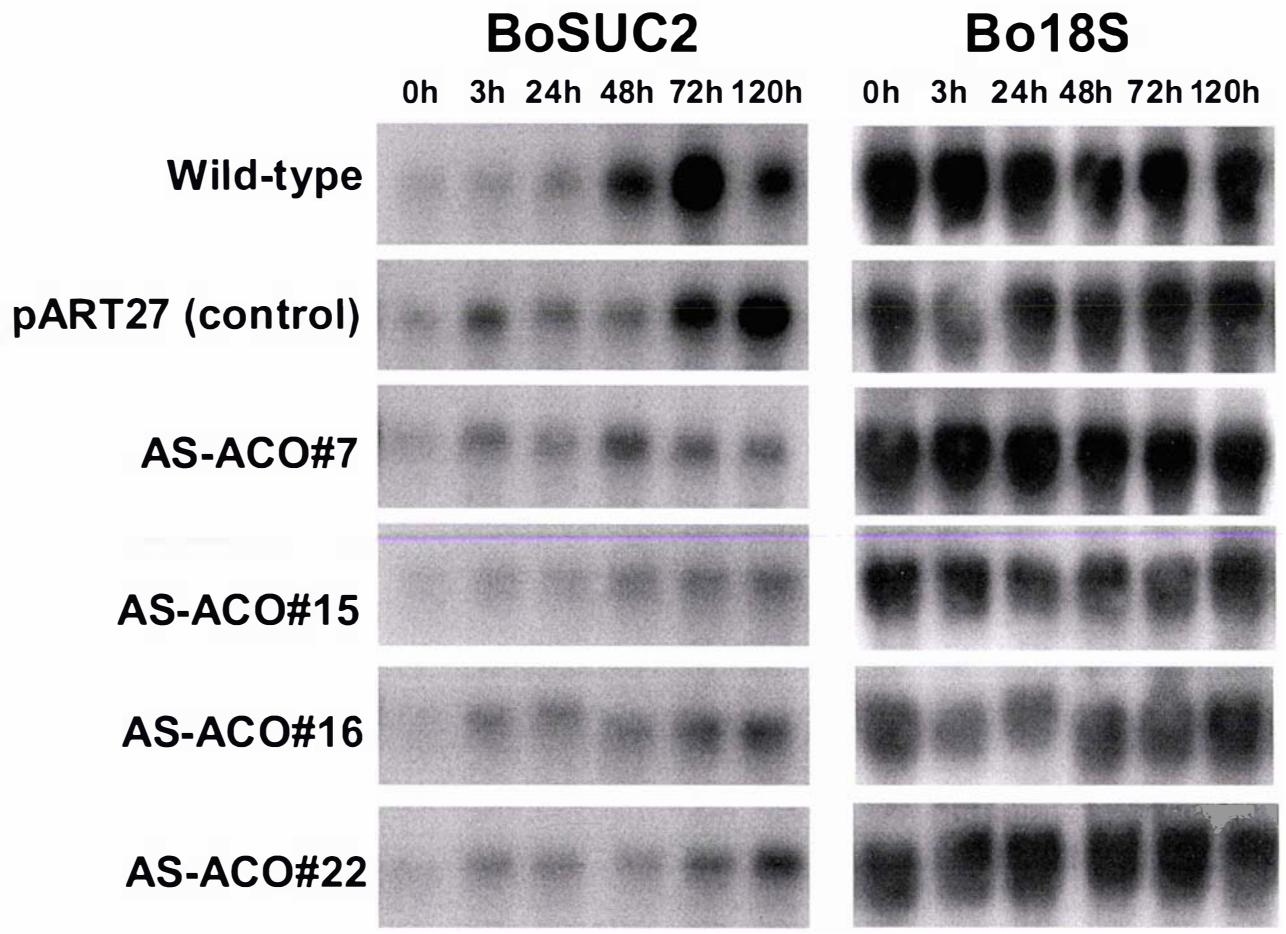

Figure 5.15 Autoradiographs showing the northern hybridisation of a 1.7 kb ^{32}P labelled sucrose transporter (*BoSUC2*) cDNA fragment and a 400 bp ^{32}P labelled *Bo18S* partial cDNA fragment with total RNA from transgenic and wild-type broccoli following harvest. Total RNA (20 μg) extracted from broccoli florets treated following harvest in air, was denatured and separated in a 1.2% (w/v) agarose gel in 2.2 M formaldehyde, and then transferred to nylon membranes. For details of hybridisation and washing conditions, see Section 2.8.

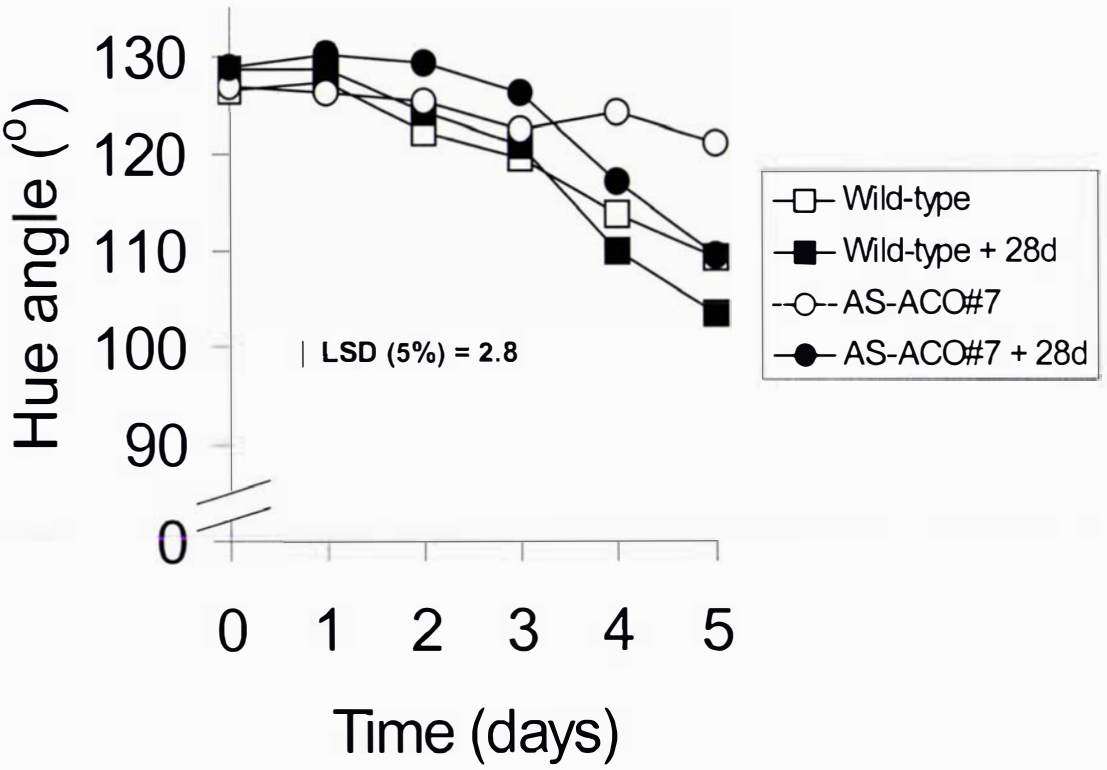

Figure 5.16 Influence of cool-storage on the shelf-life of both transgenic AS-ACO line 7 and wild-type broccoli heads following harvest as measured by hue angle. Broccoli heads were harvested at a similar stage of development and stored at either 1°C for 28 days, then at shelf conditions, or placed directly into shelf conditions at 20°C for up to five days in the dark. Each data point represents the mean hue angle value of two heads from each line (n=8).

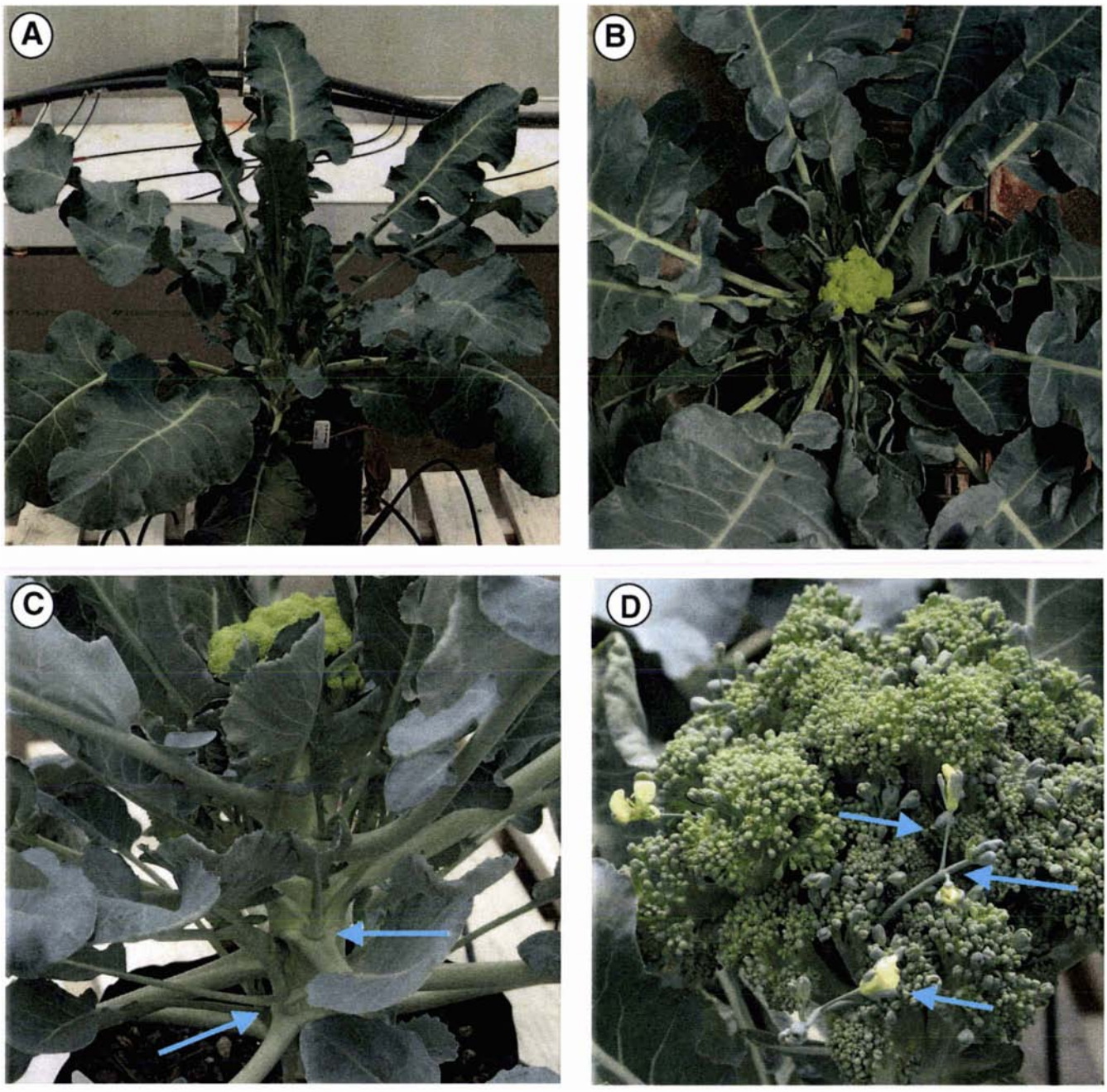

Figure 5.17 Morphological differences of transgenic broccoli plants harbouring constructs for cytokinin over-production. A, shortened plant stature; B, increased bushiness; C, released axillary shoots; and D, individual floret bolting.

5.3.7 Postharvest senescence of *ipt* heads

Plants were grown to maturity for postharvest analysis, although this proved difficult due to the dissimilar development stages observed for different plants. These experiments will be repeated by Crop & Food Research personnel once growing conditions become more suitable for broccoli.

5.4 DISCUSSION

Transgenic broccoli produced in Chapter 4 was the primary source of plant material for the analyses described in this Chapter. Detached leaf senescence assays were used to select lines for further characterisation. Leaves were taken from a number of plant lines at precise stages of development (third and fifth leaves from the apex) and were placed in the dark to induce senescence. The different development age of these leaves led to quite different rates of senescence: the younger leaves detached from the third position from the apex senesced much slower than those detached from the more mature fifth position from the apex (Figure 5.1). This is consistent with the findings of Bleecker et al. (1995). The importance of choosing the tissue at identical stages of development for senescence studies was re-iterated by Weaver et al. (1998). A number of AS-ACO transgenic lines were strong candidates for subsequent postharvest storage experiments based on how they performed in the detached leaf senescence assay. Seven of the eleven AS-ACO lines analysed in the detached leaf senescence assays showed a delayed leaf senescence phenotype. Four of the lines, 7, 15, 16 and 22, were selected and grown in larger numbers for postharvest experiments of detached heads.

The delayed senescence phenotypes were particularly interesting because *BoACO2* (and not *BoACO1*) was present in the antisense construct used to produce these plants. As *BoACO1* (but not *BoACO2*) is expressed in detached leaves (Pogson et al., 1995a), this result indicated that the AS-ACO construct was able to down-regulate *BoACO1*, so there appears to be sufficient sequence homology within the open reading frame (ORF) of *BoACO2* to down-regulate the *BoACO1* gene expressed in leaves. Consequently, as *BoACO1* and *BoACO2* are both up-regulated in detached broccoli heads (Pogson et al., 1995a), post-harvest senescence of broccoli should be delayed through the dual down-

regulation of *BoACO1* and *BoACO2* in broccoli floret tissue by the antisense *BoACO2* construct. Further, as well as expressing the appropriate ORF, it is clear that the AS promoter is driving the expression of the antisense *BoACO2* gene at a rate high enough to reduce ethylene biosynthesis to the extent that a delay in leaf senescence results.

Postharvest storage trials were conducted on heads from four AS-ACO lines, a transgenic control line (pART27 line 3) and wild-type plants. Unfortunately, due to a lack of space in the GMO glasshouse containment facility, the wild-type plants were grown separately from the transgenic lines and approximately one month apart, and so were not harvested and stored at the same time. However, the rate of harvest-induced senescence of Triathalon wild-type plants grown at different times during this project was very similar (data not shown), and so these plants were still considered to be appropriate controls for this experiment.

Harvest-induced senescence of broccoli heads, as monitored by hue angle, was delayed in all lines containing the AS-ACO construct (Figures 5.4 and 5.5) in comparison to the pART27 control and wild-type heads. Further, the expression of genes normally associated with senescence, *BoMLP* and *BoCP5*, was reduced in florets following harvest for the AS-ACO lines in comparison to both the wild-type and transgenic control (pART27) (Figures 5.10 and 5.11). Since the expression of an antisense *BoACO2* gene in broccoli caused a reduced rate of senescence, this implies that ethylene is involved in regulating senescence in broccoli, which confirms the previous work carried out by Tian et al. (1994 and 1997) and Pogson et al. (1995a).

Exactly how the antisense *BoACO2* gene caused the delayed senescence phenotype was initially investigated by assessing transcript levels of the *BoACO* genes. RNA transcription was used to make single stranded ribosomal RNA probes for analysis of both the sense and antisense *BoACO2* transcript. Northern experiments showed that these probes hybridised to a number of non-specific bands, and changes in the expression of native *BoACO2* (sense), or the introduced antisense *BoACO2* transcripts could not be ascertained (Figure 5.6).

Consequently, two further strategies were employed to assess the effect of the antisense *BoACO2* gene. Both *in vitro* ACC oxidase enzyme assays (Figure 5.8) and western analyses (Figure 5.9) confirmed that ACC oxidase activity and ACO protein accumulation was reduced in at least one of the AS-ACO transgenic lines following harvest in comparison to wild-type. It is likely that this result could be extrapolated, and that ethylene biosynthesis, and therefore, evolution is probably reduced in all the lines that show reduced senescence, and altered gene expression profiles compared to wild-type and transgenic control plants. Further, the AS promoter used to express the antisense gene was not activated in AS-ACO lines until after harvest, as basal levels of ACO enzyme activity were present until 24 h following harvest (Figure 5.8). ACO activity was only reduced after 24 h following harvest in the transgenic line analysed. This timing coincides with the normal increase in *BoACO2* transcript in wild-type florets following harvest (Figure 3.4, Chapter 3).

However, these results do not show specifically if *BoACO1* and/or *BoACO2* expression was reduced, and do not provide an answer as to the source of the basal levels of ACO enzyme activity. *BoACO1* gene expression does not appear to be very different for any of the AS-ACO lines in comparison to controls (Figure 5.7), although there may be a small reduction in levels, particularly for AS-ACO line 7. This suggests that the expression of *BoACO1* may not be a major contributor for the biosynthesis of ethylene that regulates senescence in broccoli. This data is consistent with the hypothesis suggested by Pogson et al. (1995a), that *BoACO2* expression is principally responsible for the production of the ethylene that regulates senescence in broccoli, and that expression of *BoACO1* provides basal levels of the hormone, which may or may not aid in its regulation.

However, these results do not explain why natural leaf senescence was delayed in the AS-ACO plants. It is quite possible that other unidentified *BoACO* genes are also involved, in both leaf and floret senescence. Pogson et al. (1995a) proposed the existence of at least one more member of the gene family in broccoli after completing low stringency Southern experiments. This is not surprising considering families of up to five have been observed for other species. The AS-ACO plants provide a source to

further test this hypothesis. The use of FPLC in combination with *in vitro* ACC oxidase enzyme assays and western analyses could be utilised to dissect further the roles these *BoACO* genes play in regulating senescence in broccoli.

It has been suggested that sugars play a prominent role in the regulation of senescence in broccoli and that sugars could provide a signal that regulates senescence following harvest (Irving and Joyce, 1995; Coupe et al., 2003a). In this thesis, reduction of ACO activity caused a reduction in expression of genes encoding enzymes responsible for the metabolism and transport of sugars during senescence (Figures 5.12 to 5.15). One might conclude from these findings, that ethylene may regulate the expression of those genes, which are involved in downstream regulation of senescence in broccoli. However, ethylene may not act directly on the sugar signal responsible for regulating senescence. Further biochemical characterisation of the sugar status within the florets of these transgenic plants following harvest could provide evidence indicating how an interaction between ethylene and sugar might regulate senescence.

While the AS-ACO plants showed reduced rates of postharvest deterioration, extensive field-testing will be necessary to determine if they hold a commercial advantage over other commercially available cultivars. Export of broccoli to the northern hemisphere often requires up to four weeks cool-storage. Export conditions were mimicked by cool-storing harvested broccoli, both transgenic and wild-type at 1°C for 28 days. After the initial 28 day storage period, heads were moved to 20°C for up to five days under shelf-life conditions (20°C). AS-ACO heads performed better than the wild-type cool-stored broccoli, throughout the five days of shelf-life conditions (Figure 5.16). Further, AS-ACO heads that were cool-stored had a greater hue angle at the two to three day shelf life period than wild-type heads that were subjected to shelf-life conditions immediately following harvest. Two to three days is a crucial time point for the supermarket shelf. Broccoli is considered to have a shelf-life of only two days, and heads older than two days should be removed from the super market shelf for disposal. The above result may, therefore, be of commercial significance. However, these results are only based on sepal

yellowing as measured by hue angle. Further biochemical and molecular characterisation is needed to confirm any storage advantage of the AS-ACO plants.

The AS promoter obviously has a high rate of expression to cause the reduced deterioration observed for the plants analysed. However, the horticultural performance of these plants must be ascertained and the specificity of the AS promoter must be addressed. For example, what effects would 'leaky' or non-specific expression of the antisense *BoACO2* gene have on other plant growth or developmental process that ethylene regulates? Further, ethylene regulates downstream pathways in response to both biotic and abiotic stress (O'Donnell et al., 2001). If the AS promoter were to switch on during such stress situations, the effects on the plant would need to be determined.

Natural foliar senescence was delayed in AS-ACO line 7 plants (Figure 5.3). Although this was just an observation towards the end of the growing season and an in depth analysis was not carried out, it does suggest that the AS promoter may not be as highly specific to harvest as some of the results presented in this thesis suggest. The AS promoter may be regulated by a phenomenon that is common to an upstream signal transduction that initiates senescence, whether that be harvest-induced or natural. Further, as there is frequently cross-talk between different pathways, some of the regulators of one response also may regulate another at a specific time, place or sensitivity to a hormone (e.g. ethylene).

However, the AS promoter as well as being up-regulated by harvest is also regulated negatively by sucrose, such that when sucrose levels are high, the activity of the promoter is reduced. However, when sucrose levels are low the promoter is induced (Winichayakul et al., unpublished). During senescence, the organ undergoing senescence becomes a source of carbon and sucrose is transported away. As the sucrose is lost from the site of senescence, it is possible that the down-regulation of the AS promoter by sugar is lifted, and expression of the antisense BoACO2 gene occurs, and senescence is slowed. Simple postharvest feeding experiments with sucrose to AS-BoACO2 heads could be used to address this question. If the sugar responsive element

is responsible for the expression of the antisense BoACO2 gene, then in the presence of sucrose following harvest the promoter would not be up-regulated and senescence would not be delayed.

In Chapter 4, it was suggested that the AS promoter may also respond to pathogen attack, due to the increased rate of transformation seen when using the AS-ACO construct. However, if the whole plant were to become tolerant to disease, because of the lack of ethylene, and not respond to pathogen attack, this is likely to be a disadvantage. As mentioned earlier, ethylene has been implicated in the plant-pathogen interactions between tomato and *Xanthamonas campestris* (O'Donnell et al., 2001). However, recent literature which addresses the role of ethylene in disease shows the difficulty faced with generalising the roles of hormones in defence. Ethylene insensitivity has been shown to cause reduced symptoms (Bent et al., 1992; Hoffman et al., 1999; Lund et al., 1998), increased symptoms (Knoester et al., 1998), or no differences in disease susceptibility (Hoffman et al., 1999). Further, not all ethylene-insensitive mutants responded in an equivalent way to a pathogen (Bent et al., 1992) and it appears each mutant may respond differently to different pathogens (O'Donnell et al., 2001). These observations suggest any test must be carried out with multiple pathogens to assess the horticultural performance of the crop.

Such tests were not carried out with the AS-ACO broccoli plants. However, during one growing season, there was an outbreak of *Botrytis* in the GMO containment glasshouse. This fungal pathogen appeared to affect all the broccoli plants in a similar way, and no preference by the pathogen for genotype was observed. The severity of the disease did not appear to be more or less for any plant type. This observation suggests the AS promoter is not up-regulated during pathogen attack by Botrytis. It would be interesting to test the horticultural performance of these plants in larger experiments and more controlled experiments both in the field and controlled environments with a variety of pathogens. However, both the scope of this PhD and the regulatory framework of this research in New Zealand precluded such experiments.

The response of the transgenic plants to abiotic stress would also need to be assessed. English et al. (1995) carried out an experiment with transgenic tomato plants with reduced ethylene biosynthesis. These plants were unable to produce high levels of ethylene in response to flooding-stress, and as a consequence displayed less epinastic curvature of petioles, an ethylene response, in comparison to wild-type plants. A similar experiment was carried out using AS-ACO line 7 and wild-type plants for comparison. Epinastic curvature was measured in response to both flooding and drought. Both wild-type and AS-ACO plants responded to drought by increased wilting (data not shown), but no significant differences were observed between the two plant types. However, the response may have been to temperature rather than drought, as the day in which the curvature occurred was very hot and control plants also showed increased curvature at this time. Neither the AS-ACO plants nor wild-type plants responded to flooding stress. However, plants were not fully submerged in water to the stem. It would be interesting to revisit these experiments with more controls to assess whether the AS-ACO plants respond normally to both flooding and drought stress.

As well as characterising the AS-ACO lines, a number of transgenic broccoli lines harbouring bacterial *ipt* genes are also undergoing characterisation. Three separate constructs were used: SAG_{12}-IPT, MYB_{305}-IPT and the double construct AS-ACO::MYB_{305}-IPT. Characterisation of these lines is in the very early stages. All constructs appeared to cause some morphological changes which included reduced plant stature and increased bushiness, due to a break in apical dominance, as well as a floral bolting phenotype (Figure 5.17), which could be attributed to leaky or non-specific expression of the *ipt* gene leading to enhanced levels of cytokinin. However, these were simply observations of a small number of plants growing in the containment glasshouse. Further larger experiments are in place to measure the morphological abnormalities more accurately. Number of leaves, internode length, surface area of leaves and plant height will be measured, to assess if any of the morphological abnormalities observed are significant, and caused by the ectopic expression of the *ipt* genes.

Chapter 6

Isolation of genes involved with the biosynthesis and metabolism of cytokinins from broccoli.

6.1 INTRODUCTION

Cytokinin is a key hormone involved in the regulation of growth and development in plants. The plant genes encoding cytokinin synthase enzymes (isopentenyl transferases) remained elusive until 2001, and plant biologists had had to rely on over-expressing bacterial cytokinin synthase genes to understand the role of endogenous cytokinins in plants and to manipulate cytokinin levels for commercial advantage. The enzymes involved in the metabolism of cytokinins have also been implicated as having a key role in regulating the pool of active cytokinin and recently a cytokinin receptor was also identified (Inoue et al., 2001). It appears that there could be three tiers of regulation of this hormone: regulation at the level of biosynthesis, perception and metabolism. This would provide very precise spatial and temporal control of the growth and developmental responses caused by cytokinins.

Recently, Takei et al. (2001) and Kakimoto et al. (2001a) independently isolated a multi gene family, encoding seven isopentenyl transferases (IPTs) from *Arabidopsis*. Further, Zubko et al. (2002) isolated another plant IPT from *Petunia hybrida*. Considerable progress has also been made recently in understanding the roles cytokinin oxidase enzymes play in regulating the pool of active cytokinin in plants. A gene encoding cytokinin oxidase was cloned from *Zea mays* (Houba-Herin et al., 1999; Morris et al., 1999) and, more recently, a gene family of seven cytokinin oxidases (*AtCKX1-7*) from *Arabidopsis* (Bilyeu et al., 2001). The sequences of these cytokinin biosynthesis and metabolism genes provide probes or templates on which to base gene isolation studies in other plant species. In this chapter, the aim was to exploit the homology of the *Arabidopsis* genome with that of broccoli to isolate genes involved in the biosynthesis and metabolism of cytokinin with a long-term goal of understanding how cytokinin levels are regulated in broccoli following harvest.

6.2 METHODS AND MATERIALS

6.2.1 Gene isolation

Isolation of putative cytokinin synthase and cytokinin oxidase genes was carried out by a variety of methods including PCR amplification from the genomic DNA of both *Arabidopsis* and broccoli, PCR amplification from a broccoli genomic library and RT-PCR amplification from *Arabidopsis* leaf or broccoli floret RNA (Figure 6.1). A number of DNA fragments were also cloned that showed homology to genes other than ones involved with cytokinin biosynthesis or metabolism (see Appendix 1). Amplified DNA fragments were ligated into the pGEMTeasy vector (Promega) and then sequenced.

6.2.1.1 Library screening

Reagents:

- Denaturing solution – 1.5 M NaCl, 0.5 M NaOH
- Neutralising solution – 1.5 M NaCl, 0.5 M Tris HCl, pH 7.0
- 2 x SSC – 0.3 M NaCl, 30 mM sodium citrate
- Culture medium – L-broth containing 0.2% maltose, 10 mM $MgSO_4$
- L-TOP agar - 10 g L^{-1} bacto-tryptone, 5 g L^{-1} yeast extract, 10 g L^{-1} NaCl, 10 mM $MgSO_4$, 1% agarose (w/v)
- LB plates- 10 g L^{-1} bacto-tryptone, 5 g L^{-1} yeast extract, 10 g L^{-1} NaCl, 1.5% (w/v) bactoagar
- SM buffer – 0.1 M NaCl, 8 mM $MgSO_4.7H_2O$, 50 mM tris HCl pH 7.5, 2% (v/v) gelatin

Two types of libraries were screened during this work. A Lambda ZAP cDNA library (Stratagene) previously constructed from RNA extracted from broccoli (Shogun) florets 48 h following harvest (Pogson et al., 1995a) and a Lambda FIX® II/*Xho* I broccoli genomic library (Simon Coupe, personal communication).

Plating cells were made fresh, and cells no older than 5 d were used for screening experiments. XL1-Blue MRA (P2) *E. coli* strain was used for genomic library screens and XL1-Blue MRF' *E. coli* strain was using for cDNA library screens. Cells were prepared by inoculating a liquid culture with a colony taken from freshly streaked plates. After 16 h incubation at 37°C, cells were pelleted at 1000 x g and resuspended to an optical density of 0.6 (OD_{600}) in 10 mM $MgSO_4$. Before use, it was necessary to

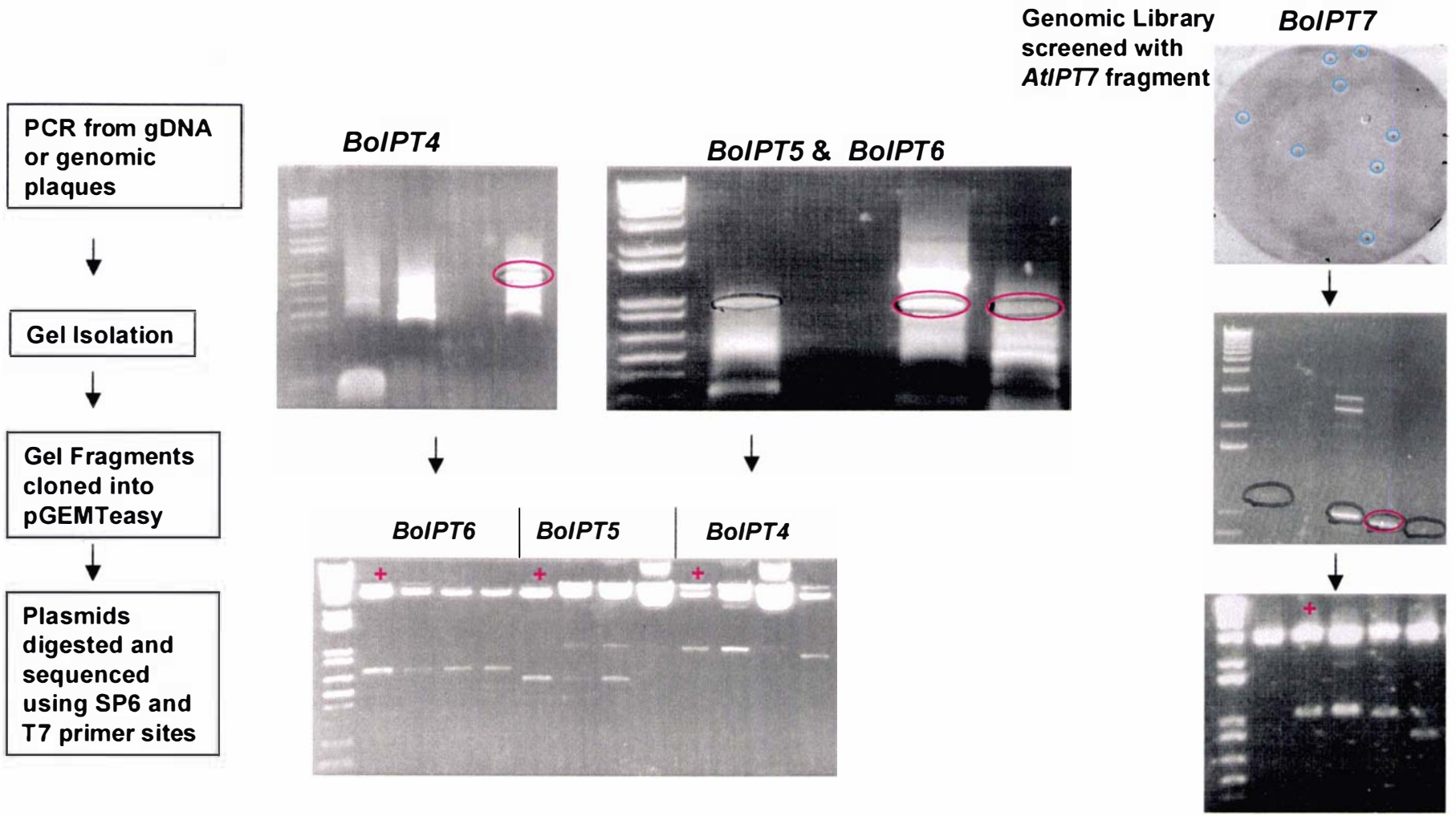

Figure 6.1 Cloning strategy for the isolation of putative BolPT genes. Blue circles on genomic library screen indicate positive plaques that were cored from plates. These were then used as DNA templates for PCR. Circled bands represent fragments that were gel isolated and cloned. + indicates positive putative *BolPT* clones following sequencing.

titre both the genomic and cDNA libraries to estimate the plaque forming unit (PFU) concentration, and also to check the efficiency of the plating cells. Dilutions of each library in a total volume of 50 μL were mixed with the appropriate plating cells (200 μL). This mixture was added and mixed with pre-warmed L-TOP agar (5-10 mL) (48°C), plated evenly onto pre-warmed LB plates (37°C), which were then incubated at 42°C for 6 h. The PFU concentration was estimated by counting the number of plaques per plate and also taking the dilution into account. For screening purposes, a plating density of 50 000 PFU was used per 20 cm plate.

Plaques were lifted from plates (precooled at 4°C) and transferred to nylon membranes (Hybond N+, Amersham), the duration of the membrane exposure to the plate for the first lift was 1 min and subsequent lifts were 3 min. Each plate was marked in a non-symmetrical fashion, and the membranes corresponding to each plate were also marked in this way. The transferred plaque DNA was denatured in denaturing solution for 3 min following by two 3 min washes in neutralising solution. The membranes were washed vigorously in 2 x SSC, then the plaques fixed to the membranes by UV cross-linking (Hoefer UVC 500 UV Cross Linker). Membranes were probed as described previously (see Section 2.8), and positive plaques from primary screens were cored and suspended in SM buffer (500 μL) with the addition of chloroform (20 μL). This was then used as either template DNA for subsequent PCR, or screened for a second (secondary screen) and third (tertiary screen) time.

6.2.2 Sequencing and phylogenetic analyses

All sequencing was carried out by either the Waikato DNA Sequencing Facility at the University of Waikato, or the Massey University DNA Sequencing Facility using the technology described in Section 2.10. DNA sequences were analysed using the DNA star software package (LASERGENE, Madison Wisconsin). Sequences were aligned using the Clustal method and phylogenetic trees drawn using the Megalign programme in the DNA star software package. This provided a fixed tree, and is based on the assumption that all sequences have diverged from one common ancestor.

6.2.3 Cross hybridisation

For both Southern and 'virtual northern' analyses, it was necessary to establish conditions that prevented cross-hybridisation of the four isolated *BoIPT* clones. Approximately 5 ng of PCR amplified *BoIPT* fragments were hybridised against each other under high-stringency wash conditions (0.1 x SSC, 0.1 % (w/v) SDS at 65°C). These wash conditions were subsequently used for both Southern and 'virtual northern' analyses.

6.2.4 Molecular analyses

PCR, Southern, northern and RT-PCR based 'virtual northern' analyses were used to isolate and verify the presence and expression of broccoli genes. For details of these techniques see Methods and Materials, Chapter 2. Plant material for gene expression analysis was taken from mature flowering plants (see results section of this chapter for details of tissue types analysed).

6.2.5 Colony hybridisation

Putative transformed bacterial (*E. coli*) colonies harbouring pART7 plasmids containing newly ligated *ipt* fragments were picked to fresh LB-plates and grown at 37°C for 16 h. The freshly grown colonies were transferred to nylon membranes, denatured, neutralised and cross-linked as described for plaque lifts (see Section 6.2.1.1). Membranes were probed as described previously using specific probes (see Section 2.8). Positive colonies were grown and plasmids subsequently extracted for further analysis.

6.2.6 Cloning of BoIPT constructs

The experimental protocols used to produce the binary vectors containing *BoIPT* clones are depicted in a flow diagram (Figure 6.2). All four putative *BoIPT* genes and *AtIPT4* fragments were released by *Not* I digestion from pGEMTeasy vectors (Promega) and the restriction sites blunt-ended using the Klenow fragment of T4 DNA polymerase (see Section 2.2.5 for details). The blunt-ended *ipt* fragments were subsequently ligated into the *Sma* I site of the multiple cloning site of pART7 (Gleave, 1992)(Figure 6.1, I). This plasmid contains the CaMV 35S promoter and the OCS3' terminator, which both flank

I

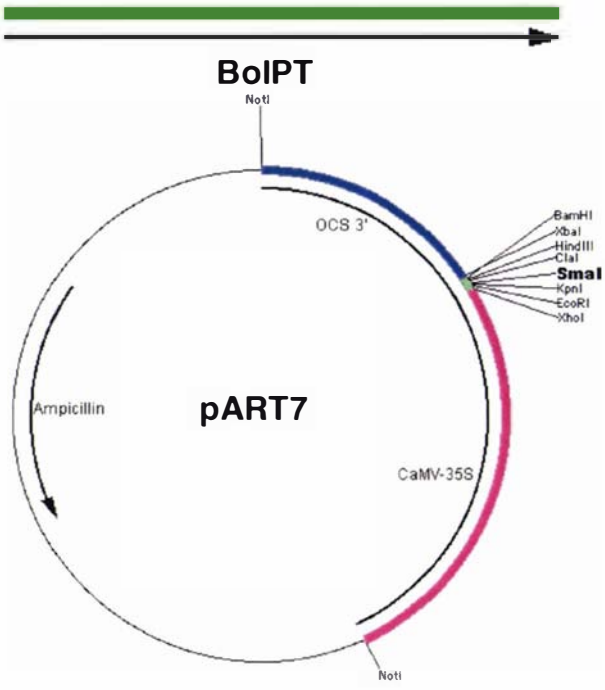

BoIPT inserts were removed from their pGEMTeasy vectors using *Not* I digestion, and the *Not* I sites blunt-ended. The *BoIPT* fragments were then cloned into the *Sma* I site of pART7.

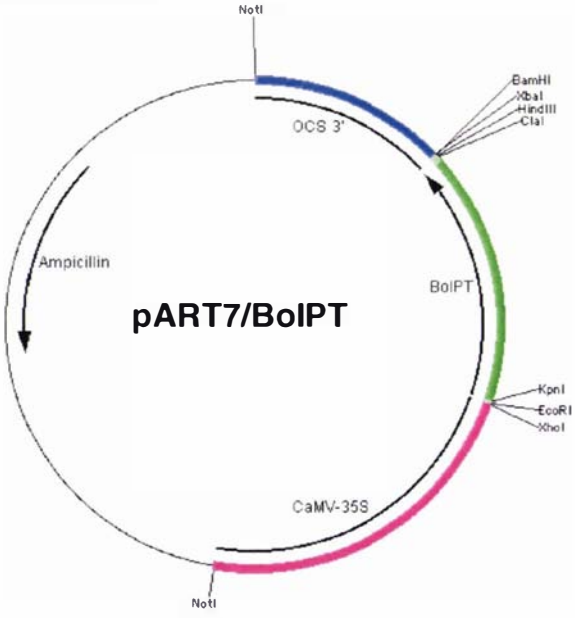

Digestion of pART7/BoIPT vectors with *Not* I liberated 3kb 35S-BoIPT-OCS3' fragments (see next page).

Diagnoses for step I of the cloning strategy: sucessful cloning of *IPT* fragments into pART7

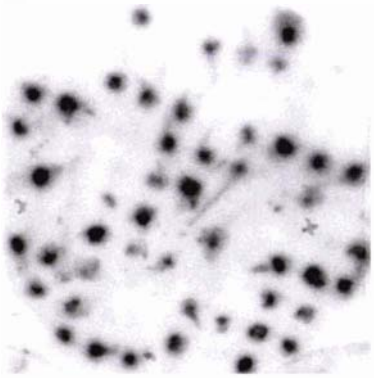

Colony hybridisation was carried out to determine which of the colonies were likely to have BoIPT inserts present. Positive colonies were subsequently picked and grown in liquid culture for plasmid preparation followed by PCR analysis.

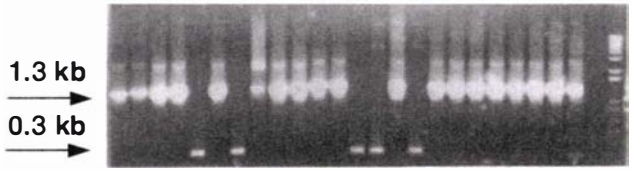

PCR across the multiple cloning site of a number of putative BoIPT/pART7 clones, using specific 35S and OCS3' primers. The presence of a 1.3 kb band suggests a BoIPT insert is present in the pART7 vector.

Further PCR was carried out to determine the correct orientation of the BoIPT inserts within the pART27 plasmids. To diagnose sense orientation, PCR products were observed using primers specific to the BoIPT of interest in the forward direction, and OCS3' in the reverse direction (lanes labelled 2-7). To diagnose antisense orientation, PCR products were observed using primers specific to the BoIPT of interest in the forward direction and 35S in the forward direction (lanes labelled 10, 17 band 18).

Figure 6.2 Cloning strategy for 35S-BoIPT-OCS3' constructs.

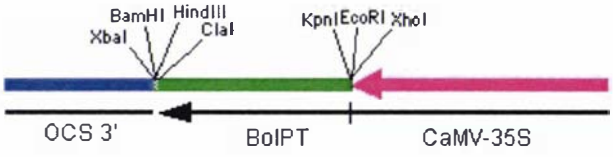

3kb Not I 35S-BolPT-OCS3' fragments were cloned into the Not I site of pART27.

II

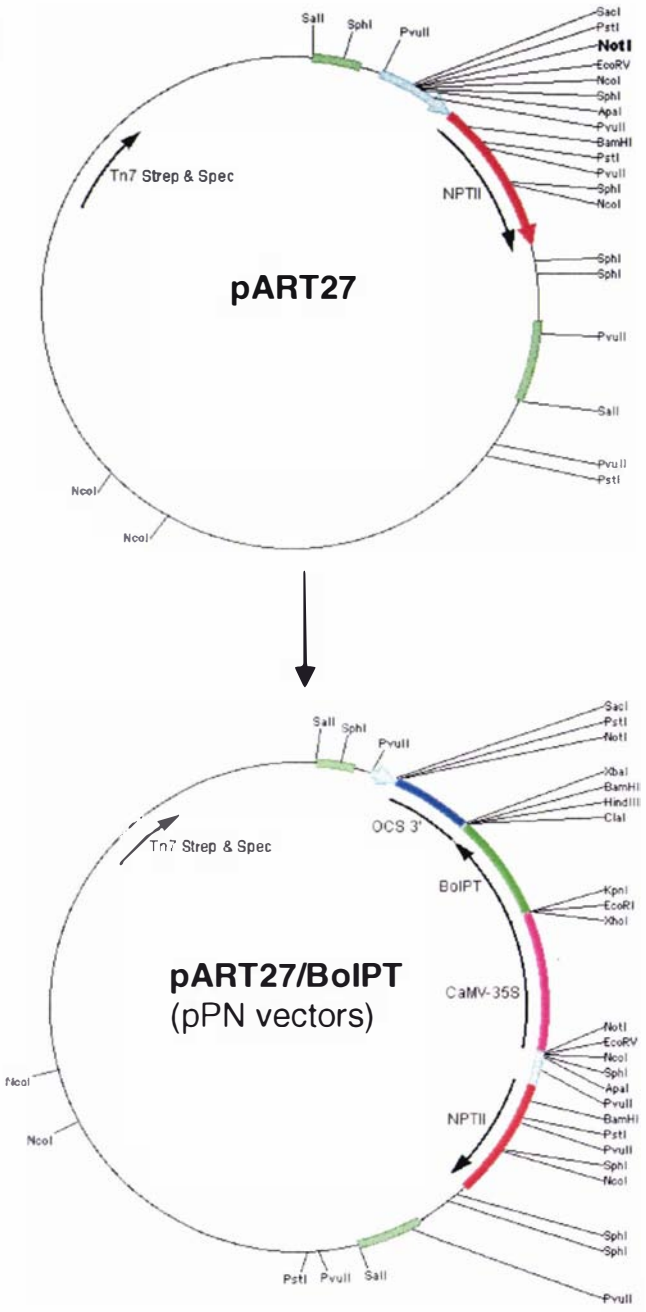

Diagnoses for step II of the cloning strategy: sucessful cloning of 35S-*IPT*-OCS3' fragments into pART27

Successful cloning was confirmed by PCR analysis using primers specific to 35S (Forward), OCS3' (Reverse), and the BolPT of interest (both Forward and Reverse). The presence of a band in lanes labelled 1 and 5 suggested the clone was a sense construct. The presence of bands in lanes labelled 2 and 4 suggested the clone was an antisense construct. Bands should be present in lanes 3 and 6 for either orientation.

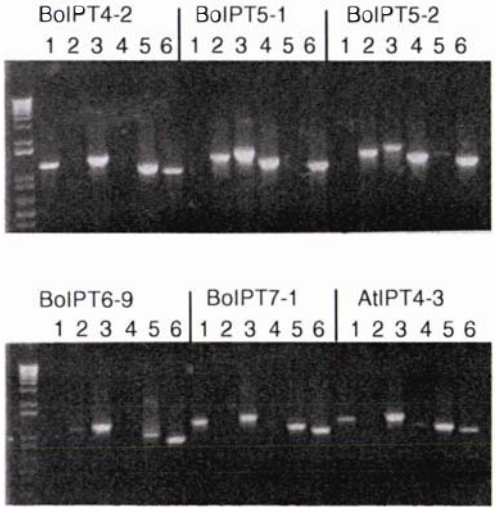

Binary vectors containg sense constructs were transformed into *A. tumefaciens* strains EHA105 and LBA4404 by electroporation.

Figure 6.2 (cont.) Cloning strategy for 35S-BolPT-OCS3' constructs.

the multiple cloning site. Putative positive colonies were then checked by colony hybridisation (see Section 6.2.5 for details) for the presence of *ipt* fragments. Up to ten positive pART7 clones for each *ipt* fragment were analysed for correct orientation using extensive PCR experiments with specific primers to the *BoIPT*, 35S and OCS3' sequences. Positive clones were then digested with *Not* I which liberated the 35S-BoIPT-OCS3' or 35S-AtIPT4-OCS3', and these fragments were ligated directly into the *Not* I site of pART27 (Gleave, 1992) (Figure 6.1, II). pART27 binary vectors harbouring the 35S-driven sense-orientated *BoIPT4*, *BoIPT6*, *BoIPT7* and *AtIPT4* were named pPN115, pPN117, pPN118 and pPN119 respectively.

The *A. tumefaciens ipt* gene under the control of its native promoter (NIK) was also cloned into pART27. The NIK insert was digested with *Eco* RI and *Kpn* I from the pUC18 based vector pNIK (McKenzie, 1994). These restriction sites were then blunt-ended using the Klenow fragment of T4 DNA polymerase (see Section 2.2.5 for details). The NIK insert was then cloned into the blunted *Not* I site of pART27, and the resulting vector was subsequently named pPN120.

A. tumefaciens strains LBA4404 and EHA105 were then transformed by electroporation (see Section 2.2.10.2 for details) with pPN115, pPN117, pPN118, pPN119 and pPN120.

6.2.7 Transformation of petunia

6.2.7.1 Plant material Leaves were harvested from *Petunia hybrida* (cv. Mitchell) plants grown in a glasshouse on site at Crop & Food Research, Palmerston North. Leaf discs (ca. 6 mm square) were used for transformation with binary vectors containing the *BoIPT* homologues, *AtIPT4* and the *A. tumefaciens* native *ipt* gene.

6.2.7.2 Transformation

Media:

- L-Broth – bacto-tryptone 10 g L^{-1}, yeast extract 5 g L^{-1}, NaCl 10 g L^{-1}
- Co-cultivation media - 1 x MS salts, B5 vitamins, 3% sucrose, 0.2 mg L^{-1} indole acetic acid (IAA), 3 mg L^{-1} 6-benzylamino purine (6-BAP), 0.75 % Phytagar, pH 5.7

- Selection media (+ 6-BAP) - 1 x MS salts, B5 vitamins, 3% sucrose, 0.2 mg L^{-1} (IAA), 3 mg L^{-1} 6-benzylamino purine (6-BAP), 500 mg L^{-1} cefataxine, 100 mg L^{-1} kanamycin, 0.75 % Phytagar, pH 5.7
- Selection media (- 6-BAP) - 1 x MS salts, B5 vitamins, 3% sucrose, 0.2 mg L^{-1} (IAA), 3 mg L^{-1}, 500 mg L^{-1} cefataxine, 100 mg L^{-1} kanamycin, 0.75 % Phytagar, pH 5.7
- Hormone free selection media - 1 x MS salts, B5 vitamins, 3% sucrose, 500 mg L^{-1} cefataxine, 100 mg L^{-1} kanamycin, 0.75 % Phytagar, pH 5.7

Petunia hybrida (cv. Mitchell) was transformed using the method described by Deroles and Gardner (1998). *Agrobacterium tumefaciens* cultures were grown in L-broth media at 28°C with the appropriate antibiotic selection. Young petunia leaves were surface sterilised in 20% commercial bleach (active ingredient, 1 g L^{-1} sodium hypochlorite) (followed by three washes in sterile water), and leaf discs were cut and briefly inoculated in the *A. tumefaciens* culture. The inoculated leaf discs were then blotted briefly on sterile 3 mm blotting paper and placed onto co-cultivation media (70 mm diameter plates) for two days at 25°C with a 16 h photoperiod. After co-cultivation, the leaf discs were transferred to selection media (medium sized tubs) at 25°C with a 16 h photoperiod.

6.3 RESULTS

6.3.1 Isolation of plant *IPT* sequences

The putative *BoIPT* genes were amplified using specific primers to *AtIPT* clones, primarily from broccoli genomic DNA (genomic DNA or genomic library, see Table 6.1 and Figure 6.1 for summary). *AtIPT* sequences were also PCR or RT-PCR amplified; *AtIPT4* and *AtIPT6* were amplified from *Arabidopsis* genomic DNA and *AtIPT7* from *Arabidopsis* leaf RNA, using specific primers (Table 6.1). The broccoli and *Arabidopsis* sequences were sequenced and the predicted proteins were aligned with other plant IPT sequences found in the GenBank™ (Figure 6.3).

This observation was confirmed by phylogenetic analysis (Figure 6.4). All the BoIPT sequences clustered individually with their *Arabidopsis* homologues. All the broccoli and *Arabidopsis* homologues clustered together away from the other plant sequence, the

Table 6.1 Putative genes isolated and how they were isolated.

Clone	Primer 1	Primer 2	Template	Fragment size
BoCKX	AtCKOX 693-Fow	AtCKOX 1222-Rev	Broccoli floret RNA[1]	530 bp
AtIPT4	AtIPT4 Fow	AtIPT4 Rev	*Arabidopsis* gDNA[2]	1.1 kb
AtIPT6	AtIPT6 Fow	AtIPT6 Rev	*Arabidopsis* gDNA[2]	1.1 kb
AtIPT7	AtIPT7 Fow	AtIPT7 Rev	*Arabidopsis* leaf RNA[3]	1.1 kb
BoIPT4	AtIPT4 Fow	AtIPT4 Rev	Broccoli gDNA[4]	1.1 kb
BoIPT5	AtIPT5 Fow	AtIPT5 Rev	Broccoli gDNA[4]	1.1 kb
BoIPT6	AtIPT6 Fow	AtIPT6 Rev	Broccoli gDNA[4]	1.0 kb
BoIPT7	AtIPT7 Fow	AtIPT7 Rev	Broccoli genomic library[5]	1.1 kb
BoCKX	T3	T7	Broccoli cDNA library[6]	1.9 kb[7]
BoACTIN	AtACTIN F	AtACTIN R	Broccoli floret RNA[1]	850 bp[7]

[1]Total RNA isolated from florets from 0-72 h postharvest heads from cv. Triathalon
[2]Genomic DNA gifted from Dr Tatsuo Kakimoto isolated from *A. thaliana*, ecotype Columbia
[3]Total RNA isolated from senescing leaves 0-96 h following detachment of *A. thaliana*, ecotype Columbia
[4]Genomic DNA isolated from broccoli cv. Triathalon
[5]Genomic library made from broccoli (Dr Simon Coupe, personal communication)
[6]Broccoli cDNA library from florets from 48 hr postharvest heads from (Pogson et al., 1995)
[7]Size determined from gel, yet to be sequenced proteins.

rice OsIPT. All plant IPT sequences were distantly related to bacterial IPTs, followed by tRNA-IPTs from both prokaryotes and eukaryotes. All the plant sequences shared the GxTxxGK[ST] ATP/GTP binding motif, where x denotes any amino acid residue and [] denotes any one of the amino acids within [].

As the sequence similarity of the individual *BoIPT* clones aligns more closely with the *Arabidopsis* homologues than within the broccoli family, there may exist sufficient difference to prevent cross-hybridisation during Southern and other molecular analyses. This was confirmed by cross-hybridisation analyses using high stringency washes (Figure 6.5). *BoIPT4*, *BoIPT5*, *BoIPT6* and *BoIPT7* did not cross hybridise under the high stringency washing conditions, which were subsequently used for Southern and 'virtual northern' analyses.

Figure 6.3 Alignment of the predicted protein sequences of plant IPT sequences. Gaps denoted by dashes were inserted to obtain maximum homology. The identical amino acid residues are indicated by white letters on a black background. BoIPTs, putative broccoli IPT homologues; AtIPTs, *Arabidopsis* IPT homologues; PhSHO, *P. hybrida* IPT homologue; OsIPT, putative *Oryza sativa* IPT homologue, deduced from the rice genome sequencing project.

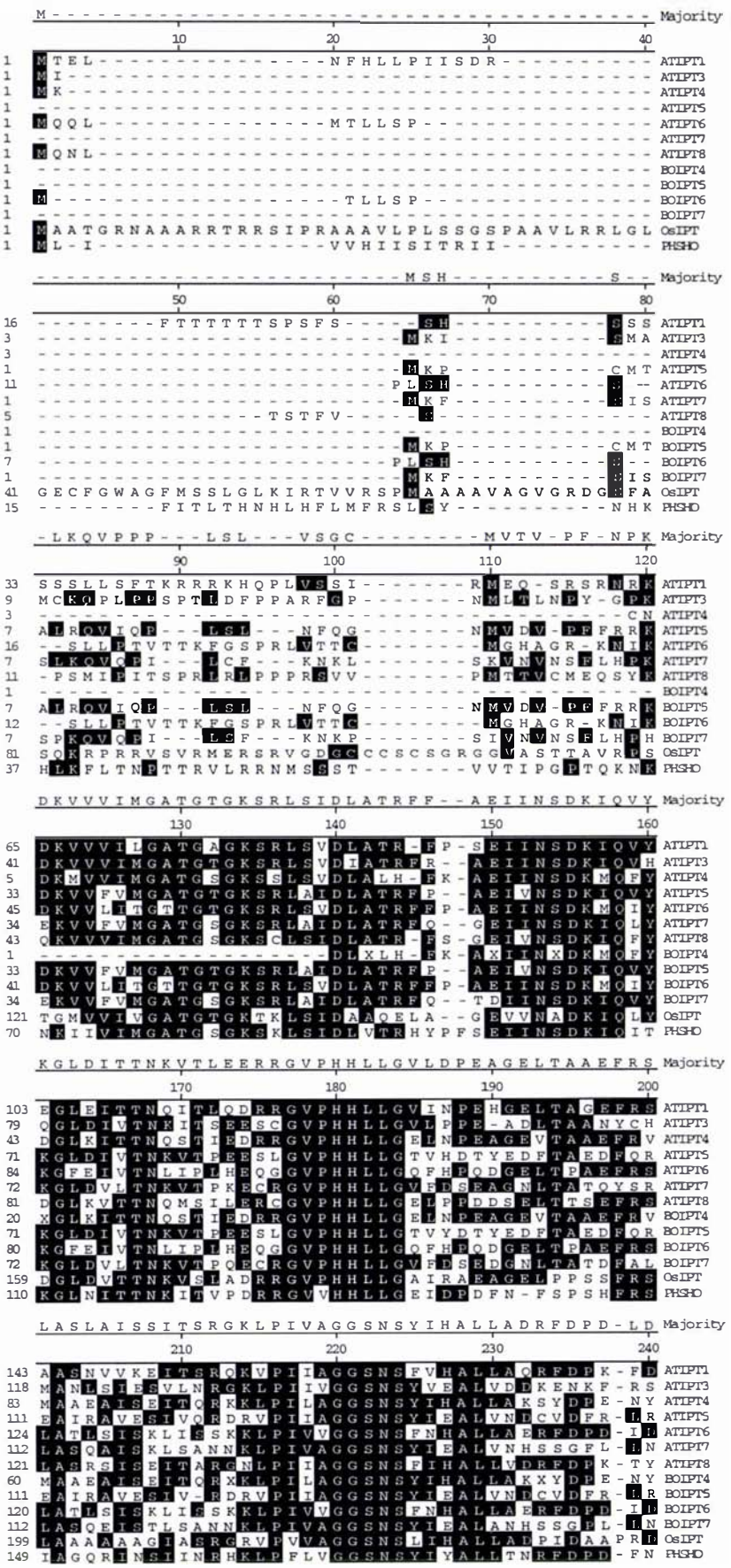
Majority
ATIPT1
ATIPT3
ATIPT4
ATIPT5
ATIPT6
ATIPT7
ATIPT8
BOIPT4
BOIPT5
BOIPT6
BOIPT7
OsIPT
PHSHO

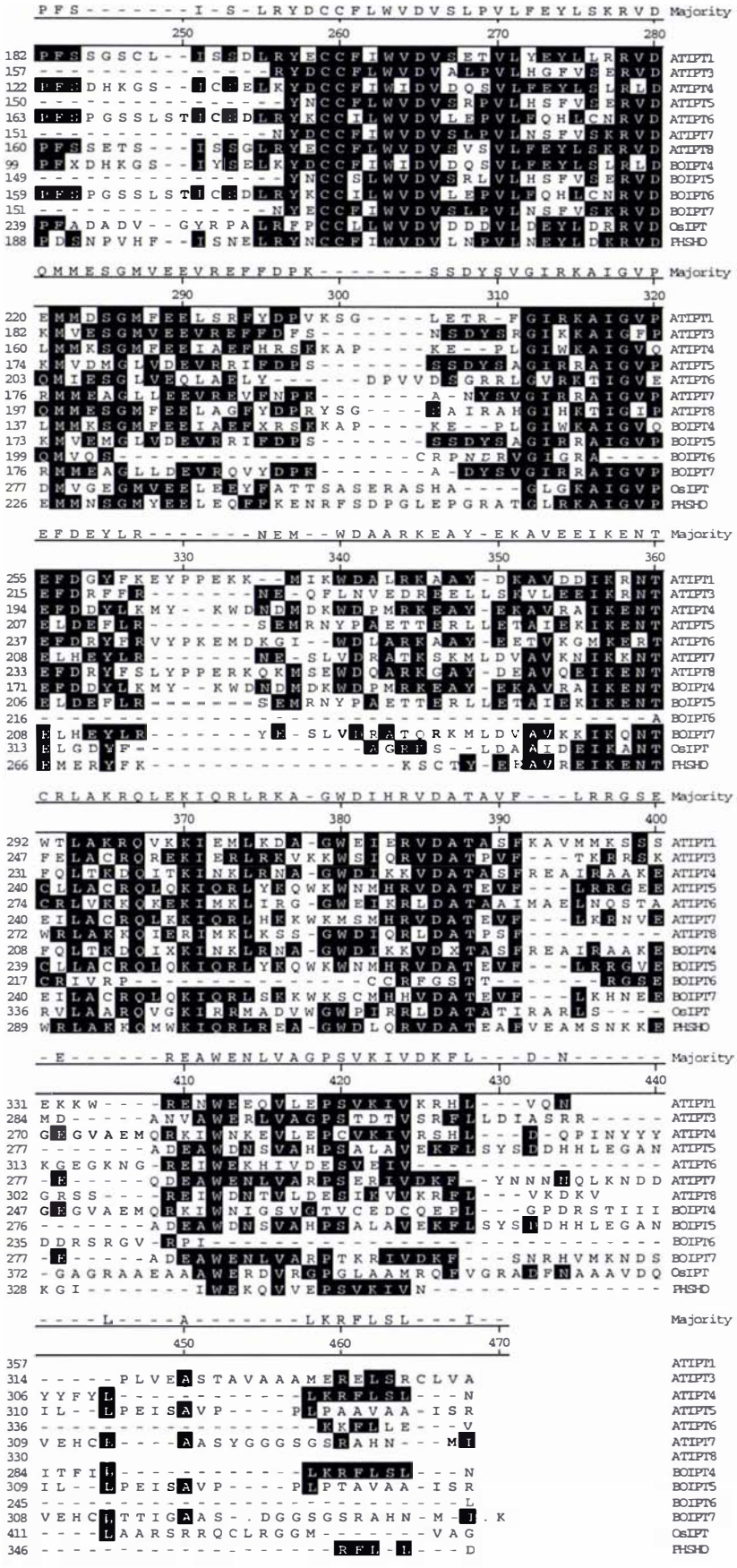
Majority
250
260
270
280
ATIPT1
ATIPT3
ATIPT4
ATIPT5
ATIPT6
ATIPT7
ATIPT8
BOIPT4
BOIPT5
BOIPT6
BOIPT7
OsIPT
PHSHO
290
300
310
320
330
340
350
360
370
380
390
400
410
420
430
440
450
460
470

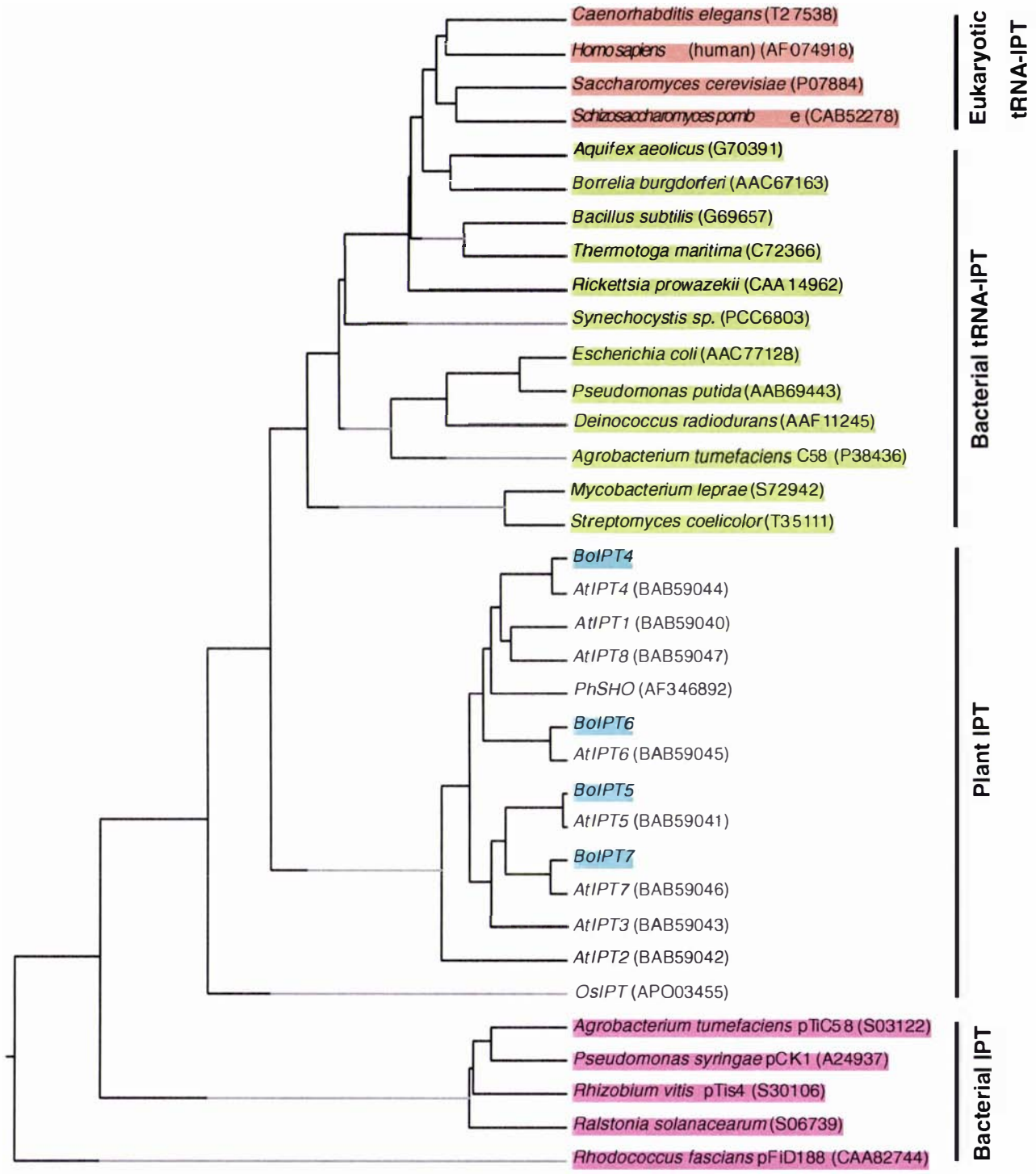

Figure 6.4 Phylogentic tree of various deduced IPT protein sequences. The tree was generated using the Clustal alignment method in The DNA Star software package. GenBank™ accession numbers are shown in brackets. BoIPTs, putative broccoli IPT homologues; AtIPTs, *Arabidopsis* IPT homologues; PhSHO, *P. hybrida* IPT homologue; OsIPT, putative *Oryza sativa* IPT homologue, deduced from rice genome sequencing project.

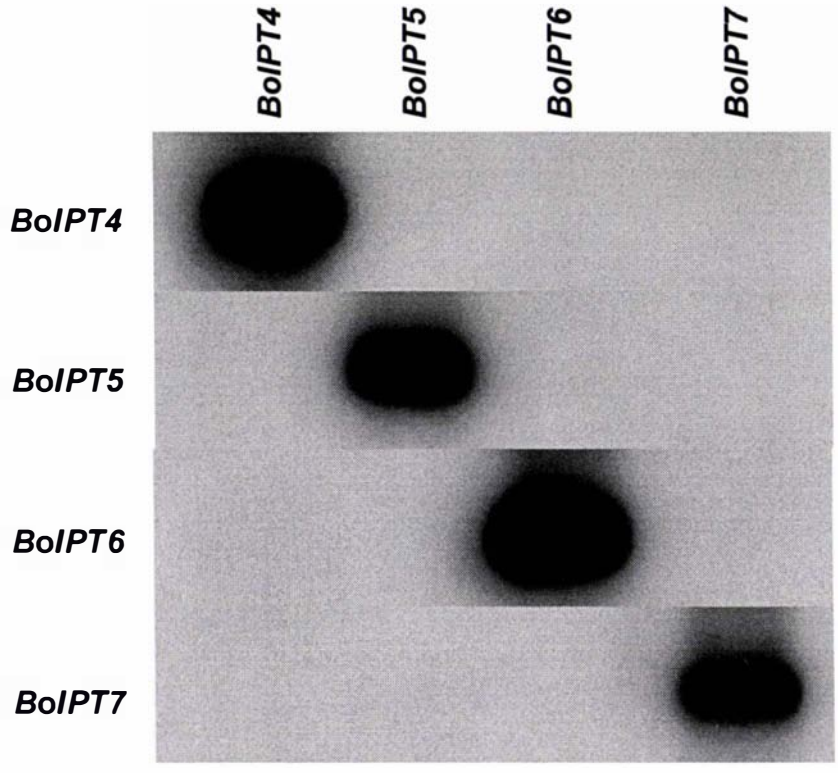

Figure 6.5 Demonstration of the lack of cross-hybridisation of the putative broccoli IPT clones. Non-specific hybridisation was removed by washing at high stringency, 65ºC at 0.1 x SSC 0.1% (w/v) SDS. For details of hybridisation and washing conditions, see Section 2.8.

6.3.2 Presence of *BoIPT* sequences in the broccoli genome

The presence of *BoIPT* clones in the broccoli genome was confirmed by Southern analyses (Figure 6.6). Genomic DNA isolated from the cv. Triathalon was digested to completion with restriction enzymes that did not cut within the putative broccoli genes. *BoIPT6* hybridised to two distinct bands when the genomic DNA was cut with *Eco* RV, *Hind* III and *Xba* I, suggesting *BoIPT6* is present as two copies in the broccoli genome (Figure 6.6c). *BoIPT7* hybridised to only one distinct band when genomic DNA was cut with *Eco* RI or *Hind* III, suggesting *BoIPT7* is present as a single copy in the broccoli genome (Figure 6.6d). For *BoIPT4* and *BoIPT5*, further Southern experiments are needed to clarify how many copies are present in the broccoli genome. *BoIPT4* hybridised weakly to uncut genomic DNA (Figure 6.6a) whereas *BoIPT5* hybridised to either two or three bands of digested broccoli genomic DNA (but not to uncut) suggesting there exists more than one copy of this gene in the broccoli genome (Figure 6.6b).

6.3.3 *BoIPTs* are differentially expressed

The expression profiles of the putative *BoIPT* genes were analysed by RT-PCR based 'virtual northern' analysis (Figures 6.7 and 6.8). Total RNA isolated from a variety of tissues from the broccoli cultivar Triathalon underwent RT-PCR, and the resulting reaction was separated and blotted on a nylon membrane, which then underwent hybridisation with specific probes. *BoIPT4* was amplified using primers specific to the *AtIPT4* homologue. *AtIPT* primers were insufficient to amplify the remaining *BoIPT* clones, so specific *BoIPT* primers were designed for *BoIPT5*, *BoIPT6* and *BoIPT7* (for primer sequences see Table 2.2, Methods and Materials).

BoIPT4 was most highly expressed in young sepals and in florets (containing young sepals) during the first 48 h following harvest (Figure 6.7). No expression was observed for *BoIPT4* in the 24 h floret sample following harvest, presumably because no *Bo18S* was detected in that sample, indicating poor or unequal loading of either RNA or cDNA. *BoIPT5* was expressed mainly in anthers and in stalk tissue, as well as stemlets, petioles and postharvest florets but at much lower levels of expression (Figure 6.8). *BoIPT6* was expressed mainly in stems, leaves, stalks, and floral tissues, and late during

Figure 6.6 Autoradiograph showing the Southern hybridisation of ^{32}P labelled *BoIPT* fragments with broccoli genomic DNA (20 µg). A. *BoIPT4*; B. *BoIPT5*; C. *BoIPT6;* and D. *BoIPT7*. Broccoli (cv. Triathalon) genomic DNA was either uncut (U) or digested with the *Eco* RI (RI), *Eco* RV (RV), *Hind* III (H3), or *Xba* I (X) restriction enzymes. The position of *Hind* III digested λ DNA markers are as indicated. Genomic DNA (20 µg) was separated on a 0.8% (w/v) agarose gel and blotted onto nylon membrane. For details of hybridisation and washing conditions, see Section 2.8.

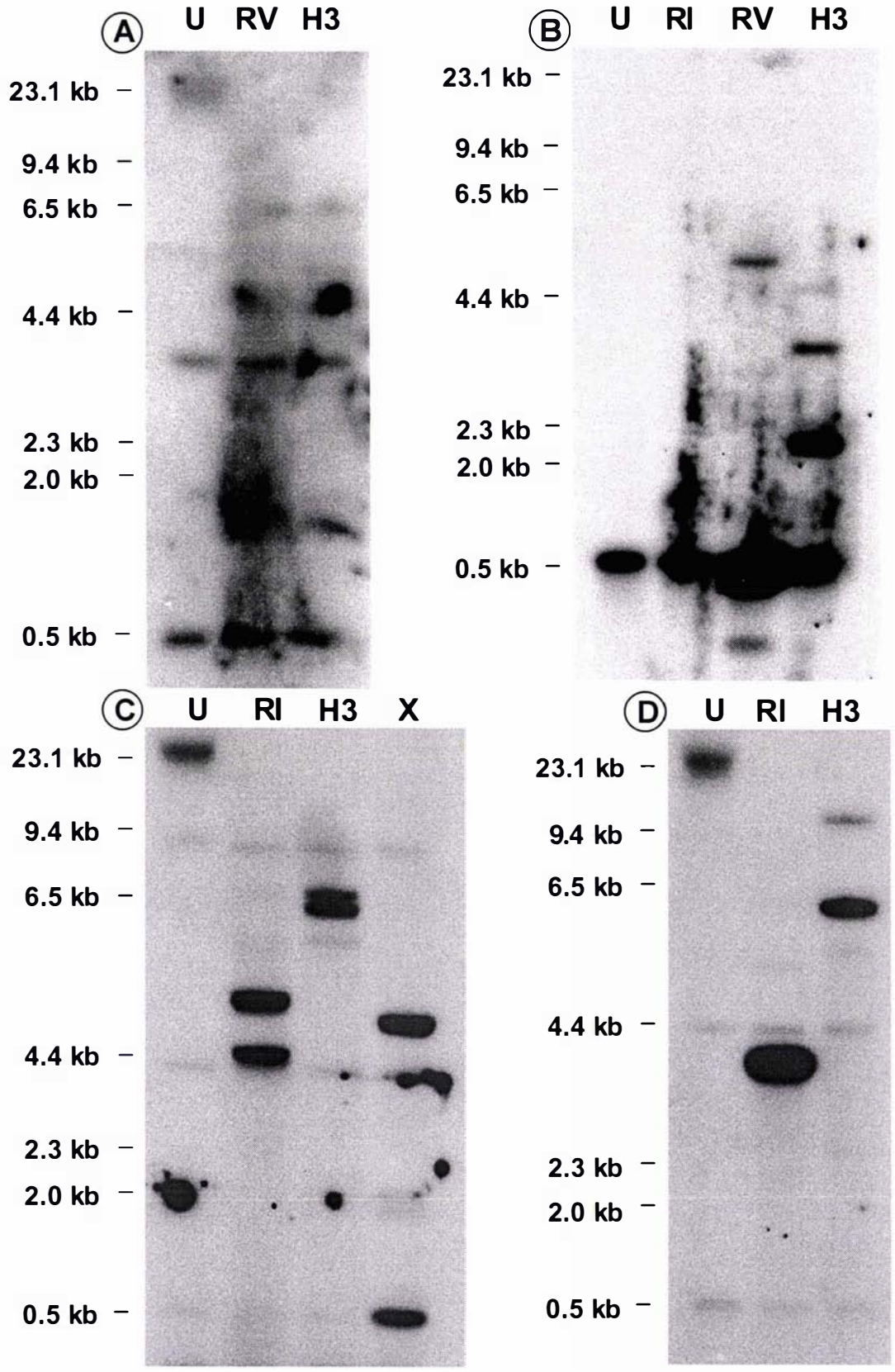
A
U
RV
H3
23.1 kb
9.4 kb
6.5 kb
4.4 kb
2.3 kb
2.0 kb
0.5 kb
B
U
RI
RV
H3
23.1 kb
9.4 kb
6.5 kb
4.4 kb
2.3 kb
2.0 kb
0.5 kb
C
U
RI
H3
X
23.1 kb
9.4 kb
6.5 kb
4.4 kb
2.3 kb
2.0 kb
0.5 kb
D
U
RI
H3
23.1 kb
9.4 kb
6.5 kb
4.4 kb
2.3 kb
2.0 kb
0.5 kb

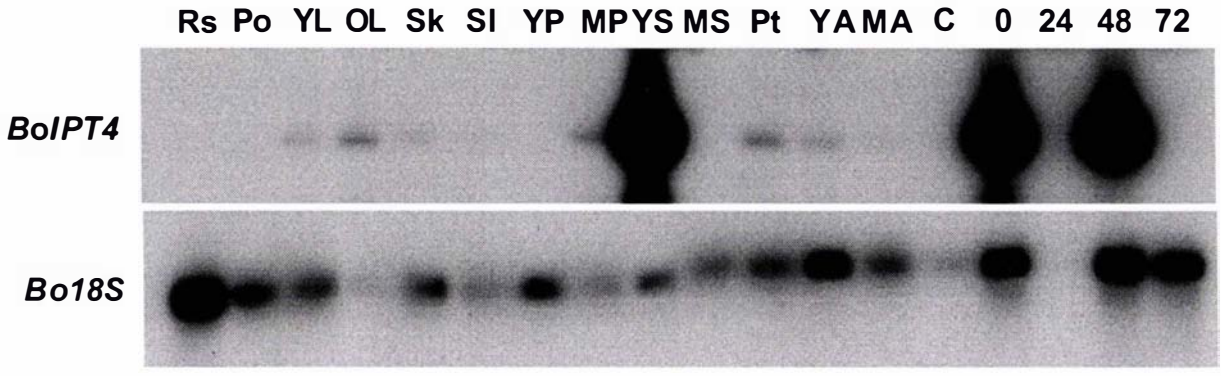

Figure 6.7 'Virtual northern' analyses of *BoIPT4* and housekeeping *Bo18S* genes in different broccoli tissues. For 'virtual northern' analyses, RT-PCR products of RNA isolated from different broccoli tissues were hybridised with ^{32}P labelled *BoIPT4* and *Bo18S* fragments. Total RNA was extracted from roots (Rs), petioles (Po), young and old leaves (YL and OL), stalks (Sk), stemlets (Sl), young and mature pedicels (YP and MP), young and mature sepals (YS and MS), mature petals (Pt), young and mature anthers (YA and MA), mature carpels (C) and postharvest florets (0, 24, 48 and 72 hours following harvest). Primers used were: for BoIPT4 amplification, AtIPT4 Fow and AtIPT4 Rev; for 18S amplification, 18S fow (39.3) and 18S Rev (39.3) (see Table 2.2 for primer sequences).

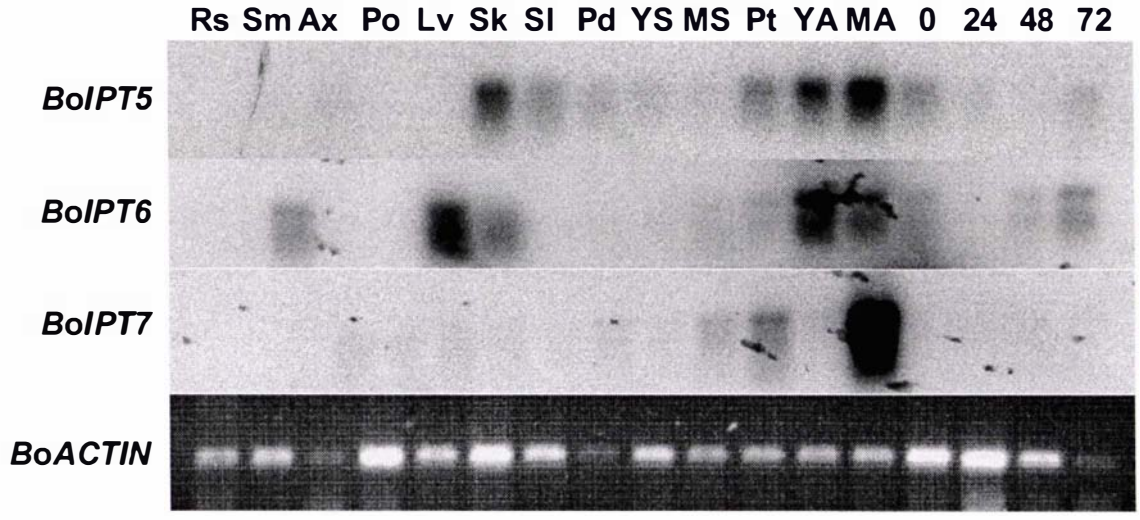

Figure 6.8 'Virtual northern' and RT-PCR analyses of *BoIPT5, 6* and *7,* and housekeeping (BoActin) genes in different broccoli tissues. For 'virtual northern' analyses, RT-PCR products of RNA isolated from different broccoli tissues were hybridised with ^{32}P labelled *BoIPT* fragments. Total RNA was extracted from roots (Rs), stems (Sm), axils (Ax), petioles (Po), leaves (Lv), stalks (Sk), stemlets (Sl), pedicels (Pd), young and mature sepals (YS and MS), mature petals (Pt), young and mature anthers (YA and MA), and postharvest florets (0, 24, 48 and 72 hours following harvest). Primer sequences used were: for BoIPT5, BoIPT5 Fow and BoIPT5 Rev; for BoIPT6, BoIPT6 Fow and BoIPT6 Rev; for BoIPT7, BoIPT7 Fow and BoIPT7 Rev; for BoACTIN, AtActin Fow and AtActin Rev (see Table 2.2 for primer sequences).

postharvest senescence (Figure 6.8). *BoIPT7* was expressed in mature anthers and petals (Figure 6.8); no expression was observed in immature florets. Both ribosomal 18S sub unit (*Bo18S*) and actin (*BoACTIN*) were used as housekeeping genes to monitor RNA/cDNA loading. In most cases either *Bo18S* or *BoACTIN* was observed, although the intensity of these bands varied, indicating loading of RNA in the initial RT-PCR reaction or amount of cDNA in the PCR reaction was not equal for each sample.

6.3.4 BoIPT over-expression *in planta*

Putative *BoIPT* genes were ectopically expressed in *P. hybrida* by *A. tumefaciens*-mediated transformation using the 35S-BoIPT-OCS3' constructs (Figure 6.9). Transformation was unsuccessful when the *A. tumefaciens* strain EHA105 was used. Transformation rate varied depending on the construct and hormone status of the media when the *A. tumefaciens* strain LBA4404 was used (data not shown). A summary of the observed shoot regeneration from these experiments is shown in Figure 6.10. Shoots regenerated from explants cultured on media either in the presence or the absence of 6-BAP for explants inoculated with pPN115 (35S-BoIPT4-OCS3'), pPN119 (35S-AtIPT4-OCS3') and pPN120 (native *ipt* pro-IPT). However, for pPN118 (35S-BoIPT7-OCS3') shoots did not regenerate on media lacking 6-BAP, although the shoot regeneration observed for this construct appeared to be very prolific compared to other constructs. Explants inoculated with, the control vector pPN92 containing 35S-GFP regenerated shoots on media containing 6-BAP. The pPN117 (35S-BoIPT6-OCS3') construct caused no regeneration at all, either in the presence or absence of 6-BAP in the media, suggesting there may have been something wrong with the *A. tumefaciens* culture for this experiment to stop transformation from occurring, or that the introduced T-DNA caused a lethal genotype.

6.3.5 Isolation of a putative cytokinin oxidase gene from broccoli

The partial length putative *BoCKX* clone was amplified by RT-PCR using broccoli floret RNA following harvest and degenerate primers (Table 6.1 and Figure 6.11). A broccoli cDNA library was screened using the 530 bp putative *BoCKX* fragment, and a positive plaque was taken through a secondary and subsequent tertiary screen. PCR

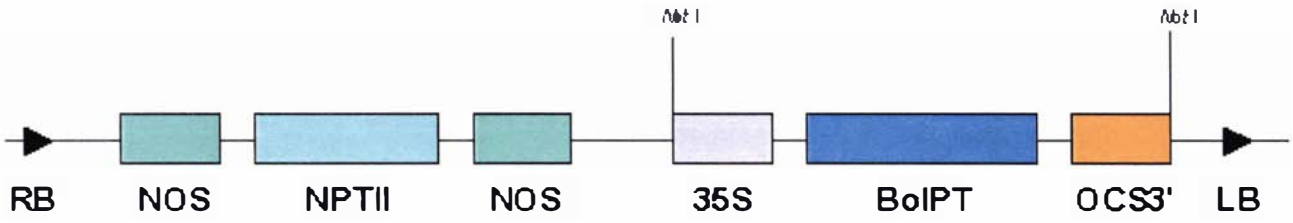

Figure 6.9 Schematic representation of the T-DNA region (not to scale) from constitutive *BoIPT* gene constructs.

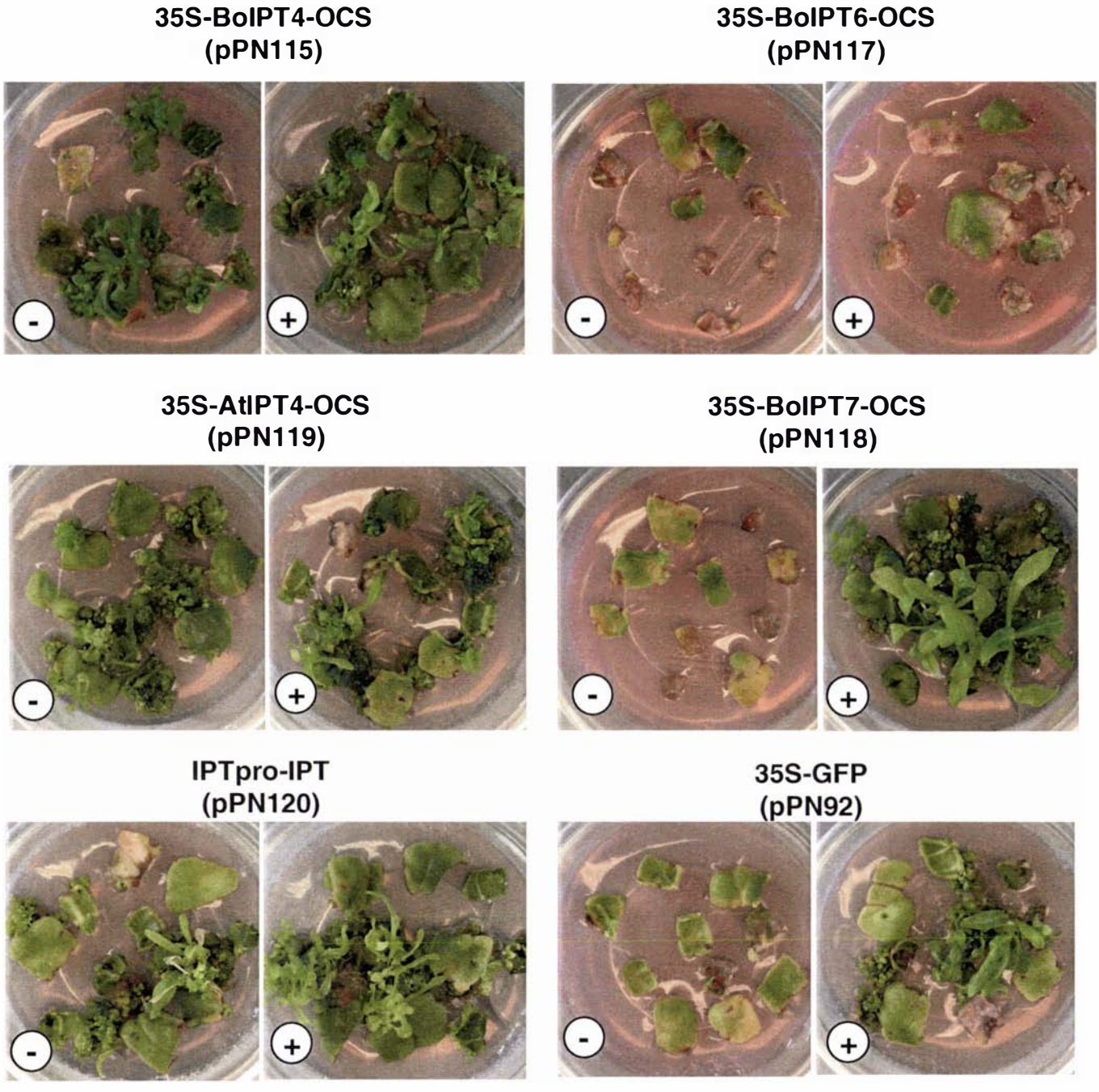

Figure 6.10 *P. hybrida* shoots regenerating from leaf discs in culture following inoculation with BoIPT containing constructs. + and – represents the presence or absence of 6-BAP in the culture media respectfully. All plant IPT binary vectors (pPN115, pPN117, pPN118 and pPN119) contained the CaMV 35S promoter and the octopine synthase 3‘ terminator. pPN120 contained the *A. tumefaciens ipt* gene under the control of its native promoter and terminator sequence. pPN92 contained a 35S driven GFP reporter construct.

RT-PCR using
degenerate primers

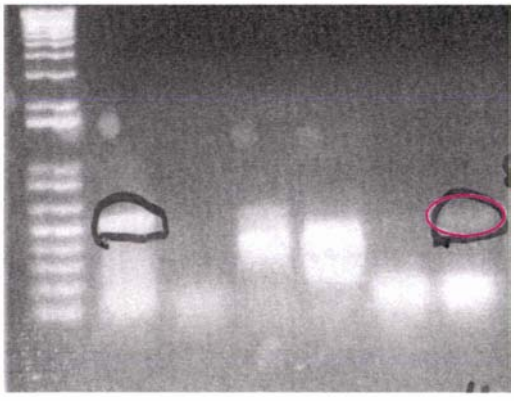

Amplified fragments gel isolated and cloned into pGEMTeasy vecotor

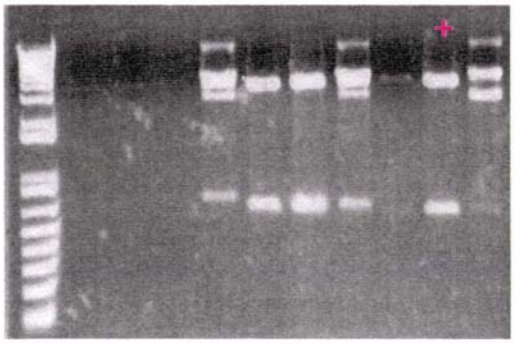

Putative clones digested then sequenced using SP6 and T7 primer sites

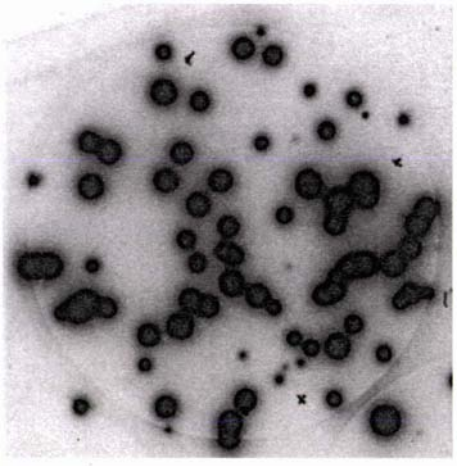

Positive 530 bp putative *BoCKX* used as a probe against broccoli cDNA library.

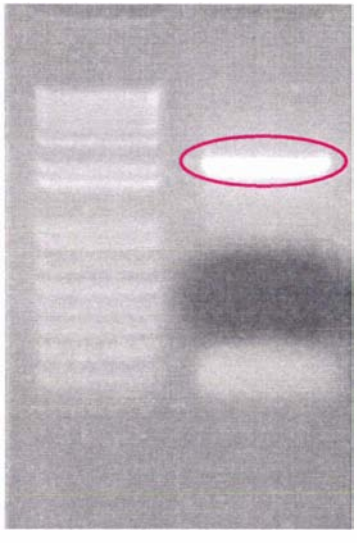

Putative full length BoCKX cDNA amplified using 3° screen as a template with T3 and T7 primers. The 2kb fragment was gel isolated and cloned into pGEMTeasy vector, then sequenced using T3 and SP6 primer sequences.

Figure 6.11 Cloning strategy for the isolation of a putative *BoCKX* cDNA. Circled bands represent fragments that were isolated from agarose gels and cloned. + indicates positive putative *BoCKX* clones following sequencing.

using T3 and T7 primers was used to amplify the full-length clone from the positive plaque tertiary core. The near 1.9 kb fragment was then cloned in pGEMTeasy (Promega), and is yet to be sequenced. The predicted protein sequence of the putative partial length (530 bp, encoding 177 amino acids) BoCKX was aligned against all other plant cytokinin oxidases in the database (Figure 6.12). The partial length BoCKX protein sequence aligned most closely with AtCKX2, with 70% sequence identity, and AtCKX5, with 60% sequence identity.

6.3.6 Presence of *BoCKX* in the broccoli genome

The presence of *BoCKX* in the broccoli genome was confirmed by Southern analyses (Figure 6.13). Genomic DNA isolated from the *cv.* Triathalon was digested to completion with the restriction enzymes *Eco* RI, *Nco* I and *Xba* I. The 530 bp partial *BoCKX* fragment hybridised weakly to at least one band for all digests and also weakly to uncut genomic DNA (Figure 6.13), confirming the presence of *BoCKX* in the broccoli genome. Further Southern experiments using the putative full-length clone as a probe will be essential to estimate the number of copies of this gene within the broccoli genome.

6.3.7 Expression of *BoCKX*

A northern analysis was carried out to show the expression profile of *BoCKX* in broccoli florets following harvest (Figure 6.14). *BoCKX* transcript was detected at very low levels in Triathalon broccoli florets 48-120 h following harvest. Further expression analysis is required to determine if this gene is also expressed in tissues other than broccoli florets.

6.4 DISCUSSION

Since cytokinin has been proposed as a regulator of senescence, the study of the function and expression of genes involved with either the biosynthesis or the metabolism of the cytokinins should provide new insights into the regulation of senescence. In this thesis, the sequence similarity between *Arabidopsis* and *B. oleracea* was exploited to isolate putative cytokinin synthase and cytokinin oxidase genes from

Figure 6.12 Alignment of the predicted protein sequences of plant CKX sequences. Gaps denoted by dashes were inserted to obtain maximum homology. The identical amino acid residues are indicated by white letters on a black background.

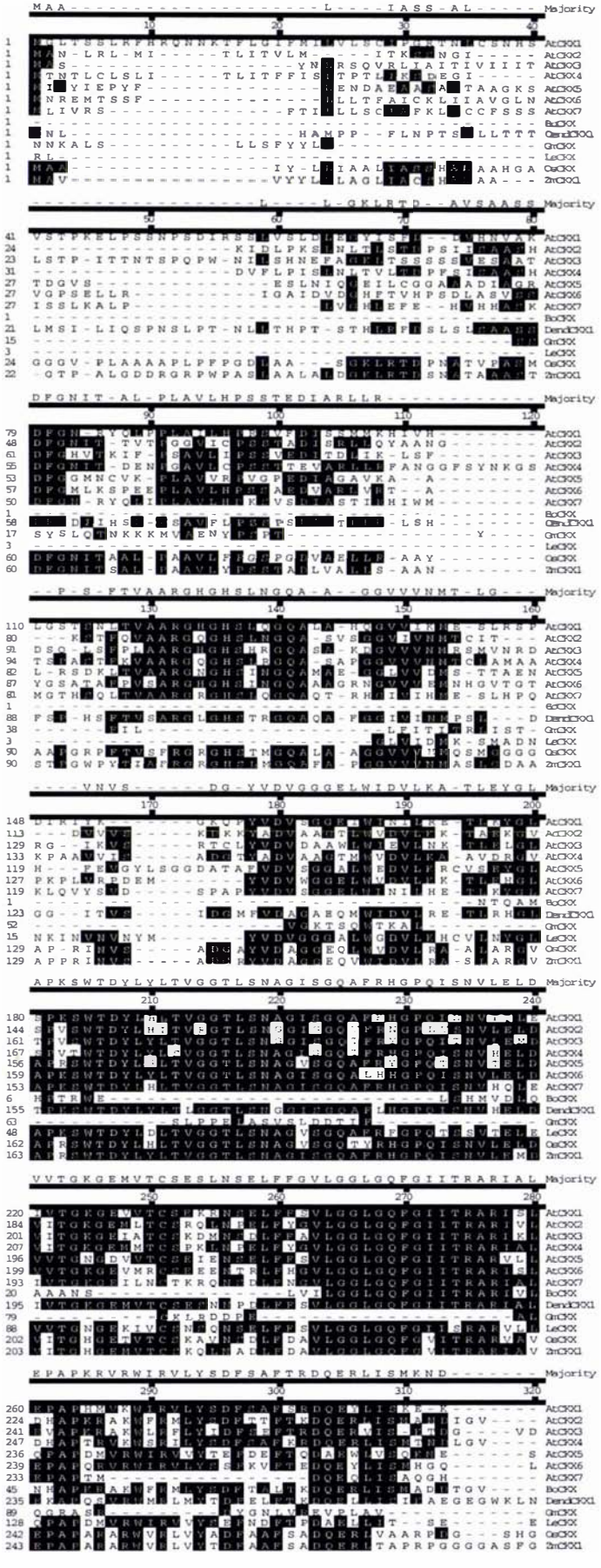

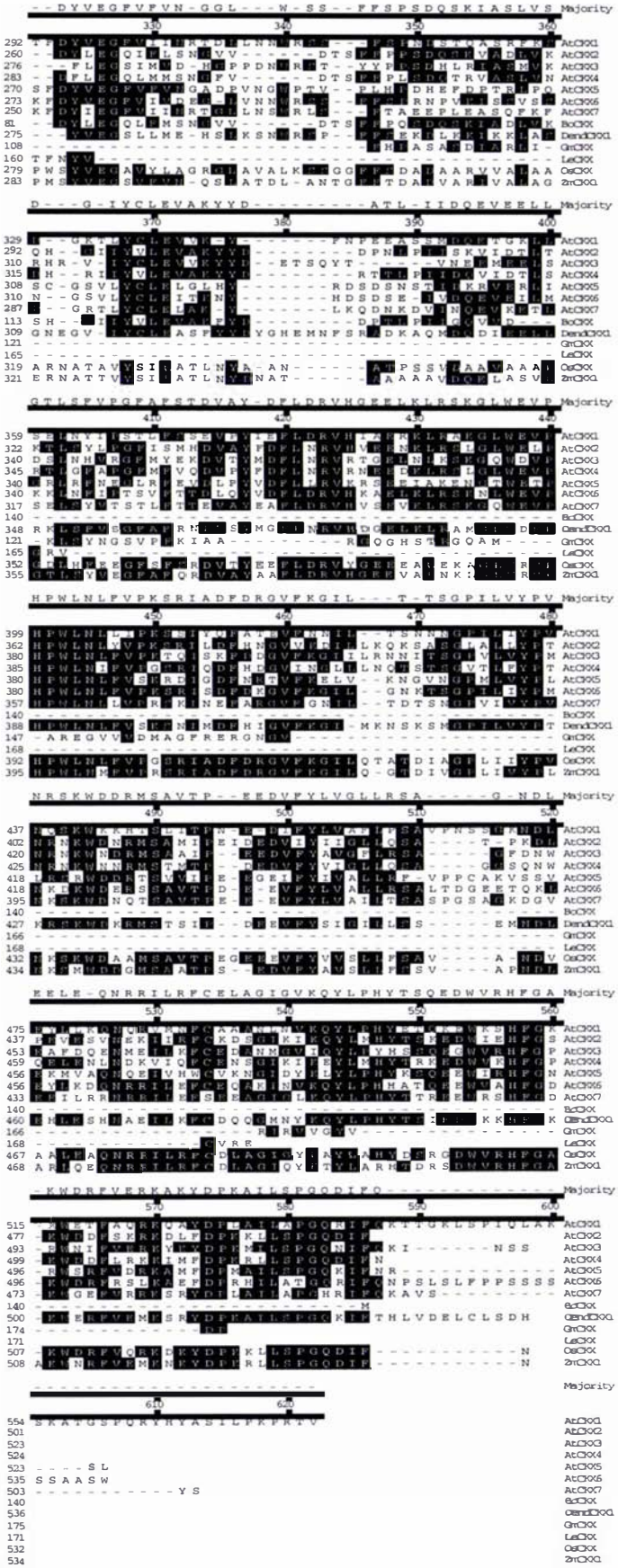

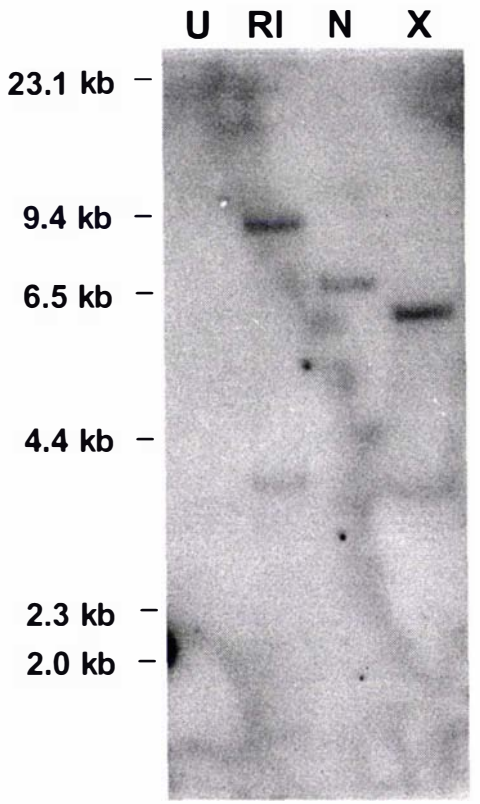

Figure 6.13 Autoradiograph showing the Southern hybridisation of the 530 bp ^{32}P labelled *BoCKX* fragment with broccoli genomic DNA (20 µg). Broccoli (cv. Triathalon) genomic DNA was either uncut (U) or digested with the *Eco* RI (RI), *Nco* I (N) or *Xba* I (X) restriction enzymes. The position of *Hind* III digested λ DNA markers are as indicated. Genomic DNA (20 µg) was separated on a 0.8% (w/v) agarose gel and blotted onto nylon membrane. For details of hybridisation and washing conditions, see Methods and Materials, Section 2.8.

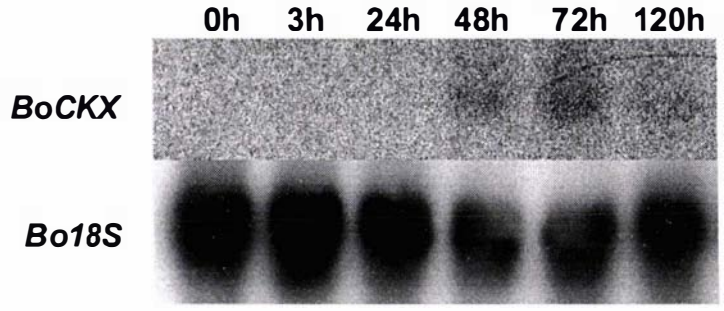

Figure 6.14 Autoradiographs showing the northern hybridisation of a 530 bp ^{32}P labeled *BoCKX* DNA fragment and a 500 bp ^{32}P labelled *Bo18S* partial cDNA fragment with total RNA from wild-type broccoli (cv. Triathalon) following harvest. Total RNA (20 μg) extracted from broccoli florets treated following harvest in air, was denatured and separated in a 1.2% (w/v) agarose gel in 2.2 M formaldehyde, and then transferred to nylon membranes. For details of hybridisation and washing conditions, see Methods and Materials, Section 2.8.

broccoli. The expression profiles of such genes could then provide key insights as to how cytokinins regulate senescence in broccoli.

Four putative *IPT* clones were amplified from broccoli using oligonucleotides specific to *Arabidopsis* sequences (Table 6.1). The presence of these clones in the broccoli genome was confirmed by Southern analyses using stringent washing conditions (Figure 6.6). *BoIPT7* is probably present as a single copy, whereas *BoIPT6* is likely to be present as two copies in the broccoli genome. Further Southern analysis is needed to estimate accurately the number of copies of both *BoIPT5*, which is likely to be present as more than one copy, and *BoIPT4* in the broccoli genome. Sequence alignment and phylogenetic analyses at the amino acid level show that the sequences isolated were more similar to their *Arabidopsis* homologues than to other broccoli homologues (Figures 6.3 and 6.4, Table 6.2). Further, all plant IPTs present in the database align closer together than bacterial IPT sequences. Eukaryote and prokaryote tRNA-IPT sequences are even more distantly related. The alignment of the broccoli sequences in this way provide additional support to the phylogenetic analyses presented by Takei et al. (2001) and Kakimoto (2001a), that the divergence of tRNA-IPTs occurred before that of plant and bacterial IPTs, and that the primary structure of the plant IPT proteins are more closely related to bacterial IPT than to tRNA-IPT proteins.

Cytokinin biosynthesis has traditionally been proposed to occur mainly in roots of plants, but also in shoot meristems and immature seeds and is highly regulated (Mok and Mok, 2001). However, new evidence is starting to arise suggesting genes responsible for cytokinin biosynthesis are also expressed in other tissues. The genes of the *AtIPT* family appear to be differentially expressed (Kakimoto et al., 2001b). Promoter-GUS constructs revealed very clear differences in tissue specificity between the genes. Further, Sun et al. (2003) observed expression of *AtIPT8* only in roots by RT-PCR based analyses, although *in situ* hybridisation studies were yet to confirm this result. The *P. hybrida AtIPT4* homologue, *PtSHO* was observed to be expressed in leaves, apex, roots and young flowers (Zubko et al. 2002). These results suggest that different IPT genes are involved in different biological processes.

Table 6.2 Structural features of putative *BoIPT* genes and predicted proteins.

Gene	Length[1]	Molecular mass (kDa)[2]	Isoelectric point[3]	% identity to AtIPT homologue (predicted protein)
BoIPT4	YTBDA	YTBDA	YTBDA	86.8 (AtIPT4)[4]
BoIPT5	332	37.5	5.9	97.3 (AtIPT5)
BoIPT6	YTBDA	YTBDA	YTBDA	83.7 (AtIPT6)
BoIPT7	332	37.1	8.4	83.6 (AtIPT7)

[1]Lengths are given as amino acids
[2]Calculated molecular mass based on predicted protein sequence
[3]Calculated isoelectric point based on predicted protein sequence
[4]Calculated using partial fragment
YTBDA – Yet to be determined accurately, due to poor sequence of the 5' end

To determine the tissue distribution of mRNA transcripts corresponding to *BoIPT4*, *BoIPT5*, *BoIPT6* and *BoIPT7* in broccoli, it was first necessary to establish conditions that prevented cross-hybridisation of the four clones (Figure 6.5). *BoIPT* fragments were hybridised against each other and under the same high-stringency wash conditions as used for both Southern (Figure 6.6) and 'virtual northern' (Figures 6.7 and 6.8) analyses. As no cross-hybridisation was detected for any of the broccoli clones, their tissue distribution was able to be analysed using specific probes at high stringency hybridisation and washing conditions. Sensitive RT-PCR based 'virtual northern' analyses of the *BoIPT* genes showed that the expression of the individual broccoli clones was also distributed in different tissues. Although this method only provides semi-quantitative gene expression data, it does provide qualitative evidence to show that all of the broccoli clones were expressed. Because these broccoli clones were isolated by PCR amplification from genomic DNA and sequencing revealed the absence of introns, it was possible that some or all of these sequences were psuedo genes. However, given that all the broccoli clones were expressed, the possibility of these broccoli clones being psuedo genes is unlikely.

It was suggested by Takei et al. (2001) that *AtIPT6* was a pseudo gene, as no expression had been observed using sensitive RT-PCR based approaches. However, in broccoli *BoIPT6* was expressed in stems, leaves, stalks and floral tissues. Takei et al. (2001) did

not report which tissues they analysed for expression of the *AtIPT6* gene. Consequently, it is possible that they did not observe expression because they did not assess the tissue(s) *AtIPT6* was expressed in. More extensive characterisation of *ipt* gene families from other plants and of *BoIPT* gene expression during broccoli development, will enable us to understand more clearly how the biosynthesis of cytokinin is regulated in plants.

It is interesting to note that the *P. hybrida ipt* homologue, *PtSHO*, is closely related to *BoIPT4* and *AtIPT4* based on sequence identity. All of these three clones are capable of causing shoot regeneration in culture in the absence of added cytokinin when ectopically expressed *in planta* (this work; Kakimoto, 2001; Zubko et al., 2002). This suggests that these three genes cause the synthesis of enhanced cytokinin when ectopically expressed, and it is this cytokinin that causes callus and shoot formation. Zubko et al. (2002) showed that this was the case for *PtSHO*; where cytokinin levels were enhanced in transgenic plants. It is very likely then that the other two *homologue*s are also responsible for cytokinin biosynthesis.

However, interpretation of data obtained for *BoIPT6* and *BoIPT7* is less straightforward. In the bioassay used, no callus or shoot regeneration was observed when either of these genes was ectopically expressed *in planta* (Figure 6.10). Although the *Arabidopsis* gene family has seven members, only *AtIPT4* has been shown to be active as discussed above (Kakimoto, 2001). There has only been one other report showing that *AtIPTs* are capable of producing cytokinins *in situ*. Sun et al. (2003) showed *AtIPT8/PGA22* mutant plants catalysed the production of iPMP and iPA.

The question arises as to which other genes in the families are also responsible for cytokinin biosynthesis *in planta*. Given that some of these clones have been shown to be expressed (*BoIPT5 BoIPT6* and *BoIPT7*), if they are not capable of cytokinin biosynthesis (as measured by shoot regeneration in the absence of cytokinin), what is their physiological role *in planta*? Northern analyses would provide a more stringent test of expression, although the expected low expression of these genes maybe a limiting factor for this approach. *In situ* hybridisation may be an approach more worth

perusing for future gene expression analyses. However, even if these genes are expressed at the level of the transcript, this does not automatically mean they are translated into functional protein *in planta*. Western analyses could be used to deduce if the plant IPT genes are translated into protein *in planta*, although this would require the production of expensive monoclonal antibodies given that there exists a multi gene family. Further, the promoters of these genes could be isolated and fused to a suitable reporter gene such as GUS or the green fluorescent protein (GFP) and ectopically expressed, thus tracing the expression pattern of the reporter *in planta*. Feeding studies could also be carried out with different precursors of cytokinins in an attempt to deduce the preferred substrate for the enzymes, and the immediate end product of the cytokinin synthase reaction *in planta*.

A similar picture with regards to differential expression is emerging now for cytokinin oxidase gene expression. As mentioned earlier, Bilyeu et al. (2001) isolated a family of seven genes from *Arabidopsis*. The promoters of three of these genes were isolated and fused to GUS and the expression profile of the reporter gene traced heterologously in tobacco (Gális et al., unpublished). *AtCKX3* appears to be expressed in various tissues, including the margins of young leaves, the hypocotyl zone, in root vasculature and in mature pollen. *AtCKX4* expression was weaker in leaf margins, and in the root restricted to the cap. *AtCKX4* was also expressed in trichomes and also in immature pollen. No expression of *AtCKX2* was observed in any of the tobacco tissue analysed. These results suggest that different cytokinin oxidase genes could be responsible for metabolising cytokinin during different biological responses or processes, such as root growth, where it is well known that cytokinin has an inhibitory effect on growth above a very minimal level.

It is interesting, that *BoIPT4* is expressed to reasonably high levels at and following harvest in broccoli (Figure 6.7). The *BoCKX* clone is also up-regulated in these tissues, albeit later (Figure 6.14). It appears that there may be a close correlation between biosynthesis of cytokinins and cytokinin oxidase activity in floret tissue. Further work will be required to elucidate whether this relationship occurs more widely and how this relationship might be controlled.

Chapter 7

Final Discussion and Conclusions

The overall aim of this thesis was to extend our understanding of how cytokinins and ethylene regulate postharvest-induced senescence in broccoli. The initial experiments focused on the effects of exogenous cytokinin, ACC and sucrose on the expression of genes associated with senescence and ethylene biosynthesis in broccoli florets following harvest. Exogenous cytokinin appeared to nullify ethylene feedback regulation of its biosynthesis by desensitising tissue to ethylene. Cytokinin caused altered expression of genes associated with senescence that was consistent with its ability to delay senescence. These results confirmed previous work conducted by Clarke et al. (1994) suggesting cytokinin is a key regulator of harvest-induced senescence in broccoli. A model is presented in Chapter 3 that integrates the role of the two hormones in postharvest senescence in broccoli.

It had been recognised that transgenic plants with altered ethylene and/or cytokinin levels, and altered senescence status are very powerful tools with which to study how ethylene and cytokinin interact to regulate senescence, and that broccoli is an excellent model plant for postharvest studies. Henzi et al. (1999b), using *A. rhizogenes*, produced broccoli plants harbouring an antisense ACO gene from tomato (*pTOM13*). However, because the results presented in Chapter 3 cast doubt on the usefulness of these plants, new transgenic plants altered for ethylene and/or cytokinin biosynthesis, using *A. tumefaciens*-mediated transformation, were produced during this thesis.

Transgenic broccoli harbouring the antisense AS-ACO, MYB_{305}-IPT, SAG_{12}-IPT and the double AS-ACO::MYB_{305}-IPT constructs were successfully produced using *A. tumefaciens*, suggesting that there is little need to use *A. rhizogenes*-mediated transformation for broccoli in the future, especially in light of the abnormal phenotypes associated with that form of transformation. The results presented in this thesis also illustrate the importance of reducing ethylene to enhance transformation rates for

broccoli and *Arabidopsis thaliana*, but they also indicated that the AS promoter was inducible under tissue culture conditions.

Although the transformation efficiency reported here for the *A. tumefaciens*-mediated method is lower than those previously published for broccoli (Toriyama et al., 1991; Metz et al., 1995), manipulating and combining some of the variables mentioned may allow an increased transformation rate. The preculture of hypocotyl and cotyledonary petiole explants prior to co-cultivation, or the use of cell feeder layers may increase transformation efficiency (Metz et al., 1995; Cho et al., 2001), although the aim in this project was to use a more simplified protocol.

The transgenic broccoli plants harbouring the antisense AS-ACO chimeric gene construct reported in Chapter 4 were characterised and described in detail in Chapter 5. Although ethylene evolution was not measured, the delayed senescence exhibited by both leaves and detached heads is indicative of reduced ethylene biosynthesis. A reduction in ACO enzyme level and activity was confirmed in AS-ACO line 7 following harvest compared to wild-type plants. In addition, differences in the expression profiles of senescence marker genes relative to controls also occurred in antisense AS-ACO florets following harvest, providing a further explanation for the delayed senescence phenotype observed.

However, the specific postharvest nature of the AS-promoter has been questioned. While it is clear that the expression of the AS-promoter is relatively strong following harvest, its temporal specificity is less clear. The AS-promoter, as well as being positively regulated in response to harvest, is negatively regulated by sucrose (Winichayakul et al., unpublished data). Biochemical analyses of the simple sugars in the antisense AS-ACO plants may provide more information on how the AS-promoter regulated the expression of the antisense ACO gene. Recently, the AS-promoter was fused to β-glucuronidase (GUS) and transformed into broccoli (Kenel et al., 1999). In depth postharvest analyses of broccoli plants expressing AS-GUS will be useful in establishing the specificity of the promoter. Deletion of the sugar-regulated element of

this promoter, or isolation of the harvest-specific component, could provide novel molecular tools for postharvest biotechnological approaches.

The antisense AS-ACO construct may be auto-regulated to some extent, in a manner similar to that proposed for the SAG_{12}-IPT construct in tobacco (Gan and Amasino, 1995), although AS-ACO auto-regulation may be less tight than that of SAG_{12}-IPT. The following sequence of events is proposed: the AS-promoter up-regulates the antisense ACO gene in response to senescence/harvest, which causes an absence of signal (ethylene) to regulate downstream consequences of senescence. The trigger, which causes the AS-promoter to up-regulate the antisense ACO gene, may no longer be sensed, so the AS-promoter is down-regulated leading to down-regulation of the antisense ACO gene, and ethylene can once again be produced. This could provide a window to produce sufficient ethylene to up-regulate senescence response pathways. The production of double transgenic plants harbouring both AS-ACO and AS-reporter constructs would be useful to test this hypothesis.

Initial characterisation of the transgenic plants harbouring constructs for enhanced cytokinin production has been carried out and are ongoing. It appears that the regulation of the promoters used to express *ipt* in these plants may also be less than specific to floral tissue (MYB_{305}) or during senescence (SAG_{12}), due to the altered morphology observed in some lines. Experiments will be conducted to assess whether the lines harbouring the cytokinin-over-production constructs show delayed senescence. The expression of the *ipt* gene will be traced by northern or RT-PCR based 'virtual northern', cytokinin levels will be measured in selected tissues, and the horticultural performance of selected lines will be tested under containment conditions. Crop & Food Research and Massey University personnel will carry out these experiments.

Although some issues have been raised about how useful the approaches used here to delay senescence could be for horticultural and agricultural purposes, the technology combined with the appropriate molecular tools does show commercial promise. However, the plants produced do provide powerful tools for the study of senescence. It is clear that blocking ethylene biosynthesis altered the expression of genes involved

with carbohydrate metabolism and transport, as well as other senescence-associated genes. Further, analyses of the expression of carbohydrate metabolising and transport genes in plants harbouring altered cytokinin status could also provide more information of how senescence is regulated in broccoli by ethylene, cytokinin and carbohydrates. In the long term, the analysis of broccoli plants altered for carbohydrate metabolism and transport could also provide tools for the study of senescence in broccoli.

Genes encoding enzymes involved with the biosynthesis and metabolism of cytokinins were also isolated and partially characterised, with the long-term aim of understanding how cytokinin levels are regulated during senescence. A multigene family exists for the cytokinin synthase (IPT) in *Arabidopsis* and broccoli. However inconclusive the picture at present, there is a common theme arising from the data presented here and that already published. It appears that the cytokinin synthase genes isolated from plants are expressed differentially throughout the plant, and may be involved with different developmental processes. It is possible that a tier of regulation is present at the level of biosynthesis of the hormone, which may be similar to the biosynthetic regulation of ethylene. Both ACC synthase and ACC oxidase, the enzymes involved with the dedicated steps of ethylene biosynthesis, are encoded by multi gene families, which are expressed in different plant tissues. Their expression is controlled both temporally and spatially in a number of plant species and therefore provide regulation of the hormone at the level of biosynthesis.

As there are seven *IPT* genes present in the *Arabidopsis* genome, it is likely, especially given the close sequence identity of the *Arabidopsis* and broccoli homologues, that there exist more than four *IPT* genes in broccoli. Further experiments are needed to isolate additional clones from broccoli. Given the success of the PCR method so far, it would seem sensible to continue with this approach using a suite of primers with homology to *AtIPT1*, *AtIPT3* and *AtIPT8*. Alternatively, the remaining *AtIPT* clones could be used as heterologous probes to screen both existing broccoli genomic and cDNA libraries.

A clearer picture of the relationship between cytokinin biosynthesis and metabolism and the role these two processes have, both alone and in tandem, on the regulation of different biological processes is now possible. Careful monitoring of the expression profiles of *IPT* and *CKX* gene families will provide useful information. Further, the developmental effects of up- or down-regulation of these genes can now be monitored as well as their effects on other genes. Furthermore, tandem reporter gene analyses could provide some key insights as to the roles, function and interaction of the cytokinin biosynthesis and metabolising genes during different developmental processes.

The biotechnological potential of these new tools are three-fold. Firstly, the genes isolated could themselves be expressed using ideal spatial or temporal gene promoters to enhance the yield of certain crops and/or their marketability due to extension of shelf-life. Secondly, given that the regulation of cytokinin biosynthesis and metabolism is tight, the promoters from these genes may also provide excellent new tools to drive the expression of genes at a certain time or in a certain tissue or at a certain metabolic status. The importance of specific gene promoters for biotechnological approaches is well publicised. Thirdly, the over-expression of a plant cytokinin synthase gene could bring an end to the use of antibiotic selectable marker genes during plant transformation. Shoot regeneration could be carried out using cytokinin-less culture media.

From the work of Kakimoto (2001) and Takei et al. (2001), it may be that ATP, ADP and AMP are the preferred substrates for different IPT enzymes. It might be conceivable that the different isoforms of cytokinin synthases may have a preference for different precursors. Further, the metabolising enzymes (CKXs) may have stronger affinity for certain cytokinin forms. The perception of the hormone adds another layer of control. Only when we understand how all three of these layers fit together will we really understand how cytokinin regulates the many physiological processes it does in such a tight manner. Some of the tools are now in place to provide information about how cytokinin regulates senescence in broccoli at the level of biosynthesis and metabolism.

A summary of the proposed regulation of senescence by cytokinin, ethylene and simple carbohydrates is presented in Figure 7.1. It is clear from the data presented in this thesis that ethylene plays an important role in the regulation of senescence-associated gene expression. Further, ethylene was responsible for up-regulating genes involved with the transport and metabolism of sugars during senescence, either directly or indirectly: when ethylene was reduced during senescence (AS-ACO plants), the expression of these genes was reduced. However, it appears that regulation of cytokinin levels during senescence may provide the ultimate level of control. Exogenous cytokinin caused a reduction of the carbohydrate and senescence-associated gene expression. Further, ethylene biosynthesis gene expression was altered: *BoACS* transcript levels rose, whereas *BoACO* transcript did not rise above basal levels, during senescence in the presence of exogenous cytokinin, results which have been interpreted as indicating that cytokinin was affecting the sensitivity of the tissue to ethylene.

BoIPT4 was expressed in florets early during senescence, and *BoCKX* expression followed later. Synthesis of active cytokinin (by *BoIPT4*) early during senescence may suppress the senescence signal that is responsible for up-regulation of ethylene biosynthesis. Later during senescence cytokinins may be irreversibly inactivated by cytokinin oxidase activity (*BoCKX*), and the suppression of the signal lifted. The ethylene signal would then up-regulate downstream senescence-associated gene expression as depicted in Figure 7.1.

The effect of elevating endogenous cytokinin levels following harvest on the rate of senescence of broccoli heads and expression of genes involved with ethylene biosynthesis and carbohydrate metabolism will be extremely interesting.

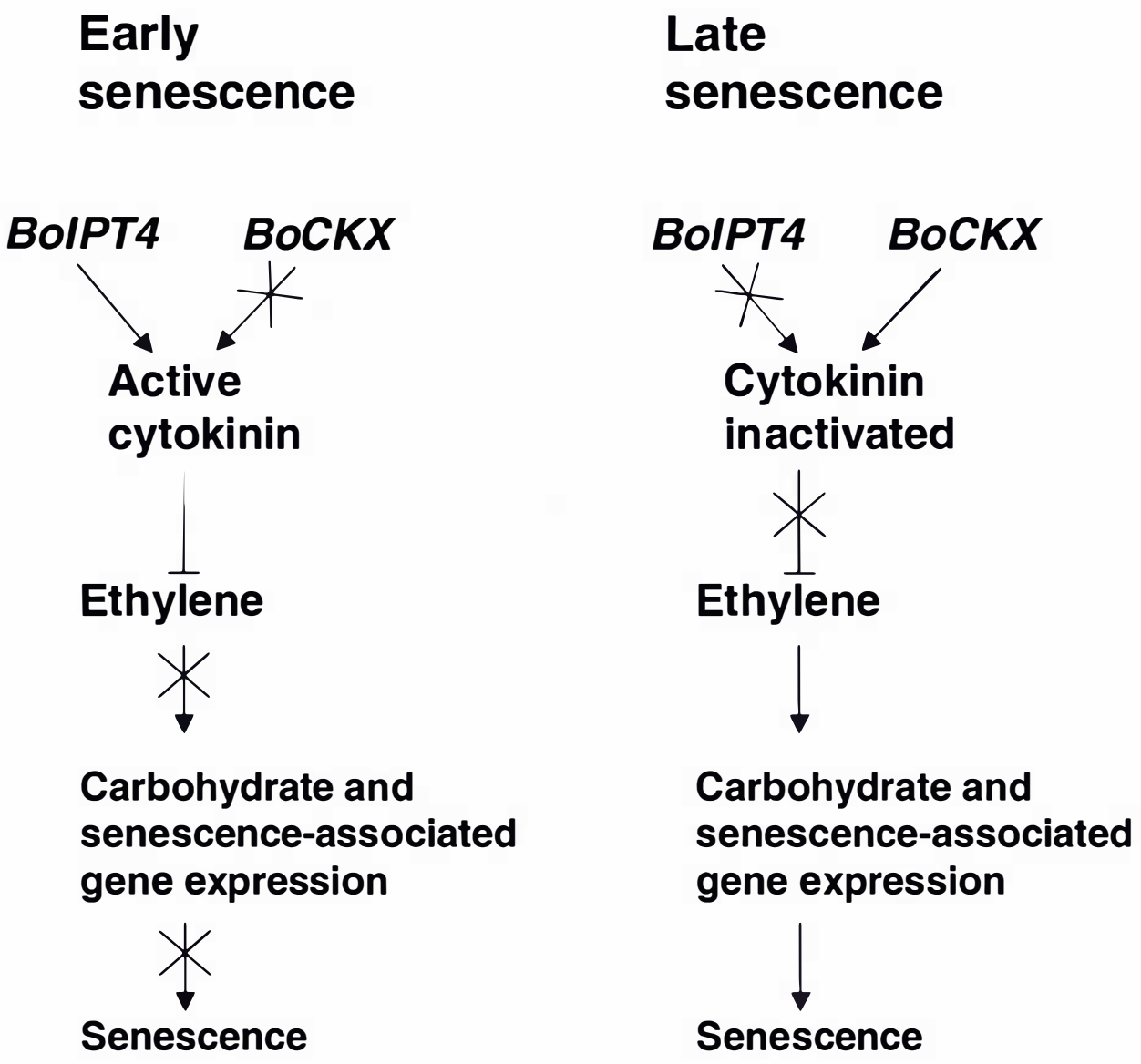

Figure 7.1 A schematic representation of the proposed regulation of senescence by cytokinin biosynthesis and metabolism in broccoli florets following harvest. A. Early senescence signalling is inhibited by active cytokinin that is produced by *BoIPT4*. B During late senescence, the inhibition of the senescence signal is lifted, due to metabolism of cytokinin by *BoCKX*.

Bibliography

Abeles FB, 1973. Ethylene in plant Biology. Abeles FB ed., Academic Press, New York.

Abeles FB, 1992. *Ethylene in Plant Biology*. 2nd ed Abeles FB, Morgan PW, Saltveit ME eds., Academic Press, San Diego, California. pp 414-.

Adam DO, Yang SF, 1979. Ethylene Biosynthesis: identification of 1-aminocyclopropane-1-carboxylic acid as an intermediate in the conversion of methionine to ethylene. *Proceedings of the National Academy of Science of the USA*. 76: 170-174.

Adedipe NO, Fletcher RA, 1971. Retardation of leaf senescence by benzyladenine in bean plants is not dependent on mobilization. *Canadian Journal of Botany*. 49: 59-61.

Aharoni N, Anderson JD, Lieberman M, 1979. Production and action of ethylene in senescing leaf discs: effect of indole acetic acid, kinetin, silver ion, and carbon dioxide. *Plant Physiology*. 64: 805-809.

Alonso JM, Hirayama T, Roman G, Nourizadeh S, Ecker JR, 1999. EIN2, a bifunctional transducer of ethylene and stress responses in *Arabidopsis*. *Science* 284: 2148–2152.

Bartz JK, Söll D, 1972. N^6-(Δ^2-isopentenyl) adenosine: biosynthesis *in vitro* in transfer RNA by an enzyme purified from *Eschericha coli*. *Biochemie*. 54: 31-39.

Bassil NV, Mok DWS, Mok MC, 1993. Partial purification of a *cis-trans*-isomerase of zeatin from immature seed of *Phaseolus vulgaris* L. *Plant Physiology*. 102: 867-872.

Becker W, Apel K, 1993. Differences in gene expression between natural and artificially induced leaf senescence. *Planta*. 189(1): 74-79.

Bent A, Innes R, Ecker J, Staskawitcz B, 1992. Disease development in ethylene-insensitive Arabidopsis thaliana infected with virulent and avirulaent *Pseudomonas* and *Xanthomonas* pathogens. *Molecular Plant-Microbe Interactions*. 5: 372-378.

Berthomieu P, Jouanin L, 1992. Transformation of rapid cycling cabbage (*Brassica oleracea* var. *capitata*) with *Agrobacterium rhizogenes*. *Plant Cell Reports*. 11: 334-338.

Bilyeu KD, Cole JL, Laskey JG, Riekhof WR, Esparza TJ, Kramer MD, Morris RO, 2001. Molecular and biochemical characterization of a cytokinin oxidase from maize. *Plant Physiology*. 125: 378-386.

Bleecker AB, Kende H, 2001. Ethylene: A gaseous signal molecule in plants. *Annual Review of Cell and Developmental Biology*. 16: 1-18.

Bleecker AB, Patterson SE, 1997. Last exit: senescence, abscission, and meristem arrest in *Arabidopsis*. *The Plant Cell*. 9: 1169–1179.

Bleecker AB, Estelle, MA, Sommerville C, Kende H, 1988. Insensitivity to ethylene conferred by a dominant mutation in *Arabidopsis thaliana*. *Science*. 241: 1086-1089.

Bradford MM, 1976. A rapid and sensitive method for the quantitation of microgram quantities of protein utilizing the principle of protein dye binding. *Analytical Biochemistry*. 72: 248-254.

Brock TG, Cleland RG, 1989. Role of acid efflux during growth promotion of primary leaves of *Phaseolus vulgaris* L. by hormones and light. *Planta*. 177: 476-482.

Buchanan-Wollaston V, 1994. Isolation of cDNA clones for genes that are expressed during leaf senescence in *Brassica napus*. *Plant Physiology*. 105: 839-846.

Buchanan-Wollaston V, 1997. The molecular biology of leaf senescence. *Journal of Experimental Botany*. 48: 181-199.

Buchanan-Wollaston V, Ainsworth, 1997. Leaf senescence in *Brassica napus*: cloniong of senescence related genes by subtractive hybridisation. *Plant Molecular Biology*. 33: 821-834.

Bufler G, 1984. Ethylene-enhanced 1-aminocyclopropane-1-carboxylic acid synthase activity in ripening apples. *Plant Physiology*. 75: 192-195.

Cao J, Tang JT, Strizhov N, Shelton AM, Earle ED, 1999. Transgenic broccoli with high levels of *Bacillus thuringiensis* Cry1C protein control diamondback moth larvae resistant to Cry1A or Cry1C. *Molecular Breeding*. 5: 131-141.

Cary AJ, Liu W, Howell SH, 1995. Cytokinin action is coupled to ethylene in its effects on the inhibition of root and hypocotyls elongation in *Arabidopsis thaliana* seedlings. *Plant Physiology*. 107: 1075-1082.

Chandlee J M, 2001. Current molecular understanding of the genetically programmed process of leaf senescence. *Physiologia Plantarum*. 113: 1-8 2001.

Chang CC, 1996. The ethylene signal transduction pathway in *Arabidopsis*: an emerging paradigm? *Trends in Biochemical Science*. 21: 129-133.

Chang HH, Chan MT, 1991. Improvement of potato (*Solanum tuberosum* L.) transformation efficiency by *Agrobacterium* in the presence of silver thiosulfate. *Botanical Bulletin of Academia Sinica*. 32: 63-70.

Chang CC, Meyerowitz EM, 1995. The ethylene hormone response in Arabidopsis: a eukaryotic two-component signalling system. *Proceedings of the National Academy of Sciences of the USA*. 92: 4129-4133.

Chang CC, Kwok SF, Bleecker AB, Meyerowitz EM, 1993. Arabidopsis ethylene response gene ETR1: similarity of product to two-component regulators. *Science*. 262: 539-544.

Chao Q, Rothenberg M, Solano R, Roman G, Terzaghi W, Ecker JR, 1997. Activation of the ethylene gas response pathway in *Arabidopsis* by the nuclear protein ETHYLENEINSENSITIVE3 and related proteins. *Cell*. 89: 1133–1144.

Chen CM, Christopeit SM, 1981a. Dephosphorylation of cytokinin ribonucleotide by 5'-nucleotidases from wheat germ cytosol. *Plant Physiology*. 67: 494-498.

Chen CM, Christopeit SM, 1981b. Metabolism of cytokinin: Deribosylation of cytokinin ribonucleoside by adenine nucleosidase from wheat germ cells. *Plant Physiology*. 68: 1020-1023.

Chen CM, Hall RH, 1969. Biosynthesis of N^6-(Δ^2-isopentenyl) adenosine in the transfer of ribonucleic acid of cultured tobacco pith tissue. *Phytochemistry*. 8: 1687-1695.

Chen LFO, Hwang JY, Charng YY, Sun CW, Yang SF, 2001. Transformation of broccoli (*Brassica oleracea* var. *italica*) with isopentenyltransefearse gene via *Agrobacterium tumefaciens* for post-harvest yellowing retardation. *Molecular Breeding*. 7: 243-257.

Chi GL, Barfield DG, Sim GE, Pua EC, 1990. Effect of $AgNO_3$ and aminoethoxyvinyl glycine on *in vitro* shoot and root organogenesis from seedling explants of recalcitrant *Brassica* genotypes. *Plant Cell Reports*. 9: 195-198.

Cho HS, Cao J, Ren JP, Earle ED, 2001. Control of Lepidopteran insect pests in transgenic Chinese cabbage (*Brassica rapa* ssp. *Pekinsis*) transformed with a synthetic *Bacillus thuringiensis cry1C* gene. *Plant Cell Reports*. 20: 1-7.

Chomczynski P, 1992. One hour downward alkaline capillary transfer for blotting DNA and RNA. *Analytical Biochemistry*. 201: 134-139.

Church GM, Gilbert W, 1984. Genomic sequencing. *Proceedings of the National Academy of Science of the USA*. 81: 1991-1995.

Christey MC, 1997. Transgenic crop plants using Agrobacterium rhizogenes-mediated transformation. In: *Hairy roots: culture and applications*. Doran, PM (ed.), Harwood Academic Publishers.

Christey MC, Sinclair BK, 1992. Regeneration of transgenic kale (*Brassica oleracea* var. *acephala*), rape (*B. napus*) and turnip (*B. campestris* var. *rapifera*) plants via *Agrobacterium rhizogenes*-mediated transformation. *Plant Science*. 87: 161-169.

Christey MC, Sinclair BK, Braun RH, Wyke L, 1997. Regeneration of transgenic vegetable brassicas (*Brassica oleracea* and *B. campestris*) via Ri-mediated transformation. *Plant Cell Reports*. 16: 161-169.

Clark DG, Richards C, Hiliti Z, Lind-Iversen S, Brown K, 1997. Effect of pollination on accumulation of ACC synthase and ACC oxidase transcripts, ethylene production and flower petal abscission in geranium (*Pelargonium* X *hortorum* L.H. Bailey), *Plant Molecular Biology*. 34: 855-865.

Clark KL, Larsen PB, Wang X, Chang CC, 1998. Association of the *Arabidopsis* CTR1 Raf-like kinase with the ETR1 and ERS ethylene receptors. *Proceedings of the National Academy of Sciences of the USA*. 95: 5401–5406.

Clarke SF, Jameson PE, Downs C, 1994. The influence of 6-benzylaminopurine on post-harvest senescence of floral tissues of broccoli (*Brassica oleracea* var. *Italica*). *Plant Growth Regulation*. 14: 21-27.

Clough SJ, Bent AF, 1998. Floral dip: a simplified method for *Agrobacterium*-mediated transformation of *Arabidopsis thaliana*. *The Plant Journal*. 16: 735-743.

Coupe SA, Sinclair BK, Watson LM, Gapper NE, Pinkney TT, Eason JR, Greer LA, Heyes JA, unpublished. The isolation and characterisation of sucrose transporter homologues from

broccoli and their role in sucrose mobilisation during senescence. *Manuscript in preparation for submission.*

Coupe SA, Sinclair BK, Greer LA, Gapper NE, Watson LM, Hurst PL, 2003a. Analysis of acid invertase gene expression during the senescence of broccoli florets. *Postharvest Biology and Technology.* 28: 27-37

Coupe SA, Sinclair BK, Watson LM, Heyes JA, Eason JR, 2003b. Identification of dehydration-responsive cysteine proteases during post-harvest senescence of broccoli florets. *Journal of Experimental Botany.* 54 (384): 1045-1056.

Dai N, Schaffer A, Petreikov M, Shahak Y, Giller Y, Ratner K, Levine A, Granot D, 1999. Overexpression of Arabidopsis hexokinase in tomato plants inhibits growth, reduces photosynthesis and induces rapid senescence. *The Plant Cell.* 11: 1253-1266.

Davies K, King GA, 1993. Isolation and characterisation of a cDNA clone for a harvest-induced asparagine synthetase from *Asparagus officinalis*. *Plant Physiology.* 102: 1337-1340.

Davies KM, Seelye JF, Irving DE, Borst WM, Hurst PL, King GA, 1996. Sugar regulation of harvest-related genes in asparagus. *Plant Physiology.*111(3): 877-883.

De Block M, De Brouwer D, Tenning P, 1989. Transformation of *Brassica napus* and *Brassica oleracea* using *Agrobacterium tumefaciens* and the expression of the *bar* and *neo* genes in transgenic plants. *Plant Physiology.* 91: 694-701.

Dedolph RR, Wittwer SH, Tuli V, Gilbart D, 1962. Effect of N^6-benzylaminopurine on respiration, and storage behaviour of broccoli (*Brassica oleracea* var. *Italica*). *Plant Physiology.* 37: 509-512.

Deroles SC, Gardner RC, 1998. Expression and inheritance of kanamycin resistance in a large number of transgenic petunias generated by *Agrobacterium*-mediated transformation. *Plant Molecular Biolology.* 11: 355-364.

Deruere J, Kieber JJ, 2002. Molecular mechanisms of cytokinin signaling. *Journal of Plant Growth Regulation.* 21(1): 32-39.

Dong JG, Kim WT, Yip WK, Thompson GA, Li L, Bennett AB, Yang SF, 1991. Cloning of a cDNA encoding 1-aminocyclopropane-1-carboxylate synthase and expression of its mRNA in ripening apple fruit. *Planta.* 185: 38-45.

Dostal HC, Dedolph RR, Tuli V, 1965. Changes in nonvolatile organic acid constituents in broccoli (*Brassica oleracea* var. *Italica*) following postharvest N^6-benzyladenine treatment. *Proceedings of the American Society of Horticultural Science.* 86; 387-391.

Downs CG, Somerfield SD, 1997. Asparagine synthetase gene expression increases as sucrose declines in broccoli after harvest. *New Zealand Journal of Crop and Horticultural Science.* 25: 191-195.

Downs CG, Davey MC, Somerfield SD, 1997. Cytokinin treatment delays senescence but not sucrose loss in harvested broccoli. *Postharvest Biology and Technology.* 11: 93-100.

Dyer TA, Osbourne DJ, 1971. Leaf nucleic acids. II. Metabolism during senescence and the effect of kinetin. *Journal of Experimental Botany.* 22: 552-560.

Edwards K, Johnstone C, Thompson, 1991. A Simple and rapid method for the preparation of plant genomic DNA for PCR analysis. *Nucleic Acids Research.* 19: 1349.

English PJ, Lycett GW, Roberts JA, Jackson MB, 1995. Increased 1-aminocyclopropane-1-carboxylic acid oxidase activity in shoots of flooded tomato plants raises ethylene production to physiologically active levels. *Plant Physiology.* 109: 1435-1440.

Estelle M, 2001. Cytokinin receptor: Just another histidine kinase. *Current Biology* 11: R271-R273.

Eulgem T, Rushton PJ, Robatzek S, Somssich IE, 2000. The WRKY superfamily of plant transcription factors. *Trends in Plant Science.* 5: 199-206.

Ferrarese L, Trainotti L, Moretto P, De3-Laureto PP, Rasicio N, Cassadoro G, 1995. Differential ethylene-inducible expression of cellulase in pepper plants. *Plant Molecular Biology.* 29: 735-747.

Fletcher RA, 1969. Retardation of leaf senescence by benzyladenine in intact bean plants. *Planta.* 89: 1-8.

Forney CF, Jordan MA, 1998. Induction of volatile compounds in broccoli by postharvest hot-water dips. *Journal of Agricultural and Food Chemistry.* 46: 5295-5301.

Frugis G, Giannino D, Mele G, Nicolodi C, Chiappetta A, Bitonti MB, Innocenti AM, Dewitte W, Van Onckelen H, Mariotti D, 2001. Overexpression of *KNAT1* in lettuce shifts leaf determinate growth to a shoot-like indeterminate growth associated with an accumulation of isopentenyl-type cytokinins. *Plant Physiology.* 126: 1370-1380.

Fu YC, Ding YY, Liu XF, Sun CQ, Cao SY, Wang DJ, He SJ, Wang XK, Li LC, Tian WZ, 1998. Rice transformation with a senescence-inhibition chimeric gene. *Chinese Science Bulletin.* 42(21): 1810-1815.

Gális I, Bilyeu KD, Godhino M, Jameson PE, unpublished. Expression of three cytokinin oxidase promoter::GUS chimeric constructs in tobacco: response to developmental and biotic factors. *Manuscript in preparation for submission.*

Galuska P, Frébort I, Šebela M, Sauer P, Jacobsone S, Peč, 2001. Cytokinin oxidase or dehydrogenase? *European Journal of Biochemistry.* 268: 450-461.

Gamble RL, Coonfield ML, Schaller GE, 1998. Histidine kinase activity of the ETR1 ethylene receptor from Arabidopsis. *Proceedings of the National Academy of Sciences USA.* 95: 7825–29.

Gan S, Amasino RM, 1995. Inhibition of leaf senescence by autoregulated production of cytokinin. *Science.* 270: 1986-1987.

Gapper NE, McKenzie MJ, Christey MC, Braun RH, Coupe SA, Lill RE, Jameson PE, 2002. *Agrobacterium tumefaciens*-mediated transformation to alter ethylene and cytokinin biosynthesis in broccoli. *Plant Cell Tissue and Organ Culture.* 70(1): 41-50.

Gerhäuser D, Bopp M, 1990. Cytokinin oxidases in mosses 2. Metabolism of kinetin and benzyladenine *in vitro*. *Journal of Plant Physiology.* 135: 714-718.

Gleave AP, 1992. A versatile binary vector system with a T-DNA organisational structure conductive to efficient integration of cloned DNA into the plant genome. *Plant Molecular Biology*. 20: 1203-1207.

Gong D, McManus MT, 2000. Purification and characterisation of two ACC oxidases expressed differentially during leaf ontogeny in white clover. *Physiologia Plantarum.* 110: 13-21.

Gonzalez N, Botella JR, 2003. Characterisation of three ACC synthase gene family members during post-harvest-induced senescence in broccoli (*Brassica oleracea* var. *italica*). *Manuscript in preparation for submission.*

Grbić V, Bleecker AB, 1993. Role of ethylene in the control of leaf senescence in *Arabidopsis thaliana. Plant Physiology (Supplement).* 102: 131.

Grierson D, Kaber AA, 1986. *Fruit ripening and quality.* In: The tomato crop: a scientific basis for improvement. Atherton JG & Rudich J. eds., Chapmann and Hall, London, UK. pp 241-280.

Grossman S, Lesham Y, 1978. Lowering endogenous lipoxygenase activity in *Pisum sativum* by cytokinin as related to by senescence. *Physiologia Plantarum.* 43: 359-362.

Gilbart DA, Dedolph RR, 1965. Phytokinin effects on respiration and photosynthesis in roses and broccoli. *Proceedings of the American Society for Horticultural Science.* 86: 774-778.

Grant JE, Dommisse EM, Christey MC, Conner AJ, 1991. Gene transfer to plant using *Agrobacterium.* In: *Advanced methods in plant breeding and biotechnology.* Murray DR (ed.) CAB, international Biotechnology in Agriculture No. 4.

Hall RH, 1973. Cytokinin as a probe of developmental processes. *Annual Review of Plant Physiology*. 24: 425-444.

Hamant O, Nogué F, Belles-Boix E, Jublot D, Grandjean O, Traas J, Pautot V, 2002. The KNAT2 homeodomain protein interacts with ethylene and cytokinin signalling. *Plant Physiology.* 130: 657-665.

Hamilton M, Lycett GW, Grierson D, 1990. Antisense gene that inhibits synthesis of the hormone ethylene in transgenic plants. *Nature.* 346: 437-439.

Hall MA, Moshkov IE, Novikova GV, Mur LAJ, Smith AR, 2001. Ethylene signal perception and transduction: Multiple paradigms? *Biological Reviews.* 76: 103-128.

Harberer G, Kieber JJ, 2002. Cytokinins. New insights into a classic phytohormone. *Plant Physiology.* 128: 354-362.

He Y, Tang W, Swain JD, Green AL, Jack TP, Gan S, 2001. Networking senescence-regulating pathways using Arabidopsis enhancer trap lines. *Plant Physiology*. 126: 707-716.

Henzi MX, 1999. Genetically modified broccoli (*Brassica oleracea* L. var. *Italica*) containing an antisense ACC oxidase gene. PhD thesis, Lincoln University, Canterbury, New Zealand.

Henzi MX, McNeil DL, Christey MC, Lill RE, 1999a. A tomato antisense 1-aminocyclopropane-1-carboxylic acid oxidase gene causes reduced ethylene production in transgenic broccoli. *Australian Journal of Plant Physiology.* 26: 179-183.

Henzi MX, Christey MC, McNeil DL, Davies KM, 1999b. *Agrobacterium rhizogenes*-mediated transformation of broccoli (*Brassica oleracea* L. var. *italica*) with an antisense 1-aminocyclopropane-1-carboxylic acid oxidase gene. *Plant Science*. 143: 55-62.

Hinderhofer K, Zentgraf U, 2001. Identification of a transcription factor specically expressed at the onset of leaf senescence. *Planta*. 213: 469-473.

Hoffman T, Schmidt JS, Zheng XY, Bent AF, 1999. Isolation of ethylene-insensitive soybean mutants that are altered in pathogen susceptibility and gene-for-gene disease resistance. *Plant Physiology*. 119: 935-949.

Holdsworth MJ, Bird CR, Ray J, Schuch W, Grierson D, 1987. Structure and expression of an ethylene-related mRNA from tomato. *Nucleic Acids Residues*. 15: 731-739.

Horgan R, 1984. *Cytokinins*. In: Advanced Plant Physiology. M.B. Wilkins (ed.) Longman Scientific and Technical. pp 53-75.

Houba-Herin N, Pethe C, d'Alayer J, Laloue M, 1999. Cytokinin oxidase from Zea mays: purification, cDNA cloning and expression in moss protoplasts. *Plant Journal*. 17(6): 615-626.

Houdebine L, Puissant C, 1995. An improvement of the single-step method of RNA isolation. *BioTechniques*. 8(2): 148-149.

Hua J, Chang C, Sun Q, Meyerowitz EM, 1995. Ethylene insensitivity conferred by *Arabidopsis ERS* gene. *Science* 269: 1712–1714.

Hua J, Sakai H, Nourizadeh S, Chen QG, Bleecker AB, 1998. *EIN4* and *ERS2* are members of the putative ethylene receptor gene family in *Arabidopsis*. *Plant Cell* 10: 1321–1332.

Huang PL, Parks JE, Rottman WH, Theologis A, 1991. Two genes encoding1-aminocyclopropane-1-carboxylate synthase in zucchini (*Cucurbita pepo*) are clustered and similar but differentially regulated. *Proceedings for the National Academy of Science of the USA*. 88: 7021-7025.

Humbeck K, Quast S, Krupinska K, 1996. Functional and molecular changes in photosynthetic apparatus during senescence of flag leaves from field-grown barley plants. *Plant Cell and Environment*. 19: 337-344.

Hunter DA, Yoo SD, Butcher SM, McManus MT, 1999. Expression of 1-aminocyclopropane-1-caboxylate oxidase during leaf ontogeny in white clover. *Plant Physiology*. 120: 131-141.

Hwang I, Sheen J. 2001. Two-component circuitry in *Arabidopsis* cytokinin signal transduction. *Nature*. 413: 383–389.

Inskeep WP, Bloom PR, 1985. Extinction coefficients of chlorophyll *a* and *b* in *N,N*-Dimethylformamide and 80% acetone. *Plant Physiology*. 77: 483-485.

Inoue T, Higuchi M, Hashimoto Y, Seki M, Kobayashi M, Kato T, Tabata S, Shinozaki K, Kakimoto T, 2001. Identification of CRE1 as a cytokinin receptor from *Arabidopsis*. *Nature*. 409: 1060–1063

Inze D, Folliin A, van Lijsebettens M, Simoens C, Genetello C, van Montagu M, Schell J, 1984. *Molecular and General Genetics.* 194: 265-274.

Irving DE, Joyce DC, 1995. Sucrose supply can increase longevity of broccoli (*Brassica oleracea*) branchlets kept at 22°C. *Plant Growth Regulation.* 17: 251-256.

Ishige F, Yamazaki K, Mori H, Imaseki H, 1991. The effects of ethylene on the coordinated synthesis of multiple proteins: accumulation of an acidic chitinase and a basic glycoprotein induced by ethylene in leaves of azuki bean, *Vigna angularis. Plant and Cell Physiology.* 32: 681-690.

Izumi H, Watada AE, Douglas W, 1996. Optimum O_2 or CO_2 atmosphere for storing broccoli florets at various temperatures. *Journal of the American Society for Horticultural Science.* 121(1): 127-131.

Jameson PE, 1994. Cytokinin metabolism and compartmentation. In: *Cytokinins: chemistry, activity, and function.* Mok DWS and Mok MC (eds.) pp.113-128. CRC Press, Florida.

Jones ML, Larsen PB, Woodson WR, 1995. Ethylene-regulated expression of a carnation cysteine protease during flower petal senescence. *Plant Molecular Biology.* 28: 505-512.

Jones RJ, Schreiber BMN, 1997. Role and function of cytokinin oxidases in plants. *Plant Growth Regulation.* 23: 122–134

Kakimoto T, 1996. CKI1, a histidine kinase homolog implicated in cytokinin signal transduction. *Science.* 274(5289): 982-985.

Kakimoto T, 2001. Identification of plant cytokinin biosynthetic enzymes as dimethylallyl diphophate:ATP/ADP isopentenyltransferases. *Plant Cell Physiology.* 42: 677-685.

Kakimoto T, Miyawaki K, Inoue T, Higuchi M, Matsumoto M, 2001. Biosynthesis and perception of cytokinins. *Proceedings of the 17th International Conference on Plant Growth Substances Brno, Czech Republic.* pp 146.

Kanyuka K, Couch D, Hooley R, 2001. Correction: A higher plant seven membrane reseptor that influences sensitivity to cytokinins. *Current Biology.* 11: 535.

Kato M, Kamo, T Wang R, Nishikawa F, Hyodo H, Ikoma Y, Sugiura M Yano M, 2002. Wound-induced ethylene synthesis in the stem tissue of harvested broccoli and its effects on senescence and ethylene synthesis in broccoli florets. *Postaharvest Biology and Technology.* 24: 69-78.

Kende H, 1993. Ethylene biosynthesis. *Annual Review of Plant Physiology and Plant Molecular Biology.* 44: 283-307.

Kenel FO, 2000. Expression of two promoter-GUS fusion genes in *Brassica oleracea* var. *italica.* Masters Thesis, Lincoln University, Canterbury, New Zealand.

Kenel FO, Braun RH, Coupe SA, Christey MC, 1999. A promoter GUS fusion in broccoli. Proceedings of the International Association of Plant Tissue Culture, Rotorua, New Zealand, February 1999.

Kieber JJ, Rothenberg M, Roman G, Feldmann KA, Ecker JR, 1993. *CTR1*, a negative regulator of the ethylene response pathway in *Arabidopsis*, encodes a member of the Raf family of protein kinases. *Cell.* 72: 427–441.

Kim JH, Kim WT, Kang BG, 2001. IAA and N^6-benzyladenine inhibit ethylene-regulated expression of ACC oxidase and ACC synthase genes in mungbean hypocotyls. *Plant Cell Physiology.* 42: 1056-1061.

Kim WT, Yang SF, 1994. Structure and expression of cDNAs encoding 1-aminocyclopropane-1-carboxylate oxidase homologs isolated and excised from mung bean hypocotyls. *Planta.* 194: 223-229.

King GA, Morris SC,1994. Physiological changes of broccoli during early postharvest senescence and through the preharvest-postharvest continuum. *Journal of the American Society for Horticultural Science.* 119: 270-275.

King GA, Davies KM, Stewart RJ, Borst WM, 1995. Similarities in gene expression during postharvest-induced senescence of spears and natural foliar senescence of asparagus. *Plant Physiology.* 108: 125-128.

Klee HJ, 1993. Ripening physiology of fruit from transgenic tomato (*Lycopersicon esculentum*) plants with reduced ethylene synthesis. *Plant Physiology.* 102(3): 911-916.

Klee H, Clark D, 2001. The tortuose road to success: Ethylene insensitive transgenic plants. *Proceedings of the 17th International Conference on Plant Growth Substances Brno, Czech Republic.* pp 64.

Knoester M, Van Loon LC, Van Den Heuvel J, Henning J, Bol JF, Linthorst HJM, 1998. Ethylene-insensitive tobacco lacks non-host resistance against soil-borne fungi. *Proceedings of the National Academy of Science of the USA.* 95: 1933-1937.

Laemmli UK, 1970.Cleavage of structural proteins during assembly of the head of bacteriaphage T4. *Nature.* 227: 680-685.

Laloue M, Fox JE, 1989. Cytokinin oxidase from wheat. Partial purification and general properties. *Plant Physiology.* 90: 899-906.

Lasserre E, Bouquin T, Hernandez JA, Bull J, Pech J-C, Balgue C, 1996. Structure and expression of three genes encoding ACC homologs from melon (*Cucumis melo* L.). *Molecular and General Genetics.* 251: 81-90.

Letham DS, Wilson MM, Parker CW, Jenkins ID, MacLeod JK, Summons RE, 1975. Regulators of cell division in plant tissues XXIII. The identity of and unusual metabolite of 6-benzylaminopurine. *Biochim. Biophys. Acta.* 399: 61-70.

Lewis DH, Burge GK, Schmierer DM, Jameson PE, 1996. Cytokinins and fruit development in the kiwifruit (*Actinidia deliciosa*). I. Changes during fruit development. *Physiologia Plantarum.* 98: 179-186.

Li CJ, Bangerth F, 1992. The possible role of cytokinins, ethylene and linolenic acid in apical dominance. In: *Progress in Plant Growth Regulation.* C.M Karssen, L.C. van Loon and D. Vreugdenhill (eds.) Kluwer, Dordretcht. pp 431-433.

Liang X, Abel S, Keller JA, Shen NF, Theologis A, 1992. The 1-aminocyclopropane-1-carboxylate synthase gene family of *Arabidopsis thaliana. Proceedings of the National Academy of the USA*. 89: 11046-11050.

Liang X, Shen NF, Theologis A, 1996. Li^+-regulated 1-aminocyclopropane-1-carboxylate synthase gene expression in *Arabidopsis thaliana. The Plant Journal*. 10: 1027-1036.

Lincoln JE, Campbell AD, Oetiker J, Rottmann WH, Oeller PW, Shen NF, Theologis A, 1993. LE-ACS4, a fruit ripening and wound-induced 1-aminocyclopropane-1-carboxylate synthase gene of tomato (*Lycopersicon esculentum*). *The Journal of Biological Chemistry*. 268: 19422-19430.

Liu J-H, Lee-Tamon SH, Reid DM, 1997. Differential and wound inducible expression of 1-aminocyclopropan-1-carboxylate oxidase genes in sunflower seedlings. *Plant Molecular Biology*. 34: 923-933.

Liu X, Shiomi S, Nakatsuka A, Kubho Y, Nakamura R, Inaba A, 1999. Chacterization of ethylene biosynthesis associated with ripening in banana fruit. *Plant Physiology*. 121: 1257-1265.

Lipton WJ, Harris CM, 1974. Controlled atmosphere effects on the market quality of stored broccoli. *Journal of the American Society for horticultural Science*. 99: 200-205.

Lund ST, Stall RE, Klee HJ, 1998. Ethylene regulates the susceptible response to pathogen infection in tomato. *The Plant Cell*. 10: 371-382.

Makhlouf J, Willemot C, Arul J, Castaigne F, Emond J, 1989. Regulation of ethylene biosynthesis in broccoli flower buds in controlled atmosphere. *Journal of the American Society for Horticultural Science*. 114: 955-958.

Martieau B, Houch CM, Sheehy RE, Hiatt WR, 1994. Fruit specific expression of the *A. tumefaciens* isopentenyl transferase gene in tomato: effects on fruit ripening and defense-related gene expression in leaves. *The Plant Journal*. 5(1): 11-19.

Matile P, 1992. Chloroplast senescence. In: *Crop Photosynthesis: Spatial and Temporal Determinants*. Baker N, Thomas H, eds. Amsterdam: Elsvier, 413-440.

McGaw BA, 1987. Cytokinin biosynthesis and metabolism. In: *Plant hormones and their role in plant growth and development*. Davies, PJ (ed.) pp. 76-93. Martinus Nijhoff Publishers, Dordrecht.

McGaw BA, Horgan R,1983. Cytokinin oxidase from *Zea mays* kernals and *Vica rosea* crown-gall tissue. *Planta*. 159: 30-37.

McGaw BA, Horgan R, Heald JK, 1985. Cytokinin metabolism and the modulation of cytokinin activity in radish. *Phytochemistry*. 24: 9-13.

McGlasson WB, Poovaiah BW, Dostal HC, 1975. Ethylene production and respiration in aging leaf segments and in disks of fruit tissue of normal and mutant tomatoes. *Plant Physiology*. 56: 547-549.

McKenzie MJ, 1996.Controlled synthesis of cytokinins in transgenic plants. PhD Thesis, University of Otago, Dunedin, New Zealand.

McKenzie MJ, Jameson PE, Poulter RTM, 1994. Cloning an *ipt* gene from *Agrobacterium tumefaciens*: characterisation of cytokinins in derivative transgenic plant tissue. *Plant Growth Regulation.* 14: 217-228.

McKenzie MJ, Mett V, Reynolds PHS, Jameson PE, 1998. Controlled cytokinin production in transgenic tobacco using a copper-inducible promoter. *Plant Physiology.* 116: 969-977.

McKeon TA, Fernandez-Maculet JC, Yang SF, 1995. Biosynthesis and metabolism of ethylene. In: *Plant Hormones: Physiology and Molecular Biology, 2nd*. Davies PJ. Ed., Kluwer Academic, Dordrecht, The Netherlands, pp 118-139.

McManus MT, Laing WA, Christeller JT, White DWR, 1994. Posttranslational modification of an isoinhibitor from the potatoe proteinase inhibitor II gene family in transgenic tobacco yields a peptide with homology to potato chymotrypsin inhibitor I. *Plant Physiology.* 106: 771-777.

Medford JI, Horgan R, El-Sawi Z, Klee HJ, 1989. Alterations of endogenous cytokinins in transgenic plants using a chimeric isopentenyl transferase gene. *Plant Cell.* 1: 403-413.

Metz TD, Dixit R, Earle ED, 1995. *Agrobacterium tumefaciens*-mediated transformation of broccoli (*Brassica oleracea* var. *italica*) and cabbage (*B. oleracea* var. *capitata*). *Plant Cell Reports.* 15: 287-292.

Miller CO, Skoog F, Okomura FS, Von Salta MH, Strong FW, 1956. Isolation, structure and synthesis of kinetin, a substance promoting cell division. *Journal of the American Chemical Society.* 78: 1345-1350.

Mo H, Pua EC, 2000. Polyamine modulation by down regulation of SPDS expression affects shoot morphogenesis of transgenic mustard *in vitro. Proceedings of The Asia Pacific Conference on Plant Tissue Culture & Agribiotechnology.* pp79.

Mok MC, 1994. Cytokinins and plant development - an overview. In: *Cytokinins: chemistry, activity and function.* DWS Mok and MC Mok (eds.) CRC Press. Boca Raton. pp 155-166.

Mok DWS, Mok MC, 2001. Cytokinin metabolism and action. *Annual Review of Plant Physiology and Plant Molecular Biology.* 52: 89-118.

Moloney MM, Walker JM, Sharma KK, 1989. High efficiency transformation of *Brassica napus* using *Agrobacterium* vectors. *Plant Cell Reports.* 8: 238-242.

Moran R, Porath D, 1980. Chlorophyll determination in intact tissues using *N,N*-Dimethylformamide. *Plant Physiology.* 65: 478-479.

Morris K, A-H-Mackerness S, Page T, John FC, Murphy AM, Carr JP, Buchanan-Wollaston, 2000. Salicylic acid has a role in regulating gene expression during leaf senescence. *The Plant Journal.* 23(5): 677-685.

Morris RO, Bilyeu KD, Laskey JG, Cheikh NN, 1999. Isolation of a gene encoding a glycosylated cytokinin oxidase from maize. *Biochemical and Biophysical Research Communications.* 255(2): 328-333.

Moyle RL, 1997. Molecular and biological studies of asparagines synthetase in asparagus. PhD Thesis, The University of Otago, Dunedin, New Zealand.

Murashige T, Skoog F, 1962. A revised medium for rapid growth and bioassays with tobacco tissue cultures. *Physiologia Plantarum.* 15: 743-497.

Nadeau JA, Zhang XS, Nair H, O'Neill SD, 1993. Temporal and spatial regulation of 1-aminocyclopropane-1-carboxylate oxidase in the pollination-induced senescence of orchid flowers. *Plant Physiology.* 103: 31-39.

Nakatsuka A, Murachi S, Okunishi H, Shiomi S, Nakano R, Kubo Y, Inaba A, 1998. Differential expression and internal feedback regulation of 1-aminocyclopropane-1-carboxylate synthase, 1-aminocyclopropane-1-carboxylate oxidase, and ethylene receptor genes in tomato fruit during development and ripening. *Plant Physiology.* 118(4): 1295-1305.

Nam HG, 1997. The molecular genetic analysis of leaf senescence. *Current Opinion in Biotechnology.* 8: 200-207.

Neljubow DN, 1901. Über die horizontale nutation der stengel von *Pisum sativum* und einiger anderer. *Pflanzen. Beih. Bot. Zentralle.* 10: 128-139.

Noodén LD, Singh S, Letham DS, 1990. Correlation of xylem sap cytokinin levels with monocarpic senescence in soybean. *Plant Physiology.* 93: 33-39.

Novikova GV, Moshkov IE, Smith AR, Hall MA, 1997. The effect of ethylene on GTP binding extracts from pea seedlings. *Planta.* 2001: 1-8.

Novikova GV, Moshkov IE, Smith AR, Kulaeva ON, Hall MA, 1999. The effect of ethylene and cytokinin on guanosine 5'-triphosphate binding and protein phosphorylation in leaves of *Arabidopsis thaliana. Planta.* 208: 239-246.

Novikova GV, Moshkov IE, Smith AR, Hall MA, 2000. The effect of ethylene on MAPKinase-like activity in *Arabidopsis thaliana. FEBS letters.* 474: 29-32.

O'Donell PJ, Jones BJ, Antoine FR, Ciardi J, Klee HJ, 2001. Ethylene-dependent salicylic acid regulates an expanded cell death response to a plant pathogen. *Plant Journal.* 25: 315-323.

Oeller PW, Wong LM, Taylor LP, Pike DA, Theologis A, 1991. Reversible inhibition of tomato fruit senescence by antisense 1-aminocyclopropane-1-carboxylate synthase in tomato fruit. *Proceedings of the National Academy of Sciences of the USA.* 88: 5340-5344.

Oh SA, Lee SY, Chung IK, Lee CH, Nam HG, 1996. A senescence-associated gene of *Arabidopsis thaliana* is distinctly regulated during natural and artificially-induced leaf senescence. *Plant Molecular Biology.* 30: 739-754.

Ohme-Takagi M, Shinshi H, 1995. Ethylene-inducible DNA binding proteins that interact with an ethylene responsive element. *The Plant Cell.* 7: 173-182.

Olsen DC, White JA, Edelman L, Harkins RN, Kende H, 1991. Differential expression of two genes for 1-aminocyclopropane-1-caboxylic synthase in tomato fruit. *Proceedings of the National Academy of Science of the USA.* 88: 5340-5344.

Osbourne DJ, Walters J, Milborrow BV, Norville A, Stange LMC, 1996. Evidence for a non-ACC ethylene biosynthesis pathway in lower plants. *Phytochemistry.* 42: 51-60.

Ori N, Juaarez MT, Jackson D, Yamaguchi J, Banowetz GM, Hake S, 1999. Leaf senescence is delayed in tobacco plants expressing the maize homeobox gene *knotted1* under the control of a senescence-activated promoter. *The Plant Cell.* 11: 1073-1080.

Page T, Griffiths G, Buchanan-Wollaston V, 2001. Molecular and biochemical characterisation of postharvest senescence in broccoli. *Plant Physiology.* 125: 718-727.

Palmer CE, 1992. Enhanced shoot regeneration from *Brassica campestris* by silver nitrate. *Plant Cell Reports.* 11: 541-545.

Palmer MV, Horgan R, Wareing PF, 1981. Cytokinin metabolism in *Phaseolus vulgaris* L. I. Variations in cytokinin levels in leaves of decapitated plants in relation to lateral bud outgrowth. *Journal of Experimental Botany.* 32: 1231-1241.

Palni LMS, Horgan R, 1983. Cytokinin biosynthesis in crown gall tissue of *Vinca rosea*: metabolism of isopentenyladenine. *Phytochemistry.* 22: 1597-1601.

Park JH, Oh SA, Kim YH, Woo HR, Nam HG, 1998. Differential expression of senescence-associated mRNAs during leaf senescence induced by different senescence-inducing factors in *Arabidopsis. Plant Molecular Biology.* 37: 445-454.

Picton S, Barton SL, Bouzayen M, Hamilton AJ, Grierson D, 1993. Altered fruit ripening and senescence in tomatoes expressing an antisense ethylene-forming enzyme transgene. The *Plant Journal.* 3: 469-481.

Pogson BJ, Downs CG, Davies KM, 1995a. Differential expression of two 1-aminocyclopropane-1-carboxylic acid oxidase genes in broccoli after harvest. *Plant Physiology.* 108: 651-657.

Pogson BJ, Downs CG, Davies KM, Morris SC, 1995b. Nucleotide sequence of a cDNA clone encoding 1-aminocyclopropane-1-carboxylic acid synthase from broccoli. *Plant Physiology.* 108: 857-858.

Pontier D, Gan S, Amasino RM, Roby D, Lam E, 1999. Markers for hypersensitive response and senescence show distinct patterns of expression. *Plant Molecular Biology.* 39(6): 1243-1255.

Plakidou-Dymock S, Dymock D, Hooley R, 1998. A higher plant seven-membrane receptor that influences sensitivity to cytokinins. *Current Biology.* 8: 315-324.

Pua EC, 2000. Study of shoot morphogenesis *in vitro* in relation to ethylene and polyamines using metabolic engineering. *Proceedings of The Asia Pacific Conference on Plant Tissue Culture & Agribiotechnology.* pp 77.

Puddephat IJ, Riggs TJ, Fenning TM, 1996. Transformation of *Brassica oleracea* L.: a critical review. *Molecular Breeding.* 2: 185-210.

Quirino BF, Normanly J, Amasino RM, 1999. Diverse range of gene activity during *Arabidopsis thaliana* leaf senescence includes pathogen-independent induction of defense-related genes. *Plant Molecular Biology.* 40: 267-278.

Quirino BF, Noh YS, Himelblau E, Amasino RM, 2000. Molecular aspects of leaf senescence. *Trends in Plant Science.* 5: 278-282.

Register JC, 1997. Approaches to evaluating the transgenic status of transformed plants. *Trends in Biotechnology.* 15: 141-146.

Richmond AE, Lang A, 1957. Effect of kinetin on protein content and survival of detached *Xanthium* leaves. *Science.* 125: 650-651.

Riou-Khamlichi C, Huntley R, Jacqmard A, Murray JAH, 1999. Cytokinin activation of *Arabidopsis* cell division through a D-type cyclin. *Science.* 238: 1541-1544.

Rodriguez FI, Esch JJ, Hall AE, Binder BM, Schaller GE, Bleecker AB, 1999. A copper cofactor for the ethylene receptor ETR1 from *Arabidopsis. Science* 283: 996–98

Rottmann WH, Peter GF, Oeller PW, Keller JA, Shen NF, Nagy BP, Taylor LP, Campbell AD, Theologis A, 1991. 1-aminocyclopropane-1-carboxylate synthase in tomato is encoded by a multigene family whose transcription is induced during fruit and floral senescence. *Journal of Molecular Biology.* 222: 937-961.

Rushing JW, 1990. Cytokinins affect respiration, ethylene production and chlorophyll retention of packaged broccoli florets. *HortScience.* 25: 88-90.

Ryall AL, Lipton WJ, 1979.Handling, transportation and storage of fruits and vegetables, Vol. 1, 2nd ed. Vegetables and Melons, AVI publishing Co., Westport, Conneticut, 587 pp.

Ryan DJ, Watson LM, Heyes JA, Coupe SA, Eason JR, 2002. Controlled atmosphere(CA) storage of broccoli: Delayed senescence-associated gene expression. *Proceedings of the Annual Meeting for the New Zealand Society of Plant Physiologists.* Microbes and Molecules, University of Canterbury, Christchurch New Zealand. pp 56.

Sablowski RWM, Moyano E, Culianez-Macia FA, Schuch W, Martin C, Bevan M, 1994. A flower-specific Myb protein activates transcription of phenylpropanoid biosynthetic genes. *The EMBO Journal.* 13(1): 128-137.

Sablowski RWM, Baulcombe DC, Bevan M, 1995. Expression of a flower-specific Myb protein in leaf cells using a viral vector causes ectopic activation of a target promoter. *Proceedings of the National Academy of Science of the USA.* 92: 6901-6905.

Sakai H, Hua J, Chen QG, Chang C, Medrano LJ, et al. 1998. *ETR2* is an *ETR1*-like gene involved in ethylene signaling in *Arabidopsis. Proceedings of the National Academy of Science of the USA.* 95: 5812–5817.

Salisbury FB, Ross CW, 1985. Hormones and Growth regulators. In: *Plant Physiology 3rd ed.* Caery JC. Ed., Wadsworth Pulishing Company, Belmont, California, USA pp 330-349.

Sambrook J, Fritsch EF, Maniatis T, 1989. Molecular Cloning, a Laboratory Manual. 2nd Edition. *Cold Spring Harbour Laboratory Press.*

Sato T, Oeller PW, Thelogis A, 1991. The 1-aminocyclopropane-1-carboxylate synthase of *Cucurbita. Journal of Biological Chemistry.* 266: 3752-3759.

Schaller GE, Bleecker AB, 1995. Ethylene-binding sites generated in yeast expressing the *Arabidopsis ETR1* gene. *Science.* 270: 1809–11.

Schmülling T, 2001. CREam of cytokinin signalling: receptor identified. *Trends in Plant Science.* 6: 281-284.

Schmülling T, 2002. New insights into the functions of cytokinins in plant development. *Journal of Plant Growth Regulation.* 21 (1): 40-49 2002.

Schultz C, Small JGC, 1991. Inhibition of lettuce seed germination by cycloheximide and chloramphenicol is alleviated by kinetin and oxygen. *Plant Physiology.* 97(2): 836-838.

Shewfelt RL, Heaton EK, Batal KM, 1983. Non-destructive color measurement of fresh broccoli. *Journal of Food Science.* 49: 1612-1613.

Shinshi H, Usami S, Ohme-Takagi M, 1995. Identification of an ethylene-responsive region in the promoter of a tobacco class I chitinase gene. *Plant Molecular Biology.* 27: 923-932.

Singh S, Letham DS, Palni LMS, 1992. Cytokinin biochemistry in relation to leaf senescence. VIII. Translocation, metabolism and biosynthesis of cytokinin in relation to sequential leaf senescence of tobacco. *Physiologia Plantarum.* 86: 398-406.

Sisler EC, Reid MS, Yang SF, 1986. Effect of antagonists of ethylene action on binding on binding of ethylene in cut carnations. *Plant Growth Regulation.* 4: 213-218.

Skoog F, Miller CO, 1957. Chemical regulation of growth and organ formation plant tissue cultured *in vitro. Symposium for the Society of Experimental Biology.* 11: 118-131.

Smalle J, Van der Straeten D, 1997. Ethylene and vegetative development. *Physiologia Plantarum.* 100: 593-605.

Smart CM, 1994. Tansley review No. 64. Gene expression during leaf senescence. *New Phytologist.* 126: 419-448.

Smart CM, Scofield SR, Bevan MW, Dyer TA, 1991. Delayed senescence in tobacco plants transformed with *tmr*, a gene for cytokinin production from *Agrobacterium. The Plant Cell.* 3: 647-656.

Smeekens S, 2000. Sugar-induced signal transduction in plants. Annual Review of Plant Biology. 51(1): 49-81.

Smith CJS, Slater A, Grierson D, 1986. rapid appearance of a mRNA correlated with ethylene synthesis encoding a protein of molecular weight 35000. *Planta.* 168: 94-100.

Solano R, Stepanova A, Chao QM, Ecker JR, 1998. Nuclear events in ethylene signaling: a transduction cascade mediated by ETHYLENE-INSENSITIVE3 and ETHYLENE-RESPONSE-FACTOR1. *Genes and Development.* 12: 3703–3714

Stabel P, Erikkson T, Engström P, 1990.Changes in protein synthesis upon cytokinin-mediated adventitious bud induction and during seedling development in Norway spruce (*Picea abies*). *Plant Physiology.* 92: 1174-1183.

Statistics New Zealand, 1996. Household Economics survey 1995/96.

Statistics New Zealand, 1988-1996. Overseas trade.

Stoddart JL, Thomas H, 1982. Leaf senescence. In: *Encyclopedia of Plant Physiology, vol 14A.* Boulter D, Parthier B, eds. Berlin Heidleberg, New York: Springer-Verlag. 592-636.

Stuchbury T, Palni LMS, Horgan R, Wareing PF, 1979. The biosynthesis of cytokinins in crown gall tissue of *Vinca rosea. Planta.* 147: 97-102.

Summons RE, Entsch B, Parker CW, Letham DS, 1979. Mass spectrometric analysis of cytokinins in plant tissues. III. Quantitation of the cytokinin glycoside complex of lupin pods by stable isotope dilution. *FEBS letters.* 107: 21-25.

Sun J, Niu Q-W, Tarkowski P, Zheng B, Tarkowska D, Sandburg G, Chua N-H, Zuo J, 2003. The Arabidopsis *AtIPT8/PGA22* gene encodes an isopentenyl transferase that is involved in *de novo* cytokinin biosynthesis. *Plant Physiology.* 131: 167-176.

Suzuki T, Sakurai K, Ueguchi C, Mizuno T, 2001. Two types of putative nuclear factors that physically interact histidine-containing phosphotransfer (Hpt) domains, signaling mediators in His-to-Asp phosphorelay, in *Arabidopsis thaliana. Plant Cell Physiology.* 42: 37–45.

Takei K, Sakakibaraq H, Sugiyama T, 2001. Identification of genes encoding adenylate isopentenyltransferase, a cytokinin biosynthesis enzyme, in *Arabidopsis thaliana. Journal of Biological Chemistry. 276*: 26405-26410.

Tang X, Gomes AMTR, Bhatia A, Woodson WR, 1994. Pistil-specific and ethylene-regulated expression of 1-aminocyclopropane-1-carboxylate oxidase genes in petunia flowers. *Plant Cell.* 6: 1227-1239.

ten Have A, Woltering EJ, 1997. Ethylene biosynthetic genes are differentially expressed during carnation (*Dianthus carophyllus* L.) flower senescence. *Plant Molecular Biology.* 34: 89-97.

Tepfer D, 1989. Ri T-DNA from *Agrobacterium rhizogenes*: a source of genes having applications in rhizosphere biology and plant development, ecology and evolution. In: *Plant microbe interactions: Molecular and Genetic Perspectives.* Kosuge, T and Nester EW, eds., vol3, pp. 294-342. McGrae-Hill, USA.

Thomas H, Stoddart JL, 1980. Leaf senescence. *Annual Review of Plant Physiology.* 31: 83-111.

Tian MS, Downs CG, Lill RE, King GA, 1994. A role for ethylene in the yellowing of broccoli after harvest. *Journal of the American Society of Horticultural Science.* 119(2):276-281.

Tian MS, Woolf, AB, Bowen JH, Ferguson IB, 1996. Changes in color and chlorophyll fluorescence of broccoli florets following hot water treatment. *Journal of the American Society for Horticultural Science.* 121(2): 310-313.

Tian MS, Islam T, Stevenson DG, Irving DE, 1997. Color, ethylene production, respiration, and compositional changes in broccoli dipped in hot water. *Journal of the American Society for Horticultural Science.* 122(1):112-116.

Toriyama K, Stein JC, Nasrallah ME, Nasrallah JB, 1991. Transformation of *Brassica oleracea* with an *S*-locus gene from *B. campestris* changes the self compatibility phenotype. *Theoretical and Applied Genetics.* 81: 769-776.

Towbin H, Staehelin T Gordan J, 1979. Electrophoretic transfer from polyacrylamide gels to nitrocellulose sheets: procedure and some applications. *Proceedings of the National Academy of Sciences of the USA*. 76: 4350-4354.

Trewavas A, 1970. The turnover of nucleic acids in *Lemna minor*. *Plant Physiology*. 45: 742-751.

Wang CY, 1977. Effect of aminoethoxy analogue of rhizobitoxine and sodium benzoate and senescence of broccoli. *HortScience* 14: 54-56.

Wang CY, Hrushka HW, 1977. Quality maintenance and anaerobic off-odour and off-flavour production and dissipation in consumer polyethylene-packaged broccoli. Market. Res. Rep. No 1085, USDA, Beltsville, MD.

Weaver LM, Himelblau E, Amasino RM, 1997. Leaf senescence: gene expression and regulation. In: *Genetic Engineering, Vol. 19, Principles and Methods*. Setlow JK ed. Plenum Press, New York. pp 215-234

Weaver LM, Gan S, Quirino B, Amasino RM, 1998. A comparison of the expression patterns of several senescence-associated genes in response to stress and hormone treatment. *Plant Molecular Biology*. 37: 455-469.

Werner T, Motyka C, Strnad M, Schmülling T, 2001. Regulation of plant growth by cytokinin. *Proceedings of the National Academy of Sciences of the USA*. 98(18): 10487-10492.

Whitty CD, Hall RH. 1974. A cytokinin oxidase in *Zea mays*. *Canadian Journal of Biochemistry*. 52: 789-799.

Wickson M, Thimann KV, 1958. The antagonist of auxin and kinetin in apical dominance. *Physiologia Plantarum*. 11: 62-69.

Winefield C, Lewis D, Arathoon S, Deroles S, 1999. Alteration of Petunia plant form through the introduction of the *rolC* gene from *Agrobacterium rhizogenes*. *Molecular Breeding*. 5(6): 543-551.

Wingler A, Schaewen A, Leegood R C, Lea PJ, Quick WP, 1998. Regulation of leaf senescence by cytokinin, sugars, and light. Effects on NADH-dependent hydroxypyruvate reductase. *Plant Physiology*. 116(1): 329-335.

Winichayakul S, Moyle RL, Ryan DJ, Farnden KJF, Davies KM, Coupe SA, unpublished. Distinct *cis*-elements in the *Asparagus officinalis* asparagine synthetase promoter respond to carbohydrate and senescence signals. *Manuscript in preparation for submission.*

Wurgler-Murphy SM, Saito H, 1997. Two-component signal transducers and MAPK cascades. *Trends Biochemical Science*. 22: 172–76.

Van Der Straeten D, Van Wiemeersch L, Van Demme J, Goodman H, Van Montagu M, 1989. Purification and amino acxid sequence analysis of 1-aminocyclopropane-1-carboxylic acid synthase from tomato pericarp. In: *Biochemical and Physiological Aspects of Ethylene Production in Lower and Higher Plants*. Clijsters H, De Proft M, Marcelle R, Van Poucke M. eds., Kluwer Academic, Dordrecht, The Netherlands. pp93-100.

Van der Straeten D, van Wiemeerrsch L, Goodman HM, van Montagu M, 1990. Cloning sequence of two different cDNAs encoding 1-aminocyclopropane-1-carboxylate synthase in tomato. *Proceedings of the National Academy of Science of the USA*. 87: 4859-4863.

van Staden J, Cook EL, Noodén LD, 1988. *Cytokinins and senescence.* In: Noodén LD, Leopold AC eds. Senescence and ageing in plants. San Diego: Academic Press, 281-238.

van Wordragen MF, Dons HJM, 1992. *Agrobacterium-tumefaciens*-mediated transformation of recalcitrant crops. *Plant Molecular Biology Reports*. 10: 12-36.

Venkatarayappa T, Fletcher RA, Thompson JE, 1984. Retardation and reversal of senescence in bean leaves by benzyladenine and decapitation. *Plant and Cell Physiology*. 25: 407-418.

Vervederdis P, John P, 1991. Complete recovery *in vitro* of ethylene-forming enzyme activity. *Phytochemistry*. 30: 725-727.

Vogel JP, Woeste KE, Theoloigs A, Kieber JJ, 1998. Rercessivce and dominant mutations in the ethylene biosynthetic gene *ACS5* of *Arabidopsis* confer cytokinin insensitivity and ethylene overproduction, respectively. *Proceedings of the National Academy of Sciences of the USA*. 95: 4766-4771.

Yang SF, Dong JG, 1993. Recent progress in research of ethylene biosynthesis. *Botanical Bulletin of Academia Sinica*. 34 (2): 89-101.

Yang SF, Hoffman NE, 1984. Ethylene biosynthesis and its regulation in higher plants. *Annual Review of Plant Physiology*. 35: 155-158.

Yip WK, Moore T, Yang SF, 1992. Differential accumulation of transcripts for four tomato 1-aminocyclopropane-1-carboxylate synthase homologs under various conditions. *Proceedings of the National Academy of Science of the USA*. 89: 2475-2479.

Yoshii H, Watanabe A, Imaseki H, 1980. Biosynthesis of auxin-induced ethylene in mung bean hypocotyls. *Plant and Cell Physiology*. 21(2): 279-291.

Zhang H, 1998. Cytokinins and phase change in *Pinus radiata*: Morphological, physiological and molecular studies. PhD Thesis, Massey University, Palmerston North.

Zubko E, Adams CJ, Macháèková I, Malbeck Jiri, Scollan C, Meyer P, 2002. Activation tagging identifies a gene from *Petunia hybrida* responsible for the production of active cytokinins in plants. *The Plant Journal*. 29(6): 797-808.

Appendix I

Table A.1 Partial length putative genes isolated during this thesis using RT-PCR from broccoli floret RNA as an initial template.

Description[1]	Primer 1	Primer 2	Fragment size (bp)[2]
Hypothetical protein (unknown)	AtCKOX-693 Fow	Oligo dT	830
PM H^+ ATPase type 1	AtIPT-190 Fow	Oligo dT	800
Scarecrow protein	AtCKOX-165 Fow	AtCKOX-706 Rev	500
rRNA 60S subunit	AtIPT-362 Fow	AtIPT-844 Rev	450
PM H^+ ATPase type 2	AtIPT-190 Fow	AtIPT-506 Rev	500
19S protesome subunit	AtIPT-362 Fow	AtIPT-769 Rev	400
Envelope glycoprotein	AtCKOX-190 Fow	Oligo dT	800
Helicase	AtCKOX-693 Fow	Oligo dT	300
Hypothetical protein (unknown)	AtIPT-362 Fow	Oligo dT	600
Homeobox leucine zipper transcriptional factor	AtIPT-362 Fow	AtIPT-844 rev	380

[1]Description of nearest homologous protein sequence in GenBank™ database
[2]Fragment size estimated by gel electrophoresis

Appendix II

Figure A1 *BoIPT4* DNA sequence. Translation start codon ATG and termination codon TAA are highlighted. Primer binding sites (used in the isolation) are underlined.

5'ATGAAGTGTAATGACAAAATGGTTGTGATCATGGGTTCTCACCGGTTCTGGCAAGTCA
TCACTCTCTGGTGATCTCGNTTTACATTTTAAAGCCGNGATCATCAACTNTGACAAAATG
CAGTTCTACGANGGCTTGAAGATCACCACGAATCAATCGACCATTGAAGATCGACGTGG
AGTGCCACATCACCTTCTCGGTGAACTAAACCCGGAGGCTGGAGAAGTCACAGCGGCN
GAATTTCGCGTTATGGCGGCTGAAGCCATCTCCGAGATTACTCAACGTAANAAGCTCCC
AATCCTTGCCGGTGGATCCAACTCATACATTCATGCTCTCCTTGCNAAATNTTATGACCC
TGAAAACTATCCGTTTNCTGATCACAAGGGCTCAATCTACTCCGAGTTGAAATATGATTG
TTGTTTCATTTGGATAGATGTGGATCAGTCTGTGTTATTCGAGTATCTTTCTTTACGTTTG
GATCTTATGATGAAGTCAGGTATGTTCGAGGAGATCGCTGAGTTCCNCCGCTCTAAGAA
GGCCCCGAAAGAGCCATTGGGGATATGGAAGGCTATAGGAGTGCAAGAGTTTGATGAC
TACCTCAAAATGTACAAGTGGGACAATGACATGGATAAATGGGACCCTATGAGAAAGGA
GGCTTATGAGAAGGCGGTNAGAGCCATCAAAGAAAACACATTTCAGCTCACAAAGGATC
AAATCNCNAAGATCAACAAGCTGAGAAATGCCGGGTGGGACATAAAGAAGGTGGATGN
TACAGCATCGTTTCGAGAGGCAATTAGGGCAGCCAAGGAAGGCGAAGGTGTAGCCGAG
ATGCAGAGAAAGATATGGAACATAGGAAGTGTTGGAACCGTGTGTGAAGATTGTCAGGA
GCCACTTGGACCAGACCGATCAACTATTATTATTATTACTTTTATTCTACTAAAAAGATTT
TTAAGTCTTAACTAGTTTGGACTAATATCACCGCAA3'

Appendix III

Figure A2 *BoIPT5* DNA sequence. Translation start codon ATG and termination codon TGA are highlighted. Primer binding sites (used in the isolation) are underlined.

5'ATGAAGCCATGCATGACGGCTCTAAGACAAGTGATTCAACCATTGTCGTTGAACTTCC
AAGGAAACATGGTGGACGTTCCGTTTTTCCGGCGAAAAGACAAGGTTGTTTTCGTCATG
GGAGCCACCGGAACCGGCAAATCTCGTCTAGCCATTGACCTAGCCACTCGTTTTCCGG
CGGAGATTGTAAACTCCGACAAGATCCAGGTCTATAAAGGTCTAGACATTGTGACTAAC
AAAGTCACTCCTGAGGAAAGCCTTGGCGTTCCTCACCACCTTCTCGGCACCGTCTACGA
CACTTACGAAGATTTCACGGCGGAGGATTTTCAGCGTGAAGCAATCAGGGCCGTCGAG
TCAATCGTGAGAGACCGTGTCCCGATCATAGCCGGTGGTTCCAATTCTTACATCGAGGC
TCTGGTCAACGATTGCGTTGACTTCCGGTTAAGGTATAATTGTTGCTCCTTGTGGGTCGA
CGTCTCTAGACTGGTTTTACACTCGTTTGTCTCGGAGCGAGTCGATAAGATGGTTGAGA
TGGGTCTCGTCGACGAGGTTCGCCGCATCTTCGATCCGTCTTCGTCGGATTACTCCGCT
GGAATTCGCCGAGCCATTGGAGTTCCAGAGCTCGACGAATTTCTCCGTTCGGAGATGC
GGAATTATCCGGCGGAGACGACGGAGAGACTTCTTGAAACGGCGATCGAGAAGATTAA
AGAGAACACTTGTTTGCTTGCGTGTAGACAATTGCAGAAGATTCAAAGGCTTTACAAGCA
GTGGAAGTGGAACATGCACCGTGTCGACGCGACGGAGGTTTTTCTCCGACGAGGAGTG
GAAGCTGATGAGGCTTGGGATAACTCAGTGGCTCATCCGAGCGCACTCGCCGTCGAAA
AGTTCCTTAGTTACAGCGATGACCACCATTTGGAAGGCGCCAATATTCTCCTACCGGAG
ATCTCTGCCGTTCCGCCTCTTCCAACCGCCGTGGCGGCGATTTCCCGGTGAGGTAAAA
CAGG3'

Appendix IV

Figure A3 *BoIPT6* DNA sequence. Start codon ATG and termination codon TGA are highlighted. Primer binding sites (used in the isolation) are underlined.

5'ATGACCTTGTTATCACCACCACTCTCTCATTCTTCTCTCCTTCCCACCGTCACTACCAA
ATTCGGGTCACCACGATTAGTCACTACGTGCATGGGCCATGCAGGGCGTAAAAATATCA
AGGATAAGGTGGTTCTCATCACAGGTACAACAGGCACAGGCAAGTCACGCCTCTCAGTC
GATCTTGCCACCCGTTTTTTTCCCGCCGAGATCATAAACTCGGACAAAATGCAAATCTAC
AAGGGATTCGAGATTGTCACAAATCTAATCCCACTGCATGAGCAAGGAGGAGTCCCGCA
CCATCTTCTAGGTCAGTTCCACCCACAAGACGGTGAACTCACCCCTGCAGAGTTCCGTT
CTTTGGCGACACTGTCCATCTCTAAACTAATTTCTAGCAAGAAACTCCCGATTGTAGTTG
GTGGATCCAACTCCTTCAATCACGCTCTACTCGCCGAGCGTTTTGACCCGGATATTGAT
CCATTCTCTCCCGGATCGAGTCTTTCAACGATCTGCTCTGACCTAAGGTACAAATGTTGC
ATCTTATGGGTTGATGTTTTAGAGCCGGTTCTGTTCCAACACTTGTGCAATCGTGTCGAC
CAAATGGTGCAATCGTGTCGACCAAATGATCGAGTCGGGATTGGTCGAGCAGCTTGCC
GAATTGTACGACCCTGTTGTAGATTCGGGTCGACGACTAGGGGTTCGGAAGACGATAG
GAGTAGAGGAGTTCGACCGATACTTTAGAGTATACCCTAAGGAGATGGACAAGGGAATT
TGGGACTTAGCGAGAAAGGCGGCGTACGAGGAGACAGTGAAGGGGATGAAAGAGAGG
ACATGTCGGTTGGTGAAGAAGCAGAAAGAGAAGATCATGAAGCTGATAAGAGGTGGTGA
AACAAGGTCAT3'

Appendix V

Figure A4 *BoIPT7* DNA sequence. Start codon ATG and termination codon TGA are highlighted. Primer binding sites (used in the isolation) are underlined.

5'ATGAAGTTCTCAATCTCATCACCGAAGCAGGTACAACCAACCTTGAGCTTCAAAAACAA
ACCATCCATTGTCAACGTCAACTCTTTCCTCCATCCTCACGAAAAAGTCGTCTTCGTAAT
GGGAGCCACTGGATACGGCAAGTCTCGTCTCGCCATCGACCTAGCAACACGGTTTCAA
ACAGATATCATAAACTCCGACAAGATCCAAGTTTACAAGGGCCTCGACGTCCTTACAAAT
AAAGTGACACCTCAAGAATGTCGAGGCGTGCCTCACCACTTGCTCGGGGTATTTGACTC
GGAAGATGGAAACCTAACGGCCACCGACTTCGCTCTCCTTGCGTCACAAGAGATCTCAA
CACTCTCAGCTAACAACAAGCTTCCTATAGTAGCCGGTGGATCAAACTCATACATCGAA
GCACTTGCGAACCATTCGTCTGGACCATTGTTAAACAACTACGAATGTTGTTTCATTTGG
GTCGACGTTTCCTTACCAGTTCTTAACTCTTTCGTCTCAAAACGTGTCGATCGTATGATG
GAAGCAGGATTACTAGATGAAGTAAGACAAGTATATGATCCCAAAGCGGATTATTCTGTC
GGGGTACGACGAGCTATCGGAGTCCCcGAGCTCCACGAGTACTTACGGTACGAATCTCT
AGTGGACCGTGCCACACAAAGAAAGATGCTTGACGTAGCGGTTAAAAAGATCAAACAGA
ACACAGAGATATTAGCTTGTCGACAGTTACAAAAGATTCAACGCCTGAGCAAGAAGTGG
AAGTCGTGTATGCACCATGTGGACGCCACGGAAGTGTTCTTGAAACATAATGAAGAAGA
AGCAGACGAGGCTTGGGAGAATCTTGTAGCGAGACCAACAAAGAGAATCGTCGACAAG
TTTTCTAATAGACATGTGATGAAAAATGATTCTGTTGAGCATTGTTTGACCACCATTGGA
GCGGCGTCATAGGACGGAGGAAGTGGAAGTAGGGCCCACAATATGATATGAAAAG3'

Appendix VI

Figure A5 *BoCKX* DNA sequence. 5' primer binding site (used in the isolation) is underlined (only 5' region has been sequenced, in one direction only).

5'TTAGGAGGTTTGGGTCAATTCGGAATAATCACGAGAGCCAGAATTGTTTTGAACCATG
CACCTAAAAGGGCGAAATGGTTTCGAATGCTGTACAGTGACTTCACAGCTTTAACAAAG
GACCAAGAACGTTTGATATCAATGGCCGATGATACTGGAGTTGACTATTTAGAAGGTCAA
CTATTCATGTCAAACGGCGTCGTAGACACCTCTTTTTTTCCACAGTCTGATCAATCTAAA
ATCGCTGATTTAGTGAAGAGCCACGGTATCATATATGTTCTTGAAGTAGCCAAGTTTTAT
GATGATCCTACACTTCCCATCATTGGCCAGGTGGTTGACATG3'